Lūkass Tomass Lukašēvics

KOBALTA KATALIZĒTA C–H SAITES FUNKCIONALIZĒŠANA

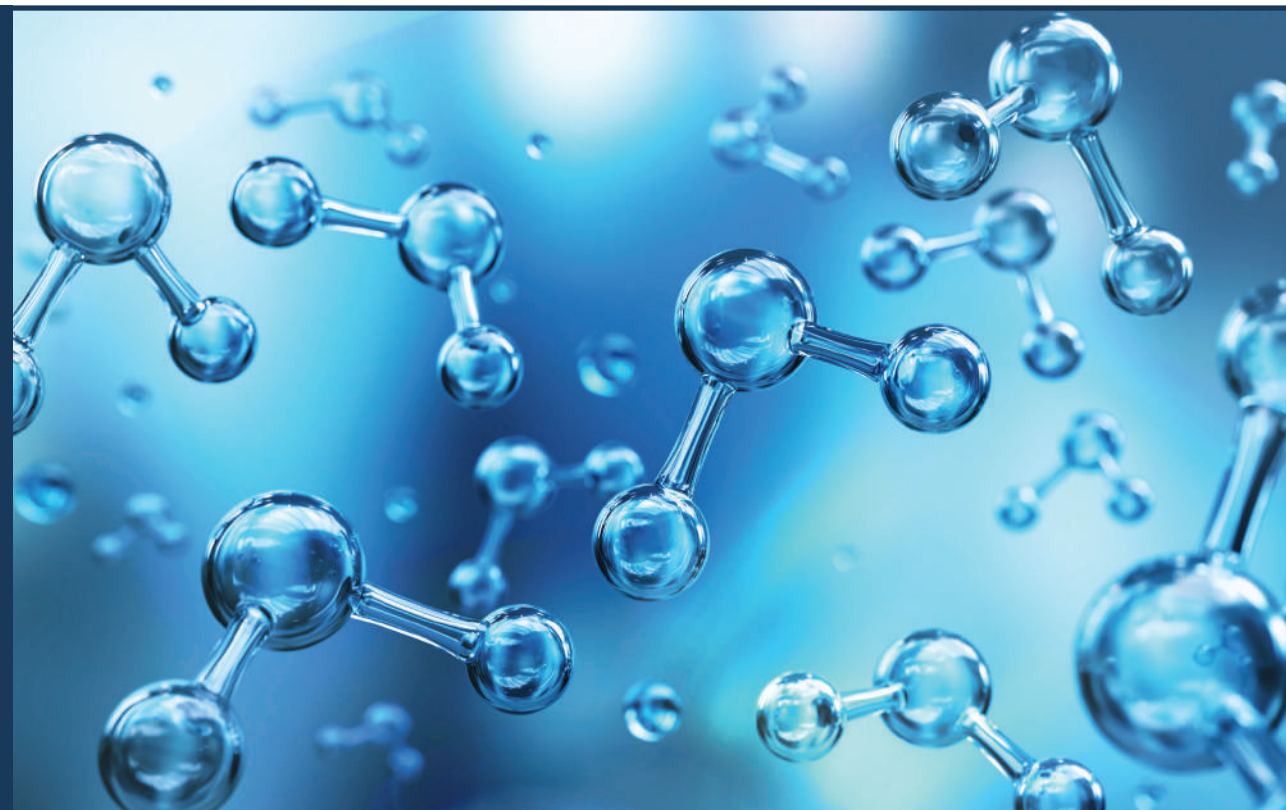Promocijas darbs

COBALT CATALYZED C–H BOND FUNCTIONALIZATION

Doctoral Thesis

RĪGAS TEHNISKĀ UNIVERSITĀTE

Materiālzinātnes un lietišķās ķīmijas fakultāte
Organiskās ķīmijas tehnoloģijas institūts
Bioloģiski aktīvo savienojumu ķīmijas tehnoloģijas katedra

RIGA TECHNICAL UNIVERSITY

Faculty of Materials Science and Applied Chemistry
Institute of Technology of Organic Chemistry
Department of Chemical Technology of Biologically Active Compounds

Lūkass Tomass Lukašēvics

Doktora studiju programmas "Ķīmija" doktorants
Student of the Doctoral Program "Chemistry"

KOBALTA KATALIZĒTA C–H SAITES FUNKCIONALIZĒŠANA

COBALT CATALYZED C–H BOND FUNCTIONALIZATION

Promocijas darbs
Doctoral Thesis

Zinātniskā vadītāja
Scientific supervisor

Docente *Dr. chem.* L. Grigorjeva
Docent *Dr. chem.* Liene Grigorjeva

Pateicības

Īpašs paldies:
- *Dr. phys.* Anatolijam Mišņevam par savienojumu rentgenstruktūranalīžu uzņemšanu;
- Aleksandram Čižikovam un Jekaterinai Boļšakovai par ieguldījumu promocijas darba tapšanā;
- Annai Nikitjukai, Elīnai Līdumniecei un Dacei Rasiņai par manuskriptu labošanu;
- Renātei Melngailei par emocionālo atbalstu;
- visiem OSM grupas kolēģiem, it īpaši prof. *Dr. chem*. A. Jirgensonam par zinātniskajām diskusijām un padomiem;
- docentei *Dr. chem*. Lienei Grigorjevai par promocijas darba vadīšanu.

Aknowledgments

Special thanks go to:
- *Dr. phys.* Anatolijs Misnevs for the X-ray analysis;
- Aleksandrs Cizikovs and Jekaterina Bolsakova for their collaboration in the reseach on the Doctoral Thesis;
- Anna Nikitjuka, Elina Lidumniece and Dace Rasina for the proofreading of the publication manuscripts;
- Renate Melngaile for the emotional support;
- all of the OSM group colleagues, especially Professor Dr. chem. A. Jirgensons for the scientific discussions and advice.

PROMOCIJAS DARBS IZVIRZĪTS ZINĀTNES DOKTORA GRĀDA IEGŪŠANAI RĪGAS TEHNISKĀJĀ UNIVERSITĀTĒ

Promocijas darbs zinātnes doktora (*Ph. D.*) grāda iegūšanai tiek publiski aizstāvēts 2022. gada 7. jūlijā. Rīgas Tehniskās universitātes Materiālzinātnes un lietišķās ķīmijas fakultātē, Rīgā, Paula Valdena ielā 3, 272 auditorijā.

OFICIĀLIE RECENZENTI

Vadošais pētnieks, *Dr. chem.* Pāvels Arsenjans, Latvijas Organiskās sintēzes institūts, Latvija
Profesors, *Ph. D.* Olafs Daugulis, Hjūstonas Universitāte, ASV
Profesors, *Dr. chem.* Edgars Sūna, Latvijas Universitāte, Latvija

APSTIPRINĀJUMS

Apstiprinu, ka esmu izstrādājis šo promocijas darbu, kas iesniegts izskatīšanai Rīgas Tehniskajā universitātē zinātnes doktora (*Ph. D.*) grāda iegūšanai. Promocijas darbs zinātniskā grāda iegūšanai nav iesniegts nevienā citā universitātē.

Lūkass Tomass Lukašēvics ……………………………. (paraksts)

Datums ………………………….

Promocijas darbs sagatavots kā tematiski vienota zinātnisko publikāciju kopa. Tas satur kopsavilkumu, četras publikācijas, trīs apskatrakstus un divas grāmatu nodaļas. Publikācijas uzrakstītas angļu valodā, to kopējais apjoms, ieskaitot elektroniski pieejamo informāciju, ir 743 lpp.

SATURS

PROMOCIJAS DARBA VISPĀRĒJS RAKSTUROJUMS

Tēmas aktualitāte

Medicīna, materiālzinātne, agroķīmija un citas ar ķīmiju saistītas zinātnes un tautsaimniecības nozares nav iedomājamas bez organiskajiem savienojumiem. Līdz ar to, organisko vielu efektīvu un lētu iegūšanas metožu izstrāde ir viens no priekšnoteikumiem šo jomu sekmīgai attīstībai. C–H saites aktivēšana un funkcionalizēšana ir salīdzinoši jauna pieeja organiskajā sintēzē. Metode ļauj vienā stadijā molekulā ievadīt jaunas grupas, tādējādi aizstājot agrāk izmantotās laikietilpīgās reakcijas sekvences un izvairoies no nevēlamu blakusproduktu veidošanās (1 att.).
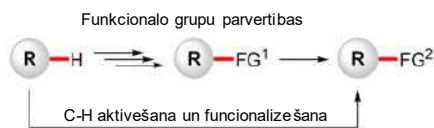
1. att. C–H saites funkcionalizēšana

Termins "C–H aktivēšana" metālorganiskajā ķīmijā bieži tiek lietots, lai aprakstītu procesu, kurā metāla centrs saistās pie substrātā esošās C–H saites, padarot to reaģētspējīgāku, un sekojošajā C–H funkcionalizēšanas solī pārveido substrātu. Lai gan organisko savienojumu struktūrās C–H saites ir visbiežāk sastopamas, tomēr to ķīmiskā reaģētspēja ir zema. Salīdzinot saišu disociācijas enerģijas ($C(sp^3)$-H = 105 kcal/mol, $C(sp^2)$-H = 110 kcal/mol, $C(sp^3)$-Cl = 83 kcal/mol, $C(sp^3)$-Br = 70 kcal/mol un $C(sp^3)$-I = 56 kcal/mol), ir redzams, ka C–H saites aktivēšanu un funkcionalizēšanu panākt ir daudz grūtāk, salīdzinot ar C–Hal saitēm, kas tradicionāli tiek izmantotas pārejas metālu katalizētās reakcijās.[1-6]

C–H saites aktivēšanai parasti izmanto dārgmetālu katalizatorus, taču pašlaik ir pieaudzis pieprasījums pēc lētākiem un videi draudzīgākiem katalizatoriem, jo mūsdienās arvien aktuālāks kļūst jautājums par "zaļās ķīmijas" pamatprincipiem, kas paredz ilgtspējīgu, videi draudzīgu un ekonomisku ķīmisko metožu izstrādi.[7] Neskatoties uz to, galvenie rezultāti C–H saites funkcionalizēšanas jomā ir sasniegti, izmantojot dārgmetālus (Rh, Ru, Pd), kas ir dabā reti sastopami, dārgi un toksiski.[1-6] Tikai salīdzinoši nesen 3d metāliem (Fe, Co, Ni) tika pievērsta lielāka uzmanība un tika sākta to katalītiska izmantošana C–H saites funkcionalizēšanas reakcijās. Viena no šādām alternatīvām ir kobalts, kas veido aptuveni 0,0029% no Zemes garozas pretstatā ķīmiskajās reakcijās tradicionāli bieži lietotajam palādijam, kā krājumi novērtēti vien triljonajās daļās Zemes garozas masas. Tikai kopš 2010. gada ir manāma ļoti strauja izaugsme kobalta katalizētas C–H funkcionalizēšanas metodoloģijā, tāpēc tas varētu tikt uzskatīts par, iespējams, visdaudzsološāko alternatīvu dārgmetālu katalizatoriem.[1]

Kobalta katalizētas C–H saites funkcionalizēšanas reakcijas ir iespējams iedalīt divās kategorijās:

1) zemas valences kobalta katalīze, šajā kategorijā esošajiem Co katalizatoriem ir raksturīga 0 vai +1 oksidēšanās pakāpe, ko iegūst no Co(I) vai Co(II) sāļiem *in situ* reducējošos apstākļos;

2) augstas valences kobalta katalīze, šajā kategorijā esošajiem kobalta katalizatoriem raksturīga +3 oksidēšanās pakāpe, ko iegūst no Co(III) vai Co(II) sāļiem *in situ* oksidējošos apstākļos. Kopš kobalta katalizētu C–H funkcionalizēšanas reakciju atklāšanas, lielākā daļa pārvētību bija panāktas, izmantojot zemas valences kobalta katalīzes pieeju. Tikai ap 2013., 2014. gadu sāka parādīties tendence izmantot augstas valences Co(III) vai prekursora Co(II) katalizatorus. Nākamajos gados kobalta katalizētām C–H funkcionalizēšanas reakcijām tika pievērsta īpaša uzmanība, un pašreiz šajā jomā izdoto publikāciju aptuvenais skaits sasniedz piecus simtus. Promocijas darbā izstrādātās metodes ir balstītas uz augstas valences kobalta katalīzi, izmantojot Co(II) sāļus un bidentātu virzošo grupu kā Co(III) prekursoru.

Neskatoties uz to, ka Co katalizētas C–H funkcionalizēšanas reakcijas pēc savas būtības ir daudz ''zaļākas'' nekā dārgmetālu gadījumā, eksistē papildus virzieni, kuros ir iespējams attīstīties, lai procesu padarītu vēl ekonomiski pievilcīgāku un dabai draudzīgāku. Viens no šiem virzieniem ir virzošo grupu stratēģija.[6] Virzošo grupu izmantošana ir priekšnosacījums selektīvai reakcijas norisei, jo tādējādi ir iespējams virzīt metālu vēlamās aktivējamās C–H saites tuvumā. Tomēr liela daļa virzošo grupu izmantošana pieprasa to ievadīšanu molekulā pirms C–H funkcionalizēšanas ar sekojošu nošķelšanu pēc pārvērtības, tādējādi daļēji atspēkojot priekšrocības, ko tās sniedz. Lai risinātu šo problēmu, ir ieviestas vairākas virzošo grupu klases (2. att.):

1) Aizejošās virzošās grupas (*traceless directing groups*) tiek ievadītas molekulā pirms C–H funkcionalizēšanas, taču tiek nošķeltas reakcijas apstākļos pēc veiksmīgas savas funkcijas izpildes. Patlaban šajā jomā ir panākts labs progress un literatūrā ir atrodami daudzi piemēri Co-katalizētām C–H funkcionalizēšanas reakcijām ar dažādām aizejošām virzošajām grupām, taču lielākā daļa pārvērtību ir limitētas tieši uz karbonilēšanas un annelēšanas reakcijām ar alkīniem un alkēniem;[6]

2) Pārejošās virzošās grupas (*transient directing groups*) tiek ievadītas molekulā un pēc tam nošķeltas reakcijas apstākļos, viena reaktora sintēzē. Šāda pieeja Co katalizētās C–H funkcionalizēšanas reakcijās ir parādījusies relatīvi nesen, tāpēc patlaban literatūrā ir zināmi tikai divi piemēri;[6]

3) Vājās virzošās grupas ir molekulā jau esošās funkcionālās grupas (karbonskābes, esteri, ketoni, aldehīdi, amīdi u. c.), kas spēj koordinēt metālu. Šāda pieeja ir šķietami vispievilcīgākā, it īpaši vēlīnajās stadijās, taču tajā pašā laikā visgrūtāk realizējamā. Šī iemesla dēļ, piemēru, kuros izmantotu vājas virzošās grupas, ir maz.[6]

2. att. Virzošo grupu stratēģija
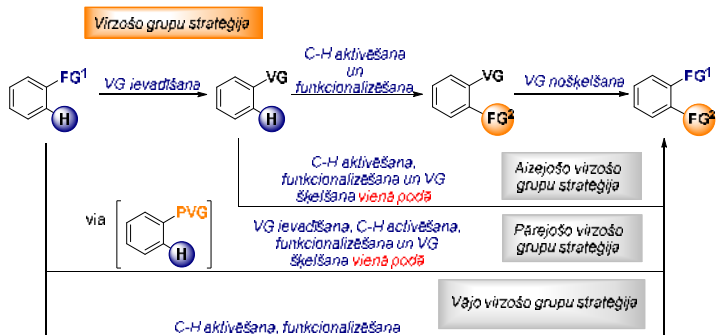
Aminoskābju un aminospirtu struktūrelementi ir ļoti bieži sastopami zāļvielās gan kā peptīdmimētiķu, gan kā proteīnu sastāvdaļas.[8] Turklāt tie ir daudzpusīgi būvbloki, ko plaši izmanto organiskajā sintēzē un asimetriskajā katalīzē.[8] Jaunu metožu izstrāde, ar kurām varētu iegūt aminoskābju un aminospirtu atvasinājumus, potenciāli spētu padarīt tirgū esošo farmaceitisko preparātu izmakas lētākas, kā arī attīstīt jaunas to iegūšanas metodes. Šo iemeslu dēļ, mūsu pētījumi ir vērsti uz kobalta-katalizētu fenilglicinola un fenilalanīna atvasinājumu C–H saites aktivēšanu, un funkcionalizēšanu ar tādiem reaģentiem kā alkīni, oglekļa monoksīds un izocianīdi (3. att.).
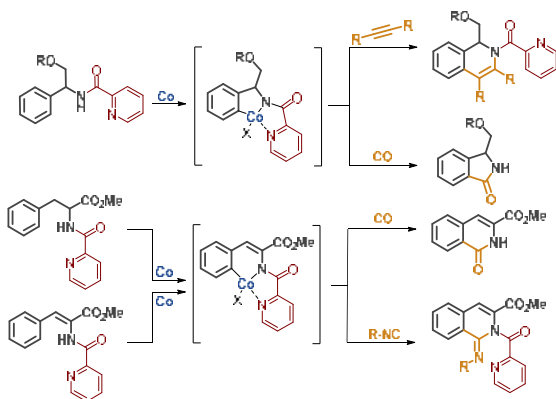
3. att. Fenilglicīnu un fenilalanīnu atvasinājumu funkcionalizēšanas iespējas

Pētījuma mērķis un uzdevumi

Promocijas darba mērķis ir jaunu, ērtu un praktisku metožu izstrāde, kas balstīta uz kobalta katalizētu C–H saites funkcionalizēšanu.

Darba mērķa īstenošanai tika definēti divi uzdevumi:

1. Iegūt aminospirtu un aminoskābju atvasinājumus, ko potenciāli varētu izmantot C–H saites funkcionalizēšanai, par modeļsubstrātiem izvēloties fenilglicinolu un fenilalanīnu (3. att.);

2. Izpētīt literatūru, atrast piemērotus reaģentus, kas spētu piedalīties kobalta katalizētā C–H saites funkcionalizēšanas reakcijā. Veikt tālāku reakcijas apstākļu optimizēšanu un substrātu ierobežojumu.

Zinātniskā novitāte un galvenie rezultāti

Darbā ir izstrādātas četras jaunas aminospirtu un aminoskābju atvasinājumu C–H saites funkcionalizēšanas metodes:

1. Kobalta katalizēta fenilglicinola atvasinājumu C–H saites alkenilēšana;

2. Kobalta katalizēta fenilglicinola atvasinājumu C–H saites karbonilēšana;

3. Kobalta katalizēta fenilalanīna atvasinājumu C–H saites karbonilēšana;

4. Kobalta katalizēta fenilalanīna atvasinājumu C–H saites iminēšana.

Darba struktūra un apjoms

Promocijas darbs sagatavots kā tematiski vienota zinātnisko publikāciju kopa par kobalta katalizētām fenilglicinola un fenilalanīna atvasinājumu C–H saites alkenilēšanas, karbonilēšanas un iminēšanas reakcijām, kā arī par iegūto produktu atvasināšanas iespējām.

Darba aprobācija un publikācijas

Promocijas darba galvenie rezultāti apkopoti četrās zinātniskajās oriģinālpublikācijās, trīs apskatrakstos un divās grāmatu nodaļās. Pētījuma rezultāti prezentēti trijās konferencēs.

Zinātniskās publikācijas:

1. Bolsakova, J.; Lukasevics, L.; Grigorjeva, L. Cobalt-Catalyzed, Directed C–H Functionalization/Annulation of Phenylglycinol Derivatives with Alkynes. *J. Org. Chem.* **2020**, *85* (6), 4482–4499. DOI:10.1021/acs.joc.0c00207

2. Lukasevics, L.; Cizikovs, A.; Grigorjeva, L. Synthesis of 3-Hydroxymethyl Isoindolinones via Cobalt-Catalyzed C(sp^2)–H Carbonylation of Phenylglycinol Derivatives. *Org. Lett.* **2020**, *22* (7), 2720-2723. DOI:10.1021/acs.orglett.0c00672

3. Lukasevics, L.; Grigorjeva, L. Cobalt-catalyzed carbonylation of the C–H bond. *Org. Biomol. Chem.* **2020**, *18*, 7460-7466. DOI:10.1039/D0OB01633K

4. Lukasevics, L.; Cizikovs, A.; Grigorjeva, L. Cobalt-Catalyzed C(sp^2)–H Carbonylation of Amino Acids Using Picolinamide as a Traceless Directing Group. *Org. Lett.* **2021**, *23* (7), 2748-2753. DOI:10.1021/acs.orglett.1c00660

5. Lukasevics, L.; Cizikovs, A.; Grigorjeva, L. C–H bond functionalization by high-valent cobalt catalysis: current progress, challenges and future perspectives. *Chem. Commun.* **2021**, *57*, 10827-10841. DOI:10.1039/D1CC04382J

6. Cizikovs, A.; Lukasevics, L.; Grigorjeva, L. Cobalt-catalyzed C–H bond functionalization using traceless directing group. *Tetrahedron* **2021,** *93*, 132307. DOI:10.1016/j.tet.2021.132307

7. Lukasevics, L.; Cizikovs, A.; Grigorjeva, L. Synthesis of 1-Aminoisoquinolines via Cobalt-Catalyzed C(sp^2)-H Bond Imination of Phenylalanine Derivatives. *Iesniegts manuskripts.*

Grāmatu nodaļas:

1. Lukasevics, L.; Grigorjeva, L. Cobalt-Catalyzed Picolinamide-Directed Synthesis of Heterocycles *Targets Heterocycl. Syst. (grāmatu sērija)* **2021**, *25,* 144-161. DOI:10.17374/targets.2022.25.144

2. Lukasevics, L.; Grigorjeva, L. Mechanistic studies on cobalt-catalyzed, bidentate chelation-assisted C–H bond functionalization *Handbook of CH-Functionalization. Pieņemts publicēšanai Wiley-VCH GmbH.*

Zinātniskās konferences, kurās prezentēti darba rezultāti:

1. Lukasevics, L. Cobalt Catalyzed Tandem C(sp^2)-H/C(sp^3)-H Functionalization of Amino Acids with Alkenes. *11th Paul Walden Symposium on Organic Chemistry.* Rīga, Latvija, 19-20. septembris **2019**.

2. Lukasevics, L. Cobalt catalyzed C–H bond functionalization. *12th Paul Walden Symposium on Organic Chemistry.* Tiešsaistē, 28-29. oktobris **2021.**

3. Lukasevics, L. Cobalt catalyzed C–H bond functionalization. *6th International Conference on Catalysis and Chemical Engineering.* Sanfrancisko, ASV, 22-26. februāris **2022**.

PROMOCIJAS DARBA GALVENIE REZULTĀTI

1. Kobalta katalizēta fenilglicinolu C–H saites alkenilēšana

Pirmais pētījuma virziens ietvēra fenilglicinola **1** C–H saites alkenilēšanas metodes izstrādi. Sākotnējiem eksperimentiem par modeļsubstrātu izvēlējāmies fenilglicinolu **1** un tercbutilacetilēnu kā alkenilēšanas reaģentu. Paredzējām, ka substrāta **1** reakcijā ar *t*butilacetilēnu potenciāli varētu veidoties četri iespējamie produkti **2a-d**, taču reakcijā novērojām selektīvu viena produkta **2a** veidošanos (4. att). Reakcijas apstākļu optimizēšanas eksperimentos nonācām līdz piemēroti katalītiskai sistēmai – Co(dpm)$_2$ katalizators, NaOPiv piedeva, un Mn(OAc)$_3$·2H$_2$O/ O$_2$ oksidētāju sistēma, kas ļāva iegūt produktu **2a** ar ļoti labu iznākumu – 83 %.
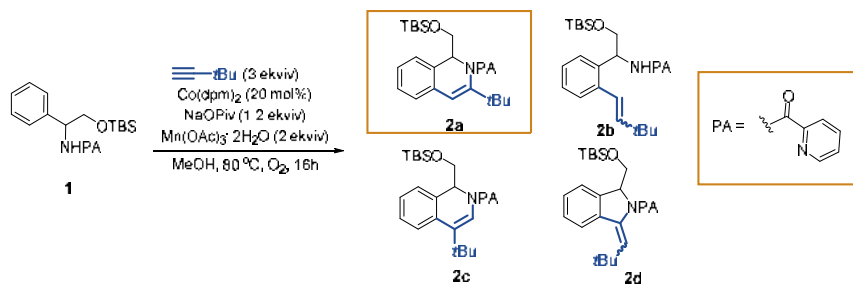
4. att. Fenilglicīna **1** C–H saites alkenilēšana ar *t*butilacetilēnu

Sākotnēji mēs vēlējāmies pārbaudīt dažādu benzilpozīcijas aizvietotāju ietekmi uz reakcijas gaitu (5. att.). Noskaidrojām, ka *O*-neaizsargāts aminospirts **4a** nav savietojams ar reakcijas apstākļiem un produkta veidošanās netika novērota, kas, iespējams, varētu būt saistīts ar katalizatora deaktivēšanu, ko izraisa brīvās hidroksilgrupas koordinēšanās pie kobalta katalizatora. Substrāti ar TBS, MOM un PMB aizsarggrupām **1a**, **1b,c**, kā arī metil- un fenilgrupu saturoši substrāti **1d**, **1e** reaģēja labi un deva attiecīgos produktus ar ļoti labiem iznākumiem – 70-88%.
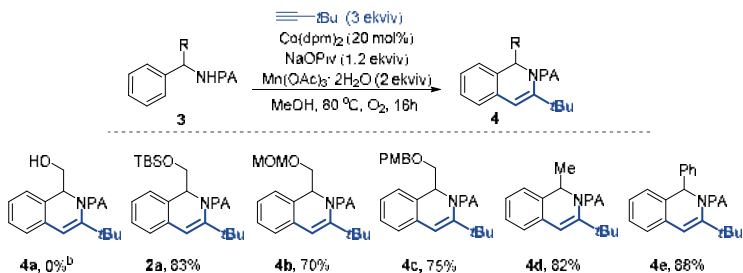
5. att. Dažādu benzilpozīcijas aizvietotāju ietekme uz reakcijas gaitu

Tālāk pārbaudījām dažādu funkcionālo grupu savietojamību ar optimizētajiem reakcijas apstākļiem (6. att.). Pārbaudījām dažādus aizvietotājus benzola gredzena *orto-*, *meta-* un *para-* pozīcijās. Interesanti, ka *meta-* aizvietotu substrātu gadījumā, novērojām tikai viena izomēra rašanos, reaģējot mazāk stēriski apgrūtinātajai *orto-* C–H saitei. Novērojām, ka substrāti ar tādiem elektronus-donējošiem aizvietotājiem kā alkil- (produkti **5c,e**), metoksi- (produkti **5a,g**) un metoksimetil- (produkts **5h**) grupas, bija reaģētspējīgi reakcijas apstākļos un deva produktus ar labiem un ļoti labiem iznākumiem - 55-90%. Līdzīgu reaģētspēju novērojām arī substrātiem, kas saturēja elektronus-atvelkošu aizvietotāju, dodot produktus **5d** un **5i** ar 65% un 75% iznākumu. Halogēnaizvietoti substrāti arī bija savietojami ar reakcijas apstākļiem (produkti **5b,f,j**). Interesanti, ka tādi strukturāli atšķirīgi substrāti kā β-fenilalaninols **1l** un tiofēns **1k** arī bija piemēroti substrāti un viegli veidoja attiecīgos C–H saites alkenilēšanas produktus (**5k,l**) ar labiem un ļoti labiem iznākumiem. Jāatzīmē, ka tiofēna **5k** gadījumā reakcija nebija selektīva un produkts tika iegūts kā reģioizomēru maisījums ar attiecību 2.5 : 1.
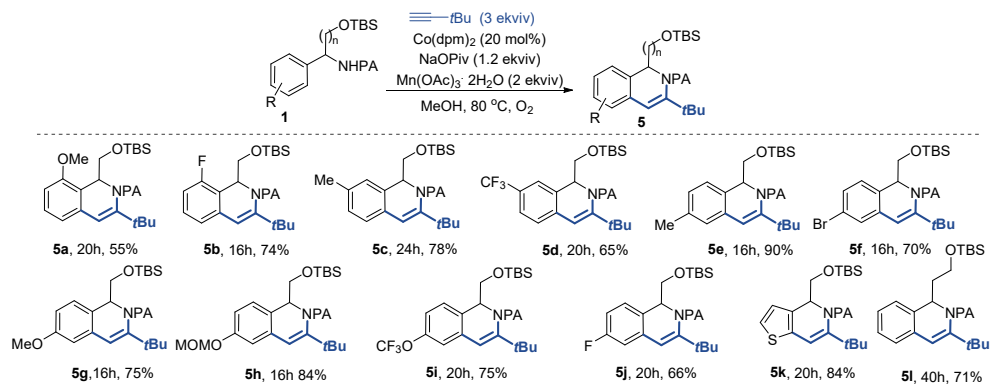
6. att. Substrātu klāsta pētījumi

Nākamais pētījuma solis ietvēra alkīnu klāsta izpēti (7. att.). Šim nolūkam izvēlējāmies gan simetriskus, gan nesimetriskus dialkil-, diaril-, kā arī terminālos alkīnus. Simetriskie dialkil- un diarilacetilēni uzrādīja labu reaģētspēju un deva produktus **6a-e** ar ļoti labiem iznākumiem – 70–80 %. Terminālo alkīnu gadījumā ieguvām produktus **6f-m** kā vienu reģioizomēru ar iznākumiem – 65–88 %. Interesanti, ka fenilglicinola **1** reakcijā ar 4-nitrofenilacetilēnu novērojām, gan sagaidāmā C–H saites alkenilēšanas produkta **6m**, gan arī dialkenilēšanas produkta **6m'** veidošanos. Lai demonstrētu attīstītās metodes praktisko pielietojumu, mēs veicām fenilglicinola **1** C–H saites alkenilēšanas reakciju 1g apjomā, un ieguvām produktu **6i** ar ļoti labu iznākumu - 80%.
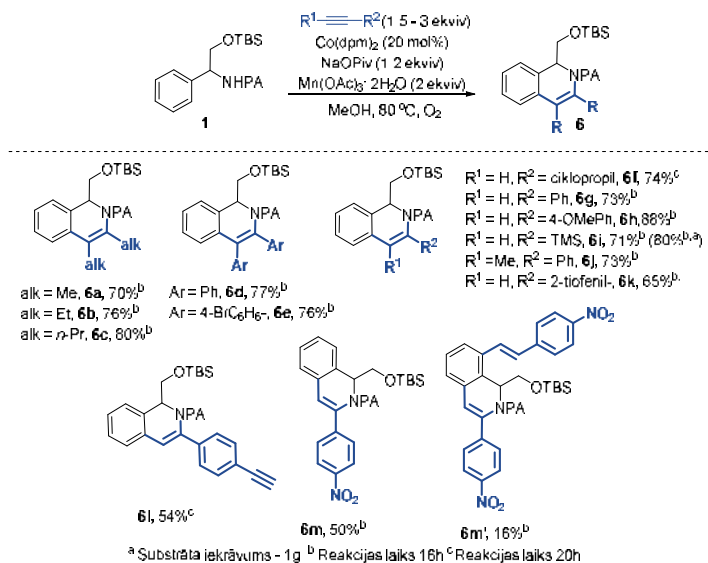
7. att. Alkīnu klāsta pētījumi

Papildus mēs vēlējāmies noskaidrot, vai reakcijas apstākļos potenciāli notiktu hirālā centra saglabāšana, ja tiktu izmantoti enantiobagātināti substrāti. Šim nolūkam mēs pakļāvām (*S*)-1 substrātu reakcijā ar pieciem dažādiem aromātiskajiem un alifātiskajiem, diazvietotiem, kā arī termināliem alkīniem (8. att.). Novērojām, ka visos gadījumos, produkti (*S*)-2a, 6a,g,d,i tika iegūti ar labiem iznākumiem un pilnīgu stereoķīmijas saglabāšanos (*ee* > 99 %).
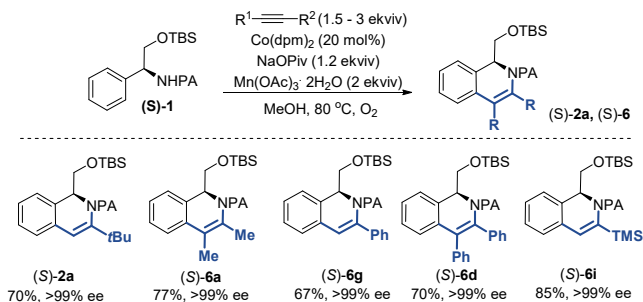
8. att. Enantiobagātinātu fenilglicinolu (*S*)-1 C–H saites alkenilēšana

Visbeidzot, mēs parādījām, ka iegūtajiem produktiem ir iespējams nošķelt pikolīnamīda virzošo grupu, lai iegūtu tetrahidroizohinolīnu atvasinājumus (*S*)-6i (9 att.). Sākumā enantiotīrs (*S*)-6i C–H saites alkenilēšanas produkts tika reducēts Bērča reducēšanas apstākļos ar Na/NH₃, iegūstot produktu 7 ar augstu diastereoselektivitāti (*d. r.* > 20 : 1). Sekojošā pikolīnamīda

13

šķelšanas solī ar LiAlH$_4$ tika iegūts tetrahidroizohinolīns **8** ar ļoti labu iznākumu un pilnībā saglabātu sākotnējo hirālo informāciju (*ee* > 99 %).
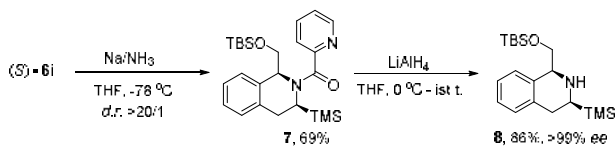
9. att. Virzošās grupas nošķelšana

2. Kobalta katalizēta fenilglicinolu C–H saites karbonilēšana

Turpinot izstrādāt jaunas metodes fenilglicinolu **1** C–H saites funkcionalizēšanai, mēs pievērsāmies C–H saites karbonilēšanai. Sākotnēji izmantojām tādu pašu katalītisko sistēmu, kas uzrādīja labus rezultātus C–H saites alkenilēšanas reakcijā. CO gāzes ģenerēšanai *in situ* izmantojām DIAD, kas pēc literatūras datiem izmantots līdzīgiem mērķiem. Šādos reakcijas apstākļos ieguvām karbonilēšanas produktu **9** ar 10 % KMR iznākumu (10. att.). Interesanti, ka pikolīnamīda virzošā grupa šajā gadījumā tika nošķelta reakcijas apstākļos pēc veiksmīgas C–H saites karbonilēšanas.
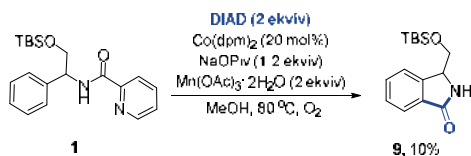
10. att. Fenilglicinola **1** C–H saites karbonilēšana

Reakcijas apstākļu optimizēšanas eksperimentos noskaidrojām, ka veiksmīgai reakcijas norisei nepieciešams Co(dpm)$_2$ katalizators, PivOH piedeva, Ag$_2$CO$_3$ oksidētājs un DIAD kā CO avots. Sākotnēji pārbaudījām dažādas spirta aizsarggrupas (11. att.). Līdzīgi kā C–H saites alkenilēšanas reakcijā, neaizsargāts aminospirts **10a** attiecīgo produktu nedeva. Lai gan PMB, MOM aizsargāti substrāti veidoja produktus **11b,c**, tie tika iegūti ar zemākiem iznākumiem nekā TBS aizsarggrupas gadījumā.
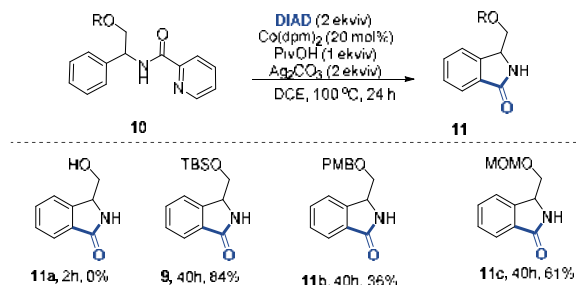
11. att. Dažādu aizsarggrupu ietekme uz C–H saites karbonilēšanu

Substrāta klāsta pētījumos tika parādīts, ka reakcijas apstākļi ir maigi un savietojami ar dažādām funkcionālajām grupām (12. att.). Līdzīgi kā C–H saites alkenilēšanas reakcijā, *meta*-aizvietotu substrātu gadījumos novērojām tikai viena reģioizomēra veidošanos, C–H saites karbonilēšanai notiekot mazāk stēriski traucētajā *orto*-pozīcijā. Gan elektroniem bagāti **1a,c,f-h**, gan elektroniem nabadzīgi substrāti **1d,i** deva produktus ar labiem un izciliem iznākumiem – 66-96%. Līdzīgu rezultātu novērojām arī halogēnsaturošu substrātu gadījumos, iegūstot produktus **12e,j,k** ar iznākumiem 75–91 %. Demonstrējām, ka tiofēnaminospirts arī ir piemērots substrāts C–H saites karbonilēšanai, taču šajā gadījumā reakcija nebija selektīva un produkts tika iegūts kā reģioizomēru **12l,l'** maisījums ar kopējo iznākumu 67%. Stēriski apjomīgāks **1m** kā arī kvarternārs substrāts **1n** bija reaģētspējīgi un deva produktus ar vidēju iznākumu. Tomēr abu substrātu gadījumos bija nepieciešams izmantot papildus katalizatora un oksidētāja daudzumu.
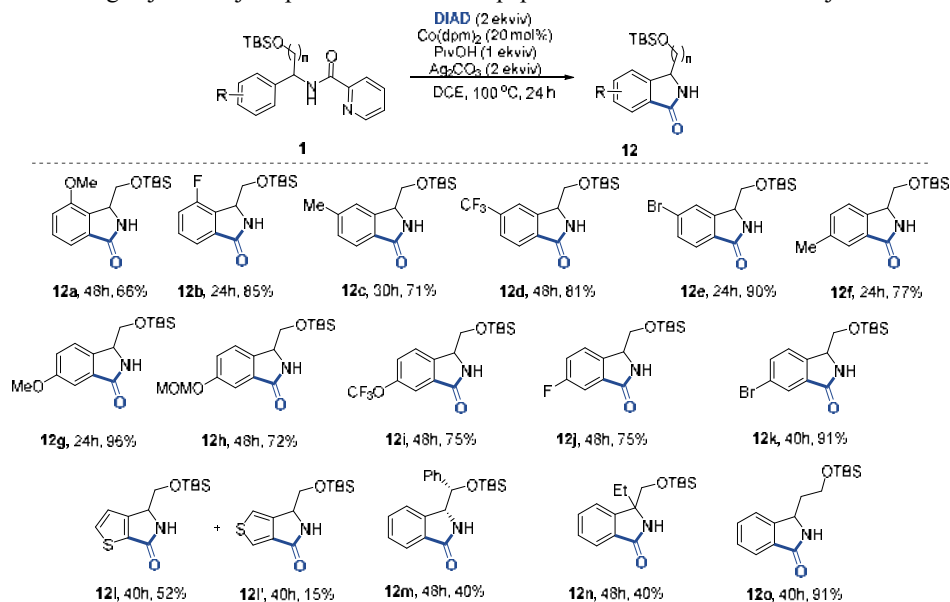
12. att. Substrātu klāsts fenilglicīnola **1** karbonilēšanā

Līdzīgi kā C–H saites alkenilēšanas reakcijas pētījumos, mēs vēlējāmies pārbaudīt vai C–H saites karbonilēšanas apstākļos būtu iespējams iegūt enantiobagātinātus produktus. Šim nolūkam izmantojām **(S)-1** fenilglicīnu un noskaidrojām, ka reakcijas apstākļos hirālā centra racemizēšanās nenotiek (13. att.).
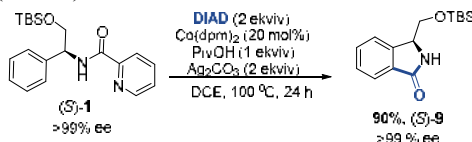
13. att. Stereoķīmijas saglabāšanās C–H saites karbonilēšanas reakcijā

3. Kobalta katalizēta fenilalanīna C–H saites karbonilēšana

Turpmākajos pētījumos mēs vēlējāmies pārbaudīt, vai C–H saites karbonilēšanas metodoloģiju varētu pielietot arī fenilalanīna atvasinājumiem. Kā modeļsubstrātu izvēlējāmies fenilalanīnu **13** ar pikolīnamīda virzošo grupu, kas līdz šim bija uzrādījusi labus rezultātus. Bijām priecīgi uzzināt, ka, izmantojot reakcijas apstākļus, kas bija piemēroti fenilglicīna **1** C–H saites karbonilēšanai, arī šajā gadījumā deva vēlamo karbonilēšanas produktu **14**, lai gan ar zemu iznākumu – 17% (14. att.). Interesanti, ka reakcijas apstākļos notiek ne tikai C–H saites karbonilēšana, bet arī dubultsaites veidošanās starp α un β oglekļiem substrātā, kā arī virzošās grupas nošķelšana.
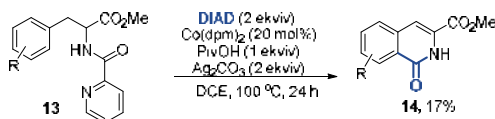
14. att. Fenilalanīna **13** C–H saites karbonilēšana

Pievēršoties reakcijas apstākļu optimizēšanai, noskaidrojām, ka labākos rezultātus iespējams sasniegt izmantojot, CO gāzi, Co(dpm)$_2$ katalizatoru, PivOH piedevu un Ag$_2$CO$_3$/Mn(OAc)$_3$·2H$_2$O oksidētāju sistēmu, PhCl šķīdinātājā, 120 °C temperatūrā. Sākotnēji pārbaudījām dažādu estera aizvietotāju ietekmi uz reakcijas iznākumu (15. att.). Substrāts **13**, kas saturēja metilestera aizvietotāju, reaģēja labi un deva attiecīgo izohinolīnona produktu **14** ar izcilu iznākumu - 94%. Substrāta iekrāvuma palielināšana līdz 1.7 mmol nedaudz samazināja produkta iznākumu, dodot produktu ar 75% iznākumu. Citi esteri Et-, *t*Bu- un Bn- reaģēja līdzīgi un deva vēlamos produktus **16a-c** ar ļoti labiem iznākumiem -70-83%. Lai gan alilaizvietots esteris izrādījās piemērots substrāts C–H saites karbonilēšanai, tas deva vēlamo produktu **16d** ar vidēju iznākumu – 50%.
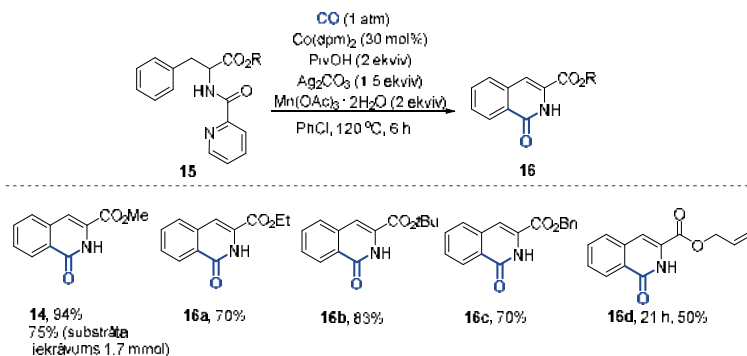
15. att. Dažādu esteru aizvietotāju ietekme uz reakcijas iznākumu

Substrāta klāsta pētījumi parādīja, ka fenilalanīna C–H saites karbonilēšanas reakciju ir iespējams realizēt ar plašu aizvietotāju klāstu benzola gredzena *orto-*, *meta-*, *para-* pozīcijās (16. att.). *Meta-* aizvietotu substrātu gadījumā arī šoreiz novērojām tikai viena reģioizomēra veidošanos, pat arī tāda maza aizvietotāja kā fluora atoma gadījumā. Dažādas funkcionālās grupas kā alkil- (produkti **18c,f**), halogēn- **18b,d,m,n**, trifluormetil- **18h**, fenil- **18g**, etilesteris **18p**, metoksi- **18i**, metoksimetil- **18j**, *t*-butilakinil- **18o** bija savietojamas ar reakcijas apstākļiem un deva reakciju produktus ar labiem un ļoti labiem iznākumiem. Mazāk veiksmīgs substrāts izrādījās 4-OAc aizvietots fenilalanīna atvasinājums, kas veidoja produktu **18l** ar 57% iznākumu, kas ir saistīts ar daļēju acetilgrupas nošķelšanu reakcijas apstākļos. Naftilaizvietotas **18r,s** kā arī tiofēnaizvietotas aminoskābes izrādījās piemēroti substrāti C–H saites karbonilēšanai, dodot attiecīgos produktus **18t** ar ļoti labiem un izciliem iznākumiem. Novērojām, ka arī amīda atvasinājums **18u**, kas potenciāli spētu koordinēt un deaktivēt katalizatoru, bija reaģētspējīgs un deva reakcijas produktu ar 52% iznākumu.
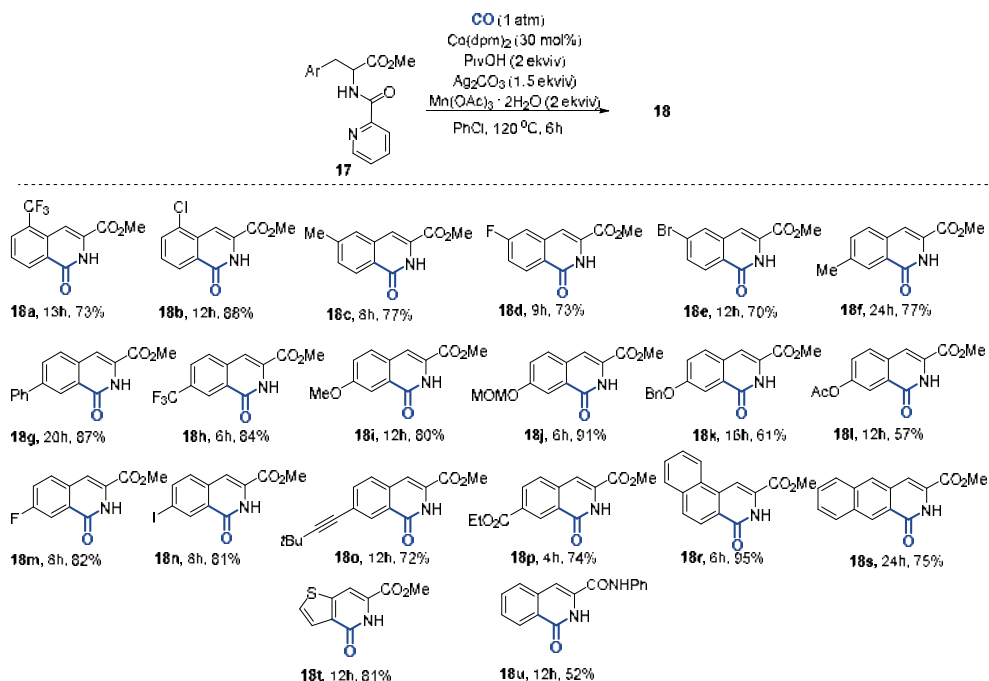
16. att. Fenilalanīnu **17** substrātu klāsts C–H saites karbonilēšanas reakcijā

Pētot reakcijas substrātu klāstu, mēs atklājām reakcijas ierobežojumus (17. att.). Benzoilaizvietota substrāta **19a** gadījumā, reakcijas produkta veidošanos nenovērojām, kas liecina par virzošās grupas svarīgo nozīmi. Reakcijas produktu veidošanās netika novērota arī kvaternārā substrāta **19b,** homofenilalanīna **19d** vai arī homobenzilamīda **19c** gadījumos. Šāds rezultāts liecina, ka veiksmīgas transformācijas veikšanai ir nepieciešama estera funkcionālā grupa, kā arī dubultsaites klātbūtne.
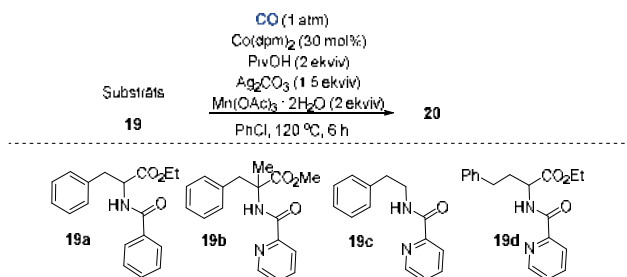
17. att. Neveiksmīgie substrāti C–H saites karbonilēšanas reakcijā

Ir zināms, ka amīdsaites peptīdu molekulās var viegli helatēt metāla jonus un tādējādi deaktivēt katalizatoru. Šī iemesla dēļ, mēs vēlējāmies pārbaudīt, vai izstrādāto metodi varētu

pielietot arī uz sarežģītākiem substrātiem - īsiem peptīdiem. Šim nolūkam mēs izmantojām dažādu dipeptīdu **12a-c** un tripeptīdu **22d** substrātus. Sākotnēji pakļaujot tos standarta reakcijas apstākļiem, mēs novērojām vēlamo produktu veidošanos, tomēr ar zemiem iznākumiem, kas ir skaidrojams ar neidentificētu blakusproduktu veidošanos. Mums izdevās uzlabot reakcijas produktu iznākumu, atmetot Mn(OAc)$_3$·2H$_2$O oksidētāju un vienlaicus palielinot Ag$_2$CO$_3$ iekrāvumu līdz 2,5 ekvivalentiem. Novērojām, ka šādos reakciju apstākļos C–H saites karbonilēšanas produktus **22a-d** bija iespējams iegūt ar pieņemamiem un labiem iznākumiem. Tomēr enantiomērā pārākuma analīze parādīja, ka diemžēl reakcijas apstākļos notiek daļēja blakus esošā hirālā centra racemizācija substrātos **22a** un **22b**, attiecīgi iegūstot produktus ar 86% un 93% *ee*. Visticamāk, ka līdzīga racemizācija notiek arī substrātā **21d**, taču produkta attīrīšanas laikā ieguvām tikai vienu diastereomēru **22d** (18.att.).
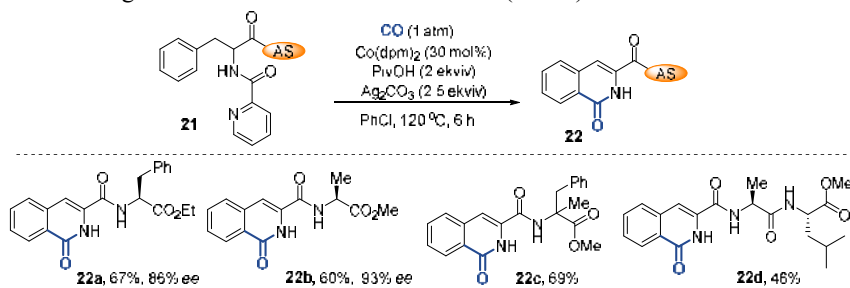
18. att. Vēlīnās stadijas C–H saites funkcionalizēšana peptīdos **22a-d**

Lai labāk izprastu reakcijas mehānismu, mēs veicām papildus kontroleksperimentus. Pakļaujot nepiesātināto fenilalanīna atvasinājumu **23** standarta reakcijas apstākļiem, mēs ieguvām karbonilēšanas produktu **14** ar 91% iznākumu (17. att., a)). Šāds rezultāts liecina, ka **14** ļoti iespējams ir karbonilēšanas reakcijas intermediāts. Turklāt, izmantojot UPLC-MS analīzi, mēs arī detektējām, abu ēnamīna **14** reģioizomēru klātbūtni reakcijas maisījumā. Interesanti, ka, pievienojot vienu vai trīs ekvivalentus radikāļu ķērāju TEMPO katalītiskajā sistēmā, mēs novērojām nozīmīgu reaktivitātes samazināšanos, un ieguvām karbonilēšanas produktu **14** ar 36% un 7% iznākumiem. Savukārt, izmantojot ēnamīnu **23** kā substrātu, tik ievērojamu reaģētspējas samazināšanos nenovērojām un ieguvām produktus ar 75% un 66% iznākumu (19. att., b)). Iegūtie rezultāti liecina par iespējamu SET reakcijas mehānismu, kas nodrošina intermediāta enamīna **23** veidošanos pirms C–H saites aktivēšanas. Papildus ieguvām Co(III) kompleksu **24**, ko mums izdevās izdalīt no reakcijas maisījuma un pierādīt tā struktūru ar rentgenstruktūranalīzi. Novērojām, ka Co(III) komplekss **24** CO atmosfērā veidoja vēlamo reakcijas produktu ar kvantitatīvu iznākumu (19. att., c)).
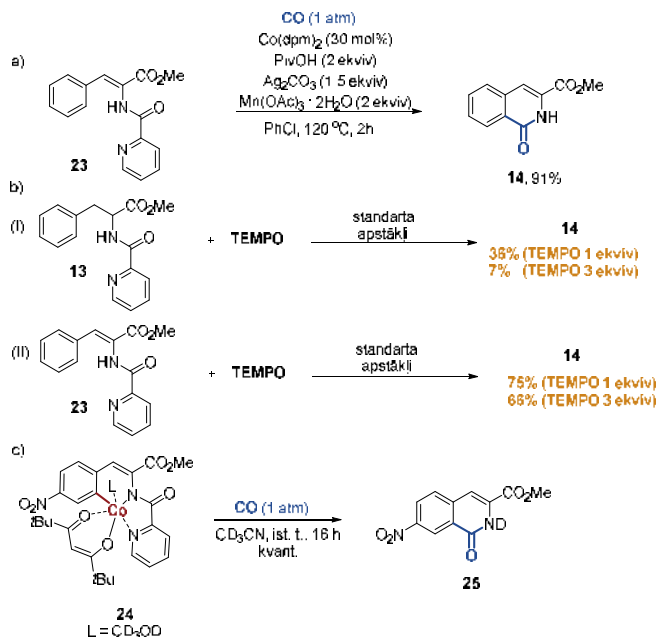
19. att. Fenilalanīna **13** C–H saites karbonilēšanas kontroleksperimenti

Balstoties uz reakcijas mehānisma pētījumiem, kā arī uz literatūras datiem, mūsu piedāvātais reakcijas mehānisms ir redzams 20. attēlā. Sākotnēji fenilalanīna atvasinājums **15** reakcijas apstākļos SET reakcijā tiek oksidēts līdz imīnam **23a**, kas tālāk tautomerizējas par ēnamīnu **23**. Sekojošos koordinēšanās/oksidēšanas soļos veidojas Co(III) komplekss **A**, kas C–H saites aktivēšanas rezultātā dod intermediātu **B**. Intermediāts **B** var tālāk tikt oksidēts līdz Co(IV), kam seko CO molekulas koordinēšana un migrējošā iespiešanās, dodot acil-Co(IV) intermediātu **C'** (ceļš a). Sekojošas reducējošās eliminēšanas stadijā tiek iegūts produkts **D**. Saskaņā ar ceļu b, intermediātā **B** vispirms varētu notikt CO koordinēšana/migrējošā ievietošana, kam seko reducējošā eliminēšana no kompleksa **C**. Alternatīvi nevar izslēgt arī iespējamu **C** oksidēšanu līdz Co(IV) intermediātam **C'** (ceļš c). Visticamāk, ka mūsu gadījumā ceļš b ir galvenais C–H saites funkcionalizēšanas mehānisms, jo kontroleksperimentā, kur izmantojām Co(III) kompleksu, produkts **14** veidojās bez papildus oksidētāja pievienošanas.Tālāk hidrolīzes rezultātā tiek nošķelta pikolīnamīda virzošā grupa, dodot galaproduktu **14** un atgriežot Co(I) katalītiskajā ciklā, kurš tālāk tiek oksidēts līdz Co(III) kompleksam **E**. Notiekot ligandu apmaiņas reakcijai starp kompleksu **E** un ēnamīnu **23**, tiek atsākts katalītiskais cikls.
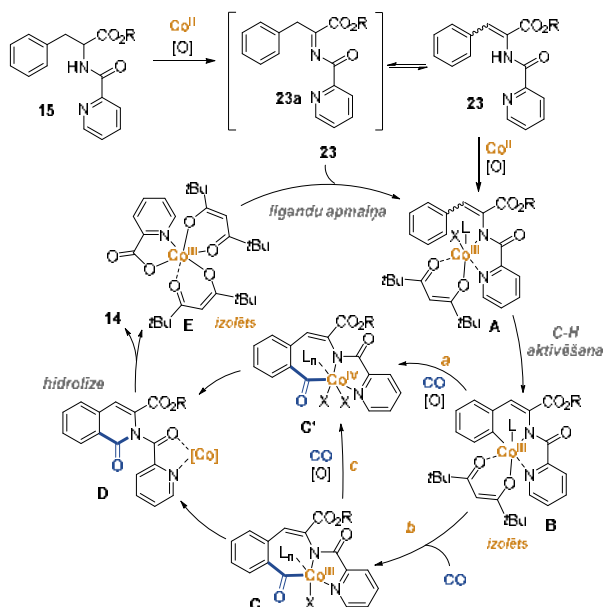
20. att. Iespējamais fenilalanīna **15** C–H saites karbonilēšanas mehānisms

4. Kobalta katalizēta fenilalanīna C–H saites iminēšana

Pēc kobalta katalizētas fenilalanīna **13** C–H saites karbonilēšanas metodes izstrādes, mēs vēlējāmies attīstīt līdzīgu virzienu, izmantojot izocianīdus kā funkcionalizēšanas reaģentus. Literatūrā ir zināmi piemēri kobalta katalizētai C–H saites iminēšanai ar izocianīdiem, taču uz doto brīdi šāda veida pārvērtības nav realizētas uz aminoskābju atvasinājumiem.[9-12] Sākotnēji par modeļsubstrātu izvēlējāmies fenilalanīnu **13** un *t*-butilizocianīdu kā C–H saites iminēšanas reaģentu. Tas reakcijas apstākļos, kas bija piemēroti C–H saites karbonilēšanai, veidoja imīnu **25a** ar 41% (21. att.). Reakcijas apstākļu optimizēšanas eksperimentos diemžēl produkta iznākumu uzlabot neizdevās, kas, mūsuprāt, visdrīzāk ir skaidrojams ar strauju izocianīda bojāšanos. Fenilalanīna **13** C–H saites karbonilēšanas metodes izstrādes laikā mēs parādījām, ka reakcijas pirmajā solī notiek ēnamīna **23** veidošanās caur SET mehānismu. Visticamāk, ka *t*butilizocianīds spēj piedalīties nevēlamās blakusreakcijās ar brīvajiem radikāļiem, kas rodas šajā solī un tādējādi degradējas.[13] Lai novērstu šo problēmu, mēs nolēmām izmantot ēnamīnu **23** kā modeļsubstrātu. Novērojām, ka izocianīds šajos reakcijas apstākļos ir ievērojami stabilāks, tas ļāva iegūt produktu **25a** ar 71% iznākumu.
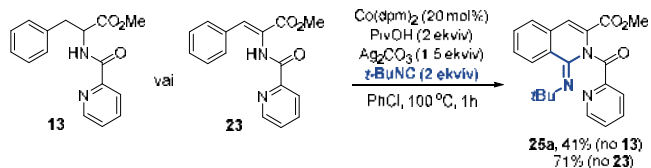
21. att. Fenilalanīnu **13** un **23** C–H saites iminēšana ar *t*-butilizocianīdu

Lai palielinātu reakcijas produkta iznākumu, veicām reakcijas apstākļu optimizēšanas eksperimentus un nonācām pie šādas katalītiskās sistēmas: Co(dpm)$_2$ katalizators, NaOPiv piedeva, Ag$_2$CO$_3$ oksidētājs, THF šķīdinātājs. Sākotnēji mēs vēlējāmies pārbaudīt dažādu izocianīdu ietekmi uz C–H saites iminēšanas reakcijas iznākumu (22. att.). Mūsu optimizētajos reakcijas apstākļos ēnamīns **23** reakcijā ar *t*-butilizocianīdu deva attiecīgo produktu **25a** ar ļoti labu iznākumu - 86%. Palielinot substrāta iekrāvumu līdz 1,8 mmol, novērojām līdzīgu rezultātu – produkts veidojās ar 72% iznākumu. Līdzīgi cikloheksil-, *n*-pentil- un feniletilaizvietoti izocianīdi bija savietojami ar reakcijas apstākļiem un deva produktus **25b-d** ar ļoti labiem un izciliem iznākumiem 79-95%.
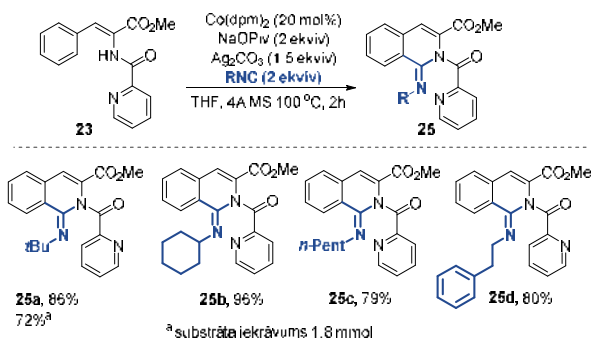
22. att. Izocianīdu klāsts fenilalanīna **23** C–H saites iminēšanas reakcijā

Turpmākos substrāta klāsta pētījumos mēs pārbaudījām dažādu *orto*-, *meta*-, *para*-aizvietotāju savietojamību ar reakcijas apstākļiem (23. att.). Elektronus-donējošas Me-, OMe-, OAc- un Ar-grupas uzrādīja labu savietojamību ar reakcijas apstākļiem un deva attiecīgos produktus **27a-d**,**f** ar labiem un izciliem iznākumiem – 74-96%. Interesanti, ka 4-OAc aizvietota substrāta **27e** gadījumā notika ne tikai C–H saites iminēšana, bet arī *trans*-acilēšana, kas ļāva iegūt 4-OPiv aizvietotu produktu. Gan BocNH-, gan PhthN- *meta*-pozīcijā aizvietoti substrāti reaģēja labi un veidoja produktus **27g,h** ar 84% un 83% iznākumu. Jāatzīmē, ka *meta*-aizvietotu substrātu gadījumā arī šoreiz novērojām tikai viena reģioizomēra veidošanos, C–H saites aktivēšanai notiekot ar mazāk stēriski apgrūtināto *orto*-C–H saiti. Pārbaudot dažādu halogēnatomu aizvietotājus *orto*- un *para*-pozīcijās noskaidrojām, ka F-, Cl- Br-, I- aizvietototi substrāti ir savietojami ar reakcijas apstākļiem un dod attiecīgos produktus **27i-l** ar 61-65% iznākumu. Papildus noskaidrojām, ka arī citas aromātiskās sistēmas var tikt funkcionalizētas,

izmantojot mūsu izstrādāto metodi. To labi demonstrēja tiofenil- un furanil-alanīni, kas reakcijas apstākļos veidoja attiecīgos imīnus **27o,p** ar 64% un 67% iznākumu.

27a, 1h, 96% **27b**, 1h, 89% **27c**, 1h, 84% **27d**, 1h, 75% **27e**, 1h, 74%

27f, 2h, 95% **27g**, 2h, 84% **27h**, 1h, 83% **27i**, 2h, 63% **27j**, 2h, 65%

27k, 2h, 62% **27l**, 2h, 63% **27m**, 1h, 61% **27n**, 1h, 66% **27o**, 2h, 64%

27p, 2h, 67% **27r**, 1h, 72%
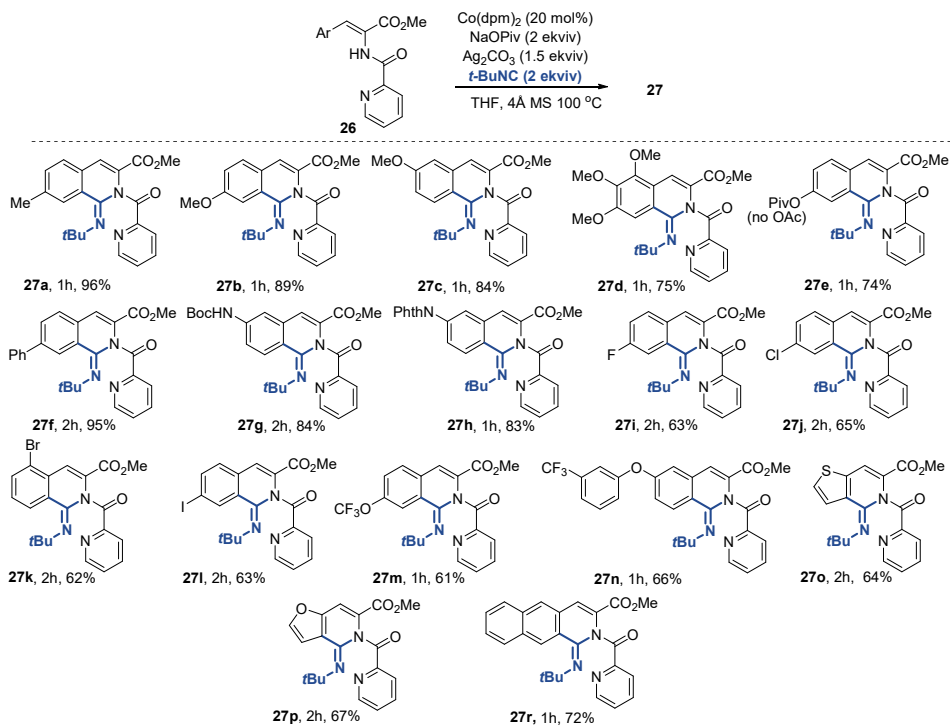
23. att. Nepiesātinātu fenilalanīnu **26** substrātu klāsts C–H saites karbonilēšanas reakcijā

Lai demonstrētu izstrādātās metodes praktisko pielietojumu, mēs parādījām, ka iegūtie C–H saites iminēšanas produkti var tikt izmantoti 1-aminoizohinolīnu **28a,b** sintēzē (24. att.). Mēs atklājām, ka pikolīnamīda virzošo grupu var nošķelt reducējošos apstākļos, izmantojot LiAlH$_4$, lai iegūtu produktu **28a** ar pilnībā reducētu estera grupu. Savukārt, izmantojot Zn/AcOH maisījumu virzošās grupas šķelšanai, ieguvām metilesteri **28b** ar labu iznākumu -67%.
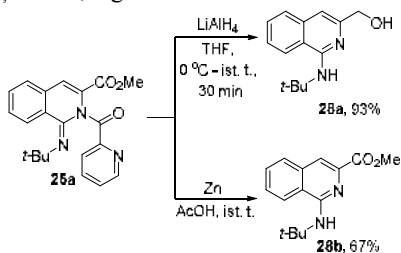
24. att. Virzošās grupas nošķelšana reducējošos apstākļos

Mēs veicām kontroleksperimentus, lai labāk izprastu C–H iminēšanas mehānismu (25. att.). Vispirms noskaidrojām, ka katalītiskā cikla pirmais solis ir Co(dpm)$_2$ katalizatora koordinēšana pie substrāta, nevis Co(II) oksidēšana uz Co(III).
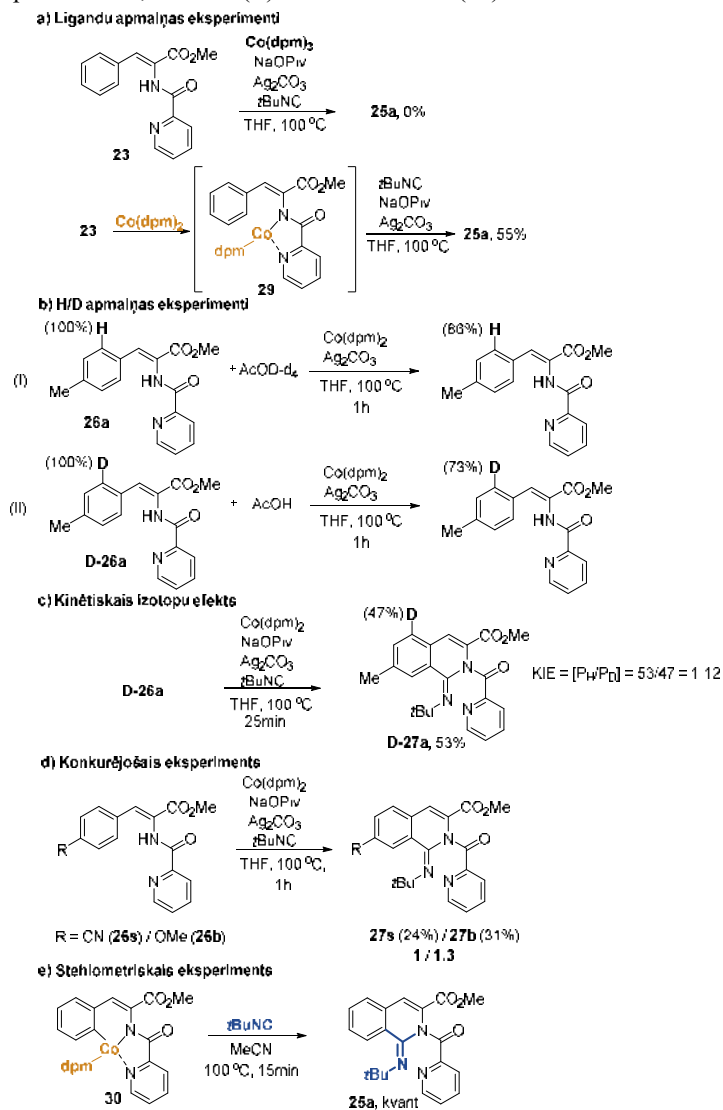
25. att. Kontroleksperimenti C–H saites iminēšanas reakcijā

To labi parādīja ligandu apmaiņas kontroleksperiments, kurā, pakļaujot substrātu **23** reakcijas standartapstākļiem, tas izrādījās nereaģētspējīgs, ja Co(dpm)$_2$ katalizators tika aizstāts

ar Co(dpm)₃ (25. att., a)). Turklāt, stehiometriskajā eksperimentā, kur Co(II)-substrāta komplekss **29** tika pakļauts reakcijas standartapstākļiem, tas deva vēlamo imīnēšanas produktu **25a** ar 55% iznākumu (25. att., a)). Tālāk pievērsāmies H/D apmaiņas eksperimentiem. Izmantojot AcOD-d₄ kā papildus šķīdinātāju reakcijas apstākļos, mēs novērojām 14% H/D apmaiņu substrāta **26a** *orto*- pozīcijā. Līdzīgu rezultātu novērojām, izmantojot AcOH šķīdinātāju un ar deitēriju iezīmētu substrātu **D-26a** (25. att., b)).Turpinot D-iezīmes eksperimentus, mēs noteicām kinētiskā izotopa efekta vērtību konkurences eksperimentā KIE = 1.12 (23. att., c)). Šāda vērtība, kā arī rezultāti, ko ieguvām H/D apmaiņas eksperimentos, liecina, ka C–H saites aktivēšanas solis katalītiskajā ciklā visticamāk ir apgriezenisks un nav reakcijas limitējošā stadija. Tālākos konkurences eksperimentos, kur pakļāvām reakcijas apstākļiem ekvimolāru daudzumu elektroniem bagāta un nabadzīga substrāta **26b** un **26s**, novērojām mazliet lielāku reaģētspēju elektroniem bagātākā substrātā, kas varētu liecināt, ka C–H saites aktivēšana notiek saskaņā ar S$_E$Ar mehānismu (25. att., d)).[14-16] Mums izdevās izdalīt Co(III) kompleksu **30** no reakcijas maisījuma līdzīgi kā C–H saites karbonilēšanas reakcijās. Kompleksam **30** reakcijā ar *t*BuNC degazētā MeCN novērojām imīnēšanas produkta **25a** veidošanos ar kvantitatīvu iznākumu (25. att., e)).

Balstoties uz veiktajiem mehānisma pētījuma eksperimentiem, piedāvātais katalītiskais cikls ir redzams 26. attēlā. Katalītiskais cikls tiek iniciēts Co(dpm)₂ katalizatoram koordinējoties pie substrāta **23**, veidojot kompleksu **A**. Sekojošā oksidēšanas solī tiek iegūts Co(III) komplekss **B**, kas tālāk C–H saites aktivēšanas solī dod kompleksu **C**. CO molekulai koordinējoties un migrējoši ievietojoties Co-C saitē, rodas iminoil-Co komplekss **D**, kas reducējošās eliminēšanas ceļā dod gala produktu **25a** un Co(I), kas tiek oksidēts un atgriezts katalītiskajā ciklā.
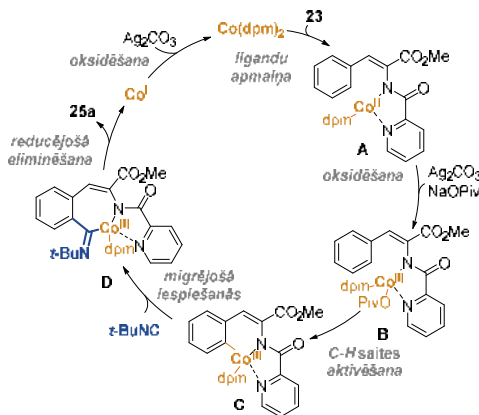
26. att. Piedāvātais cikls kobalta katalizētai nepiesātinātā fenilalanīnu **23** C–H saites imīnēšanai ar izocianīdiem

SECINĀJUMI

1. Kobalta-katalizētā fenilglicinolu C–H saites alkenilēšanas reakcijā ir iespējams iegūt dihidroizohinolīna atvasinājumus. C–H saites alkenilēšanai ir iespējams izmantot gan simetriskus, gan nesimetriskus iekšējos, kā arī terminālos alkīnus. Substrātā esošā hirālā informācija tiek pārnesta uz produktu bez enantiomērā pārākuma zuduma.
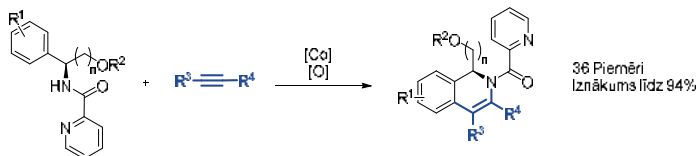
2. Izmantojot terminālos alkīnus kobalta-katalizētai fenilglicīnolu C–H saites alkenilēšanai, alkīna aizvietotājs vienmēr novietojas C(3) pozīcijā dihidroizohinolīna produktā, kas ir saskaņā ar literatūras datiem. Izmantojot nesimetriskus iekšējos alkīnus kobalta-katalizētai fenilglicīnolu C–H saites alkenilēšanai, lielākais alkīna aizvietotājs vienmēr novietojas C(3) pozīcijā dihidroizohinolīna produktā, savukārt mazākais – C(4) pozīcijā.
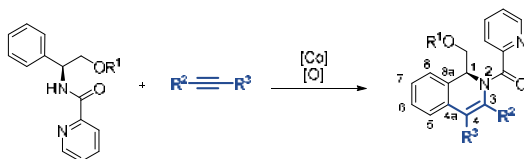
3. Kobalta-katalizētā fenilglicinolu C–H saites karbonilēšanas reakcijā ir iespējams iegūt izoindolīnona atvasinājumus. CO gāzes ģenerēšanai *in situ* ir iespējams izmantot diizopropilazodikarboksilātu (DIAD). Līdzīgi kā C–H saites alkenilēšanas gadījumā, hirālā informācija tiek saglabāta reakcijas gaitā. Pikolīnamīda virzošā grupa tiek nošķelta reakcijas apstākļos, pēc veiksmīgas C–H saites funkcionalizēšanas.
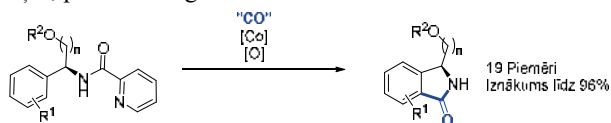
4. Kobalta-katalizētā fenilalanīna C–H saites karbonilēšanas reakcijā ir iespējams iegūt izohinlīnona atvasinājumus. Kobalta katalizatora un oksidētāja klātbūtnē reakcijas vidē vispirms veidojas nepiesātināts fenilalanīna intermediāts, kam seko C–H saites funkcionalizēšana un visbeidzot virzošās grupas nošķelšana *in situ*.
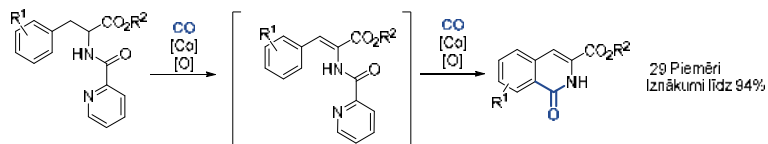
5. Kobalta-katalizētā nepiesātināta fenilalanīna C–H saites iminēšanas reakcijā ir iespējams iegūt izohinolīn-1(2H)-imīna atvasinājumus. Turklāt, C–H saites iminēšanas reakcijā iegūtajiem izohinlīn-1(2H)-imīna produktiem var viegli nošķelt virzošo grupu reducējošos apstākļos, lai iegūtu 1-aminoizohinolīna atvasinājumus.
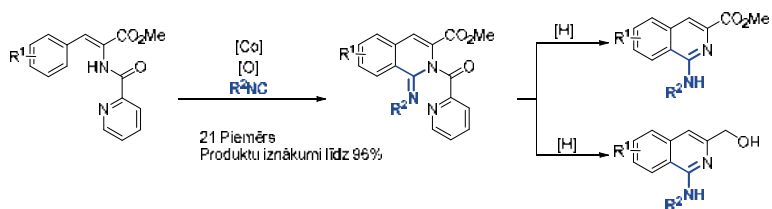
**DOCTORAL THESIS PROPOSED TO
RIGA TECHNICAL UNIVERSITY FOR THE PROMOTION
TO THE SCIENTIFIC DEGREE OF DOCTOR OF SCIENCES**

To be granted the scientific degree of Doctor of Sciences (*Ph.D.*), the present Doctoral Thesis has been submitted for the defence at the open meeting of RTU Promotion Council on July 7, 2022 at the Faculty of Materials Science and Applied Chemistry of Riga Technical University, 3 Paula Valdena Street, Room 272.

OFFICIAL REVIEWERS
Senior researcher, *Dr. chem.* Pāvels Arsenjans,
 Latvian Institute of Organic Synthesis, Latvia

Professor *Ph. D.* Olafs Daugulis,
 University of Houston, USA

Professor *Dr. Chem.* Edgars Sūna,
 University of Latvia, Latvia

DECLARATION OF ACADEMIC INTEGRITY

I hereby declare that the Doctoral Thesis submitted for the review to Riga Technical University for the promotion to the scientific degree of Doctor of Sciences (Ph. D.) is my own. I confirm that this Doctoral Thesis has not been submitted to any other university for the promotion to other scientific degree.

Lukass Tomass Lukasevics ……………………………. (signature)

Date…………………………….

The Doctoral Thesis has been prepared as thematically united collection of scientific publications. It consists of summary, 4 scientific publications, 3 reviews and 2 book chapters and a summary. Publications and book chapters have been written in English. The total number of pages is 743, including electronical data.

CONTENTS

GENERAL OVERVIEW OF THE THESIS

Introduction

Medicine, material science, agrochemistry and other chemistry-related sciences cannot be imagined without organic compounds. Therefore, the development of efficient and inexpensive methods for organic compounds is one of the preconditions for the successful development of these areas. C–H bond activation and functionalization is a relatively novel synthetic approach in organic synthesis. This approach allows installing functional groups into the molecule in a single step, therefore replacing previously employed time-consuming reaction sequences and avoiding the formation of unwanted by-products (Fig. 1).
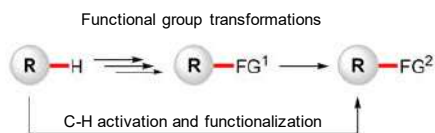
Fig. 1. C–H bond functionalization

The term "C–H activation" is often used in organometallic chemistry to describe the process in which the metal center binds to the C–H bond in the substrate, making it more reactive and transforming the substrate in the subsequent C–H functionalization step. Although C–H bonds are very common in the organic compounds, their chemical reactivity is low. By comparing the dissociation energies of the bonds ($C(sp^3)$-H = 105 kcal/mol, $C(sp^2)$-H = 110 kcal/mol, $C(sp^3)$-Cl = 83 kcal/mol, $C(sp^3)$-Br = 70 kcal/mol and $C(sp^3)$-I= 56 kcal/mol) it can be clearly seen that the activation and functionalization of the C–H bond is much more difficult compared to the C–Hal bonds traditionally used in transition metal catalyzed reactions.[1-6]

Precious metal catalysts are commonly used for the activation of C–H bonds, even though nowadays there is a growing demand for cheaper and more environmentally friendly catalysts, due to the strong emphasis on the basic principles of "green chemistry", which prefer sustainable, environmentally friendly and economical synthetic methodology.[7] Despite this, the main results in the field of C–H bond functionalization have been achieved using precious metals (Rh, Ru, Pd), which are rare, expensive, and toxic.[1-6] Only relatively recently 3d transition metals (Fe, Co, Ni) have witnessed the growth of interest among chemists and have been used in catalytic C–H bond functionalization reactions. One of such alternatives is cobalt which accounts for about 0.0029% of the Earth's crust in contrast to the palladium, which is traditionally used in chemical reactions, and is estimated to be a trillion parts of the Earth's crust mass. Only since 2010 has there been a very rapid growth in cobalt-catalyzed C–H functionalization methodology, therefore it can be considered as a one of the most promising alternative to precious metal catalysts.[1]

Cobalt catalyzed C–H bond functionalization reactions can be distinguished into two categories:

1. Low valent cobalt catalysis. Co catalysts in this category have an oxidation state of 0 or +1 and are obtained from Co(I) or Co(II) pre-catalysts under reductive conditions;

2. High-valent cobalt catalysis. Cobalt catalysts in this category have an oxidation state of +3 and are obtained from Co(III) or Co(II) pre-catalysts under in situ oxidative conditions. Since the discovery of cobalt-catalyzed C–H functionalization reactions, most of the transformations have been achieved using a low-valent cobalt catalysis approach. It was only between 2013 and 2014 that the use of high-valent Co(III) or precursor Co(II) catalysts began to emerge. In the following years, special attention was paid to cobalt-catalyzed C–H functionalization reactions, and the number of publications currently published in this field is close to five hundred. The methodology developed in the Doctoral Thesis is based on the high-valent cobalt catalysis approach, using Co(II) pre-catalyst in combination with bidentate directing group as a Co(III) precursor.

Despite that the cobalt-catalyzed C–H bond functionalization reactions by their nature being „greener" options than precious metal catalyzed counterparts, there are still some research directions which can make the process even more economically attractive and environmentally friendly. One of these directions is the directing group strategy.[6] The use of directing groups is an important precondition for regioselective transformation, as it enables to coordinate and direct the metal catalyst in close proximity of the target C–H bond. However, majority of the directing groups require additional installation step prior to the C–H functionalization followed by a cleavage step after the transformation, thus partially negating the benefits they provide. To overcome this problem, several types of directing groups have been introduced (Fig. 2.):

1. Traceless directing groups are introduced in the molecule before the C–H bond functionalization step, however are removed under the same reaction conditions after successful transformation. Thus far, a decent progress in this field has been achieved and many examples can be found in the literature exploiting a variety of directing groups. However, unfortunately, most of the reported transformations are limited to carbonylation and annulation reactions with alkynes, diynes and alkenes.[6]

2. Transient directing groups are installed and removed under the reaction conditions *in situ*. Such directing groups are relatively recent additions to the field of cobalt catalysis, therefore there are only two examples reported in the literature.[6]

3. Weakly directing groups are preexisting functional groups (carboxylic acids, esters, ketones, aldehydes, amides, etc.) in the molecule, that can coordinate to the metal catalyst. This directing group approach is seemingly the most attractive one, especially in late stages of the synthesis, although is the most challenging. For this reason, examples where weak directing groups have been exploited are rare.[6]
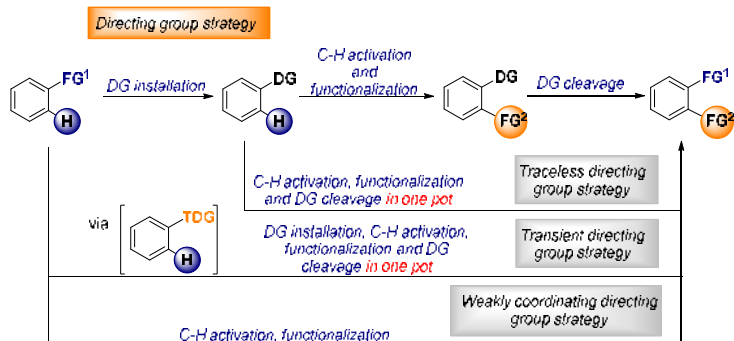
Fig. 2. The directing group strategy

Amino acid and amino alcohol fragments are frequently present in many pharmaceuticals as a part of peptidomimetics and protein building blocks. In addition, they are useful building blocks, which are widely used both in organic synthesis and asymmetric catalysis.[8] Development of novel amino alcohol and amino acid synthetic methodologies could potentially reduce the production cost of the pharmaceuticals that already exist in the market as well as introduce novel synthetic pathways. For these reasons, the Thesis is dedicated to the development of novel cobalt-catalyzed C–H bond functionalization methodologies using alkyne, CO, isocyanide reagents (Fig. 3.)
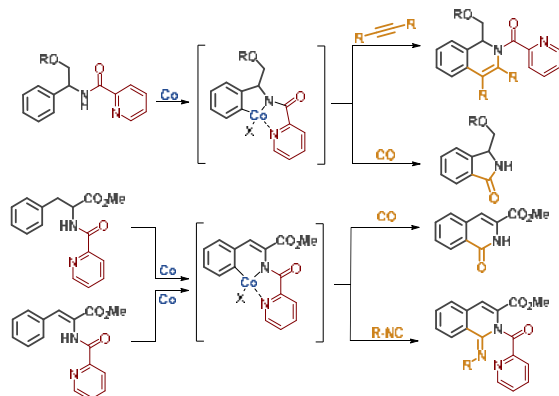
Fig. 3. Cobalt-catalyzed C–H bond functionalization of amino acid and amino alcohol derivatives

Aims and objectives

The aim of the thesis is to develop novel, efficient and practical methodology for cobalt-catalyzed C–H bond functionalization.

The following tasks were set:

1. Obtain amino acid and amino alcohol derivatives, which could be employed as substrates for C–H bond functionalization reaction. Phenylglycinol and phenylalanine as model substrates were chosen (Fig. 3.);

2. Explore the literature and select appropriate reagents that could be used for C–H bond functionalization reactions. Perform optimization of reaction conditions, investigate the substrate scope

Scientific novelty and main results

As a result of the thesis, 4 novel C–H bond functionalization methods of amino acid and amino alcohol derivatives were developed:

1. Cobalt catalyzed C–H bond alkenylation of phenylglycinol derivatives;

2. Cobalt catalyzed C–H bond carbonylation of phenylglycinol derivatives;

3. Cobalt catalyzed C–H bond carbonylation of phenylalanine derivatives;

4. Cobalt catalyzed C–H bond imination of phenylalanine derivatives

Structure of the thesis

The thesis is a collection of scientific publications on the cobalt-catalyzed C–H bond alkenylation, carbonylation and imination of phenylglycinol and phenylalanine derivatives as well as derivatization options of the obtained products.

Publications and approbation of the thesis

Main results of the Thesis were summarized in 4 scientific publications, 3 reviews and 2 book chapters. Results of the research were presented at three conferences.

<u>**Scientific publications:**</u>

1. Bolsakova, J.; <u>Lukasevics, L.</u>; Grigorjeva, L. Cobalt-Catalyzed, Directed C–H Functionalization/Annulation of Phenylglycinol Derivatives with Alkynes. *J. Org. Chem.* **2020**, 85, 6, 4482–4499. DOI:10.1021/acs.joc.0c00207

2. Lukasevics, L.; Cizikovs, A.; Grigorjeva, L. Synthesis of 3-Hydroxymethyl Isoindolinones via Cobalt-Catalyzed $C(sp^2)$–H Carbonylation of Phenylglycinol Derivatives. *Org. Lett.* 2020, *22* (7), 2720-2723. DOI:10.1021/acs.orglett.0c00672

3. Lukasevics, L.; Grigorjeva, L. Cobalt-catalyzed carbonylation of the C–H bond. *Org. Biomol. Chem.*, **2020**, 18, 7460-7466. DOI:10.1039/D0OB01633K

4. Lukasevics, L.; Cizikovs, A.; Grigorjeva, L. Cobalt-Catalyzed $C(sp^2)$–H Carbonylation of Amino Acids Using Picolinamide as a Traceless Directing Group. *Org. Lett.* **2021** 23 (7), 2748-2753. DOI:10.1021/acs.orglett.1c00660

5. Lukasevics, L.; Cizikovs, A.; Grigorjeva, L. C–H bond functionalization by high-valent cobalt catalysis: current progress, challenges and future perspectives. *Chem. Commun.*, 2021, **57**, 10827-10841. DOI:10.1039/D1CC04382J

6. Cizikovs, A.; Lukasevics, L.; Grigorjeva, L. Cobalt-catalyzed C–H bond functionalization using traceless directing group. *Tetrahedron* **2021**, *93*, 132307. DOI:10.1016/j.tet.2021.132307

7. Lukasevics, L.; Cizikovs, A.; Grigorjeva, L. Synthesis of 1-Aminoisoquinolines via Cobalt-Catalyzed $C(sp^2)$-H Bond Imination of Phenylalanine Derivatives. *Submitted manuscript.*

Book chapters:

1. Lukasevics, L.; Grigorjeva, L. Cobalt-Catalyzed Picolinamide-Directed Synthesis of Heterocycles *Targets Heterocycl. Syst. (book series)* **2021**, *25,* 144-161. DOI:10.17374/targets.2022.25.144

2. Lukasevics, L.; Grigorjeva, L. Mechanistic studies on cobalt-catalyzed, bidentate chelation-assisted C–H bond functionalization *Handbook of CH-Functionalization*. *Accepted for publication by Wiley-VCH GmbH.*

Results of the thesis were presented at the following conferences:

1. Lukasevics, L. Cobalt Catalyzed Tandem $C(sp^2)$-H/$C(sp^3)$-H Functionalization of Amino Acids with Alkenes. *11th Paul Walden Symposium on Organic Chemistry.* Riga, Latvia, 19-20 September **2019**.

2. Lukasevics, L. Cobalt catalyzed C–H bond functionalization. *12th Paul Walden Symposium on Organic Chemistry.* Online, 28-29 October **2021.**

3. Lukasevics, L. Cobalt catalyzed C–H bond functionalization. *6th International Conference on Catalysis and Chemical Engineering.* San Francisco, USA, 22-26. February **2022**.

MAIN RESULTS OF THE THESIS

1. Cobalt-catalyzed C–H bond alkenylation of phenylglycinol

The development of the C–H bond alkenylation methodology was chosen as the first direction of the research. For the initial experiments phenylglycinol **1** was chosen as the model substrate and *t*-butyl acetylene as the functionalization reagent. We envisioned that substrate **1** in the reaction with alkyne could form four potential products **2a-d**, however we observed the formation only of product **2a** (Fig. 4.). During the optimization of the reaction conditions, we arrived to the following catalytic system: Co(dpm)$_2$ catalyst, NaOPiv additive and Mn(OAc)$_3$·2H$_2$O/ O$_2$ oxidant system.
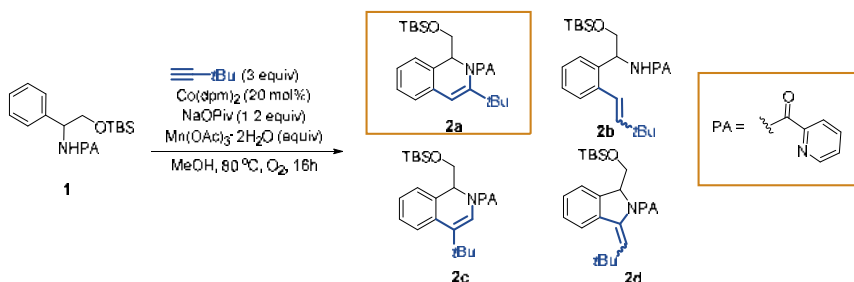
Fig. 4. C–H bond alkenylation of phenylglycinol **1**

First, we determined the benzylic substituent effects on the reaction yield (Fig. 5.). We found that *O*-unprotected amino alcohol **4a** is not compatible with the reaction conditions and the formation of the product was not observed, which potentially could be explained by deactivation of the catalyst caused by the excessive chelation of the free hydroxyl group to the cobalt catalyst. Substrates **2a**, **4b-e** bearing TBS, MOM and PMB protecting groups as well as methyl and phenyl group containing substrates **3e** and **3d** reacted well under the reaction conditions and gave products in good and very good yields – 70-88%.
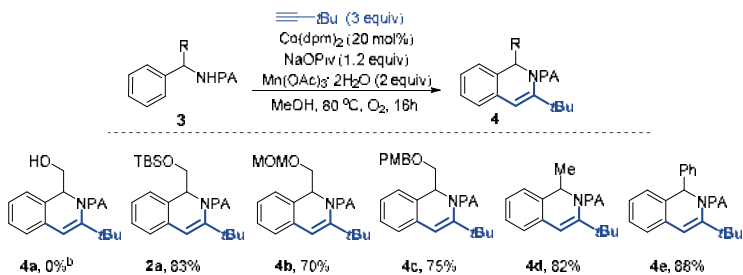
Fig. 5. Benzylic substituent scope in C–H bond alkenylation reaction

Next we examined the compatibility of phenylglycinol **1** scope for the optimized reaction conditions. We tested various substituents in the *ortho*-, *meta*- and *para*-positions of the benzene ring (Fig. 6). Interestingly, *meta*-substituted substrates delivered products as a single regioisomers, by reacting at the less sterically hindered C–H *ortho*-bond. We found that substrates bearing electron-donating substituents such as alkyl (product **5c,e**), methoxy (**5a,g**), and methoxymethyl **5h**, were well tolerated and furnished products in good and very good yields – 55–90 %. Similar reactivity we observed also in substrates bearing electron-withdrawing substituents, providing products **5d** and **5i** in 65% and 75% yields respectively. Halogen-substituted substrates were also compatible with the reaction conditions (products **5b,f,j**). Interestingly, phenylalaninol **1l**, and thiophene **1k** were also competent substrates for the C–H bond alkenylation, giving products **5k,l** in very good yields. It should be noted that in the case of thiophene **5k**, the reaction was not selective and the product was obtained as a mixture of regioisomers with the ratio of 2.1:1.
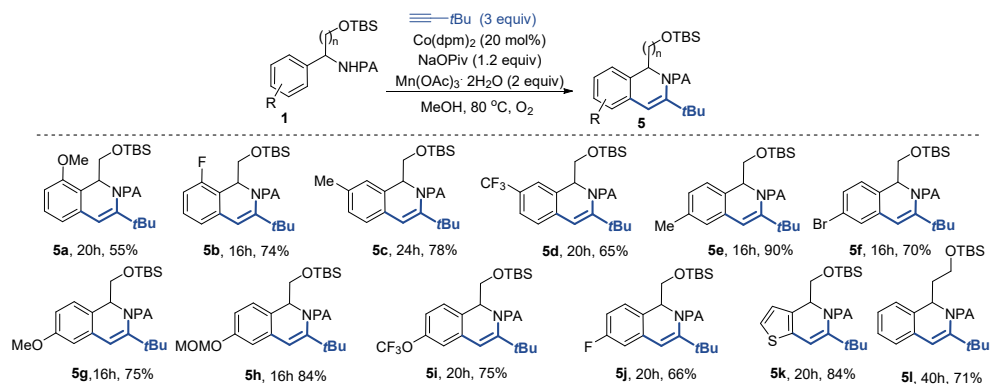
Fig. 6. The substrate scope in the C–H bond alkenylation reaction

Next step of the research involved the examination of alkyne scope for the C–H bond alkenylation of phenylglycinols **1** (Fig. 7.). For this purpose we selected symmetric and non-symmetric dialkyl, diaryl, as well as terminal alkynes. Symmetric dialkyl and diary acetylenes displayed good reactivity and gave products **6a-e** in very good yields – 70-80%. In case of terminal alkynes, we obtained products **6f-m** as single regioisomers in yields ranging from 65 to 88%. Interestingly, in the reaction of phenylglycinol **1** with 4-nitrophenylacetylene, we observed the formation not only of the C–H bond alkenylation product **6m**, but also the formation of dialkenylation product **6m'**. To show the utility of the developed method, we performed the reaction in 1g scale and obtained the product **6i** in a very good yield – 80%.
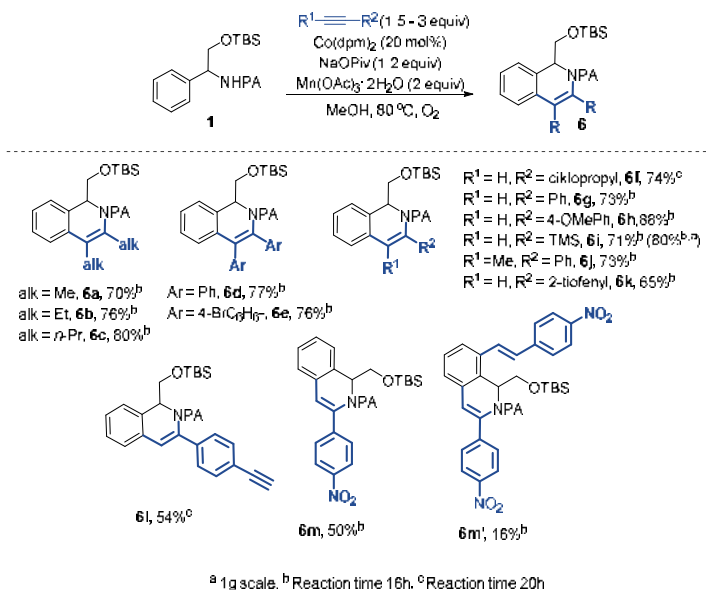
Fig. 7. Alkyne scope in the C–H bond alkenylation reaction

Additionally we wanted to test whether the chiral information of enantioenriched substrates can be preserved under the reaction conditions. For this reason we used substrate (*S*)-1 for the reaction with various aromatic, aliphatic, internal as well as terminal alkynes under the optimized reaction conditions. Gratifyingly, we found that in all of the cases, racemization of the chiral center did not occur and no erosion of enantiopurity was observed in the products (*S*)-2a, 6a,g,d,i (Fig. 6.).
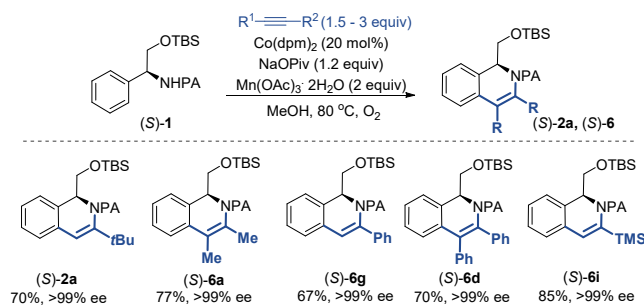
Fig. 8. Preservation of the chirality

We demonstrated that the picolinamide directing group can be cleaved in the products to obtain tetrahydroisoquinoline **8** derivatives (Fig. 9.) Initially, enantiopure substrate (*S*)-6i was

reduced under Birch reduction conditions in the presence of Na/NH$_3$ to afford product **7** with high diastereoselectivity (*d.r.* > 20:1). Subsequently, the picolinamide directing group was cleaved with LiAlH$_4$ to obtain tetrahydroisoquinoline **8** in very good yield with full preservation of initial enantiopurity (*ee* > 99%).
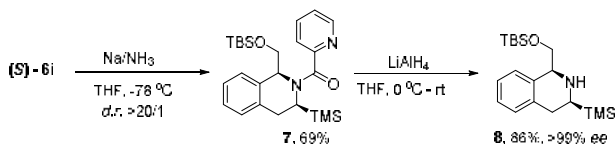
Fig. 9. Cleavage of the directing group

2. Cobalt-catalyzed C–H bond carbonylation of phenylglycinols

Moving forward with the development of the phenylglycinol **1** C–H bond functionalization methodology, we turned our attention to C–H bond carbonylation. Initially we employed the same catalytic system that had displayed good reactivity for the C–H bond alkenylation reactions. For the generation of the CO gas *in situ*, we used DIAD, which has been exploited for the similar purpose in the literature. We observed the formation of carbonylation product **9** in 10% NMR yield (Fig. 10.). Interestingly, the picolinamide directing group was cleaved under the reaction conditions after successful C–H bond carbonylation.
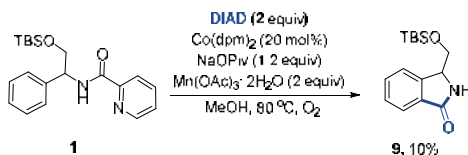
Fig. 10. C–H bond carbonylation of phenylglycinol **1**

During the optimization of the reaction conditions we found that the successful transformation required Co(dpm)$_2$ catalyst, PivOH additive, Ag$_2$CO$_3$ oxidant and DIAD as CO surrogate. First, we tested several alcohol protecting groups (Fig. 11.). Similarly as in the C–H bond alkenylation reactions, unprotected amino alcohol did not furnish the desired product **11a**. Even though PMB, MOM protecting groups were suitable for C–H bond carbonylation and afforded products **11b,c**, they were obtained in lower yields compared to product **9** with TBS protecting group.
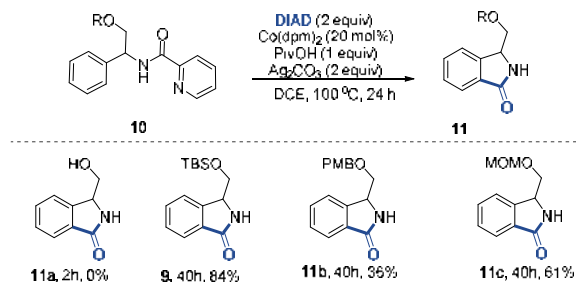
Fig. 11. Directing group scope for the C–H bond carbonylation

The substrate scope experiments showed that the reaction conditions are mild and compatible with various functional groups (Fig. 12.). Similarly to the C–H bond alkenylation reaction, *meta*-substituted substrates delivered only regioisomer, by reacting in the sterically hindered *ortho*-C–H bond. Both electron rich **12a**,**c**,**f-h** and electron poor substrates **12d**,**i** gave products in good and excellent yields – 66-96%. Similar result was also observed using halogen-substituted substrates, affording products **12b**,**e**,**j**,**k** in 75-91% yields. We demonstrated that thiophene amino alcohol was also competent substrate for the C–H carbonylation, however the reaction was not selective and the product **12l**,**l'** was obtained as a mixture of regioisomers in total yield of 67%. Bulkier substrate **12m** as well as quaternary substrate **12n** gave products in medium yield. However, in the case of both substrates **12m**,**n**, additional catalyst and oxidant loading was necessary after 24h.
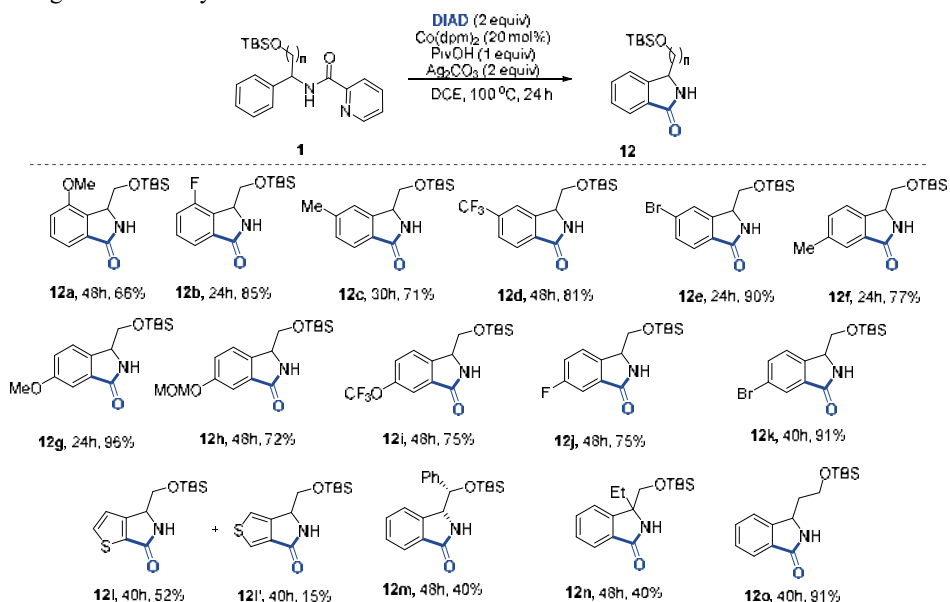
Fig. 12. Substrate scope for the C–H bond carbonylation of phenylglycinol **1**

We demonstrated that the original stereochemistry of substrate can be preserved under the reaction conditions during the C–H bond carbonylation by affording product **(S)-9** in high yield and >*99% ee* (Fig. 13.)
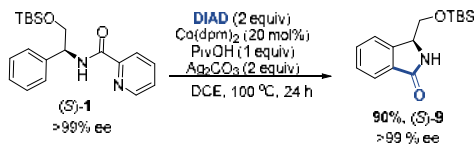
Fig. 13. Preservation of the stereochemistry in C–H bond carbonylation reaction

3. Cobalt-catalyzed C–H bond carbonylation of phenylalanine

As the next step of our study, we chose to transfer C–H bond carbonylation methodology to phenylalanine derivatives. We used phenylalanine **13** as the model substrate and picolinamide directing group that had displayed good results in our previous research. We were pleased to find that the employment the same reaction conditions, that were suitable for C–H bond carbonylation of phenylglycinols **1**, gave the desired carbonylation product **14**, albeit in low yield – 17% (Fig. 14.) Interestingly, besides C–H bond carbonylation, we also observed the formation of double bond between α and β carbons, and the cleavage of the picolinamide directing group *in situ*.
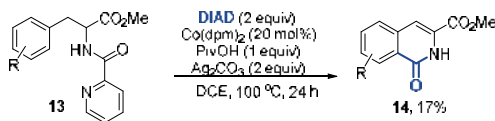
Fig. 14. Cobalt catalyzed C–H bond carbonylation of phenylalanine **13**

The reaction optimization study showed that the best results can be achieved by employing the following catalytic system: $Co(dpm)_2$ catalyst, PivOH additive and $Ag_2CO_3/Mn(OAc)_3 \cdot 2H_2O$ oxidant system in PhCl solvent at 120 °C under CO atmosphere (1atm). Initially, we tested the compatibility of several ester moieties with the reaction conditions (Fig. 15.). Methyl ester substrate **13** displayed good reactivity and provided product **14** in excellent yield – 94%. Upscaling the reaction to 1.7 mmol gave the product in 75% yield. Other ester substrates such as Et-, *t*Bu- and Bn-substituted substrates reacted similarly and gave products **16a-c** in very good yield – 70-83%. Although allyl substituted ester was competent substrate for C–H bond carbonylation, we obtained the corresponding product **16d** in acceptable yield – 50%.
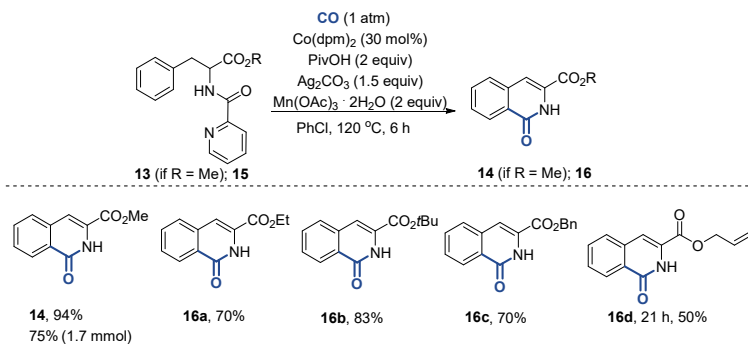
Fig. 15. Ester scope for the C–H bond carbonylation

Next, substrate scope study revealed that the C–H bond carbonylation reaction conditions can be applied for a wide range of phenylalanine **17** substrates with various substitution patterns in *ortho-*, *meta-* and *para-*positions of the benzene ring moiety (Fig. 16.). In case of *meta-*substituted substrates, we observed the formation of a single regioisomer. Several functionalities such as alkyl (products **18c,f**), halogen **18b,d,m,n**, trifluoromethyl **18h**, phenyl **18g**, ethyl ester **18p**, methoxy **18i**, MOM **18j** and *t*butylakynyl **18o** were compatible with the reaction conditions and gave corresponding products in good and very good yields. Less successful 4-OAc substituted substrate **18l** afforded product in 57% yield, which was a result of partial acetyl group cleavage under the reaction conditions. Naphthyl **18r,s** and thiophene amino acids **18t** were competent substrates and underwent C–H bond carbonylation to give products in very good and excellent yields. We were pleased to find that more challenging amide **18u**, which could potentially coordinate and deactivate the catalyst, also was reactive and delivered the product in 52% yield.
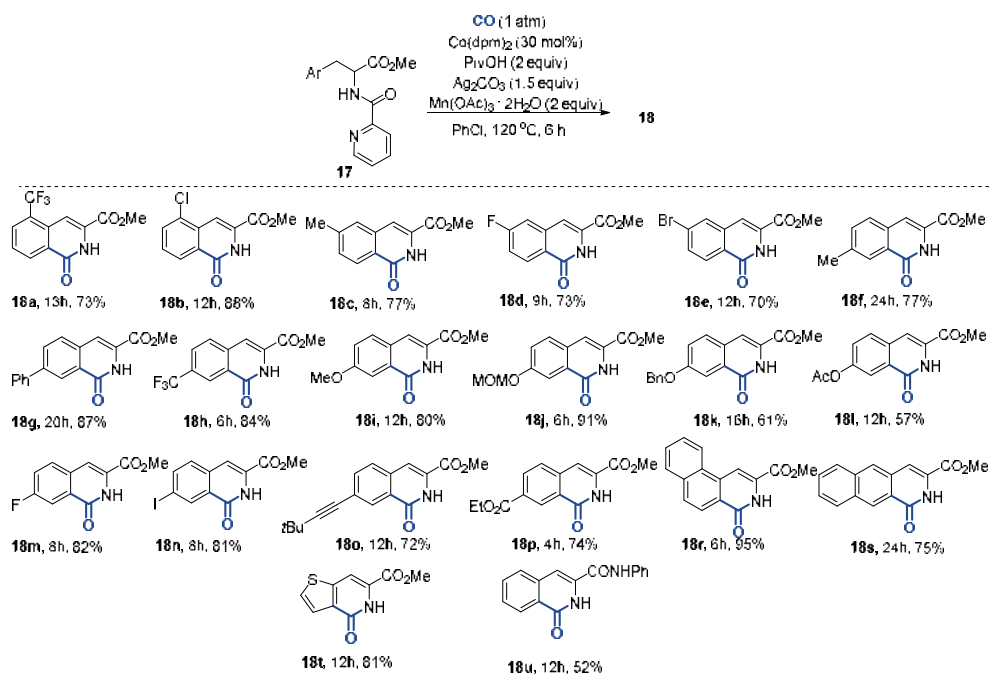
Fig. 16. Phenylalanine **17** scope for C–H bond carbonylation

During the substrate scope investigation, we found some limitations (Fig. 17.). First, benzoyl-protected phenylalanine **19a** was unreactive, which shows the important role of the directing group. Additionally, we did not observe formation of the product in case of homophenylalanine **19d**, homobenzylamide **19c** or quaternary **19b** substrates. Such a result indicates that the presence of ester moiety as well as the double bond is crucial for the successful transformation.
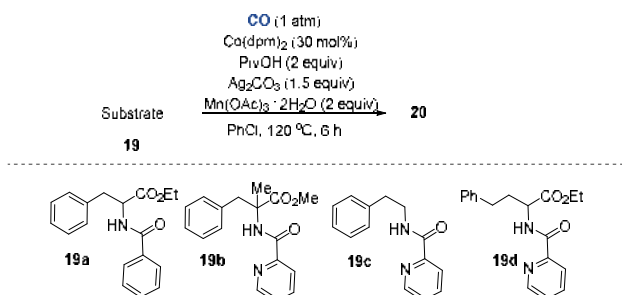
Fig. 17. Unsuccessful substrate for C–H bond carbonylation

It is known, that amide bonds within peptides can chelate metal ions and thereby deactivate the catalyst. For this reason we examined more challenging substrates for C–H bond carbonylation – short peptides. We selected several dipeptide **22a,-c** and tripeptide **22d** substrates, which initially we subjected to the developed reaction conditions. The formation of products, although with low yields due to the formation of undesired byproducts, was observed. We were able to overcome this problem by excluding $Mn(OAc)_3 \cdot 2H_2O$ oxidant from the catalytic system and increasing the loading of Ag_2CO_3 to 2.5 equivalents. We were pleased to find that under these reaction conditions C–H bond carbonylation products were obtained in acceptable and good yields (Fig. 18.). Unfortunately we observed partial racemization of the adjacent stereo centre in amino acids **22a** and **22b** obtaining products with 86% and 93% *ee,* respectively. Notably, in the carbonylation of enantiopure **21d**, partial racemization most likely occurred, but purification led to the isolation of the pure major diasteroisomer **22d** in 46% yield.
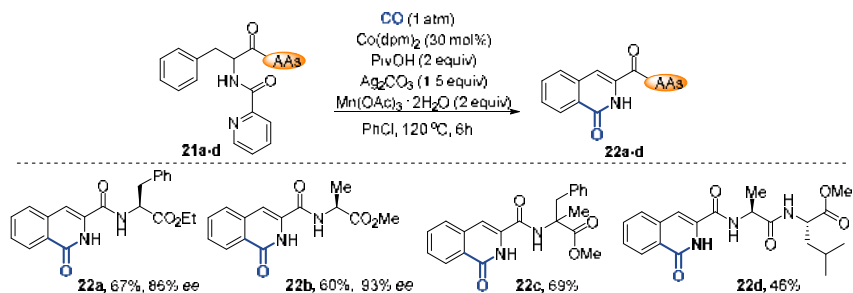
Fig.18. Late stage C–H bond carbonylation of peptides **21a-d**

To understand the reaction mechanism, we conducted several control experiments (Fig. 19.). We subjected the unsaturated phenylalanine derivative **23** to the standard reaction conditions and observed the formation of product **14** in 91% yield (Fig. 19., a)). Such a result suggests that **14** very likely is an intermediate of the catalytic cycle. Moreover, in the reaction mixture we detected both of the unsaturated intermediate **23** regioisomers by the UPLC-MS analysis. Interestingly, addition of one or three equivalents of radical scavenger TEMPO to the catalytic system resulted in significant suppression of the reactivity in substrate **13**, affording product in 36% and 7% yields, respectively. On the other hand, addition of radical scavenger TEMPO, did not significantly affect the reactivity of the unsaturated intermediate **23** (Fig. 19., b)). The obtained results indicate the SET reaction within the catalytic cycle that ensures the formation of the unsaturated intermediate **23**, before the C–H bond activation step. We were able to isolate and the Co(III) C–H bond activation complex **24** confirmed the structure by X-ray diffraction. Noteworthy, that Co(III) complex **24** under CO atmosphere at room temperature formed carbonylation product **25** in quantitative yield (Fig. 19., c)).
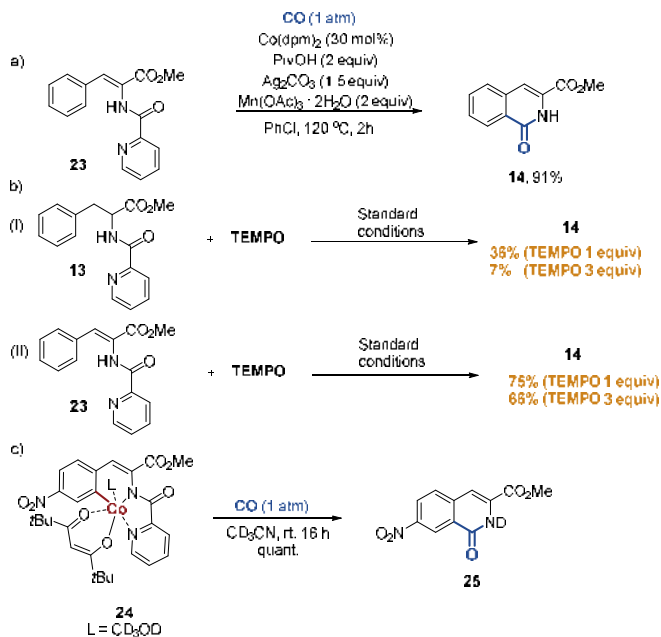
Fig. 19. Control experiments for the phenylalanine **13** C–H bond carbonylation

Based on the mechanistic experiments as well as literature precedents, the proposed catalytic cycle is depicted in the Fig. 20. Initially, under the reaction conditions phenylalanine **15** is oxidized to imine **23a** via SET mechanism. The imine **23a** is tautomerized to enamine **23**, which then coordinates to the Co(II) catalyst and in the subsequent oxidation step gives complex **A**. In the following C–H bond activation step, complex **B** is formed. Further oxidation of complex **B**, followed by coordination and migratory insertion of CO into Co-C bond yields Co(IV) intermediate **C'**, which reductively eliminates complex **D** (path a). According to the path b, CO coordination/migratory insertion would occur in the complex **B** first, followed by an oxidation of the resulting complex **C** to obtain **C'**. Alternative pathway c involves subsequent CO coordination/migratory insertion in the complex **B** directly followed by reductive elimination. The control experiment, in which Co(III) C–H bond activation complex **B** readily reacted with CO in the absence of external oxidant, suggests that in our case path c is dominant in C–H bond functionalization mechanism. Upon the hydrolysis of the complex **D**, final product **14** is liberated and Co(I) is reoxidized to Co(III) complex **E**, which we detected in all of the C–H bond carbonylation experiments by TLC analysis. Ligand exchange between **E** and enamine **23** restarts the catalytic cycle.
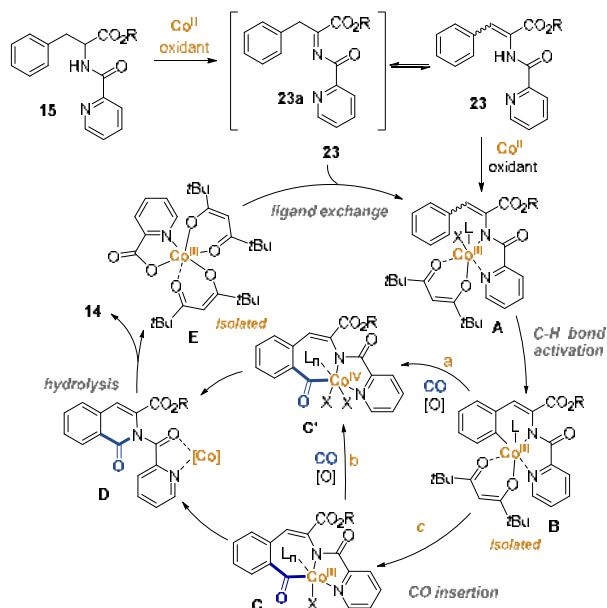
Fig. 20. The proposed mechansim for C–H bond carbonylation of phenylalanine **15**

4. Cobalt-catalyzed phenylalanine C–H bond imination

After successful development of novel C–H bond carbonylation method for phenylalanine **13**, we turned our attention to isocyanides as potential derivatization reagents. In the literature, cobalt-catalyzed C–H bond imination reactions are known, although amino acid derivatives have not been exploited as substrates in such reactions.[9-12] Initially we chose phenylalanine **13** as a model substrate and *t*butyl isocyanide as a C–H bond imination reagent. We subjected the model substrate **13** to the reaction conditions, which had proven to be effective in phenylalanine **13** C–H bond carbonylation and observed the formation of corresponding imine **25a** in 41% yield (Fig. 21.). The efforts to optimize the reaction conditions to obtain product in higher yield were not successful, which we attribute to the rapid decomposition of isocyanide. In the previous research where we reported C–H bond carbonylation of phenylalanine **13**, we demonstrated that in the first step of the catalytic cycle, unsaturated intermediate **23** was formed via SET mechanism. We speculate that *t*butyl isocyanide can participate in undesired side reactions with free radicals that arise in this step and thereby decompose.[13] To overcome this issue, we chose to use enamine **23** as the model substrate. We were pleased to find that *t*butyl isocyanide was much more stable under the reaction conditions and furnished the imination product **25a** in 71% yield.
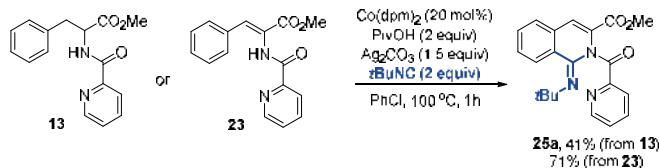
Fig. 21. C–H bond imination of phenyalanines **13,23** with *t*butyl isocyanide

To increase the product yield, we conducted optimization of the reaction conditions and found the final reaction conditions: Co(dpm)$_2$ catalyst, NaOPiv additive, Ag$_2$CO$_3$ oxidant, THF solvent. We tested the isocyanide scope for the C–H bond imination of model substrate **23** (Fig. 22.). Under the optimized reaction conditions, *t*butyl isocyanide gave imination product in very high yield – 86%. Furthermore, upscaling the reaction to 1.8 mmol did not significantly affect the product yield. Similarly, cyclohexyl, *n*-pentyl, and phenylethyl-substituted isocyanides were compatible with the reaction conditions and furnished the products **25b-d** in very good and excellent yields – 79-95%.
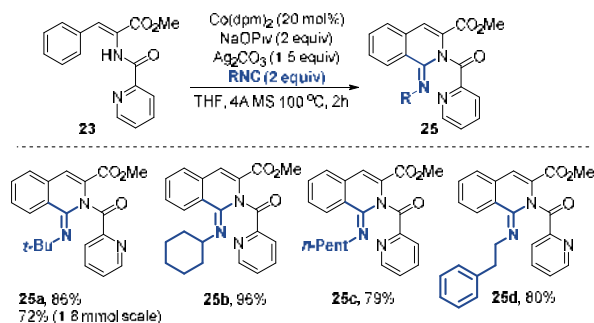
Fig. 22. The isocyanide scope for C–H bond imination of phenylalanines **23**

Next, we examined the substrate **26** scope with various substitution patterns in *ortho*-, *meta*-, *para*-positions of the benzene ring moiety (Fig. 23.) Electron donating Me-, OMe-, OAc- and Ar- groups displayed good compatibility with the reaction conditions and provided the corresponding products **27a-d,f** in good to excellent yields -74-96%. Interestingly, in case of 4-OAc substituted substrate **26e**, we not only observed the C–H bond imination, but also transacylation to obtain 4-OPiv product **27e**. Both BocNH- as well as PhthN- *meta*-substituted substrates **27g,h** were reactive and gave products in 84% and 83% yields. It should be noted that also in this case, *meta*-substituted substrates provided reaction products as single regioisomers. Various halogen substituents in substrates were well tolerated under the reaction conditions and provided products **27i-l** in 61-65% yields. Additionally, we found that different aromatic systems can be functionalized by employing our method. It was well demonstrated by thiophenyl and furanyl alanines, which under the reaction conditions gave imines **27o,p** in 64% and 67% yields.
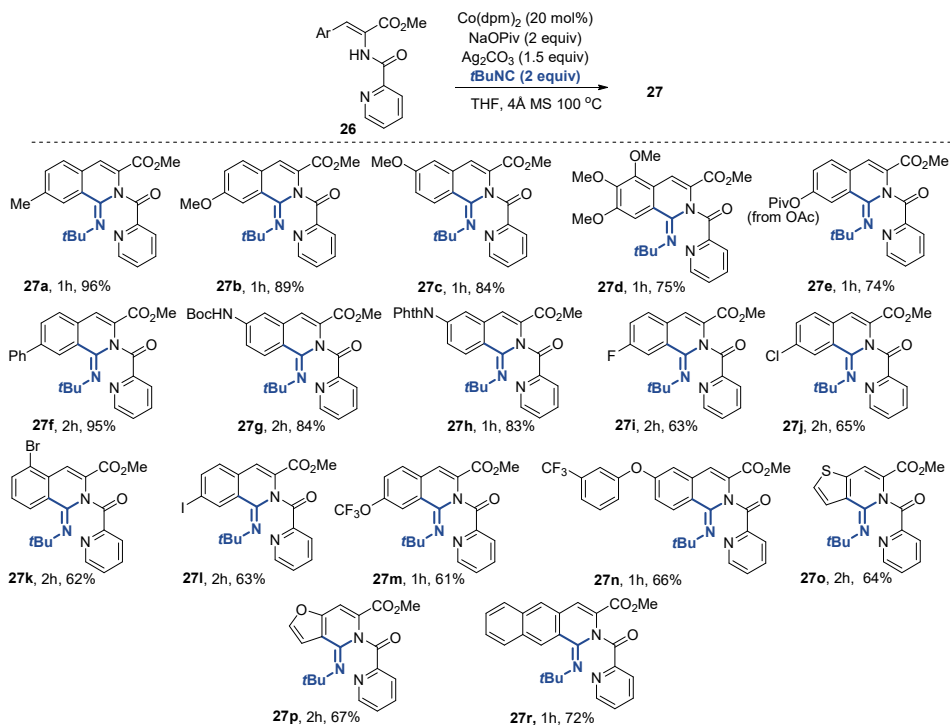
Fig. 23. Unsaturated phenylalanine **26** scope for the C–H bond imination reaction

To demonstrate the utility of the developed method, the obtained imine **25a** products were employed for the synthesis of 1-aminoisoquinolines **28a**,**b** (Fig. 24). We found that the picolinamide directing group can be cleaved under reductive conditions in the presence of LiAlH$_4$ to obtain 1-aminoisoquinoline **28a** in 93% yield, although with complete reduction of ester moiety. Alternatively, methyl ester **28b** was obtained in 67% yield when Zn/AcOH mixture was used.
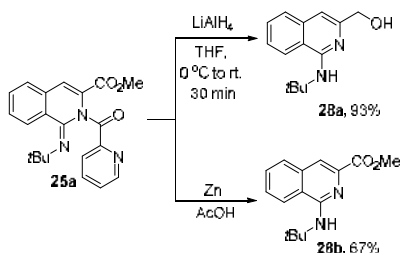
Figure. 24. Synthesis of 1-aminoisoquinolines **28a,b**

In order to better understand the reaction mechanism, we conducted several control experiments (Fig. 25.).
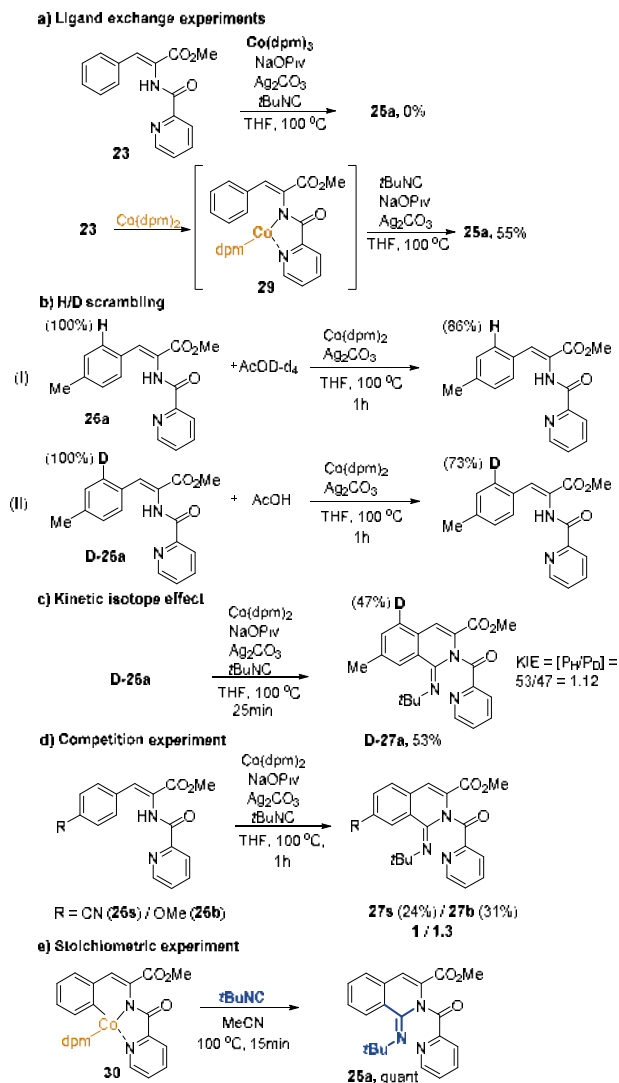
Fig. 25. Mechanistic control experiments for the C–H bond imination of phenylalanines **23**

We found that the first step of the catalytic cycle is the coordination of the catalyst to the substrate **23** and not the oxidation of Co(II) to Co(III). It was well demonstrated by the ligand

exchange experiment, in which model substrate **23** under the standard reaction conditions was to unreactive if Co(dpm)$_2$ catalyst was substituted to Co(dpm)$_3$ (Fig. 25., a)). Additionally, in the stoichiometric experiments Co(II)-substrate complex **29** was subjected to the reaction conditions and imination product **25a** was obtained in 55% yield (Fig. 25., a)). Next, we performed H/D scrambling experiments. By employing AcOD-d$_4$ as a co-solvent under the reaction conditions, we observed 14% of deuterium incorporation in the *ortho*-position of the substrate **26a**. Similar result was observed by employing deuterium-labeled substrate **D-26a** and AcOH co-solvent (Fig. 25., b)). Additionally, we determined the kinetic isotope effect in a competition experiment to be KIE = 1.12 (Fig. 25., c)). Such a value in combination with the observations in H/D scrambling experiments indicates that most likely C–H bond activation step within the catalytic cycle is reversible and not rate determining step. In the competition experiments, where equimolar loading of electron-rich **26b** and electron-poor substrates **26s** were subjected to the reaction conditions, we observed a slightly better reactivity in electron-rich substrates, which suggests that the C–H bond activation step might occur via S$_E$Ar mechanism (Fig. 25., d)).[14-16] We were successful in isolation of Co(III) C–H bond activation complex **30** from the reaction mixture. Reacting the complex **30** with *t*BuNC in the degassed THF led to the formation of imination product **25a** in quantitative yield (Fig. 25., e)).

Based on the control experiments and literature precedents, the proposed catalytic cycle is depicted in the Fig. 26. The catalytic cycle is initiated by the coordination of the catalyst to the substrate **23** to form complex **A**. In the subsequent oxidation step Co(III) complex **B** is obtained, which further undergoes C–H bond activation to furnish complex **C**. Next, CO molecule is coordinated and migratory inserted in the Co-C bond, giving iminoyl-Co complex **D**, which upon reductive elimination yields the product **25a** and Co(I) that is oxidized and returned to the catalytic cycle.
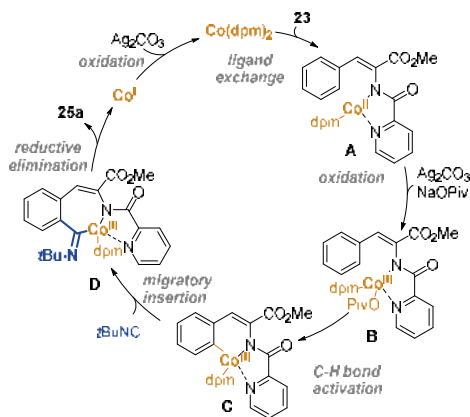
Figure 26. The proposed catalytic cycle for the C–H bond imination

CONCLUSIONS

1. Cobalt-catalyzed phenylglycinol C–H bond alkenylation can be used to obtain dihydroisoquinoline derivatives. Both symmetric and non-symmetric internal as well as terminal alkynes for the C–H bond alkenylation can be employed. The chiral information is preserved during the reaction without erosion of enantiopurity.
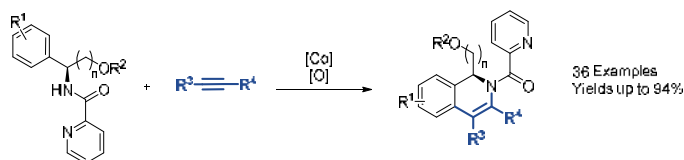
2. If terminal alkynes are used for the cobalt-catalyzed C–H bond alkenylation, alkyne substituent is always positioned in the C(3) position of the dihydroisoquinoline product, which is in the accordance with literature. If non-symmetrical internal alkynes are used for the cobalt-catalyzed C–H bond alkenylation, the largest of the alkyne substituents is always positioned in the C(3) position of the dihydroisoquinoline product, however the smallest – in the C(4) position.
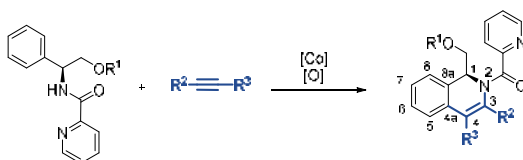
3. Cobalt-catalyzed phenylglycinol C–H bond carbonylation can be used to obtain isoindolinone derivatives. Diisopropylazodicarboxylate (DIAD) can be employed for the generation of CO gas *in situ*. Similarly as in the C–H bond alkenylation reaction, chiral information in the substrate can be preserved under the reaction conditions. Picolinamide directing group is cleaved under the reaction conditions after successful C–H bond functionalization step.
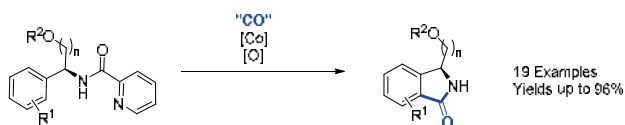
4. Cobalt-catalyzed phenylalanine C–H bond carbonylation can be used to obtain isoquinolinone derivatives. Under the reaction conditions, substrate is firstly transformed into unsaturated phenylalanine derivative in the presence of the cobalt catalyst and oxidant, followed by the C–H bond functionalization and finally cleavage of the directing group *in situ*.
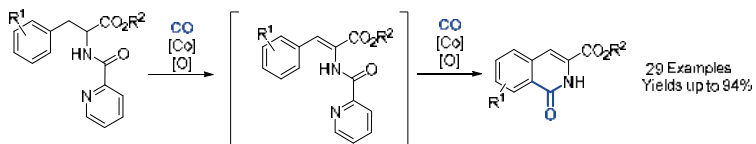
5. Cobalt-catalyzed unsaturated phenylalanine derivative C–H bond carbonylation can be used to obtain isoquinolinyl-1(2H)-imine derivatives. Additionally, isoquinolinyl-1(2H)-imine products obtained in the C–H bond imination reaction can be used for the synthesis of 1-aminoisoquinoline derivatives via cleavage of the directing group under reductive conditions.
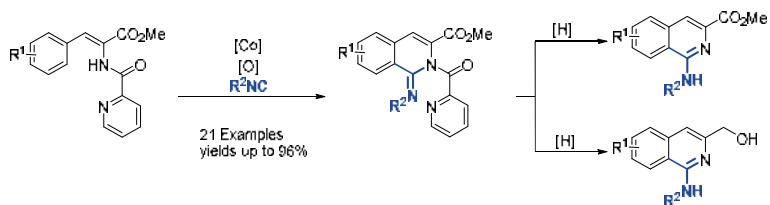
ATSAUCES/REFERENCES

1. Gandeepan, P.; Müller, T.; Zell, D.; Cera,G.; Warratz, S.; Ackermann, L. Chem. Rev. **2019**, *119*, 2192-2452.
2. Moselage, M.; Li, J.; Ackermann, L. *ACS Catal*. **2016**, *6*, 498-525.
3. Kommagalla, Y.; Chatani, N. *Coord. Chem. Rev.* **2017**, *350*, 117-135.
4. Daugulis, O.; Roane, J.; Tran, L. D. *Acc. Chem. Res.* **2015**, *48*, 1053-1064.
5. Hyster, T. K. *Catal. Lett*. **2015**, *145*, 458-467.
6. Lukasevics, L.; Cizikovs, A.; Grigorjeva, L. *Chem. Commun.* **2021**, *57*, 10827-10841.
7. Dalton, T.; Faber, T.; Glorius, F. *ACS Cent. Sci.* **2021**, *7*, 2, 245–261.
8. T. Brandhofer, O. García Mancheño, *European J. Org. Chem.* **2018**, *2018*, 6050–6067.
9. Tian, C.; Massignan, L.; Meyer, T. H.; Ackermann, L. *Angew. Chem., Int. Ed.* **2018**, *57* (9), 2383-2387.
10. Mei, R; Sauermann, N.; Oliveira, J. C. A.; Ackermann, L. *J. Am. Chem. Soc*. **2018**, *140*, 7913-7921.
11. Zell, D.; Bursch, M.; Müller, V.; Grimme, S.; Ackermann, L. *Angew. Chem., Int. Ed*. **2017**, *56* (35), 10378-10382.
12. Zhu, T. H.; Wang, S. Y.; Tao, Y. Q.; Wei, T. Q.; Ji, S. J. *Org. Lett.* **2014**, *16* (4), 1260-1263.
13. Nelson, D. E.; Li, R.; Kenttämaa, H. I. *Int. J. Mass Spectrom*. **1999**, *185*, 91-96.
14. Tian, C.; Massignan, L.; Meyer, T. H.; Ackermann, L. *Angew. Chem., Int. Ed.* **2018**, 57 (9), 2383-2387.
15. Mei, R; Sauermann, N.; Oliveira, J. C. A.; Ackermann, L. *J. Am. Chem. Soc*. **2018**, *140*, 7913-7921.
16. Zell, D.; Bursch, M.; Müller, V.; Grimme, S.; Ackermann, L. *Angew. Chem., Int. Ed*. **2017**, 56 (35), 10378-10382.

PIELIKUMI/PUBLICATIONS

Bolsakova, J.; <u>Lukasevics, L.</u>; Grigorjeva, L. Cobalt-Catalyzed, Directed C–H Functionalization/Annulation of Phenylglycinol Derivatives with Alkynes. *J. Org. Chem.* **2020**, 85, 6, 4482–4499.

Cobalt-Catalyzed, Directed C−H Functionalization/Annulation of Phenylglycinol Derivatives with Alkynes

Jekaterina Bolsakova, Lukass Lukasevics, and Liene Grigorjeva*

Read Online

ACCESS | Metrics & More | Article Recommendations | Supporting Information
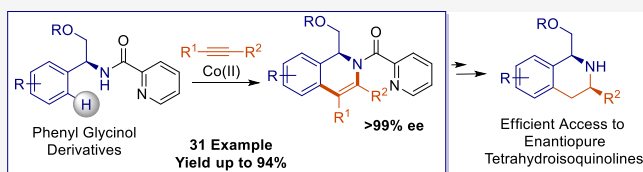
ABSTRACT: A new method for cobalt-catalyzed C(sp²)−H functionalization of phenylglycinol derivatives with terminal and internal alkynes directed by picolinamide auxiliary has been developed. This method offers an efficient and highly regioselective route for the synthesis of 1-hydroxymethyltetrahydroisoquinolines. The reaction employs commercially available Co(II) catalyst in the presence of Mn(III) cooxidant and oxygen as a terminal oxidant and proceeds with full preservation of original stereochemistry.

■ INTRODUCTION

Transition metal-catalyzed C−H bond functionalization during the past decades has become an important tool that allows simplification of synthetic schemes and allows the use of less complex starting materials.[1] In the past few years, C−H functionalization using 3d-transition metals has emerged as an attractive alternative to noble metals.[2a] Because of its earth-abundance, lower toxicity, and unique catalytic activity, cobalt has stood out as one of the promising alternatives.[2] In 2014, Daugulis group demonstrated that simple Co(II) salts in combination with bidentate directing group assistance can be efficiently exploited for C−H functionalization as high-valent cobalt(III) precursors.[3] Since the discovery, a large number of other C−H functionalization reactions based on this approach have been reported showing the potential of this methodology starting from readily available Co(II) salts and co-oxidants (e.g., C−H functionalization with alkynes,[4a−c] alkenes,[4d−f] allenes,[4g,h] isonitriles,[4i] carbonylation,[4j−f] etc.).[4]

There is no literature precedent for the Co-catalyzed C−H functionalization of phenylglycinol derivatives. However, several studies have been devoted to benzylamine derivatives. In 2014, Daugulis group demonstrated the first example of the cobalt(II)-catalyzed 1-methylbenzylamine-derived picolinamide reaction with 2-butyne yielding a cyclized product in moderate yields (Scheme 1A).[3] In 2017, Carretero group published an extended study and improved methodology for cobalt-catalyzed, picolinamide-directed C−H functionalization/alkyne annulation of benzylamine derivatives (Scheme 1B).[5a] In the same year, Cui group demonstrated the cobalt-catalyzed annulation of benzylamides with alkynes to synthesize isoquinolines by using picolinamide as a traceless directing group (Scheme 1C).[5b] Despite the significant

Scheme 1. Cobalt(II)-Catalyzed C−H Functionalization with Alkynes
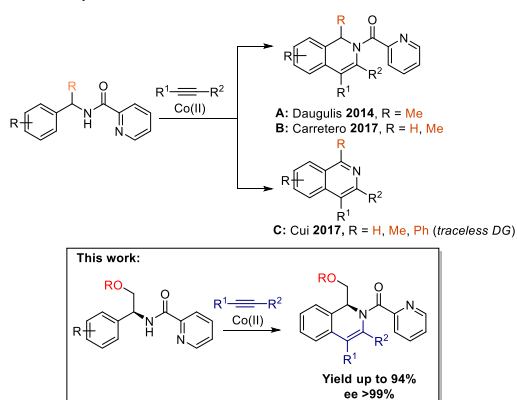
progress made in picolinamide-directed benzylamide alkynylation and annulation, the methodology developed so far unfortunately lack the substituent diversity at the benzylamine benzylic position (Scheme 1).[6] Typically only methyl
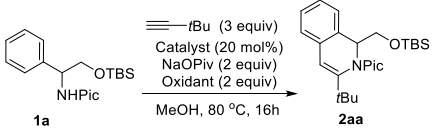
substituted or nonsubstituted benzylamine derivatives were exploited that may limit the use of developed methodology in total synthesis or synthesis of pharmaceutically relevant targets.

1-Substituted tetrahydroisoquinoline is a structural backbone of a large number of alkaloids that commonly possess a broad range of biological activity.[7] 1-Substituted 1,2-dihydroisoquinoline derivatives are especially valuable as intermediates in the synthesis of alkaloid natural products that has led to increasing interest for their synthesis.[8] Herein, we report an efficient method for the synthesis of 1-hydroxymethyl-1,2-dihydroisoquinolines via cobalt-catalyzed C—H annulation of phenylglycinol derivatives using terminal and internal alkynes.

■ RESULTS AND DISCUSSION

For optimization studies, the model reaction between phenylglycinol derivative **1a** and 3,3-dimethyl-1-butyne was chosen. During the optimization studies, a range of cobalt catalysts, oxidants, base additives, and reaction solvents were evaluated. Treatment of **1a** with 3,3-dimethyl-1-butyne in the presence of $Co(OAc)_2$ catalyst, NaOPiv base, and AgOAc oxidant in MeOH at 80 °C led to the regioselective formation of **2aa** in 5% yield (Table 1, entry 1).[9] Screening of alternative oxidants

Table 1. Optimization of Reaction Conditions[a]

entry	Catalyst	oxidant	yield, %[b]
1	$Co(OAc)_2$	AgOAc	5
2	$Co(OAc)_2$	MnO_2	4
3	$Co(OAc)_2$	$Mn(OAc)_2 \cdot 4H_2O$	5
4	$Co(OAc)_2$	$Mn(OAc)_3 \cdot 2H_2O$	12
5	$Co(OAc)_2$	$Mn(OAc)_3 \cdot 2H_2O/O_2$	16
6	$Co(OAc)_2$	under air	0
7[c]	$Co(OAc)_2$	$Mn(OAc)_3 \cdot 2H_2O/O_2$	28
8[c,d]	$Co(OAc)_2$	$Mn(OAc)_3 \cdot 2H_2O/O_2$	1
9[c,e]	$Co(OAc)_2$	$Mn(OAc)_3 \cdot 2H_2O/O_2$	13
10[c]	$CoCl_2$	$Mn(OAc)_3 \cdot 2H_2O/O_2$	trace
11[c]	$Co(acac)_2$	$Mn(OAc)_3 \cdot 2H_2O/O_2$	30
12[c]	$Co(dpm)_2$	$Mn(OAc)_3 \cdot 2H_2O/O_2$	82
13[c,f]	**$Co(dpm)_2$**	**$Mn(OAc)_3 \cdot 2H_2O/O_2$**	**84**
14	w/o $Co(dpm)_2$	$Mn(OAc)_3 \cdot 2H_2O/O_2$	0

[a]Reaction conditions: **1a** (0.1 mmol), 3,3-dimethyl-1-butyne (0.3 mmol, 3 equiv), catalyst (0.02 mmol, 20 mol %), NaOPiv (0.2 mmol, 2 equiv), $Mn(OAc)_3 \cdot 2H_2O$ (0.2 mmol, 2 equiv), MeOH (1 mL), 80 °C. [b]NMR yield using triphenylmethane as an internal standard. [c]NaOPiv (0.12 mmol, 1.2 equiv). [d]Solvent: EtOH (1 mL). [e]Solvent: CF_3CH_2OH (1 mL). [f]Time: 24 h. Pic—picolinyl. $Co(dpm)_2$—bis(2,2,6,6-tetramethyl-3,5-heptanedionato)cobalt(II), CAS: 13986-53-3.

(entries 2−5) showed that product **2aa** yield can be slightly improved by using of $Mn(OAc)_3 \cdot 2H_2O$ in combination with oxygen (entry 5). Reducing the amount of NaOPiv enhanced the product **2aa** yield to 28% (entry 7). The results in entries 8 and 9 indicated that MeOH is the solvent of choice. Studies using alternative Co(II) and Co(III) salts (entries 10−13) identified the $Co(dpm)_2$ catalyst as the crucial factor for the

successful reaction, yielding product **2aa** in 84% yield as a single regioisomer (entry13). Control experiments excluding catalyst (entry 14) and oxidant (entry 6) showed no product **2aa** formation.

With the optimized conditions in hand, we next examined the substrate scope with respect to picolinamides **1** (Scheme 2). We found that O-unprotected phenylglycinol picolinamide

Scheme 2. Reaction Scope with Respect to Picolinamides 1[a]
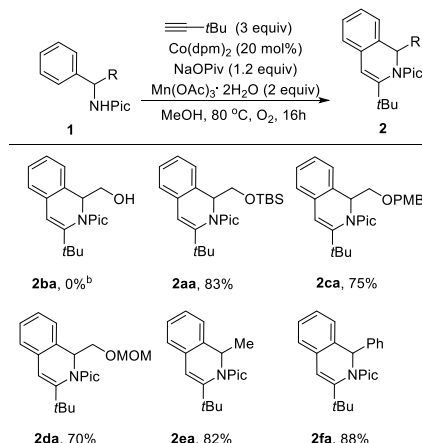
[a]Reaction conditions: **1** (0.5 mmol), 3,3-dimethyl-1-butyne (1.5 mmol, 3 equiv), $Co(dpm)_2$ (0.1 mmol, 20 mol %), NaOPiv (0.6 mmol, 1.2 equiv), $Mn(OAc)_3 \cdot 2H_2O$ (1.0 mmol, 2 equiv), MeOH (5 mL), O_2, 80 °C; Isolated yields are given. [b]Decomposition of substrate **1b**.

1b completely decomposed under the reaction conditions, and product **2ba** did not form. TBS, PMB, and MOM-protected phenylglycinol derivatives gave corresponding products (**2aa**, **2ca**, and **2da**, respectively) in very good yields (70−83%) as single regioisomers (regiochemistry of products was confirmed by 2D-NOESY experiments, see Supporting Information for details). We were pleased to find that under optimized reaction conditions, benzamide derivatives gave products in excellent yields (**2ea** and **2fa**) as well.

Subsequently, the scope of phenylglycinol derivatives **1** with diverse functional groups was examined under the optimized conditions (Scheme 3). As shown in Scheme 3, we found that reactions were successful on phenylglycinol derivatives **1** with para-, meta-, and ortho-substitution patterns. Using meta-substituted substrates (**1ia** and **1ja**), we observed that the reaction favors less hindered C—H bonds, yielding products in excellent regioselectivity that is consistent with literature examples.[3,5a]

Different functional groups on phenylglycinol derivatives **1** were tolerated, including electron-donating groups, such as alkyl (products **2ia** and **2ka**), methoxy (products **2ga** and **2la**), and methoxymethyl ether (product **2ma**), and electron-withdrawing groups, such as trifluoromethyl (product **2ja**) and trifluoromethoxy group (product **2na**). Fluoro and bromo functionalities are compatible with reaction conditions (products **2ha**, **2oa**, and **2pa**). β-Phenylalaninol derivative **1r** was also a competent substrate and gave corresponding product **2ra** in very good yield. Moreover, the reaction worked

Scheme 3. Reaction Scope with Respect to Phenylglycinol Derivatives 1[a]

2ga, 55%[c]   **2ha**, 74%[b]   **2ia**, 78%[d]   **2ja**, 65%[c]   **2ka**, 90%[b]   **2la**, 75%[b]

2ma, 84%[b]   **2na**, 75%[c]   **2oa**, 66%[d]   **2pa**, 70%[b]   **2qa**, 84%[c,f]   **2ra**, 71%[e]

[a]Reaction conditions: **1** (0.5 mmol), 3,3-dimethyl-1-butyne (1.5 mmol, 3 equiv), Co(dpm)$_2$ (0.1 mmol, 20 mol %), NaOPiv (0.6 mmol, 1.2 equiv), Mn(OAc)$_3$·2H$_2$O (1.0 mmol, 2 equiv), MeOH (5 mL), O$_2$, 80 °C; isolated yields are given; all products were isolated as single regioisomers unless stated. [b]Time: 16−17 h. [c]Time: 20 h. [d]Time: 24 h. [e]Time: 40 h. [f]Isolated as 2.5:1 mixture of thiophene regioisomers, major product shown.

Scheme 4. Reaction Scope with Respect to Alkynes[a]

2ab, 73%[c]   **2ac**, 70%[b]   **2ad**, 76%[b]   **2ae**, 80%[b]   **2af**, 73%[b,d]   **2ag**, 88%[b,d]

2ah, 50%[b]   **2ah'**, 16%[b]   **2ai**, 54%[c]   **2aj**, 65%[b,d]   **2ak**, 77%[b]

2al, 76%[b]   **2am**, 73%[b,d]   **2an**, 71%[b,d] 80%[e]

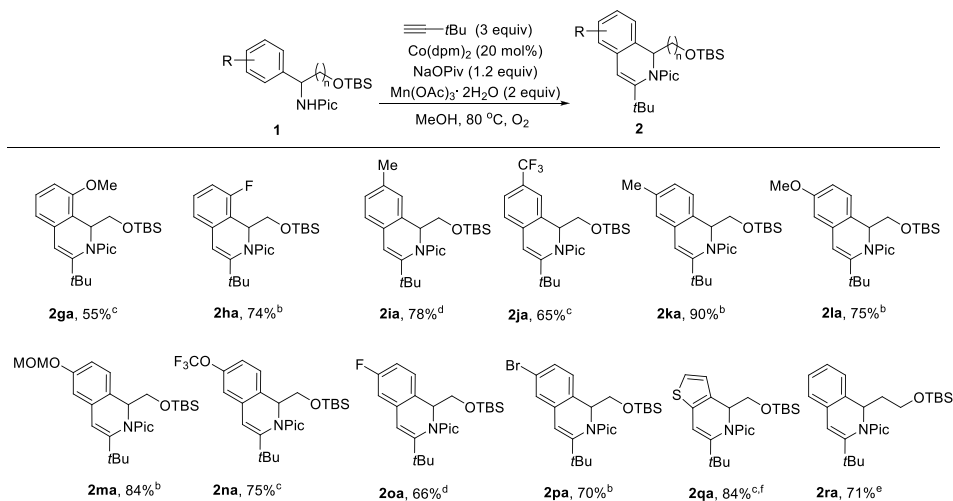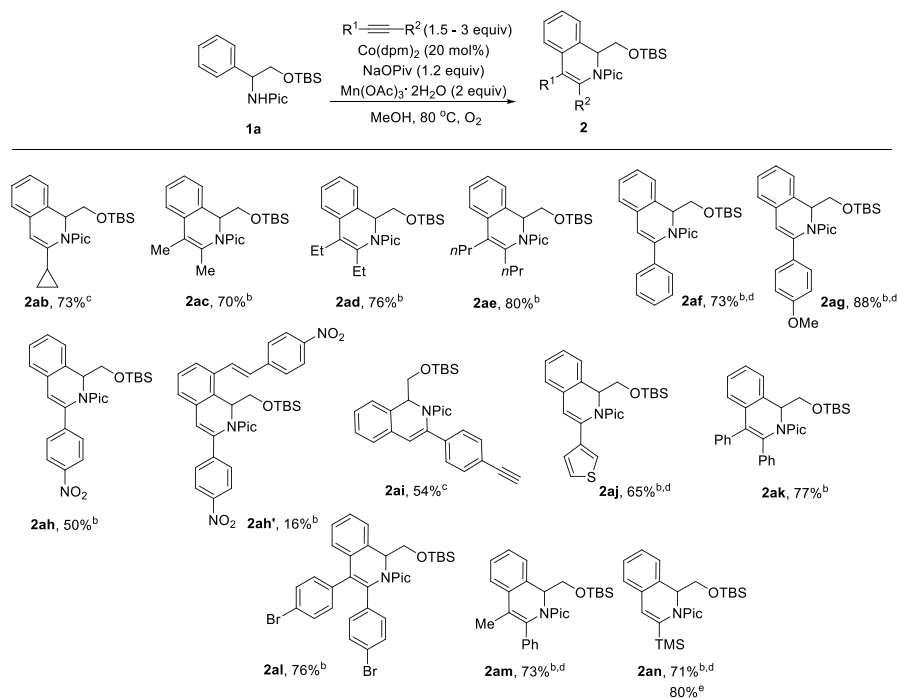[a]Reaction conditions: **1a** (0.5 mmol), alkyne (0.75−1.5 mmol, 1.5−3 equiv), Co(dpm)$_2$ (0.1 mmol, 20 mol %), NaOPiv (0.6 mmol, 1.2 equiv), Mn(OAc)$_3$·2H$_2$O (1.0 mmol, 2 equiv), MeOH (5 mL), O$_2$, 80 °C; isolated yields are given. [b]Time: 16−17 h. [c]Time: 20 h. [d]Isolated as a single regioisomer. [e]Gram-scale synthesis, starting from 1 g picolinamide **1a**.

not only with benzyl amides but also with thiophene amino alcohol derivative **1q** and gave product **2qa** in very good yield. Unfortunately, using substrate **1q**, C−H functionalization with 3,3-dimethyl-1-butyne was not selective, and both regioisomers (thiophene 2nd vs 4th position) were obtained as 2.5/1 mixture.

Thereafter, we investigated the reaction scope with respect to alkynes (Scheme 4). Both internal and terminal alkynes were competent reagents for C−H functionalization. Cyclopropylacetylene was compatible with reaction conditions and afforded product **2ab** as a single regioisomer in 73% yield. Dialkyl-substituted alkynes reacted smoothly and gave corresponding products in high yields (70−80%; **2ac**, **2ad**, and **2ae**). Terminal alkynes with either aromatic or heteroaromatic substituent (**2af**−**2aj**) gave products as single regioisomers. Interestingly, 4-nitrophenylacetylene afforded mono C−H alkenylation/cyclization product **2ah** (50%) and bisalkenylation product **2ah′** (16%). In the case of *p*-diethynylbenzene, product **2ai** was isolated in 54% yield. 3-Ethynylthiophene and trimethylsilylacetylene were competent substrates and selectively formed products **2aj** and **2an**, as well as 1-phenyl-1-propyne — **2am**. Diarylacetylenes displayed excellent reactivity under the reaction conditions (**2ak** and **2al**). The synthetic application of the developed methodology was demonstrated through gram-scale synthesis of annulation product **2an** which was obtained in excellent yield — 80%.

To find out whether stereochemical integrity for α-position of phenylglycinol derivative **1** is preserved during the reaction, enantiopure (*S*)-phenylglycinol derivative (*S*)-**1a** was tested under the optimized reaction conditions (Scheme 5). Aliphatic

Scheme 5. Preservation of Stereochemistry
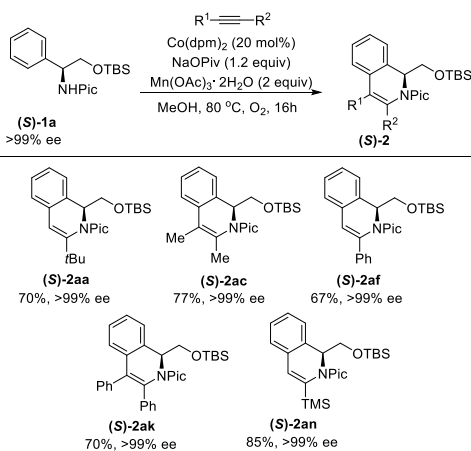
and aromatic terminal and internal alkynes were tested (**2aa**, **2ac**, **2af**, **2ak**, and **2an**). We were pleased to find that the stereocenter was preserved completely, and no loss of enantiopurity was detected exploiting either terminal or internal alkynes.

The application of the developed methodology was shown by accessing valuable tetrahydroisoquinoline derivative (*S*,*S*)-**4an** (Scheme 6). Reduction of enantiopure (*S*)-**2an** using Na/NH₃ proceeded in a highly diastereoselective manner (>20/1) and gave tetrahydroisoquinoline (*S*,*S*)-**3an**. Subsequent

Scheme 6. Synthesis of Tetrahydroisoquinoline (*S*,*S*)-4an
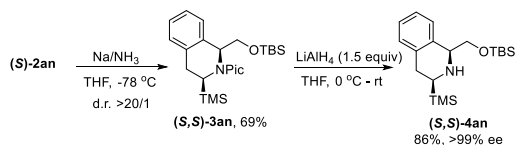
directing group removal using LiAlH₄ gave corresponding tetrahydroisoquinoline (*S*,*S*)-**4an** in good yield and without the loss of enantiopurity.

Based on literature data[3,5a,10] and experimental observations,[9] a possible reaction mechanism was proposed (Scheme 7).

Scheme 7. Mechanistic Considerations
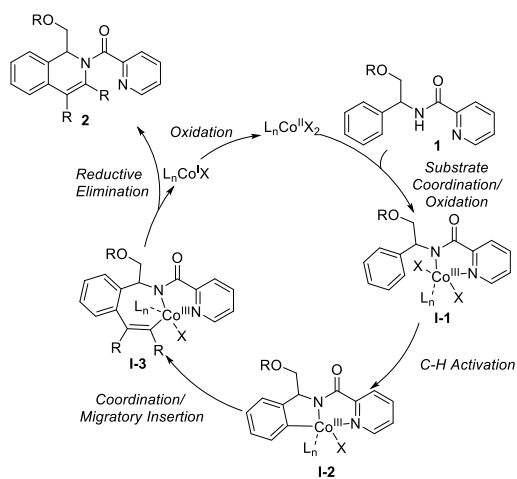
Accordingly, oxidation of the Co(II) catalyst in the presence of substrate **1** would generate Co(III) species **I-1**.[5a] C−H bond activation would form intermediate **I-2**. Coordination followed by insertion of alkyne into Co−Ar bond would result in the formation of **I-3**. Subsequent reductive elimination would form dihydroisoquinoline **2** and Co(I) species which is reoxidized to Co(II) and returned to the catalytic cycle. The protodemetallation pathway from **I-3** was excluded as no cyclization product **2af** formation was observed under standard reaction conditions (Scheme 8).[9]

In conclusion, we have developed a general method for cobalt-catalyzed C−H functionalization of phenylglycinol derivatives with terminal and internal alkynes, directed by picolinamide auxiliary. The reactions proceed in the presence

Scheme 8. Possible Cyclization of Picolinamide 1s
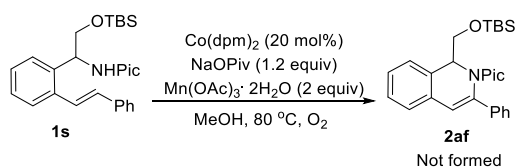
of commercially available cobalt(II) tetramethylheptanedionate catalyst, NaOPiv base, O_2 oxidant, and $Mn(OAc)_3 \cdot 2H_2O$ cooxidant. Major advantages of the methodology are substituent diversity at benzylamine benzylic position, excellent regioselectivity, and full preservation of original stereochemistry.

◼ EXPERIMENTAL SECTION

General Comments. Reactions were performed using standard glassware or were run in 4 mL vials with polytetrafluoroethylene/liner screw caps or 30 mL vials using w/polyseal screw caps. Reactions were heated using Chemglass aluminium reaction blocks. Column chromatography was performed using Kieselgel silicagel (35−70 and 60−200 μm). Thin layer chromatography (TLC) was performed on silica gel using Merck TLC Silica gel 60 F254 Aluminum sheets and was visualized by a UV lamp, staining with $KMnO_4$. ^{1}H, ^{13}C, ^{19}F, and 2D-NMR spectra were recorded on a 400 MHz Bruker spectrometer using residual solvent peak as a reference. Compounds for HRMS were analyzed by positive mode electrospray ionization (ESI) using a Waters Synapt G2-Si mass spectrometer. High-performance liquid chromatography (HPLC) data were obtained using a Waters Alliance 2695 HPLC system with a Phenomenex Lux Amylose-1 (4.6 × 150 mm) or CHIRALPAK IC-1 (4.6 × 250 mm) column (conditions specified on attached HPLC chromatograms). Infrared (IR) spectra were obtained using a Shimadzu IR Prestige-21 Fourier-transform IR spectroscopy (FT-IR) spectrometer. Optical rotations were measured at 20 °C on a Rudolph Research Analytical Autopol VI Polarimeter, cell length 50 mm, using solvent and concentration stated, at 589 nm. All procedures were performed under ambient air unless otherwise noted. Reagents and starting materials were obtained from commercial sources and used without further purification unless otherwise noted.

Substrate Synthesis. Amide substrates **1a−c,g−q,s** were synthesized through methyl-2-aryl-2-(picolinamido)acetates (**5a,g−q,s**). Corresponding methyl-2-aryl-2-(picolinamido)acetates were synthesized in two steps from commercially available amino acids.

Methyl 2-Phenyl-2-(picolinamido)acetate (5a). Procedure A: Step 1: 2-amino-2-phenylacetic acid (6.00 g, 39.69 mmol, 1 equiv) was suspended in MeOH (48 mL) under an argon atmosphere. The solution was cooled to 0 °C, and oxalyl chloride (6.9 mL, 79.38 mmol, 2 equiv) was slowly added dropwise. The reaction mixture was stirred overnight at room temperature. The solvent was evaporated under vacuum to obtain a crude product as a pale solid. The crude product was used in the next step without further purification. Step 2: under an argon atmosphere, methyl 2-amino-2-phenylacetate hydrogen chloride (39.69 mmol, 1 equiv), picolinic acid (5.12 g, 41.58 mmol, 1.05 equiv), and N,N,N',N'-tetramethyl-O-(1H-benzotriazol-1-yl)uronium hexafluorophosphate (30.03 g, 79.38 mmol, 2 equiv) were dissolved in dimethylformamide (DMF) (48 mL). Pyridine (9.6 mL, 119.07 mmol, 3 equiv) was added to the solution directly. The reaction mixture was stirred at room temperature overnight. Then, the reaction mixture was diluted with EtOAc (60 mL) and H_2O (40 mL) and filtered. The organic phase was separated, and the aqueous phase was extracted with EtOAc (50 mL); the combined organic phase was washed with dist. H_2O (20 mL) and brine (20 mL), dried over Na_2SO_4, and filtered. The solvent was evaporated under reduced pressure to afford the crude product, which was further purified by flash chromatography on silica gel using petroleum ether/EtOAc (3/1) as an eluent to give corresponding product 8.07 g (75%) as a white solid. This compound is known.[11] ^{1}H NMR (400 MHz, CDCl$_3$): δ 8.94 (d, J = 6.9 Hz, 1H), 8.59 (ddd, J = 4.8, 1.7, 0.9 Hz, 1H), 8.16 (dt, J = 7.8, 1.1 Hz, 1H), 7.83 (td, J = 7.7, 1.7 Hz, 1H), 7.5 −7.46 (m, 2H), 7.46−7.30 (m, 4H), 5.78 (d, J = 7.6 Hz, 1H), 3.77 (s, 3H).

Methyl 2-(2-Methoxyphenyl)-2-(picolinamido)acetate (5g). **5g** was synthesized according to procedure A. Step 1: (2-methoxyphenyl)glycine (1.28 g, 7.10 mmol, 1 equiv), $C_2O_2Cl_2$ (1.2 mL, 14.20 mmol, 2 equiv), and MeOH (12 mL) were mixed. Step 2: crude reaction mixture from step 1, picolinic acid (873 mg, 7.10 mmol, 1 equiv), N,N,N',N'-tetramethyl-O-(1H-benzotriazol-1-yl)-

uronium hexafluorophosphate (5.38 g, 14.20 mmol, 2 equiv), DMF (15 mL), pyridine (1.7 mL, 21.30 mmol, 3 equiv) were mixed. After column chromatography (gradient hexanes/EtOAc from 3:1 to 2:1), 900 mg (42%) of product was obtained as a colorless oil. This compound is known.[11] ^{1}H NMR (400 MHz, CDCl$_3$): δ 8.98 (d, J = 8.4 Hz, 1H), 8.56 (d, J = 4.1 Hz, 1H), 8.16 (d, J = 7.8 Hz, 1H), 7.81 (td, J = 7.7, 1.7 Hz, 1H), 7.48−7.35 (m, 2H), 7.35−7.27 (m, 1H), 7.05−6.81 (m, 2H), 6.00 (d, J = 8.6 Hz, 1H), 3.89 (s, 3H), 3.73 (s, 3H).

Methyl 2-(2-Fluorophenyl)-2-(picolinamido)acetate (5h). **5h** was synthesized according to procedure A. Step 1: (2-fluorophenyl)glycine hydrochloride (1.84 g, 9.00 mmol, 1 equiv), $C_2O_2Cl_2$ (1.6 mL, 18.00 mmol, 2 equiv), and MeOH (10 mL) were mixed. Step 2: crude reaction mixture from step 1, picolinic acid (1.16 g, 9.50 mmol, 1.04 equiv), N,N,N',N'-tetramethyl-O-(1H-benzotriazol-1-yl)uronium hexafluorophosphate (6.80 g, 18.00 mmol, 2 equiv), DMF (18 mL), and pyridine (2.2 mL, 27.00 mmol, 3 equiv) were mixed. After column chromatography (gradient hexanes/EtOAc from 3:1 to 2:1), 1.50 g (58%) of product was obtained as a colorless oil. R_f = 0.36 (petroleum ether/EtOAc 2:1). ^{1}H NMR (400 MHz, CDCl$_3$, ppm): δ 8.98 (d, J = 7.4 Hz, 1H), 8.58 (d, J = 4.7 Hz, 1H), 8.15 (d, J = 7.8 Hz, 1H), 7.82 (td, J = 7.7, 1.6 Hz, 1H), 7.52−7.38 (m, 2H), 7.39−7.27 (m, 1H), 7.20−7.05 (m, 2H), 6.02 (d, J = 7.9 Hz, 1H), 3.78 (s, 3H). ^{13}C{^{1}H} NMR (100 MHz, CDCl$_3$, ppm): δ 170.6, 163.9, 160.7 (d, J_{C-F} = 248.5 Hz), 149.3, 148.5, 137.4, 130.5 (d, J_{C-F} = 8.3 Hz), 129.9 (d, J_{C-F} = 3.5 Hz), 126.6, 124.7 (d, J_{C-F} = 3.6 Hz), 124.4 (d, J_{C-F} = 14.3 Hz), 122.5, 116.1 (d, J_{C-F} = 21.3 Hz), 53.1, 51.5 (d, J_{C-F} = 2.6 Hz). ^{19}F NMR (376 MHz, CDCl$_3$, ppm): δ −117.06. HR-MS (ESI-TOF) m/z: calcd for $[M + H]^+$ $C_{15}H_{14}N_2O_3F$, 289.0988; found, 289.0999. FT-IR (thin film, cm^{-1}) ν: 3387, 2955, 1750, 1683, 1510, 1233.

Methyl 2-(3-Methylphenyl)-2-(picolinamido)acetate (5i). **5i** was synthesized from commercially available methyl amino(3-methylphenyl)acetate hydrochloride using procedure A. Step 2: amino(3-methylphenyl)acetate hydrochloride (1.00 g, 4.60 mmol), picolinic acid (599 mg, 4.80 mmol, 1.05 equiv), N,N,N',N'-tetramethyl-O-(1H-benzotriazol-1-yl)uronium hexafluorophosphate (3.52 g, 9.20 mmol, 2 equiv), DMF (10 mL), and pyridine (1.1 mL, 13.80 mmol, 3 equiv) were mixed. After column chromatography (gradient hexanes/EtOAc from 3:1 to 2:1), 1.00 g (76%) of product was obtained as a colorless oil. R_f = 0.59 (petroleum ether/EtOAc 1:1). ^{1}H NMR (400 MHz, CDCl$_3$, ppm): δ 8.93 (d, J = 7.0 Hz, 1H), 8.60 (ddd, J = 4.8, 1.7, 0.9 Hz, 1H), 8.18 (dt, J = 7.8, 1.0 Hz, 1H), 7.85 (td, J = 7.7, 1.7 Hz, 1H), 7.45 (ddd, J = 7.6, 4.8, 1.2 Hz, 1H), 7.32−7.23 (m, 3H), 7.20−7.11 (m, 1H), 5.75 (d, J = 7.5 Hz, 1H), 3.79 (s, 3H), 2.38 (s, 3H). ^{13}C{^{1}H} NMR (100 MHz, CDCl$_3$, ppm): δ 171.3, 163.9, 149.4, 148.4, 138.9, 137.4, 136.5, 129.5, 129.0, 128.2, 126.5, 124.6, 122.5, 56.7, 52.9, 21.5. HR-MS (ESI-TOF) m/z: calcd for $[M + H]^+$ $C_{16}H_{17}N_2O_3$, 285.1239; found, 285.1250. FT-IR (thin film, cm^{-1}) ν: 3388, 2953, 1744, 1685, 1512, 1437.

Methyl 2-(3-Trifluoromethylphenyl)-2-(picolinamido)acetate (5j). **5j** was synthesized according to procedure A. Step 1: 2-(3-trifluoromethylphenyl)glycine (1.21 g, 5.50 mmol, 1 equiv), $C_2O_2Cl_2$ (0.95 mL, 11.00 mmol, 2 equiv), and MeOH (12 mL) were mixed. Step 2: crude reaction mixture from step 1, picolinic acid (679 mg, 5.50 mmol, 1 equiv), N,N,N',N'-tetramethyl-O-(1H-benzotriazol-1-yl)uronium hexafluorophosphate (4.18 g, 11.00 mmol, 2 equiv), DMF (15 mL), and pyridine (1.34 mL, 16.50 mmol, 3 equiv) were mixed. After column chromatography (gradient hexanes/EtOAc from 3:1 to 2:1), 1.12 g (59%) of product was obtained as a colorless oil. R_f = 0.22 (petroleum ether/EtOAc 3:1). ^{1}H NMR (400 MHz, CDCl$_3$, ppm): δ 9.07 (d, J = 7.0 Hz, 1H), 8.62 (ddd, J = 4.8, 1.6, 0.9 Hz, 1H), 8.15 (d, J = 7.8, 1.0 Hz, 1H), 7.85 (td, J = 7.7, 1.7 Hz, 1H), 7.69 (d, J = 7.7 Hz, 1H), 7.60 (d, J = 7.8 Hz, 1H), 7.54−7.43 (m, 2H), 5.84 (d, J = 7.4 Hz, 1H), 3.80 (s, 3H). ^{13}C{^{1}H} NMR (100 MHz, CDCl$_3$, ppm): δ 170.6, 164.0, 149.2, 148.5, 137.9, 137.5, 131.5 (q, J_{C-F} = 32.4 Hz), 130.9 (q, J_{C-F} = 1.2 Hz), 129.6, 126.8, 125.6 (q, J_{C-F} = 3.6 Hz), 124.3 (q, J_{C-F} = 3.7 Hz), 124.0 (q, J_{C-F} = 272.5 Hz), 122.5, 56.4, 53.3. ^{19}F NMR (376 MHz, CDCl$_3$, ppm): δ −62.60. HR-MS (ESI-TOF) m/z: calcd for $[M + H]^+$ $C_{16}H_{14}N_2O_3F_3$, 339.0957;

found, 339.0957. FT-IR (thin film, cm^{-1}) ν: 2957, 1748, 1684, 1330, 1168, 1127.

Methyl 2-(4-Methylphenyl)-2-(picolinamido)acetate (5k). **5k** was synthesized according to procedure A. Step 1: (4-methylphenyl)-glycine hydrochloride (1.40 g, 7.00 mmol, 1 equiv), C$_2$O$_2$Cl$_2$ (1.2 mL, 14.00 mmol, 2 equiv), and MeOH (8 mL) were mixed. Step 2: crude reaction mixture from step 1, picolinic acid (903 mg, 7.30 mmol, 1.04 equiv), *N,N,N',N'*-tetramethyl-*O*-(1*H*-benzotriazol-1-yl)uronium hex-afluoro-phosphate (5.30 g, 14.00 mmol, 2 equiv), DMF (14 mL), and pyridine (1.7 mL, 21.00 mmol, 3 equiv) were mixed. After column chromatography (gradient hexanes/EtOAc from 3:1 to 2:1), 750 mg (38%) of product was obtained as a colorless oil. R_f = 0.40 (petroleum ether/EtOAc 2:1). ^{1}H NMR (400 MHz, CDCl$_3$, ppm): δ 8.90 (d, J = 6.8 Hz, 1H), 8.62−8.45 (m, 1H), 8.15 (d, J = 7.8 Hz, 1H), 7.82 (td, J = 7.7, 1.7 Hz, 1H), 7.50−7.37 (m, 1H), 7.36 (d, J = 8.1 Hz, 2H), 7.18 (d, J = 7.9 Hz, 2H), 5.73 (d, J = 7.5 Hz, 1H), 3.76 (s, 3H), 2.34 (s, 3H). ^{13}C{^{1}H} NMR (100 MHz, CDCl$_3$, ppm): δ 171.4, 163.9, 149.5, 148.4, 138.6, 137.4, 133.7, 129.8, 127.4, 126.5, 122.5, 56.5, 52.9, 21.3. HR-MS (ESI-TOF) *m/z*: calcd for [M + H]$^+$ C$_{16}$H$_{17}$N$_2$O$_3$, 285.1239; found, 285.1243. FT-IR (thin film, cm^{-1}) ν: 3388, 2951, 1743, 1684, 1507, 1437, 1180.

Methyl 2-(4-Hydroxyphenyl)-2-(picolinamido)acetate (5lm). **5lm** was synthesized according to procedure A. Step 1: 4-hydroxyphenyl-glycine (1.50 g, 9.00 mmol, 1 equiv), C$_2$O$_2$Cl$_2$ (1.6 mL, 18.00 mmol, 2 equiv), and MeOH (10 mL) were mixed. Step 2: crude reaction mixture from step 1, picolinic acid (1.16 g, 9.45 mmol, 1.05 equiv), *N,N,N',N'*-tetramethyl-*O*-(1*H*-benzotriazol-1-yl)uronium hexafluoro-phosphate (6.80 g, 18.00 mmol, 2 equiv), DMF (18 mL), and pyridine (2.2 mL, 27.00 mmol, 3 equiv) were mixed. After column chromatography (gradient hexanes/EtOAc from 3:1 to 2:1), 1.20 g (47%) of the product was obtained as a colorless oil. This compound is known.[12] ^{1}H NMR (400 MHz, CDCl$_3$, ppm): δ 8.97 (d, J = 7.2 Hz, 1H), 8.59 (ddd, J = 4.8, 1.7, 0.9 Hz, 1H), 8.16 (dt, J = 7.8, 1.0 Hz, 1H), 7.85 (td, J = 7.7, 1.7 Hz, 1H), 7.45 (ddd, J = 7.6, 4.8, 1.2 Hz, 1H), 7.30−7.21 (m, 2H), 6.79−6.67 (m, 2H), 5.67 (d, J = 7.3 Hz, 1H), 3.76 (s, 3H).

Methyl 2-(4-Methoxyphenyl)-2-(picolinamido)acetate (5l). To a solution of methyl 2-(4-hydroxy-phenyl)-2-(picolinamido)acetate (**5lm**, 500 mg, 1.75 mmol) in DMF (15 mL), NaH (60% dispersion in mineral oil, 105 mg, 2.62 mmol, 1.5 equiv) was added at 0 °C. The reaction was stirred at the same temperature for 5 min, and then MeI (142 μL, 2.27 mmol 1.3 equiv) was added and further stirred for 30 min at the same temperature. The reaction mixture was quenched with ice water and then extracted with ethyl acetate (3 × 20 mL). The combined organic phase was washed with dist. H$_2$O (20 mL) and brine (20 mL), then dried over anhydrous Na$_2$SO$_4$, filtered, and evaporated under reduced pressure. After column chromatography (gradient hexanes/EtOAc from 3:1 to 2:1), 270 mg (52%) of product was obtained as a colorless oil. R_f = 0.25 (petroleum ether/EtOAc 2:1). ^{1}H NMR (400 MHz, C$_2$D$_2$Cl$_4$, ppm): δ 8.86 (d, J = 7.4 Hz, 1H), 8.61 (d, J = 4.1 Hz, 1H), 8.12 (d, J = 7.8 Hz, 1H), 7.87 (td, J = 7.7, 1.7 Hz, 1H), 7.48 (ddd, J = 7.5, 4.8, 1.2 Hz, 1H), 7.45−7.32 (m, 2H), 6.96−6.89 (m, 2H), 5.68 (d, J = 7.4 Hz, 1H), 3.81 (s, 3H), 3.78 (s, 3H). ^{13}C{^{1}H} NMR (100 MHz, CDCl$_3$, ppm): δ 171.5, 163.9, 159.9, 149.5, 148.4, 137.4, 128.8, 128.7, 126.5, 122.5, 114.5, 56.2, 55.5, 52.9. HR-MS (ESI-TOF) *m/z*: calcd for [M + Na]$^+$ C$_{16}$H$_{16}$N$_2$O$_4$Na, 323.1002; found, 323.1015. FT-IR (thin film, cm^{-1}) ν: 3385, 3007, 2954, 1745, 1682, 1513, 1259, 1179.

Methyl 2-(4-(Methoxymethoxy)phenyl)-2-(picolinamido)acetate (5m). To a solution of methyl 2-(4-hydroxy-phenyl)-2-(picolinamido)acetate (**5lm**) (1.00 g, 3.49 mmol) in DMF (15 mL), NaH (60% dispersion in mineral oil, 210 mg, 5.24 mmol, 1.5 equiv) was added at 0 °C. The reaction was stirred at the same temperature for 5 min, and then MOMCl (0.35 mL, 4.54 mmol 1.3 equiv) was added and further stirred for 30 min at the same temperature. The reaction mixture was quenched with ice water and then extracted with ethyl acetate (3 × 20 mL). The combined organic phase was washed with dist. H$_2$O (20 mL) and brine (20 mL), then dried over anhydrous Na$_2$SO$_4$, filtered, and evaporated under reduced pressure. After column chromatography (gradient hexanes/EtOAc

from 3:1 to 2:1), 550 mg (48%) of product was obtained as a colorless oil. R_f = 0.33 (petroleum ether/EtOAc 2:1). ^{1}H NMR (400 MHz, CDCl$_3$, ppm): δ 8.88 (d, J = 7.1 Hz, 1H), 8.58 (ddd, J = 4.8, 1.7, 0.9 Hz, 1H), 8.15 (dt, J = 7.8, 1.1 Hz, 1H), 7.83 (td, J = 7.7, 1.7 Hz, 1H), 7.45−7.37 (m, 3H), 7.06−7.01 (m, 2H), 5.71 (d, J = 7.4 Hz, 1H), 5.16 (s, 2H), 3.77 (s, 3H), 3.46 (s, 3H). ^{13}C{^{1}H} NMR (100 MHz, CDCl$_3$, ppm): δ 171.4, 163.9, 157.5, 149.4, 148.4, 137.4, 129.9, 128.8, 126.6, 122.5, 116.8, 94.5, 56.2, 56.1, 52.9. HR-MS (ESI-TOF) *m/z*: calcd for [M + Na]$^+$ C$_{17}$H$_{18}$N$_2$O$_5$Na, 353.1113; found, 353.1117. FT-IR (thin film, cm^{-1}) ν: 3386, 2954, 1751, 1683, 1508, 1236, 1153.

Methyl 2-(4-Trifluoromethoxyphenyl)-2-(picolinamido)acetate (5n). **5n** was synthesized according to procedure A. Step 1: (4-trifluoromethoxyphenyl)glycine (1.00 g, 4.30 mmol, 1 equiv), C$_2$O$_2$Cl$_2$ (0.74 mL, 8.60 mmol, 2 equiv), and MeOH (5 mL) were mixed. Step 2: crude reaction mixture from step 1, picolinic acid (550 mg, 4.50 mmol, 1.05 equiv), *N,N,N',N'*-tetramethyl-*O*-(1*H*-benzo-triazol-1-yl)uronium hexa-fluorophosphate (3.23 g, 8.60 mmol, 2 equiv), DMF (8 mL), and pyridine (1.0 mL, 12.9 mmol, 3 equiv) were mixed. After column chromatography (gradient hexanes/EtOAc from 3:1 to 2:1), 1.30 g (82%) of product was obtained as a colorless oil. R_f = 0.42 (petroleum ether/EtOAc 2:1). ^{1}H NMR (400 MHz, CDCl$_3$, ppm): δ 9.01 (d, J = 7.2 Hz, 1H), 8.60 (ddd, J = 4.8, 1.6, 0.9 Hz, 1H), 8.14 (dt, J = 7.8, 1.0 Hz, 1H), 7.84 (td, J = 7.7, 1.7 Hz, 1H), 7.55−7.47 (m, 2H), 7.45 (ddd, J = 7.6, 4.8, 1.2 Hz, 1H), 7.25−7.17 (m, 2H), 5.79 (d, J = 7.5 Hz, 1H), 3.79 (s, 3H). ^{13}C{^{1}H} NMR (100 MHz, CDCl$_3$, ppm): δ 170.8, 164.0, 149.4 (q, J_{C-F} = 1.6 Hz), 149.2, 148.5, 137.5, 135.4, 129.0, 126.7, 122.5, 121.5, 120.5 (q, J_{C-F} = 257.6 Hz), 56.0, 53.2. ^{19}F NMR (376 MHz, CDCl$_3$, ppm): δ −57.84. HR-MS (ESI-TOF) *m/z*: calcd for [M + H]$^+$ C$_{16}$H$_{14}$N$_2$O$_4$F$_3$, 355.0906; found, 355.0906. FT-IR (thin film, cm^{-1}) ν: 3384, 2957, 1743, 1675, 1505, 1436, 1261, 1221, 1162.

Methyl 2-(4-Fluorophenyl)-2-(picolinamido)acetate (5o). **5o** was synthesized according to procedure A. Step 1: 2-(4-fluorophenyl)-glycine (1.0 g, 5.90 mmol, 1 equiv), C$_2$O$_2$Cl$_2$ (1.5 mL, 17.70 mmol, 3 equiv), and MeOH (9 mL) were mixed. Step 2: crude reaction mixture from step 1, picolinic acid (762 mg, 6.20 mmol, 1.05 equiv), *N,N,N',N'*-tetramethyl-*O*-(1*H*-benzotriazol-1-yl)uronium hexa-fluorophosphate (4.48 g, 11.80 mmol, 2 equiv), DMF (12 mL), and pyridine (1.4 mL, 17.70 mmol, 3 equiv) were mixed. After column chromatography (gradient hexanes/EtOAc from 3:1 to 2:1), 1.30 g (76%) of product was obtained as a colorless oil. R_f = 0.37 (eluent petroleum ether/EtOAc = 2/1). ^{1}H NMR (400 MHz, CDCl$_3$, ppm): δ 8.96 (d, J = 6.8 Hz, 1H), 8.65−8.54 (m, 1H), 8.15 (d, J = 7.8 Hz, 1H), 7.89−7.76 (m, 1H), 7.50−7.40 (m, 2H), 7.12−7.00 (m, 2H), 5.75 (d, J = 7.4 Hz, 1H), 3.77 (s, 3H). ^{13}C{^{1}H} NMR (100 MHz, CDCl$_3$, ppm): δ 171.1, 163.9, 162.9 (d, J_{C-F} = 247.4 Hz), 149.3, 148.5, 137.5, 132.6 (d, J_{C-F} = 3.3 Hz), 129.3 (d, J_{C-F} = 8.4 Hz), 126.7, 122.5, 116.1 (d, J_{C-F} = 21.8 Hz), 56.0, 53.1. ^{19}F NMR (376 MHz, CDCl$_3$, ppm): δ −113.28. HR-MS (ESI-TOF) *m/z*: calcd for [M + H]$^+$ C$_{15}$H$_{14}$N$_2$O$_3$, 289.0988; found, 289.1002. FT-IR (thin film, cm^{-1}) ν: 3386, 2955, 1744, 1683, 1507, 1437, 1225, 1161.

Methyl 2-(4-Bromophenyl)-2-(picolinamido)acetate (5p). **5p** was synthesized according to procedure A. Step 1: 2-(4-bromophenyl)-glycine (1.59 g, 6.00 mmol, 1 equiv), C$_2$O$_2$Cl$_2$ (1.6 mL, 18.00 mmol, 3 equiv), and MeOH (10 mL) were mixed. Step 2: crude reaction mixture from step 1, picolinic acid (775 mg, 6.30 mmol, 1.05 equiv), *N,N,N',N'*-tetramethyl-*O*-(1*H*-benzotriazol-1-yl)uronium hexa-fluorophosphate (4.55 g, 12.00 mmol, 2 equiv), DMF (12 mL), and pyridine (1.5 mL, 18.00 mmol, 3 equiv) were mixed. After column chromatography (gradient hexanes/EtOAc from 3:1 to 2:1), 700 mg (33%) of product was obtained as a colorless oil. R_f = 0.40 (eluent petroleum ether/EtOAc = 2/1). ^{1}H NMR (400 MHz, CDCl$_3$, ppm): δ 8.99 (d, J = 7.0 Hz, 1H), 8.60 (ddd, J = 4.8, 1.7, 0.9 Hz, 1H), 8.14 (dt, J = 7.8, 1.1 Hz, 1H), 7.84 (td, J = 7.7, 1.7 Hz, 1H), 7.53−7.47 (m, 2H), 7.45 (ddd, J = 7.6, 4.8, 1.2 Hz, 1H), 7.38−7.33 (m, 2H), 5.73 (d, J = 7.4 Hz, 1H), 3.77 (s, 3H). ^{13}C{^{1}H} NMR (100 MHz, CDCl$_3$, ppm): δ 170.8, 163.9, 149.2, 148.4, 137.5, 135.8, 132.3, 129.2, 126.7, 122.8, 122.5, 56.2, 53.1. HR-MS (ESI-TOF) *m/z*: calcd for [M + H]$^+$

$C_{15}BrH_{14}N_2O_3$, 349.0188; found, 349.0190. FT-IR (thin film, cm^{-1}) ν: 3378, 2954, 1748, 1680, 1507, 1173.

Methyl 2-(Picolinamido)-2-(thiophen-3-yl)acetate (5q). **5q** was synthesized according to procedure A. Step 1: 2-amino-2-(thiophen-3-yl)acetic acid hydrochloride (1.23 g, 7.80 mmol, 1 equiv), $C_2O_2Cl_2$ (1.36 mL, 15.60 mmol, 2 equiv), and MeOH (15 mL) were mixed. Step 2: crude reaction mixture from step 1, picolinic acid (965 mg, 7.80 mmol, 1.0 equiv), N,N,N',N'-tetramethyl-O-(1H-benzotriazol-1-yl)uronium hexa-fluorophosphate (5.95 g, 15.60 mmol, 2 equiv), DMF (24 mL), and pyridine (1.89 mL, 23.40 mmol, 3 equiv) were mixed. After column chromatography (gradient hexanes/EtOAc from 3:1 to 2:1), 280 mg (13%) of product was obtained as a colorless oil. R_f = 0.51 (eluent petroleum ether/EtOAc = 1/1). ^{1}H NMR (400 MHz, CDCl$_3$, ppm): δ 8.84 (d, J = 7.2 Hz, 1H), 8.58 (ddd, J = 4.8, 1.7, 0.9 Hz, 1H), 8.17 (dt, J = 7.8, 1.1 Hz, 1H), 7.84 (td, J = 7.7, 1.7 Hz, 1H), 7.44 (ddd, J = 7.6, 4.8, 1.2 Hz, 1H), 7.41−7.36 (m, 1H), 7.33 (dd, J = 5.0, 3.0 Hz, 1H), 7.17 (dd, J = 5.0, 1.3 Hz, 1H), 5.92 (d, J = 7.9 Hz, 1H), 3.80 (s, 3H). ^{13}C{^{1}H} NMR (100 MHz, CDCl$_3$, ppm): δ 170.9, 164.0, 149.4, 148.4, 137.4, 136.6, 126.9, 126.6, 126.5, 123.5, 122.5, 53.0, 52.5. HR-MS (ESI-TOF) m/z: calcd for [M + H]$^+$ $C_{13}H_{13}N_2O_3S$, 277.0647; found, 277.0655. FT-IR (thin film, cm^{-1}) ν: 3387, 3098, 2954, 1752, 1679, 1514, 1212, 1164.

Methyl (E)-2-(Picolinamido)-2-(2-styrylphenyl)acetate (5s). Step 1: to a stirred solution of ammonium chloride (0.58 g, 10.87 mmol, 1.3 equiv) in 25 mL of ammonium hydroxide solution (25% NH$_3$ in water), sodium cyanide (0.52 g, 10.45 mmol, 1.25 equiv) was added carefully, followed by dropwise (over 30 min) addition of (E)-2-styrylbenzaldehyde[11] (1.74 g, 8.36 mmol, 1 equiv) solution in iPrOH (10 mL). The mixture was stirred at room temperature overnight. The solvent was removed under reduced pressure, and the crude mixture was diluted with water (pH > 10) and extracted with dichloromethane (DCM) (3 × 30 mL). The combined organic layers were washed with brine (1 × 30 mL), dried over Na$_2$SO$_4$, filtered, and evaporated under reduced pressure to afford the crude product, which was used in the next step without further purification. Step 2: to a stirred solution of the crude product from step 1 in 1,4-dioxane (5 mL), concentrated hydrochloric acid (37%, 5.2 mL, 167.23 mmol, 20 equiv) was added dropwise, and the resulting mixture was refluxed for 5 h. The solvent was removed under reduced pressure to afford the crude product, which was used in the next step without further purification. Step 3: the crude product from step 2 was suspended in MeOH (24 mL) under an argon atmosphere. The solution was cooled to 0 °C, and oxalyl chloride (1.5 mL, 16.72 mmol, 2 equiv) was slowly added dropwise. The reaction mixture was stirred overnight at room temperature. The solvent was evaporated under vacuum; the residue was dissolved in dist. H$_2$O (50 mL) and extracted with EtOAc (50 mL). Using 1 M NaOH, the pH of the aqueous phase was adjusted to ~8. The aqueous phase was extracted with EtOAc (3 × 50 mL). The combined organic phase was dried over Na$_2$SO$_4$ and filtered. The solvent was evaporated under reduced pressure to afford the crude product as a yellowish oil. The crude product was used in the next step without further purification. Step 4: under an argon atmosphere, the crude product from step 3, picolinic acid (1.08 g, 8.78 mmol, 1.05 equiv), and N,N,N',N'-tetramethyl-O-(1H-benzotriazol-1-yl)uronium hexafluorophosphate (6.34 g, 16.72 mmol, 2 equiv) were dissolved in DMF (10 mL). Pyridine (1.4 mL, 16.72 mmol, 2 equiv) was added to the solution directly. The reaction mixture was stirred at room temperature overnight. Then reaction mixture was diluted with EtOAc (50 mL) and H$_2$O (40 mL) and filtered. The organic phase was separated, and the aqueous phase was extracted with EtOAc (50 mL); the combined organic phase was washed with dist. H$_2$O (20 mL) and brine (20 mL), dried over Na$_2$SO$_4$, and filtered. The solvent was evaporated under reduced pressure to afford the crude product, which was further purified by flash chromatography on silica gel using petroleum ether/EtOAc (3/1) as an eluent to give corresponding product 1.04 g (34% over 4 steps) as a yellowish oil. R_f = 0.28 (petroleum ether/EtOAc 3:1). ^{1}H NMR (400 MHz, CDCl$_3$, ppm): δ 8.92 (d, J = 7.5 Hz, 1H), 8.52 (ddd, J = 4.8, 1.7, 0.9 Hz, 1H), 8.17 (dt, J = 7.8, 1.1 Hz, 1H), 7.82 (td, J = 7.7, 1.7 Hz, 1H), 7.71−7.64 (m, 2H), 7.61−7.54 (m, 2H), 7.44−7.35 (m, 5H), 7.33−7.26 (m, 2H),

7.03 (d, J = 16.0 Hz, 1H), 6.16 (d, J = 7.7 Hz, 1H), 3.76 (s, 3H). ^{13}C{^{1}H} NMR (100 MHz, CDCl$_3$, ppm): δ 171.6, 163.9, 149.4, 148.4, 137.4, 137.3, 134.2, 132.7, 129.0, 128.8, 128.4, 128.0, 127.9, 127.1, 127.0, 126.6, 125.4, 122.5, 53.9, 53.0. HR-MS (ESI-TOF) m/z: calcd for [M + H]$^+$ $C_{23}H_{21}N_2O_3$, 373.1552; found, 373.1561. FT-IR (thin film, cm^{-1}) ν: 3389, 1743, 1680, 1507, 1220.

Synthesis and Characterization of Picolinamides 1. *N-(2-((tert-Butyldimethylsilyl)oxy)-1-phenylethyl)picolinamide (1a).* Procedure B: Step 1: methyl 2-phenyl-2-(picolinamido)acetate (1.50 g, 5.55 mmol, 1 equiv) was dissolved in tetrahydrofuran (THF; 20 mL) under an argon atmosphere. The solution was cooled in water/ice bath to 0 °C and lithium borohydride (4 M in THF, 1.8 mL, 7.21 mmol, 1.3 equiv) was added slowly dropwise; then the reaction mixture was stirred at room temperature for 3 h. The reaction was monitored by TLC to achieve full conversion and then cooled in water/ice bath and quenched by 15% citric acid solution in water. The organic solvent was evaporated in vacuum, and the water phase was extracted by DCM (2 × 30 mL). The combined organic phase was dried over Na$_2$SO$_4$, filtered, and evaporated under reduced pressure to afford the crude product, which was used in the next step without further purification. Step 2: to the solution of N-(2-hydroxy-1-phenylethyl)picolinamide (5.55 mmol, 1 equiv) in DMF (18 mL) under an argon atmosphere, imidazole (1.10 g, 7.21 mmol, 1.3 equiv) and *tert*-butyldimethylsilyl chloride (491 mg, 7.21 mmol, 1.3 equiv) were added. The reaction mixture was stirred at room temperature to achieve full conversion and then was diluted with EtOAc (30 mL) and H$_2$O (20 mL). The organic phase was separated, and the water phase was extracted with EtOAc (20 mL); the combined organic phase was washed with dist. H$_2$O (20 mL) and brine (20 mL). The combined organic phase was dried over Na$_2$SO$_4$, filtered, and evaporated under reduced pressure to afford the crude product, which was further purified by flash chromatography on silica gel using petroleum ether/EtOAc (6/1) as an eluent to give corresponding product 1.60 g (81%) as a colorless oil. R_f = 0.34 (petroleum ether/EtOAc 4:1). ^{1}H NMR (400 MHz, CDCl$_3$, ppm): δ 8.86 (d, J = 7.7 Hz, 1H), 8.58 (ddd, J = 4.8, 1.6, 0.9 Hz, 1H), 8.18 (dt, J = 7.8, 1.0 Hz, 1H), 7.83 (td, J = 7.7, 1.7 Hz, 1H), 7.45−7.38 (m, 3H), 7.36−7.29 (m, 2H), 7.28−7.22 (m, 1H), 5.22 (dt, J = 8.7, 4.6 Hz, 1H), 4.01 (dd, J = 10.2, 4.6 Hz, 1H), 3.94 (dd, J = 10.2, 4.6 Hz, 1H), 0.87 (s, 9H), −0.01 (s, 3H), −0.05 (s, 3H). ^{13}C{^{1}H} NMR (100 MHz, CDCl$_3$, ppm): δ 163.9, 150.1, 148.2, 140.3, 137.4, 128.5, 127.5, 127.2, 126.3, 122.4, 66.4, 54.9, 25.9, 18.4, −5.4, −5.5. HR-MS (ESI-TOF) m/z: calcd for [M + H]$^+$ $C_{20}H_{29}N_2O_2Si$, 357.1998; found, 357.2007. FT-IR (thin film, cm^{-1}) ν: 3386, 2954, 2927, 2856, 1681, 1517, 1254, 1107.

N-(2-Hydroxy-1-phenylethyl)picolinamide (1b). **1b** was synthesized according to procedure B. Step 1: methyl 2-phenyl-2-(picolinamido)acetate (1.10 g, 4.07 mmol, 1 equiv), LiBH4 (4 M in THF 1.32 mL, 5.29 mmol, 1.3 equiv), and THF (15 mL) were mixed. After column chromatography (gradient hexanes/EtOAc from 1:1 to EtOAc), 880 mg (89%) of product was obtained as a colorless oil. This compound is known.[13] ^{1}H NMR (400 MHz, CDCl$_3$, ppm): δ 8.70 (d, J = 6.5 Hz, 1H), 8.63−8.48 (m, 1H), 8.23−8.09 (m, 1H), 7.83 (td, J = 7.7, 1.7 Hz, 1H), 7.51−7.22 (m, 6H), 5.32−5.18 (m, 1H), 4.11−3.89 (m, 2H), 3.07 (s, 1H).

N-(2-((4-Methoxybenzyl)oxy)-1-phenylethyl)picolinamide (1c). To a solution of N-(2-hydroxy-1-phenylethyl)picolinamide (300 mg, 1.24 mmol) in DMF (4 mL), NaH (60% dispersion in mineral oil, 74 mg, 1.86 mmol, 1.5 equiv) was added at 0 °C. The reaction was stirred at the same temperature for 5 min, and then PMBCl (0.22 mL, 1.61 mmol 1.3 equiv) was added and further stirred for 30 min at the same temperature. The reaction mixture was quenched with ice water and then extracted with ethyl acetate (3 × 10 mL). The combined organic phase was washed with dist. H$_2$O (10 mL) and brine (10 mL), then dried over anhydrous Na$_2$SO$_4$, filtered, and evaporated under reduced pressure. After column chromatography (gradient hexanes/EtOAc from 5:1 to 3:1), 380 mg (85%) of product was obtained as a colorless oil. R_f = 0.10 (petroleum ether/EtOAc 4:1). ^{1}H NMR (400 MHz, CDCl$_3$, ppm): δ 8.75 (d, J = 8.0 Hz, 1H), 8.58 (ddd, J = 4.8, 1.7, 0.9 Hz, 1H), 8.18 (dt, J = 7.8, 1.0 Hz, 1H), 7.83 (td, J = 7.7, 1.7 Hz, 1H), 7.46−7.38 (m, 3H), 7.38−7.30 (m, 2H), 7.31−

7.23 (m, 1H), 7.24−7.18 (m, 2H), 6.87−6.81 (m, 2H), 5.39 (dt, J = 8.2, 5.2 Hz, 1H), 4.59−4.46 (m, 2H), 3.83 (d, J = 5.3 Hz, 2H), 3.79 (s, 3H). ^{13}C{^{1}H} NMR (100 MHz, CDCl$_3$, ppm): δ 164.0, 159.3, 150.0, 148.2, 139.9, 137.4, 130.1, 129.4, 128.6, 127.5, 127.1, 126.3, 122.4, 113.9, 72.8, 72.3, 53.3, 53.1. HR-MS (ESI-TOF) m/z: calcd for [M + Na]$^+$ C$_{22}$H$_{22}$N$_2$O$_3$Na, 385.1528; found, 385.1530. FT-IR (thin film, cm^{-1}) ν: 3393, 2862, 1683, 1512, 1250, 1096.

N-(2-(Methoxymethoxy)-1-phenylethyl)picolinamide (1d). To a solution of *N*-(2-hydroxy-1-phenylethyl)picolinamide (300 mg, 1.24 mmol) in DMF (4 mL), NaH (60% dispersion in mineral oil, 74 mg, 1.86 mmol, 1.5 equiv) was added at 0 °C. The reaction was stirred at the same temperature for 5 min, and then MOMCl (0.12 mL, 1.61 mmol 1.3 equiv) was added and further stirred for 30 min at the same temperature. The reaction mixture was quenched with ice water and then extracted with ethyl acetate (3 × 10 mL). The combined organic phase was washed with dist. H$_2$O (10 mL) and brine (10 mL), then dried over anhydrous Na$_2$SO$_4$, filtered, and evaporated under reduced pressure. After column chromatography (gradient hexanes/EtOAc from 2:1 to 1:1), 185 mg (52%) of product was obtained as a colorless oil. R_f = 0.29 (petroleum ether/EtOAc 1:1). ^{1}H NMR (400 MHz, CDCl$_3$, ppm): δ 8.71 (d, J = 8.0 Hz, 1H), 8.53−8.42 (m, 1H), 8.11 (d, J = 7.8 Hz, 1H), 7.79−7.67 (m, 1H), 7.43−7.30 (m, 3H), 7.32−7.22 (m, 2H), 7.23−7.14 (m, 1H), 5.34 (dt, J = 8.5, 5.1 Hz, 1H), 4.63−4.52 (m, 2H), 3.92−3.82 (m, 2H), 3.20 (s, 3H). ^{13}C{^{1}H} NMR (100 MHz, CDCl$_3$, ppm): δ 163.9, 149.8, 148.1, 139.7, 137.3, 128.6, 127.5, 126.9, 126.3, 122.3, 96.5, 70.4, 55.4, 53.0. HR-MS (ESI-TOF) m/z: calcd for [M + Na]$^+$ C$_{16}$H$_{18}$N$_2$O$_3$Na 309.1215; found, 309.1217. FT-IR (thin film, cm^{-1}) ν: 3390, 2932, 2887, 1680, 1518, 1151, 1041.

N-(1-Phenylethyl)picolinamide (1e). Under an argon atmosphere, phenylethylamine (1.50 g, 12.38 mmol, 1 equiv), picolinic acid (1.60 g, 13.00 mmol, 1.05 equiv), and *N,N,N′,N′*-tetramethyl-*O*-(1*H*-benzotriazol-1-yl)uronium hexafluorophosphate (9.39 g, 24.76 mmol, 2 equiv) were dissolved in DMF (24 mL). Pyridine (3.0 mL, 37.14 mmol, 3 equiv) was added to the solution directly. The reaction mixture was stirred at room temperature overnight. The reaction was monitored by TLC to achieve full conversion, then was diluted with EtOAc (50 mL) and H$_2$O (50 mL), and filtered. The organic phase was separated, and the aqueous phase was extracted with EtOAc (50 mL); the combined organic phase was washed with dist. H$_2$O (20 mL) and brine (20 mL), dried over Na$_2$SO$_4$, and filtered. The solvent was evaporated under reduced pressure to afford the crude product, which was further purified by flash chromatography on silica gel using petroleum ether/EtOAc (2/1) as an eluent to give corresponding product 2.05 g (73%) as a colorless oil. This compound is known.[3] ^{1}H NMR (400 MHz, CDCl$_3$, ppm): δ 8.53 (ddd, J = 4.8, 1.6, 0.9 Hz, 1H), 8.34 (d, J = 6.6 Hz, 1H), 8.20 (d, J = 7.8 Hz, 1H), 7.83 (td, J = 7.7, 1.7 Hz, 1H), 7.45−7.38 (m, 3H), 7.38−7.33 (m, 2H), 7.26 (tt, J = 6.9, 1.3 Hz, 1H), 5.38−5.28 (m, 1H), 1.63 (d, J = 6.9 Hz, 3H).

N-Benzhydrylpicolinamide (1f). Under an argon atmosphere, diphenylmethanamine (0.66 mL, 3.82 mmol, 1 equiv), picolinic acid (470 mg, 3.82 mmol, 1 equiv), and *N,N,N′,N′*-tetramethyl-*O*-(1*H*-benzotriazol-1-yl)uronium hexafluorophosphate (2.90 g, 7.64 mmol, 2 equiv) were dissolved in DMF (15 mL). Pyridine (0.62 mL, 7.64 mmol, 2 equiv) was added to the solution directly. The reaction mixture was stirred at room temperature overnight. The reaction was monitored by TLC to achieve full conversion, then was diluted with EtOAc (30 mL) and H$_2$O (30 mL), and filtered. The organic phase was separated, and the aqueous phase was extracted with EtOAc (30 mL); the combined organic phase was washed with dist. H$_2$O (20 mL) and brine (20 mL), dried over Na$_2$SO$_4$, and filtered. The solvent was evaporated under reduced pressure to afford the crude product, which was further purified by flash chromatography on silica gel using petroleum ether/EtOAc (3/1) as an eluent to give corresponding product 931 mg (85%) as white powder. This compound is known.[14] ^{1}H NMR (400 MHz, CDCl$_3$, ppm): δ 8.75 (d, J = 8.1 Hz, 1H), 8.57 (ddd, J = 4.8, 1.6, 0.9 Hz, 1H), 8.24 (dt, J = 7.8, 1.0 Hz, 1H), 7.87 (td, J = 7.7, 1.7 Hz, 1H), 7.45 (ddd, J = 7.6, 4.8, 1.2 Hz, 1H), 7.40−7.20 (m, 10H), 6.47 (d, J = 8.6 Hz, 1H).

N-(2-((tert-Butyldimethylsilyl)oxy)-1-(2-methoxyphenyl)ethyl)-picolinamide. **1g.** was synthesized according to procedure B. Step 1: methyl 2-(2-methoxyphenyl)-2-(picolinamido)acetate (0.90 g, 2.99 mmol, 1 equiv), LiBH$_4$ (4 M in THF 0.97 mL, 3.89 mmol, 1.3 equiv), and THF (24 mL) were mixed. Step 2: crude reaction mixture from step 1, imidazole (265 mg, 3.89 mmol, 1.3 equiv), TBSCl (587 mg, 3.89 mmol, 1.3 equiv), and DMF (12 mL) were mixed. After column chromatography (hexanes/EtOAc 6:1), 627 mg (54%) of product was obtained as a colorless oil. R_f = 0.38 (petroleum ether/EtOAc 3:1). ^{1}H NMR (400 MHz, CDCl$_3$, ppm): δ 9.02 (d, J = 8.6 Hz, 1H), 8.59 (ddd, J = 4.8, 1.7, 0.9 Hz, 1H), 8.18 (dt, J = 7.8, 1.1 Hz, 1H), 7.82 (td, J = 7.7, 1.7 Hz, 1H), 7.41 (ddd, J = 7.6, 4.8, 1.2 Hz, 1H), 7.33−7.27 (m, 1H), 7.22 (td, J = 7.9, 1.7 Hz, 1H), 6.94−6.85 (m, 2H), 5.53 (dt, J = 9.0, 5.1 Hz, 1H), 3.98 (dd, J = 10.0, 5.2 Hz, 1H), 3.94−3.86 (m, 4H), 0.83 (s, 9H), −0.06 (s, 3H), −0.10 (s, 3H). ^{13}C{^{1}H} NMR (100 MHz, CDCl$_3$, ppm): δ 163.7, 157.1, 150.5, 148.3, 137.3, 128.8, 128.5, 127.9, 126.1, 122.4, 120.6, 110.7, 64.9, 55.6, 51.4, 25.9, 18.4, −5.47, −5.48. HR-MS (ESI-TOF) m/z: calcd for [M + H]$^+$ C$_{21}$H$_{31}$N$_2$O$_3$Si, 387.2104; found, 387.2108. FT-IR (thin film, cm^{-1}) ν: 3394, 2930, 2856, 1694, 1508, 1256, 1110.

N-(2-((tert-Butyldimethylsilyl)oxy)-1-(2-fluorophenyl)ethyl)-picolinamide (1h). **1h** was synthesized according to procedure B. Step 1: methyl 2-(2-fluorophenyl)-2-(picolinamido)acetate (1.40 g, 4.86 mmol, 1 equiv), LiBH$_4$ (4 M in THF 1.58 mL, 6.32 mmol, 1.3 equiv), and THF (24 mL) were mixed. Step 2: crude reaction mixture from step 1, imidazole (430 mg, 6.32 mmol, 1.3 equiv), TBSCl (952 mg, 6.32 mmol, 1.3 equiv), and DMF (10 mL) were mixed. After column chromatography (hexanes/EtOAc 6:1), 1.30 g (71%) of product was obtained as a colorless oil. R_f = 0.38 (petroleum ether/EtOAc 4:1). ^{1}H NMR (400 MHz, CDCl$_3$, ppm): δ 8.91 (d, J = 8.2 Hz, 1H), 8.59 (ddd, J = 4.8, 1.7, 0.9 Hz, 1H), 8.17 (dt, J = 7.8, 1.0 Hz, 1H), 7.83 (td, J = 7.6, 1.7 Hz, 1H), 7.42 (ddd, J = 7.6, 4.8, 1.2 Hz, 1H), 7.37 (td, J = 7.6, 1.7 Hz, 1H), 7.26−7.18 (m, 1H), 7.11−7.01 (m, 2H), 5.52 (dt, J = 8.9, 4.8 Hz, 1H), 4.01 (dd, J = 10.1, 4.8 Hz, 1H), 3.95 (dd, J = 10.1, 4.8 Hz, 1H), 0.84 (s, 9H), −0.03 (s, 3H), −0.09 (s, 3H). ^{13}C{^{1}H} NMR (100 MHz, CDCl$_3$, ppm): δ 163.9, 160.7 (d, J_{C-F} = 245.5 Hz), 150.0, 148.3, 137.4, 129.1 (d, J_{C-F} = 4.5 Hz), 129.0 (d, J_{C-F} = 8.3 Hz), 127.1 (d, J_{C-F} = 13.4 Hz), 126.3, 124.0 (d, J_{C-F} = 3.4 Hz), 122.4, 115.5 (d, J_{C-F} = 21.8 Hz), 65.2 (d, J_{C-F} = 1.2 Hz), 50.0 (d, J_{C-F} = 1.4 Hz), 25.9, 18.3, −5.5, −5.6. ^{19}F NMR (376 MHz, CDCl$_3$, ppm): δ −118.54. HR-MS (ESI-TOF) m/z: calcd for [M + H]$^+$ C$_{20}$H$_{28}$N$_2$O$_2$SiF, 375.1904; found, 375.1916. FT-IR (thin film, cm^{-1}) ν: 3388, 2955, 2928, 1685, 1514, 1107.

N-(2-((tert-Butyldimethylsilyl)oxy)-1-(3-methylphenyl)ethyl)-picolinamide (1i). **1i** was synthesized according to procedure B. Step 1: methyl 2-(3-methylphenyl)-2-(picolinamido)acetate (1.00 g, 3.52 mmol, 1 equiv), LiBH$_4$ (4 M in THF 4.26 mmol, 1.2 equiv), and THF (17 mL) were mixed. Step 2: crude reaction mixture from step 1, imidazole (312 mg, 4.58 mmol, 1.3 equiv), TBSCl (690 mg, 4.58 mmol, 1.3 equiv), and DMF (15 mL) were mixed. After column chromatography (petroleum ether/EtOAc 6:1), 441 mg (34%) of product was obtained as a colorless oil. R_f = 0.37 (petroleum ether/EtOAc 5:1). ^{1}H NMR (400 MHz, CDCl$_3$, ppm): δ 8.82 (d, J = 7.7 Hz, 1H), 8.58 (ddd, J = 4.7, 1.5, 0.8 Hz, 1H), 8.18 (d, J = 7.8 Hz, 1H), 7.83 (td, J = 7.7, 1.7 Hz, 1H), 7.42 (ddd, J = 7.6, 4.8, 1.2 Hz, 1H), 7.24−7.16 (m, 3H), 7.10−7.01 (m, 1H), 5.22−5.10 (m, 1H), 3.99 (dd, J = 10.2, 4.6 Hz, 1H), 3.92 (dd, J = 10.2, 4.6 Hz, 1H), 2.33 (s, 3H), 0.88 (s, 9H), 0.00 (s, 3H), −0.04 (s, 3H). ^{13}C{^{1}H} NMR (100 MHz, CDCl$_3$, ppm): δ 164.0, 150.2, 148.3, 140.3, 138.0, 137.3, 128.4, 128.2, 128.0, 126.2, 124.2, 122.3, 66.4, 54.9, 25.9, 21.6, 18.4, −5.4. HR-MS (ESI-TOF) m/z: calcd for [M + H]$^+$ C$_{21}$H$_{31}$N$_2$O$_2$Si, 371.2155; found, 371.2159. FT-IR (thin film, cm^{-1}) ν: 3397, 2954, 2927, 2857, 1684, 1512, 1101.

N-(2-((tert-Butyldimethylsilyl)oxy)-1-(3-trifluoromethylphenyl)-ethyl)picolinamide (1j). **1j** was synthesized according to procedure B. Step 1: methyl 2-(3-trifluoromethylphenyl)-2-(picolinamido)acetate (1.12 g, 3.30 mmol, 1 equiv), LiBH$_4$ (4 M in THF 1.07 mL, 4.29 mmol, 1.3 equiv), and THF (30 mL) were mixed. Step 2: crude reaction mixture from step 1, imidazole (292 mg, 4.29 mmol, 1.3 equiv), TBSCl (647 mg, 4.29 mmol, 1.3 equiv), and DMF (12 mL)

were mixed. After column chromatography (hexanes/EtOAc 6:1), 1.40 g (60%) of product was obtained as a colorless oil. $R_f = 0.37$ (petroleum ether/EtOAc 3:1). ^{1}H NMR (400 MHz, CDCl$_3$, ppm): δ 8.94 (d, $J = 7.9$ Hz, 1H), 8.59 (ddd, $J = 4.8, 1.7, 0.9$ Hz, 1H), 8.17 (dt, $J = 7.8, 1.0$ Hz, 1H), 7.84 (td, $J = 7.7, 1.7$ Hz, 1H), 7.69 (s, 1H), 7.60 (d, $J = 7.7$ Hz, 1H), 7.52 (d, $J = 7.8$ Hz, 1H), 7.49−7.32 (m, 2H), 5.26 (dt, $J = 8.2, 4.1$ Hz, 1H), 4.04 (dd, $J = 10.2, 4.4$ Hz, 1H), 3.94 (dd, $J = 10.2, 3.8$ Hz, 1H), 0.88 (s, 9H), 0.01 (s, 3H), −0.05 (s, 3H). ^{13}C{^{1}H} NMR (100 MHz, CDCl$_3$, ppm): δ 164.1, 149.8, 148.4, 141.7, 138.5, 130.8, 130.8 (q, $J_{C-F} = 32.1$ Hz), 128.9, 126.4, 124.4 (q, $J_{C-F} = 3.8$ Hz), 124.1 (q, $J_{C-F} = 3.8$ Hz), 124.3 (q, $J_{C-F} = 272.4$ Hz), 122.4, 66.2, 54.4, 25.8, 18.3, −5.5, −5.6. ^{19}F NMR (376 MHz, CDCl$_3$, ppm): δ −62.54. HR-MS (ESI-TOF) m/z: calcd for [M + H]$^+$ C$_{21}$H$_{28}$N$_2$O$_2$SiF$_3$, 425.1872; found, 425.1881. FT-IR (thin film, cm^{-1}) ν: 3386, 2955, 2930, 2859, 1683, 1508, 1329, 1126.

N-(2-((*tert*-Butyldimethylsilyl)oxy)-1-(4-methylphenyl)ethyl)-picolinamide (1k). 1k was synthesized according to procedure B. Step 1: methyl 2-(4-methylphenyl)-2-(picolinamido)acetate (668 mg, 2.35 mmol, 1 equiv), LiBH$_4$ (4 M in THF 0.76 mL, 3.05 mmol, 1.3 equiv), and THF (15 mL) were mixed. Step 2: crude reaction mixture from step 1, imidazole (208 mg, 3.05 mmol, 1.3 equiv), TBSCl (460 mg, 3.05 mmol, 1.3 equiv), and DMF (8 mL) were mixed. After column chromatography (hexanes/EtOAc 6:1), 514 mg (59%) of product was obtained as a colorless oil. $R_f = 0.46$ (petroleum ether/EtOAc 4:1). ^{1}H NMR (400 MHz, CDCl$_3$, ppm): δ 8.79 (d, $J = 7.8$ Hz, 1H), 8.56 (ddd, $J = 4.8, 1.6, 0.9$ Hz, 1H), 8.17 (dt, $J = 7.8, 1.0$ Hz, 1H), 7.82 (td, $J = 7.7, 1.7$ Hz, 1H), 7.41 (ddd, $J = 7.6, 4.8, 1.2$ Hz, 1H), 7.30 (d, $J = 8.1$ Hz, 2H), 7.13 (d, $J = 7.9$ Hz, 2H), 5.17 (dt, $J = 8.7, 4.7$ Hz, 1H), 3.99 (dd, $J = 10.2, 4.7$ Hz, 1H), 3.92 (dd, $J = 10.2, 4.9$ Hz, 1H), 2.32 (s, 3H), 0.88 (s, 9H), 0.01 (s, 3H), −0.02 (s, 3H). ^{13}C{^{1}H} NMR (100 MHz, CDCl$_3$, ppm): δ 163.9, 150.2, 148.2, 137.4, 137.3, 137.0, 129.2, 127.1, 126.2, 122.3, 66.4, 54.7, 25.9, 21.2, 18.4, −5.38, −5.42. HR-MS (ESI-TOF) m/z: calcd for [M + H]$^+$ C$_{21}$H$_{31}$N$_2$O$_2$Si, 371.2155; found, 371.2164. FT-IR (thin film, cm^{-1}) ν: 3389, 2952, 2859, 1679, 1518, 1257, 1115.

N-(2-((*tert*-Butyldimethylsilyl)oxy)-1-(4-methoxyphenyl)ethyl)-picolinamide (1l). 1l was synthesized according to procedure B. Step 1: methyl 2-(4-methoxyphenyl)-2-(picolinamido)acetate (260 mg, 0.87 mmol, 1 equiv), LiBH$_4$ (4 M in THF 0.28 mL, 1.12 mmol, 1.3 equiv), and THF (5 mL) were mixed. Step 2: crude reaction mixture from step 1, imidazole (77 mg, 1.12 mmol, 1.3 equiv), TBSCl (170 mg, 1.12 mmol, 1.3 equiv), and DMF (4 mL) were mixed. After column chromatography (hexanes/EtOAc 6:1), 180 mg (54%) of product was obtained as a colorless oil. $R_f = 0.33$ (petroleum ether/EtOAc 4:1). ^{1}H NMR (400 MHz, CDCl$_3$, ppm): δ 8.79 (d, $J = 7.8$ Hz, 1H), 8.56 (d, $J = 4.1$ Hz, 1H), 8.17 (d, $J = 7.8$ Hz, 1H), 7.82 (td, $J = 7.7, 1.6$ Hz, 1H), 7.45−7.37 (m, 2H), 7.37−7.29 (m, 2H), 6.94−6.80 (m, 2H), 5.16 (dt, $J = 8.7, 4.6$ Hz, 1H), 3.98 (dd, $J = 10.2, 4.7$ Hz, 1H), 3.91 (dd, $J = 10.2, 4.7$ Hz, 1H), 3.78 (s, 3H), 0.88 (s, 9H), 0.01 (s, 3H), −0.02 (s, 3H). ^{13}C{^{1}H} NMR (100 MHz, CDCl$_3$, ppm): δ 163.9, 159.0, 150.1, 148.2, 137.4, 132.6, 128.3, 126.2, 122.3, 113.9, 66.4, 55.4, 54.3, 25.9, 18.3, −5.4. HR-MS (ESI-TOF) m/z: calcd for [M + Na]$^+$ C$_{21}$H$_{30}$N$_2$O$_3$NaSi, 409.1923; found, 409.1926. FT-IR (thin film, cm^{-1}) ν: 3389, 3058, 2952, 2929, 2857, 1688, 1505, 1249, 1109.

N-(2-((*tert*-Butyldimethylsilyl)oxy)-1-(4-(methoxymethoxyphenyl)ethyl)picolinamide (1m). 1m was synthesized according to procedure B. Step 1: methyl 2-(4-methoxymethoxyphenyl)-2-(picolinamido)acetate (514 mg, 1.56 mmol, 1 equiv), LiBH$_4$ (4 M in THF 0.51 mL, 2.02 mmol, 1.3 equiv), and THF (10 mL) were mixed. Step 2: crude reaction mixture from step 1, imidazole (138 mg, 2.02 mmol, 1.3 equiv), TBSCl (305 mg, 2.02 mmol, 1.3 equiv), and DMF (5 mL) were mixed. After column chromatography (hexanes/EtOAc 6:1), 370 mg (57%) of product was obtained as a colorless oil. $R_f = 0.20$ (petroleum ether/EtOAc 4:1). ^{1}H NMR (400 MHz, CDCl$_3$, ppm): δ 8.78 (d, $J = 7.9$ Hz, 1H), 8.56 (ddd, $J = 4.8, 1.6, 0.9$ Hz, 1H), 8.17 (dt, $J = 7.8, 1.0$ Hz, 1H), 7.83 (td, $J = 7.7, 1.7$ Hz, 1H), 7.41 (ddd, $J = 7.6, 4.8, 1.2$ Hz, 1H), 7.38−7.30 (m, 2H), 7.03−6.95 (m, 2H), 5.23−5.08 (m, 3H), 3.98 (dd, $J = 10.2, 4.7$ Hz, 1H), 3.91 (dd, $J = 10.2, 4.7$ Hz, 1H), 3.46 (s, 3H), 0.88 (s,

9H), 0.01 (s, 3H), −0.02 (s, 3H). ^{13}C{^{1}H} NMR (100 MHz, CDCl$_3$, ppm): δ 163.9, 156.3, 150.2, 148.3, 137.4, 133.9, 128.4, 126.2, 122.3, 116.3, 94.6, 66.4, 56.1, 54.3, 25.9, 18.4, −5.37, −5.41. HR-MS (ESI-TOF) m/z: calcd for [M + H]$^+$ C$_{22}$H$_{33}$N$_2$O$_4$Si, 417.2210; found, 417.2206. FT-IR (thin film, cm^{-1}) ν: 3388, 2930, 1512, 1153, 1108, 1080, 1006.

N-(2-((*tert*-Butyldimethylsilyl)oxy)-1-(4-trifluoromethoxyphenyl)-ethyl)picolinamide (1n). 1n was synthesized according to procedure B. Step 1: methyl 2-(4-trifluoromethoxyphenyl)-2-(picolinamido)-acetate (1.16 g, 3.27 mmol, 1 equiv), LiBH$_4$ (4 M in THF 1.06 mL, 4.26 mmol, 1.3 equiv), and THF (24 mL) were mixed. Step 2: crude reaction mixture from step 1, imidazole (290 mg, 4.26 mmol, 1.3 equiv), TBSCl (642 mg, 4.26 mmol, 1.3 equiv), and DMF (10 mL) were mixed. After column chromatography (hexanes/EtOAc 6:1), 1.00 g (69%) of product was obtained as a colorless oil. $R_f = 0.34$ (petroleum ether/EtOAc 4:1). ^{1}H NMR (400 MHz, CDCl$_3$, ppm): δ 8.88 (d, $J = 7.9$ Hz, 1H), 8.58 (ddd, $J = 4.8, 1.7, 0.9$ Hz, 1H), 8.17 (dt, $J = 7.8, 1.1$ Hz, 1H), 7.84 (td, $J = 7.7, 1.7$ Hz, 1H), 7.48−7.40 (m, 3H), 7.21−7.12 (m, 2H), 5.21 (dt, $J = 8.3, 4.3$ Hz, 1H), 4.01 (dd, $J = 10.2, 4.5$ Hz, 1H), 3.92 (dd, $J = 10.2, 4.2$ Hz, 1H), 0.87 (s, 9H), 0.01 (s, 3H), −0.05 (s, 3H). ^{13}C{^{1}H} NMR (100 MHz, CDCl$_3$, ppm): δ 164.1, 149.9, 148.6 (q, $J_{C-F} = 1.8$ Hz), 148.3, 139.3, 137.5, 128.6, 126.4, 122.4, 121.0, 120.6 (q, $J_{C-F} = 256.8$ Hz), 66.3, 54.2, 25.9, 18.3, −5.47, −5.48. ^{19}F NMR (376 MHz, CDCl$_3$, ppm): δ −57.19. HR-MS (ESI-TOF) m/z: calcd for [M + H]$^+$ C$_{21}$H$_{28}$N$_2$O$_3$SiF$_3$, 441.1821; found, 441.1828. FT-IR (thin film, cm^{-1}) ν: 3386, 2955, 2931, 2858, 1686, 1507, 1260, 1224, 1165, 1109.

N-(2-((*tert*-Butyldimethylsilyl)oxy)-1-(4-fluorophenyl)ethyl)-picolinamide (1o). 1o was synthesized according to procedure B. Step 1: methyl 2-(4-fluorophenyl)-2-(picolinamido)acetate (742 mg, 2.57 mmol, 1 equiv), LiBH$_4$ (4 M in THF 0.84 mL, 3.34 mmol, 1.3 equiv), and THF (20 mL) were mixed. Step 2: crude reaction mixture from step 1, imidazole (228 mg, 3.34 mmol, 1.3 equiv), TBSCl (504 mg, 3.34 mmol, 1.3 equiv), and DMF (10 mL) were mixed. After column chromatography (petroleum ether/EtOAc 6:1), 590 mg (61%) of product was obtained as a colorless oil. $R_f = 0.32$ (petroleum ether/EtOAc 5:1). ^{1}H NMR (400 MHz, CDCl$_3$, ppm): δ 8.85 (d, $J = 7.7$ Hz, 1H), 8.57 (ddd, $J = 4.8, 1.6, 0.9$ Hz, 1H), 8.17 (dt, $J = 7.8, 0.9$ Hz, 1H), 7.83 (td, $J = 7.7, 1.7$ Hz, 1H), 7.46−7.33 (m, 3H), 7.05−6.94 (m, 2H), 5.18 (dt, $J = 8.4, 4.4$ Hz, 1H), 3.99 (dd, $J = 10.1, 4.6$ Hz, 1H), 3.91 (dd, $J = 10.1, 4.3$ Hz, 1H), 0.88 (s, 9H), 0.01 (s, 3H), −0.04 (s, 3H). ^{13}C{^{1}H} NMR (100 MHz, CDCl$_3$, ppm): δ 164.0, 162.2 (d, $J_{C-F} = 245.0$ Hz), 150.0, 148.3, 137.4, 136.3 (d, $J_{C-F} = 3.1$ Hz), 128.8 (d, $J_{C-F} = 8.1$ Hz), 126.3, 122.4, 115.3 (d, $J_{C-F} = 21.4$ Hz), 66.3, 54.2, 25.9, 18.4, −5.4, −5.5. ^{19}F NMR (376 MHz, CDCl$_3$, ppm): δ −115.67. HR-MS (ESI-TOF) m/z: calcd for [M + H]$^+$ C$_{20}$H$_{27}$N$_2$O$_2$Si, 375.1904; found, 375.1910. FT-IR (thin film, cm^{-1}) ν: 3388, 2954, 2929, 2858, 1687, 1514, 1258, 1223, 1103.

N-(2-((*tert*-Butyldimethylsilyl)oxy)-1-(4-bromophenyl)ethyl)-picolinamide (1p). 1p was synthesized according to procedure B. Step 1: methyl 2-(4-bromophenyl)-2-(picolinamido)acetate (335 mg, 0.96 mmol, 1 equiv), LiBH$_4$ (4 M in THF 0.31 mL, 1.24 mmol, 1.3 equiv), and THF (20 mL) were mixed. Step 2: crude reaction mixture from step 1, imidazole (85 mg, 1.24 mmol, 1.3 equiv), TBSCl (188 mg, 1.24 mmol, 1.3 equiv), and DMF (10 mL) were mixed. After column chromatography (hexanes/EtOAc 6:1), 222 mg (53%) of product was obtained as a colorless oil. $R_f = 0.33$ (petroleum ether/EtOAc 5:1). ^{1}H NMR (400 MHz, CDCl$_3$, ppm): δ 8.85 (d, $J = 7.7$ Hz, 1H), 8.61−8.49 (m, 1H), 8.16 (d, $J = 7.8$ Hz, 1H), 7.84 (td, $J = 7.7, 1.7$ Hz, 1H), 7.51−7.40 (m, 3H), 7.33−7.27 (m, 2H), 5.15 (dt, $J = 8.3, 4.3$ Hz, 1H), 3.99 (dd, $J = 10.2, 4.5$ Hz, 1H), 3.90 (dd, $J = 10.2, 4.2$ Hz, 1H), 0.88 (s, 9H), 0.01 (s, 3H), −0.03 (s, 3H). ^{13}C{^{1}H} NMR (100 MHz, CDCl$_3$, ppm): δ 164.0, 150.0, 148.3, 139.6, 137.4, 131.5, 129.0, 126.4, 122.4, 121.3, 66.1, 54.3, 25.9, 18.4, −5.4, −5.5. HR-MS (ESI-TOF) m/z: calcd for [M + H]$^+$ C$_{20}$H$_{27}$BrN$_2$O$_2$Si, 435.1103; found, 435.1102. FT-IR (thin film, cm^{-1}) ν: 2954, 2928, 2856, 1684, 1515, 1255, 1107.

N-(2-((*tert*-Butyldimethylsilyl)oxy)-1-(thiophen-3-yl)ethyl)-picolinamide (1q). 1q was synthesized according to procedure B. Step 1: methyl 2-(picolinamido)-2-(thiophen-3-yl)acetate (280 mg,

1.01 mmol, 1 equiv), LiBH$_4$ (4 M in THF 0.33 mL, 1.31 mmol, 1.3 equiv), and THF (10 mL) were mixed. Step 2: crude reaction mixture from step 1, imidazole (89 mg, 1.31 mmol, 1.3 equiv), TBSCl (197 mg, 1.31 mmol, 1.3 equiv), and DMF (5 mL) were mixed. After column chromatography (petroleum ether/EtOAc 6:1), 233 mg (64%) of product was obtained as a colorless oil. R_f = 0.36 (petroleum ether/EtOAc 5:1). ^{1}H NMR (400 MHz, CDCl$_3$, ppm): δ 8.72 (d, J = 8.4 Hz, 1H), 8.55 (ddd, J = 4.8, 1.7, 0.9 Hz, 1H), 8.20 (dt, J = 7.8, 1.0 Hz, 1H), 7.84 (td, J = 7.7, 1.7 Hz, 1H), 7.42 (ddd, J = 7.6, 4.8, 1.2 Hz, 1H), 7.32−7.23 (m, 2H), 7.16 (dd, J = 4.9, 1.4 Hz, 1H), 5.36 (dt, J = 8.5, 4.2 Hz, 1H), 4.07−3.93 (m, 2H), 0.89 (s, 9H), 0.03 (s, 3H), 0.00 (s, 3H). ^{13}C{^{1}H} NMR (100 MHz, CDCl$_3$, ppm): δ 163.8, 150.1, 148.3, 141.3, 137.4, 127.1, 126.3, 125.7, 122.4, 122.0, 65.8, 50.7, 25.9, 18.4, −5.4. HR-MS (ESI-TOF) m/z: calcd for [M + H]$^+$ C$_{18}$H$_{27}$N$_2$O$_2$SiS, 363.1563; found, 363.1573. FT-IR (thin film, cm^{-1}) ν: 2954, 2928, 1676, 1513, 1510, 1255, 1114.

N-(3-((tert-Butyldimethylsilyl)oxy)-1-phenylpropyl)picolinamide (**1r**). Procedure C: Step 1: under an argon atmosphere, 3-amino-3-phenylpropan-1-ol (700 mg, 4.62 mmol, 1 equiv), picolinic acid (570 mg, 4.62 mmol, 1 equiv), and *N,N,N',N'*-tetramethyl-*O*-(1*H*-benzotriazol-1-yl)uronium hexafluorophosphate (3.51 g, 9.24 mmol, 2 equiv) were dissolved in DMF (15 mL). Pyridine (0.75 mL, 9.24 mmol, 2 equiv) was added to the solution directly. The reaction mixture was stirred at room temperature overnight. The reaction was monitored by TLC to achieve full conversion, then was diluted with EtOAc (30 mL) and H$_2$O (30 mL), and filtered. The organic phase was separated, and the aqueous phase was extracted with EtOAc (30 mL); the combined organic phase was washed with dist. H$_2$O (20 mL) and brine (20 mL), dried over Na$_2$SO$_4$, and filtered. The solvent was evaporated under reduced pressure to afford the crude product, which was used in the next step without further purification. Step 2: to the solution of crude reaction mixture from the previous step in DMF (12 mL) under an argon atmosphere, imidazole (471 mg, 6.93 mmol, 1.5 equiv) and *tert*-butyldimethylsilyl chloride (1.04 g, 6.93 mmol, 1.5 equiv) were added. The reaction mixture was stirred at room temperature to achieve full conversion and then was diluted with EtOAc (30 mL) and H$_2$O (20 mL). The organic phase was separated, and the water phase was extracted with EtOAc (20 mL); the combined organic phase was washed with dist. H$_2$O (20 mL) and brine (20 mL). The combined organic phase was dried over Na$_2$SO$_4$, filtered, and evaporated under reduced pressure to afford the crude product, which was further purified by flash chromatography on silica gel using petroleum ether/EtOAc (5/1) as an eluent to give corresponding product 776 mg (68%) as a colorless oil. R_f = 0.40 (petroleum ether/EtOAc 3:1). ^{1}H NMR (400 MHz, CDCl$_3$, ppm): δ 8.90 (d, J = 7.6 Hz, 1H), 8.56−8.42 (m, 1H), 8.10 (d, J = 7.8 Hz, 1H), 7.76 (td, J = 7.7, 1.7 Hz, 1H), 7.35 (ddd, J = 7.6, 4.8, 1.2 Hz, 1H), 7.35−7.28 (m, 2H), 7.30−7.21 (m, 2H), 7.20−7.14 (m, 1H), 5.37−5.25 (m, 1H), 3.67−3.52 (m, 2H), 2.23−2.07 (m, 1H), 2.10−1.96 (m, 1H), 0.86 (s, 9H), −0.00 (s, 3H), −0.01 (s, 3H). ^{13}C{^{1}H} NMR (100 MHz, CDCl$_3$, ppm): δ 163.8, 150.3, 148.1, 142.1, 137.3, 128.6, 127.2, 126.7, 126.1, 122.4, 60.4, 51.9, 38.6, 26.1, 18.5, −5.30, −5.32. HR-MS (ESI-TOF) m/z: calcd for [M + H]$^+$ C$_{21}$H$_{31}$N$_2$O$_2$Si, 371.2155; found, 371.2155. FT-IR (thin film, cm^{-1}) ν: 3379, 2952, 2928, 2856, 1682, 1519, 1257, 1093.

(S)-N-(2-((tert-Butyldimethylsilyl)oxy)-1-phenylethyl)-picolinamide (**S-1a**). **S-1a** was synthesized according to procedure C. Step 1: (S)-2-amino-2-phenylethanol (1.00 g, 7.29 mmol, 1 equiv), picolinic acid (942 mg, 7.65 mmol, 1.05 equiv), *N,N,N',N'*-tetramethyl-*O*-(1*H*-benzotriazol-1-yl)uronium hexafluoro-phosphate (5.53 g, 14.58 mmol, 2 equiv), DMF (20 mL), and pyridine (1.18 mL, 14.58 mmol, 2 equiv) were mixed. The reaction mixture was filtered through a short silicagel column. Step 2: reaction mixture from the previous step, imidazole (645 mg, 9.48 mmol, 1.3 equiv), TBSCl (1.43 g, 9.48 mmol, 1.3 equiv), and DMF (25 mL) were mixed. After column chromatography (petroleum ether/EtOAc 6:1), 1.87 g (72%) of product was obtained as a colorless oil. R_f = 0.34 (petroleum ether/EtOAc 4:1). ee = 99.9% (see attached HPLC data). The NMR data matched to racemate. $[\alpha]_D^{20}$ −27.2 (c = 0.993, CHCl$_3$).

(E)-N-(2-((tert-Butyldimethylsilyl)oxy)-1-(2-styrylphenyl)ethyl)-picolinamide (**1s**). Step 1: methyl (E)-2-(picolinamido)-2-(2-styrylphenyl)acetate (918 mg, 2.47 mmol, 1 equiv) was dissolved in THF (20 mL) under an argon atmosphere. The solution was cooled in water/ice bath to 0 °C, and lithium borohydride (4 M in THF, 0.8 mL, 3.21 mmol, 1.3 equiv) was added slowly dropwise; then the reaction mixture was stirred at room temperature for 3 h. The reaction was monitored by TLC to achieve full conversion, then cooled in water/ice bath, and quenched by 15% citric acid solution in water. The organic solvent was evaporated in vacuum and the water phase was extracted by 2 × DCM (30 mL). The combined organic phase was dried over Na$_2$SO$_4$, filtered, and evaporated under reduced pressure to afford the crude product, which was used in next step without further purification. Step 2: to the solution of crude product from step 1 in DMF (7 mL) under an argon atmosphere, imidazole (218 mg, 3.21 mmol, 1.3 equiv) and *tert*-butyldimethylsilyl chloride (483 mg, 3.21 mmol, 1.3 equiv) were added. The reaction mixture was stirred at room temperature to achieve full conversion and then was diluted with EtOAc (30 mL) and H$_2$O (20 mL). The organic phase was separated, and the water phase was extracted with EtOAc (20 mL); the combined organic phase was washed with dist. H$_2$O (20 mL) and brine (20 mL). The combined organic phase was dried over Na$_2$SO$_4$, filtered, and evaporated under reduced pressure to afford the crude product, which was further purified by flash chromatography on silica gel using petroleum ether/EtOAc (6/1) as an eluent to give corresponding product 520 mg (46%) as a colorless oil. R_f = 0.37 (petroleum ether/EtOAc 5:1). ^{1}H NMR (400 MHz, CDCl$_3$, ppm): δ 8.93 (d, J = 7.8 Hz, 1H), 8.60 (ddd, J = 4.8, 1.6, 0.9 Hz, 1H), 8.22 (dt, J = 7.8, 1.0 Hz, 1H), 7.86 (td, J = 7.7, 1.7 Hz, 1H), 7.68 (d, J = 16.0 Hz, 1H), 7.65−7.56 (m, 3H), 7.52−7.38 (m, 4H), 7.37−7.25 (m, 3H), 7.02 (d, J = 16.0 Hz, 1H), 5.70 (dt, J = 8.3, 4.7 Hz, 1H), 4.05 (dd, J = 10.3, 4.7 Hz, 1H), 3.95 (dd, J = 10.3, 4.9 Hz, 1H), 0.89 (s, 9H), 0.00 (s, 3H), −0.05 (s, 3H). ^{13}C{^{1}H} NMR (100 MHz, CDCl$_3$, ppm): δ 163.9, 150.1, 148.3, 137.7, 137.6, 137.4, 136.4, 131.7, 128.8, 127.8, 127.7, 127.6, 126.9, 126.8, 126.7, 126.23, 126.21, 122.3, 65.6, 51.4, 25.9, 18.3, −5.5. HR-MS (ESI-TOF) m/z: calcd for [M + H]$^+$ C$_{28}$H$_{33}$N$_2$O$_2$Si, 459.2468; found, 459.2476. FT-IR (thin film, cm^{-1}) ν: 3390, 2953, 2928, 2856, 1682, 1519, 1254, 1105.

Synthesis and Characterization of Reaction Products 2. *General Procedure for Cobalt-Catalyzed sp^2 C−H Alkenylation/Cyclization.* A 30 mL vial equipped with a magnetic stir bar was charged with picolinamide (0.50 mmol), Co(dpm)$_2$ (42.5 mg, 0.10 mmol, 20 mol %), NaOPiv (74.5 mg, 0.60 mmol, 1.2 equiv), Mn(OAc)$_3$·2H$_2$O (268 mg, 1.00 mmol, 2 equiv), and MeOH (5 mL). The reaction mixture was purged with O$_2$ for 30 s, then alkyne (0.75−1.50 mmol, 1.5−3 equiv) was added, and the mixture was heated at 80 °C for an indicated time (16−24 h). The reaction was monitored by TLC after 16, 20, and 24 h to determine the completion time. The reaction mixture was cooled to room temperature, and the solvent was evaporated. To the residue, potassium sodium tartrate (10 mL of 1 M aqueous solution) was added, and the mixture was extracted with EtOAc (3 × 15 mL). The combined organic phase was dried over Na$_2$SO$_4$ and filtered, and the solvent was evaporated. The product was purified by column chromatography on silica gel using an appropriate eluent. After purification, the product was dried under reduced pressure. Note! It was observed that the reaction was sensitive to Mn(OAc)$_3$·2H$_2$O. Reproducible results were obtained using Mn-(OAc)$_3$·2H$_2$O purchased from Acros Organics and self-made Mn(OAc)$_3$·2H$_2$O.

(3-(tert-Butyl)-1-(((tert-butyldimethylsilyl)oxy)methyl)-isoquinolin-2(1H)-yl)(pyridin-2-yl)methanone (**2aa**). *N*-(2-((tert-Butyldimethylsilyl)oxy)-1-phenylethyl)picolinamide (178 mg, 0.50 mmol), 3,3-dimethyl-1-butyne (185 μL, 1.50 mmol, 3 equiv), Co(dpm)$_2$ (42.5 mg, 0.10 mmol, 20 mol %), NaOPiv (75 mg, 0.60 mmol, 1.2 equiv), Mn(OAc)$_3$·2H$_2$O (268 mg, 1.00 mmol, 2 equiv), and MeOH (5 mL) were mixed for 16 h at 80 °C under an O$_2$ atmosphere. After column chromatography (gradient petroleum ether/EtOAc from 6:1 to 4:1), 183 mg (84%) of a yellowish oil was obtained. R_f = 0.45 (petroleum ether/EtOAc 4:1). The product was isolated as a single regioisomer. The structure was confirmed by

2D-NMR (COSY, NOESY, see attached NMR data). ^{1}H NMR (400 MHz, CDCl$_3$, ppm): δ 8.71 (d, J = 4.7 Hz, 1H), 7.86−7.72 (m, 2H), 7.43−7.36 (m, 1H), 7.23−7.17 (m, 1H), 7.13 (d, J = 6.6 Hz, 1H), 7.05 (td, J = 7.4, 1.3 Hz, 1H), 6.86 (d, J = 7.4 Hz, 1H), 6.57 (s, 1H), 5.01 (t, J = 6.3 Hz, 1H), 3.97 (dd, J = 9.8, 7.3 Hz, 1H), 3.62 (dd, J = 9.8, 7.7 Hz, 1H), 1.38 (s, 9H), 0.85 (s, 9H), −0.08 (s, 3H), −0.09 (s, 3H). ^{13}C{^{1}H} NMR (100 MHz, CDCl$_3$, ppm): δ 171.3, 153.7, 149.5, 149.3, 136.9, 132.7, 131.7, 128.0, 126.7, 126.5, 125.7, 125.3, 124.8, 118.1, 62.3, 60.7, 36.7, 31.0, 26.0, 18.4, −5.4, −5.6. HR-MS (ESI-TOF) m/z: calcd for [M + H]$^+$ C$_{26}$H$_{37}$N$_2$O$_2$Si, 437.2624; found, 437.2624. FT-IR (thin film, cm^{-1}) ν: 2955, 2930, 2858, 1653, 1117.

(S)-(3-(tert-Butyl)-1-(((tert-butyldimethylsilyl)oxy)methyl)-isoquinolin-2(1H)-yl)(pyridin-2-yl)methanone ((S)-2aa). (S)-N-(2-((tert-Butyldimethylsilyl)oxy)-1-phenylethyl)picolinamide (178 mg, 0.50 mmol), 3,3-dimethyl-1-butyne (185 μL, 1.50 mmol, 3 equiv), Co(dpm)$_2$ (42.5 mg, 0.10 mmol, 20 mol %), NaOPiv (75 mg, 0.60 mmol, 1.2 equiv), Mn(OAc)$_3$·2H$_2$O (268 mg, 1.00 mmol, 2 equiv), and MeOH (5 mL) were mixed for 16 h at 80 °C under an O$_2$ atmosphere. After column chromatography (gradient petroleum ether/EtOAc from 6:1 to 4:1), 167 mg (77%) of a yellowish oil was obtained. R_f = 0.45 (petroleum ether/EtOAc 4:1). The product was isolated as a single regioisomer. ee = >99% (see attached HPLC data). The NMR data matched that of racemate. $[α]_D^{20}$ −225.0 (c = 0.970, CHCl$_3$).

(3-(tert-Butyl)-1-(((4-methoxybenzyl)oxy)methyl)isoquinolin-2(1H)-yl)(pyridin-2-yl)methanone (2ca). N-(2-((4-Methoxybenzyl)-oxy)-1-phenylethyl)picolinamide (181 mg, 0.50 mmol), 3,3-dimethyl-1-butyne (185 μL, 1.50 mmol, 3 equiv), Co(dpm)$_2$ (42.5 mg, 0.10 mmol, 20 mol %), NaOPiv (75 mg, 0.60 mmol, 1.2 equiv), Mn(OAc)$_3$·2H$_2$O (268 mg, 1.00 mmol, 2 equiv), and MeOH (5 mL) were mixed for 16 h at 80 °C under an O$_2$ atmosphere. After column chromatography (gradient petroleum ether/EtOAc from 6:1 to 4:1, then 2:1), 166 mg (75%) of a yellowish oil was obtained. R_f = 0.16 (petroleum ether/EtOAc 4:1). The product was isolated as a single regioisomer. The structure was confirmed by 2D-NMR (COSY, NOESY, see attached NMR data). ^{1}H NMR (400 MHz, CDCl$_3$, ppm): δ 8.68 (dt, J = 4.8, 1.3 Hz, 1H), 7.80−7.67 (m, 2H), 7.41−7.35 (m, 1H), 7.29−7.16 (m, 3H), 7.14 (d, J = 6.7 Hz, 1H), 7.07 (t, J = 8.0 Hz, 1H), 6.91−6.81 (m, 4H), 6.57 (s, 1H), 5.33−5.13 (m, 1H), 4.44 (s, 2H), 3.88−3.74 (m, 4H), 3.44 (dd, J = 9.8, 6.7 Hz, 1H), 1.35 (s, 9H). ^{13}C{^{1}H} NMR (100 MHz, CDCl$_3$, ppm): δ 171.2, 159.3, 153.7, 149.5, 149.4, 136.9, 132.8, 131.8, 130.4, 129.4, 128.1, 126.8, 126.0, 125.9, 125.3, 124.8, 118.2, 113.9, 72.9, 69.2, 58.6, 55.4, 36.8, 31.0. HR-MS (ESI-TOF) m/z: calcd for [M + H]$^+$ C$_{28}$H$_{31}$N$_2$O$_3$, 443.2335; found, 443.2341. FT-IR (thin film, cm^{-1}) ν: 2959, 2864, 1658, 1607, 1512, 1255, 1169.

(3-(tert-Butyl)-1-((methoxymethoxy)methyl)isoquinolin-2(1H)-yl)(pyridin-2-yl)methanone (2da). N-(2-(Methoxymethoxy)-1-phenylethyl)picolinamide (143 mg, 0.50 mmol), 3,3-dimethyl-1-butyne (185 μL, 1.50 mmol, 3 equiv), Co(dpm)$_2$ (42.5 mg, 0.10 mmol, 20 mol %), NaOPiv (75 mg, 0.60 mmol, 1.2 equiv), Mn(OAc)$_3$·2H$_2$O (268 mg, 1.00 mmol, 2 equiv), and MeOH (5 mL) were mixed for 24 h at 80 °C under an O$_2$ atmosphere. After column chromatography (gradient petroleum ether/EtOAc from 2:1 to 1:1), 128 mg (70%) of a yellowish oil was obtained. R_f = 0.40 (petroleum ether/EtOAc 2:1). The product was isolated as a single regioisomer. The structure was confirmed by 2D-NMR (COSY, NOESY, see attached NMR data). ^{1}H NMR (400 MHz, CDCl$_3$, ppm): δ 8.69 (ddd, J = 4.8, 1.6, 1.0 Hz, 1H), 7.81−7.67 (m, 2H), 7.39 (ddd, J = 7.4, 4.8, 1.4 Hz, 1H), 7.20 (td, J = 7.5, 1.2 Hz, 1H), 7.14 (d, J = 6.5 Hz, 1H), 7.06 (td, J = 7.4, 1.4 Hz, 1H), 6.88 (d, J = 7.4 Hz, 1H), 6.58 (s, 1H), 5.34−5.06 (m, 1H), 4.63−4.54 (m, 2H), 3.91 (dd, J = 9.8, 7.0 Hz, 1H), 3.59 (dd, J = 9.8, 7.6 Hz, 1H), 3.24 (s, 3H), 1.37 (s, 9H). ^{13}C{^{1}H} NMR (100 MHz, CDCl$_3$, ppm): δ 171.0, 153.6, 149.5, 149.0, 137.0, 132.8, 131.6, 128.0, 126.7, 126.1, 125.8, 125.4, 124.8, 118.1, 96.3, 66.7, 58.5, 55.3, 36.7, 31.0. HR-MS (ESI-TOF) m/z: calcd for [M + H]$^+$ C$_{22}$H$_{27}$N$_2$O$_3$, 367.2022; found, 367.2033. FT-IR (thin film, cm^{-1}) ν: 2956, 1662, 1653, 1365, 1149, 1116, 1038.

(3-(tert-Butyl)-1-methylisoquinolin-2(1H)-yl)(pyridin-2-yl)-methanone (2ea). N-(1-Phenylethyl)picolinamide (113 mg, 0.50

mmol), 3,3-dimethyl-1-butyne (185 μL, 1.50 mmol, 3 equiv), Co(dpm)$_2$ (42.5 mg, 0.10 mmol, 20 mol %), NaOPiv (75 mg, 0.60 mmol, 1.2 equiv), Mn(OAc)$_3$·2H$_2$O (268 mg, 1.00 mmol, 2 equiv), and MeOH (5 mL) were mixed for 16 h at 80 °C under an O$_2$ atmosphere. After column chromatography (gradient petroleum ether/EtOAc from 6:1 to 4:1), 126 mg (82%) of a yellowish oil was obtained. R_f = 0.33 (petroleum ether/EtOAc 4:1). The product was isolated as a single regioisomer. The structure was confirmed by 2D-NMR (COSY, NOESY, see attached NMR data). ^{1}H NMR (400 MHz, CDCl$_3$, ppm): δ 8.72 (d, J = 5.4 Hz, 1H), 7.78 (td, J = 7.7, 1.7 Hz, 1H), 7.64 (d, J = 7.7 Hz, 1H), 7.45−7.38 (m, 1H), 7.20−7.11 (m, 2H), 7.05 (td, J = 7.2, 1.8 Hz, 1H), 6.78 (d, J = 7.4 Hz, 1H), 6.61 (s, 1H), 5.23−5.03 (m, 1H), 1.43 (d, J = 6.8 Hz, 3H), 1.38 (s, 9H). ^{13}C{^{1}H} NMR (100 MHz, CDCl$_3$, ppm): δ 171.0, 154.2, 148.9, 148.7, 137.21, 137.19, 131.1, 127.5, 127.0, 126.0, 125.4, 124.1, 118.2, 55.7, 36.6, 30.9, 19.6. HR-MS (ESI-TOF) m/z: calcd for [M + H]$^+$ C$_{20}$H$_{23}$N$_2$O, 307.1810; found, 307.1823. FT-IR (thin film, cm^{-1}) ν: 2966, 1653, 1395, 1341, 1164.

(3-(tert-Butyl)-1-phenylisoquinolin-2(1H)-yl)(pyridin-2-yl)-methanone (2fa). N-Benzhydrylpicolinamide (144 mg, 0.5 mmol), 3,3-dimethyl-1-butyne (185 μL, 1.50 mmol, 3 equiv), Co(dpm)$_2$ (42.5 mg, 0.10 mmol, 20 mol %), NaOPiv (75 mg, 0.60 mmol, 1.2 equiv), Mn(OAc)$_3$·2H$_2$O (268 mg, 1.00 mmol, 2 equiv), and MeOH (5 mL) were mixed for 16 h at 80 °C under an O$_2$ atmosphere. After column chromatography (gradient petroleum ether/EtOAc from 6:1 to 4:1), 162 mg (88%) of a yellowish oil was obtained. R_f = 0.40 (petroleum ether/EtOAc 4:1). The product was isolated as a single regioisomer. The structure was confirmed by 2D-NMR (COSY, NOESY, see attached NMR data). ^{1}H NMR (400 MHz, CDCl$_3$, ppm): δ 8.77 (d, J = 4.3 Hz, 1H), 7.81 (t, J = 7.2 Hz, 1H), 7.70 (d, J = 6.9 Hz, 1H), 7.55−7.34 (m, 3H), 7.32−7.24 (m, 5H), 7.14 (t, J = 6.7 Hz, 1H), 6.99−6.77 (m, 1H), 6.69−6.24 (m, 2H), 1.02 (s, 9H). ^{13}C{^{1}H} NMR (100 MHz, CDCl$_3$, ppm): δ 170.5, 153.9, 150.1, 148.6, 139.3, 137.3, 133.4, 132.9, 128.9, 128.1, 127.8, 127.7, 127.0, 126.1, 125.8, 125.5, 125.1, 119.1, 60.7, 36.3, 30.6. HR-MS (ESI-TOF) m/z: calcd for [M + H]$^+$ C$_{25}$H$_{25}$N$_2$O, 369.1967; found, 369.1973. FT-IR (thin film, cm^{-1}) ν: 2967, 2905, 1653, 1648, 1375, 1364, 1334.

(3-(tert-Butyl)-1-(((tert-butyldimethylsilyl)oxy)methyl)-8-methoxyisoquinolin-2(1H)-yl)(pyridin-2-yl)methanone (2ga). N-(2-((tert-Butyldimethylsilyl)oxy)-1-(2-methoxyphenyl)ethyl)picolinamide (193 mg, 0.50 mmol), 3,3-dimethyl-1-butyne (185 μL, 1.50 mmol, 3 equiv), Co(dpm)$_2$ (42.5 mg, 0.10 mmol, 20 mol %), NaOPiv (75 mg, 0.60 mmol, 1.2 equiv), Mn(OAc)$_3$·2H$_2$O (268 mg, 1.00 mmol, 2 equiv), and MeOH (5 mL) were mixed for 20 h at 80 °C under an O$_2$ atmosphere. After column chromatography (gradient petroleum ether/EtOAc from 8:1 to 6:1, then 4:1), 127 mg (55%) of a yellowish oil was obtained. R_f = 0.48 (petroleum ether/EtOAc 3:1). The product was isolated as a single regioisomer. The structure was confirmed by 2D-NMR (COSY, NOESY, see attached NMR data). ^{1}H NMR (400 MHz, CDCl$_3$, ppm): δ 8.72−8.64 (m, 1H), 7.90 (d, J = 7.4 Hz, 1H), 7.74 (td, J = 7.7, 1.7 Hz, 1H), 7.36 (ddd, J = 7.6, 4.8, 1.1 Hz, 1H), 7.15 (t, J = 7.9 Hz, 1H), 6.76 (d, J = 7.5 Hz, 1H), 6.65 (d, J = 8.1 Hz, 1H), 6.54 (s, 1H), 5.53−5.33 (m, 1H), 3.70 (dd, J = 10.5, 9.2 Hz, 1H), 3.63 (s, 3H), 3.52 (dd, J = 10.6, 4.7 Hz, 1H), 1.38 (s, 9H), 0.91 (s, 9H), 0.01 (s, 3H), −0.01 (s, 3H). ^{13}C{^{1}H} NMR (100 MHz, CDCl$_3$, ppm): δ 171.6, 154.8, 154.0, 149.9, 149.7, 136.3, 133.5, 128.5, 124.8, 124.5, 120.7, 118.5, 118.1, 109.5, 61.1, 55.5, 55.2, 36.8, 30.9, 26.1, 18.5, −5.39, −5.40. HR-MS (ESI-TOF) m/z: calcd for [M + H]$^+$ C$_{27}$H$_{39}$N$_2$O$_3$Si, 467.2730; found, 467.2747. FT-IR (thin film, cm^{-1}) ν: 2952, 2858, 1674, 1474, 1259, 1104.

(3-(tert-Butyl)-1-(((tert-butyldimethylsilyl)oxy)methyl)-8-fluoroisoquinolin-2(1H)-yl)(pyridin-2-yl)methanone (2ha). N-(2-((tert-Butyldimethylsilyl)oxy)-1-(2-fluorophenyl)ethyl)picolinamide (187 mg, 0.50 mmol), 3,3-dimethyl-1-butyne (185 μL, 1.50 mmol, 3 equiv), Co(dpm)$_2$ (42.5 mg, 0.10 mmol, 20 mol %), NaOPiv (75 mg, 0.60 mmol, 1.2 equiv), Mn(OAc)$_3$·2H$_2$O (268 mg, 1.00 mmol, 2 equiv), and MeOH (5 mL) were mixed for 24 h at 80 °C under an O$_2$ atmosphere. After column chromatography (gradient petroleum ether/EtOAc from 6:1 to 4:1), 169 mg (74%) of a yellowish oil was obtained. R_f = 0.52 (petroleum ether/EtOAc 4:1). The product

was isolated as a single regioisomer. The structure was confirmed by 2D-NMR (COSY, NOESY, see attached NMR data). ^{1}H NMR (400 MHz, CDCl$_3$, ppm): δ 8.79−8.60 (m, 1H), 7.86−7.73 (m, 2H), 7.40 (ddd, J = 7.4, 4.8, 1.4 Hz, 1H), 7.16 (td, J = 8.0, 5.6 Hz, 1H), 6.93 (d, J = 7.5 Hz, 1H), 6.79 (t, J = 9.1 Hz, 1H), 6.59 (d, J = 1.7 Hz, 1H), 5.47 (t, J = 7.2 Hz, 1H), 3.92 (dd, J = 10.0, 7.7 Hz, 1H), 3.65 (dd, J = 10.1, 6.8 Hz, 1H), 1.38 (s, 9H), 0.85 (s, 9H), −0.04 (s, 3H), −0.06 (s, 3H). ^{13}C{^{1}H} NMR (100 MHz, CDCl$_3$, ppm): δ 171.4, 158.4 (d, $J_{C−F}$ = 245.8 Hz), 153.4, 150.9, 149.5, 136.8, 134.2, (d, $J_{C−F}$ = 4.9 Hz), 129.0 (d, $J_{C−F}$ = 8.4 Hz), 125.4, 124.7, 121.4 (d, $J_{C−F}$ = 2.9 Hz), 119.5 (d, $J_{C−F}$ = 17.5 Hz), 117.6 (d, $J_{C−F}$ = 3.4 Hz), 113.8 (d, $J_{C−F}$ = 21.9 Hz), 61.5, 54.5, 36.9, 30.9, 26.0, 18.4, −5.49, −5.52. ^{19}F NMR (376 MHz, CDCl$_3$, ppm): δ −121.12. HR-MS (ESI-TOF) m/z: calcd for [M + H]$^{+}$ C$_{26}$H$_{36}$N$_2$O$_2$SiF, 455.2530; found, 455.2543. FT-IR (thin film, cm^{-1}) ν: 2957, 2930, 2858, 1653, 1465, 1250, 1111, 1082.

(3-(tert-Butyl)-1-(((tert-butyldimethylsilyl)oxy)methyl)-7-methylisoquinolin-2(1H)-yl)(pyridin-2-yl)methanone (2ia). N-(2-((tert-Butyldimethylsilyl)oxy)-1-(3-methylphenyl)ethyl)picolinamide (185 mg, 0.50 mmol), 3,3-dimethyl-1-butyne (185 μL, 1.50 mmol, 3 equiv), Co(dpm)$_2$ (42.5 mg, 0.10 mmol, 20 mol %), NaOPiv (75 mg, 0.60 mmol, 1.2 equiv), Mn(OAc)$_3$·2H$_2$O (268 mg, 1.00 mmol, 2 equiv), and MeOH (5 mL) were mixed for 24 h at 80 °C under an O$_2$ atmosphere. After column chromatography (gradient petroleum ether/EtOAc from 6:1 to 3:1), 176 mg (78%) of a yellowish oil was obtained. R_f = 0.71 (petroleum ether/EtOAc 3:1). The product was isolated as a single regioisomer. The structure was confirmed by 2D-NMR (COSY, NOESY, see attached NMR data). ^{1}H NMR (400 MHz, CDCl$_3$, ppm): δ 8.70 (dt, J = 4.8, 1.3 Hz, 1H), 7.84−7.71 (m, 2H), 7.42−7.34 (m, 1H), 7.07−6.97 (m, 2H), 6.68 (s, 1H), 6.53 (s, 1H), 5.08−4.82 (m, 1H), 3.95 (dd, J = 9.8, 7.4 Hz, 1H), 3.59 (dd, J = 9.8, 7.6 Hz, 1H), 2.23 (s, 3H), 1.37 (s, 9H), 0.85 (s, 9H), −0.08 (s, 3H), −0.09 (s, 3H). ^{13}C{^{1}H} NMR (100 MHz, CDCl$_3$, ppm): δ 171.2, 153.9, 149.4, 148.4, 136.8, 136.3, 132.7, 129.0, 128.6, 127.4, 125.6, 125.2, 124.7, 118.0, 62.3, 60.8, 36.6, 31.0, 25.9, 21.3, 18.4, −5.48, −5.53. HR-MS (ESI-TOF) m/z: calcd for [M + H]$^{+}$ C$_{27}$H$_{39}$N$_2$O$_2$Si, 451.2781; found, 451.2794. FT-IR (thin film, cm^{-1}) ν: 2956, 2928, 2858, 1660, 1388, 1364, 1258, 1113.

(3-(tert-Butyl)-1-(((tert-butyldimethylsilyl)oxy)methyl)-7-trifluoromethylisoquinolin-2(1H)-yl)(pyridin-2-yl)methanone (2ja). N-(2-((tert-Butyldimethylsilyl)oxy)-1-(3-trifluoromethylphenyl)ethyl)picolinamide (212 mg, 0.50 mmol), 3,3-dimethyl-1-butyne (185 μL, 1.50 mmol, 3 equiv), Co(dpm)$_2$ (42.5 mg, 0.10 mmol, 20 mol %), NaOPiv (75 mg, 0.60 mmol, 1.2 equiv), Mn(OAc)$_3$·2H$_2$O (268 mg, 1.00 mmol, 2 equiv), and MeOH (5 mL) were mixed for 24 h at 80 °C under an O$_2$ atmosphere. After column chromatography (gradient petroleum ether/EtOAc from 6:1 to 4:1), 165 mg (65%) of a yellowish oil was obtained. R_f = 0.77 (petroleum ether/EtOAc 3:1). The product was isolated as a single regioisomer. The structure was confirmed by 2D-NMR (COSY, NOESY, see attached NMR data). ^{1}H NMR (400 MHz, CDCl$_3$, ppm): δ 8.71 (dt, J = 4.8, 1.3 Hz, 1H), 7.87−7.74 (m, 2H), 7.51−7.38 (m, 2H), 7.22 (d, J = 7.9 Hz, 1H), 7.13 (s, 1H), 6.60 (s, 1H), 5.11 (dd, J = 8.6, 6.5 Hz, 1H), 4.08 (dd, J = 9.4, 6.4 Hz, 1H), 3.69−3.58 (m, 1H), 1.37 (s, 9H), 0.82 (s, 9H), −0.10 (s, 3H), −0.12 (s, 3H). ^{13}C{^{1}H} NMR (100 MHz, CDCl$_3$, ppm): δ 171.2, 153.1, 152.6, 149.2, 137.2, 134.8, 133.3, 128.2 (q, $J_{C−F}$ = 32.4 Hz), 125.8, 125.7, 125.2, 124.9 (q, $J_{C−F}$ = 3.8 Hz), 124.3 (q, $J_{C−F}$ = 272.0 Hz), 124.0 (q, $J_{C−F}$ = 3.7 Hz), 117.1, 61.9, 60.3, 37.1, 31.0, 25.9, 18.3, −5.5, −5.6. ^{19}F NMR (376 MHz, CDCl$_3$, ppm): δ −62.29. HR-MS (ESI-TOF) m/z: calcd for [M + H]$^{+}$ C$_{27}$H$_{36}$N$_2$O$_2$SiF$_3$, 505.2498; found, 505.2511. FT-IR (thin film, cm^{-1}) ν: 2958, 2930, 2859, 1661, 1331, 1164, 1131, 1125, 1070.

(3-(tert-Butyl)-1-(((tert-butyldimethylsilyl)oxy)methyl)-6-methylisoquinolin-2(1H)-yl)(pyridin-2-yl)methanone (2ka). N-(2-((tert-Butyldimethylsilyl)oxy)-1-(4-methylphenyl)ethyl)picolinamide (185 mg, 0.50 mmol), 3,3-dimethyl-1-butyne (185 μL, 1.50 mmol, 3 equiv), Co(dpm)$_2$ (42.5 mg, 0.10 mmol, 20 mol %), NaOPiv (75 mg, 0.60 mmol, 1.2 equiv), Mn(OAc)$_3$·2H$_2$O (268 mg, 1.00 mmol, 2 equiv), and MeOH (5 mL) were mixed for 16 h at 80 °C under an O$_2$ atmosphere. After column chromatography (gradient petroleum ether/EtOAc from 6:1 to 4:1), 202 mg (90%) of a yellowish oil

was obtained. R_f = 0.44 (petroleum ether/EtOAc 4:1). The product was isolated as a single regioisomer. The structure was confirmed by 2D-NMR (COSY, NOESY, see attached NMR data). ^{1}H NMR (400 MHz, CDCl$_3$, ppm): δ 8.69 (dd, J = 5.4, 1.9 Hz, 1H), 7.84−7.70 (m, 2H), 7.42−7.35 (m, 1H), 6.96 (s, 1H), 6.87 (d, J = 7.6 Hz, 1H), 6.75 (d, J = 7.6 Hz, 1H), 6.52 (s, 1H), 5.09−4.87 (m, 1H), 3.93 (dd, J = 9.8, 7.4 Hz, 1H), 3.57 (dd, J = 9.8, 7.4 Hz, 1H), 2.29 (s, 3H), 1.36 (s, 9H), 0.86 (s, 9H), −0.06 (s, 3H), −0.07 (s, 3H). ^{13}C{^{1}H} NMR (100 MHz, CDCl$_3$, ppm): δ 171.3, 153.9, 149.5, 149.4, 137.6, 136.7, 131.6, 130.0, 127.2, 126.5, 126.4, 125.2, 124.7, 118.2, 62.5, 60.6, 36.7, 31.0, 26.0, 21.3, 18.5, −5.4, −5.5. HR-MS (ESI-TOF) m/z: calcd for [M + H]$^{+}$ C$_{27}$H$_{39}$N$_2$O$_2$Si, 451.2781; found, 451.2786. FT-IR (thin film, cm^{-1}) ν: 2956, 2928, 2858, 1661, 1653, 1364, 1111.

(3-(tert-Butyl)-1-(((tert-butyldimethylsilyl)oxy)methyl)-6-methoxyisoquinolin-2(1H)-yl)(pyridin-2-yl)methanone (2la). N-(2-((tert-Butyldimethylsilyl)oxy)-1-(4-methoxyphenyl)ethyl)picolinamide (161 mg, 0.41 mmol), 3,3-dimethyl-1-butyne (150 μL, 1.23 mmol, 3 equiv), Co(dpm)$_2$ (34 mg, 0.08 mmol, 20 mol %), NaOPiv (62 mg, 0.50 mmol, 1.2 equiv), Mn(OAc)$_3$·2H$_2$O (220 mg, 0.82 mmol, 2 equiv), and MeOH (4 mL) were mixed for 16 h at 80 °C under an O$_2$ atmosphere. After column chromatography (gradient petroleum ether/EtOAc from 6:1 to 4:1), 143 mg (75%) of a yellowish oil was obtained. R_f = 0.33 (petroleum ether/EtOAc 4:1). The product was isolated as a single regioisomer. The structure was confirmed by 2D-NMR (COSY, NOESY, see attached NMR data). ^{1}H NMR (400 MHz, CDCl$_3$, ppm): δ 8.74−8.65 (m, 1H), 7.82−7.72 (m, 2H), 7.42−7.37 (m, 1H), 6.77 (d, J = 8.3 Hz, 1H), 6.69 (d, J = 2.5 Hz, 1H), 6.61 (dd, J = 8.3, 2.6 Hz, 1H), 6.53 (s, 1H), 4.95 (t, J = 6.9 Hz, 1H), 3.94 (dd, J = 9.8, 7.3 Hz, 1H), 3.77 (s, 3H), 3.57 (dd, J = 9.8, 7.6 Hz, 1H), 1.37 (s, 9H), 0.85 (s, 9H), −0.07 (s, 3H), −0.08 (s, 3H). ^{13}C{^{1}H} NMR (100 MHz, CDCl$_3$, ppm): δ 171.3, 159.4, 153.8, 150.1, 149.4, 136.8, 132.9, 127.6, 125.3, 125.2, 124.8, 118.2, 112.4, 110.7, 62.5, 60.3, 55.5, 36.8, 31.0, 26.0, 18.4, −5.4, −5.5. HR-MS (ESI-TOF) m/z: calcd for [M + H]$^{+}$ C$_{27}$H$_{39}$N$_2$O$_3$Si, 467.2730; found, 467.2736. FT-IR (thin film, cm^{-1}) ν: 2955, 2930, 2858, 1653, 1246, 1154, 1110.

(3-(tert-Butyl)-1-(((tert-butyldimethylsilyl)oxy)methyl)-6-(methoxymethoxy)isoquinolin-2(1H)-yl)(pyridin-2-yl)methanone (2ma). N-(2-((tert-Butyldimethylsilyl)oxy)-1-(4-methoxymethoxyphenyl)ethyl)pico-linamide (208 mg, 0.50 mmol), 3,3-dimethyl-1-butyne (185 μL, 1.50 mmol, 3 equiv), Co(dpm)$_2$ (42.5 mg, 0.10 mmol, 20 mol %), NaOPiv (75 mg, 0.60 mmol, 1.2 equiv), Mn(OAc)$_3$·2H$_2$O (268 mg, 1.00 mmol, 2 equiv), and MeOH (5 mL) were mixed for 20 h at 80 °C under an O$_2$ atmosphere. After column chromatography (gradient petroleum ether/EtOAc from 6:1 to 4:1), 209 mg (84%) of a yellowish oil was obtained. R_f = 0.31 (petroleum ether/EtOAc 4:1). The product was isolated as a single regioisomer. The structure was confirmed by 2D-NMR (COSY, NOESY, see attached NMR data). ^{1}H NMR (400 MHz, CDCl$_3$, ppm): δ 8.73−8.64 (m, 1H), 7.85−7.63 (m, 2H), 7.43−7.35 (m, 1H), 6.85 (d, J = 2.3 Hz, 1H), 6.81−6.69 (m, 2H), 6.53 (s, 1H), 5.17−5.09 (m, 2H), 4.96 (t, J = 6.8 Hz, 1H), 3.93 (dd, J = 9.8, 7.3 Hz, 1H), 3.57 (dd, J = 9.8, 7.5 Hz, 1H), 3.45 (s, 3H), 1.36 (s, 9H), 0.86 (s, 9H), −0.06 (s, 3H), −0.07 (s, 3H). ^{13}C{^{1}H} NMR (100 MHz, CDCl$_3$, ppm): δ 171.3, 157.0, 153.8, 150.1, 149.4, 136.8, 132.9, 127.5, 126.5, 125.3, 124.8, 118.2, 114.6, 113.3, 94.6, 62.4, 60.3, 56.0, 36.8, 31.0, 26.0, 18.4, −5.4, −5.5. HR-MS (ESI-TOF) m/z: calcd for [M + H]$^{+}$ C$_{28}$H$_{41}$N$_2$O$_4$Si, 497.2836; found, 497.2840. FT-IR (thin film, cm^{-1}) ν: 2955, 2929, 2857, 1653, 1241, 1152, 1112.

(3-(tert-Butyl)-1-(((tert-butyldimethylsilyl)oxy)methyl)-6-trifluoromethoxyisoquinolin-2(1H)-yl)(pyridin-2-yl)methanone (2na). N-(2-((tert-Butyldimethylsilyl)oxy)-1-(4-trifluoromethoxyphenyl)ethyl)-picolin-amide (260 mg, 0.50 mmol), 3,3-dimethyl-1-butyne (185 μL, 1.50 mmol, 3 equiv), Co(dpm)$_2$ (42.5 mg, 0.10 mmol, 20 mol %), NaOPiv (75 mg, 0.60 mmol, 1.2 equiv), Mn(OAc)$_3$·2H$_2$O (268 mg, 1.00 mmol, 2 equiv), and MeOH (5 mL) were mixed for 17 h at 80 °C under an O$_2$ atmosphere. After column chromatography (gradient petroleum ether/EtOAc from 6:1 to 4:1), 194 mg (75%) of a yellowish oil was obtained. R_f = 0.52 (petroleum ether/EtOAc 4:1). The product was isolated as a single regioisomer. The structure was

confirmed by 2D-NMR (COSY, NOESY, see attached NMR data). ^{1}H NMR (400 MHz, CDCl₃, ppm): δ 8.70 (dd, J = 3.7, 2.4 Hz, 1H), 7.88−7.74 (m, 2H), 7.47−7.37 (m, 1H), 7.00 (s, 1H), 6.94−6.84 (m, 2H), 6.54 (s, 1H), 5.06 (t, J = 7.4 Hz, 1H), 4.01 (dd, J = 9.6, 6.8 Hz, 1H), 3.62 (dd, J = 9.6, 8.3 Hz, 1H), 1.37 (s, 9H), 0.83 (s, 9H), −0.09 (s, 3H), −0.10 (s, 3H). ¹³C{¹H} NMR (100 MHz, CDCl₃, ppm): δ 171.3, 153.3, 151.6, 149.0 (q, J_{C-F} = 1.8 Hz), 137.1, 133.4, 131.3, 128.2, 125.6, 125.0, 120.6 (q, J_{C-F} = 257.0 Hz), 118.8, 118.0, 117.2, 62.0, 60.1, 36.9, 31.0, 25.9, 18.4, −5.47, −5.54. ¹⁹F NMR (376 MHz, CDCl₃, ppm): δ −57.84. HR-MS (ESI-TOF) m/z: calcd for [M + H]⁺ C₂₇H₃₆N₂O₃F₃Si, 521.2447; found, 521.2458. FT-IR (thin film, cm⁻¹) ν: 2957, 2930, 2859, 1662, 1260, 1168, 1118.

(3-(tert-Butyl)-1-(((tert-butyldimethylsilyl)oxy)methyl)-6-fluoroisoquinolin-2(1H)-yl)(pyridin-2-yl)methanone (2oa). N-(2-((tert-Butyldimethylsilyl)oxy)-1-(4-fluorophenyl)ethyl)picolinamide (187 mg, 0.50 mmol), 3,3-dimethyl-1-butyne (185 μL, 1.50 mmol, 3 equiv), Co(dpm)₂ (42.5 mg, 0.10 mmol, 20 mol %), NaOPiv (75 mg, 0.60 mmol, 1.2 equiv), Mn(OAc)₃·2H₂O (268 mg, 1.00 mmol, 2 equiv), and MeOH (5 mL) were mixed for 24 h at 80 °C under an O₂ atmosphere. After column chromatography (gradient petroleum ether/EtOAc from 6:1 to 4:1), 151 mg (66%) of a yellowish oil was obtained. R_f = 0.76 (petroleum ether/EtOAc 2:1). The product was isolated as a single regioisomer. The structure was confirmed by 2D-NMR (COSY, NOESY, see attached NMR data). ¹H NMR (400 MHz, CDCl₃, ppm): δ 8.70 (dt, J = 4.8, 1.3 Hz, 1H), 7.83−7.74 (m, 2H), 7.44−7.37 (m, 1H), 6.87−6.78 (m, 2H), 6.75 (td, J = 8.5, 2.5 Hz, 1H), 6.51 (s, 1H), 5.02 (t, J = 7.3 Hz, 1H), 3.98 (dd, J = 9.6, 6.9 Hz, 1H), 3.59 (dd, J = 9.6, 8.1 Hz, 1H), 1.36 (s, 9H), 0.84 (s, 9H), −0.08 (s, 3H), −0.09 (s, 3H). ¹³C{¹H} NMR (100 MHz, CDCl₃, ppm): δ 171.3, 162.6 (d, J_{C-F} = 244.7 Hz), 153.5, 151.1, 149.3, 137.0, 133.5 (d, J_{C-F} = 8.6 Hz), 128.6 (d, J_{C-F} = 2.8 Hz), 128.2 (d, J_{C-F} = 8.5 Hz), 125.5, 124.9, 117.5 (d, J_{C-F} = 2.3 Hz), 113.0 (d, J_{C-F} = 21.9 Hz), 112.2 (d, J_{C-F} = 22.3 Hz), 62.2, 60.1, 36.9, 31.0, 26.0, 18.4, −5.4, −5.5. ¹⁹F NMR (376 MHz, CDCl₃, ppm): δ −114.98. HR-MS (ESI-TOF) m/z: calcd for [M + H]⁺ C₂₆H₃₆N₂O₂SiF, 455.2530; found, 455.2540. FT-IR (thin film, cm⁻¹) ν: 2956, 2929, 2858, 1662, 1652, 1365, 1240, 1146, 1109.

(3-(tert-Butyl)-1-(((tert-butyldimethylsilyl)oxy)methyl)-6-bromoisoquinolin-2(1H)-yl)(pyridin-2-yl)methanone (2pa). N-(2-((tert-Butyldimethylsilyl)oxy)-1-(4-bromophenyl)ethyl)picolinamide (202 mg, 0.46 mmol), 3,3-dimethyl-1-butyne (170 μL, 1.38 mmol, 3 equiv), Co(dpm)₂ (39 mg, 0.092 mmol, 20 mol %), NaOPiv (69 mg, 0.55 mmol, 1.2 equiv), Mn(OAc)₃·2H₂O (247 mg, 0.92 mmol, 2 equiv), and MeOH (5 mL) were mixed for 16 h at 80 °C under an O₂ atmosphere. After column chromatography (gradient petroleum ether/EtOAc from 6:1 to 4:1), 165 mg (70%) of a yellowish oil was obtained. R_f = 0.50 (petroleum ether/EtOAc 4:1). The product was isolated as a single regioisomer. The structure was confirmed by 2D-NMR (COSY, NOESY, see attached NMR data). ¹H NMR (400 MHz, CDCl₃, ppm): δ 8.76−8.61 (m, 1H), 7.83−7.71 (m, 2H), 7.45−7.35 (m, 1H), 7.28 (d, J = 1.9 Hz, 1H), 7.18 (dd, J = 8.0, 1.9 Hz, 1H), 6.74 (d, J = 8.0 Hz, 1H), 6.50 (s, 1H), 5.01 (t, J = 7.1 Hz, 1H), 3.98 (dd, J = 9.6, 6.8 Hz, 1H), 3.62−3.56 (m, 1H), 1.35 (s, 9H), 0.83 (s, 9H), −0.07 (s, 3H), −0.08 (s, 3H). ¹³C{¹H} NMR (100 MHz, CDCl₃, ppm): δ 171.2, 153.3, 151.3, 149.2, 137.0, 133.6, 131.6, 129.2, 128.4, 128.3, 125.5, 124.9, 121.6, 117.0, 62.0, 60.2, 36.9, 30.9, 26.0, 18.4, −5.4, −5.5. HR-MS (ESI-TOF) m/z: calcd for [M + H]⁺ C₂₆H₃₆N₂O₂BrSi, 515.1729; found, 515.1742. FT-IR (thin film, cm⁻¹) ν: 2957, 2929, 2858, 1662, 1653, 1365, 1111.

(6-(tert-Butyl)-4-(((tert-butyldimethylsilyl)oxy)methyl)thieno[3,2-c]pyridin-5(4H)-yl)(pyridin-2-yl)methanone (2qa). N-(2-((tert-Butyldimethylsilyl)oxy)-1-(thiophen-3-yl)ethyl)picolinamide (181 mg, 0.50 mmol), 3,3-dimethyl-1-butyne (185 μL, 1.50 mmol, 3 equiv), Co(dpm)₂ (42.5 mg, 0.10 mmol, 20 mol %), NaOPiv (75 mg, 0.60 mmol, 1.2 equiv), Mn(OAc)₃·2H₂O (268 mg, 1.00 mmol, 2 equiv), and MeOH (5 mL) were mixed for 16 h at 80 °C under an O₂ atmosphere. After column chromatography (gradient petroleum ether/EtOAc from 6:1 to 4:1), 185 mg (84%) of a yellowish oil was obtained. An unseperable mixture of regioisomers (3.1:1) was obtained. R_f = 0.54 (petroleum ether/EtOAc 3:1). Note! NMR

signals of major regioisomers are given. ¹H NMR (400 MHz, CDCl₃, ppm): δ 8.74−8.67 (m, 1H), 7.84−7.73 (m, 2H), 7.42−7.38 (m, 1H), 7.02 (d, J = 5.0 Hz, 1H), 6.65 (d, J = 5.0 Hz, 1H), 6.58 (s, 1H), 5.19−5.06 (m, 1H), 3.93 (dd, J = 9.6, 7.0 Hz, 1H), 3.61 (dd, J = 9.6, 7.9 Hz, 1H), 1.34 (s, 9H), 0.86 (s, 9H), −0.05 (s, 3H), −0.07 (s, 3H). ¹³C{¹H} NMR (100 MHz, CDCl₃, ppm): δ 171.8, 153.6, 149.4, 147.1, 136.9, 133.8, 133.6, 125.8, 125.4, 125.0, 123.0, 112.6, 62.0, 58.1, 36.9, 31.1, 26.0, 18.4, −5.4, −5.6. HR-MS (ESI-TOF) m/z: calcd for [M + H]⁺ C₂₄H₃₅N₂O₂SSi, 443.2189; found, 443.2199. FT-IR (thin film, cm⁻¹) ν: 2956, 2928, 2858, 1655, 1364, 1257, 1113.

(3-(tert-Butyl)-1-(2-((tert-butyldimethylsilyl)oxy)ethyl)-isoquinolin-2(1H)-yl)(pyridin-2-yl)methanone (2ra). N-(3-((tert-Butyldimethylsilyl)oxy)-1-phenylpropyl)picolinamide (185 mg, 0.50 mmol), 3,3-dimethyl-1-butyne (185 μL, 1.50 mmol, 3 equiv; additional 93 μL, 0.75 mmol, 1.5 equiv after 16 h), Co(dpm)₂ (42.5 mg, 0.10 mmol, 20 mol %), NaOPiv (75 mg, 0.60 mmol, 1.2 equiv), Mn(OAc)₃·2H₂O (268 mg, 1.00 mmol, 2 equiv), and MeOH (5 mL) were mixed for 40 h at 80 °C under an O₂ atmosphere. After column chromatography (gradient petroleum ether/EtOAc from 6:1 to 4:1), 160 mg (71%) of a yellowish oil was obtained. R_f = 0.51 (petroleum ether/EtOAc 4:1). The product was isolated as a single regioisomer. The structure was confirmed by 2D-NMR (COSY, NOESY, see attached NMR data). ¹H NMR (400 MHz, CDCl₃, ppm): δ 8.69 (dd, J = 6.0, 1.2 Hz, 1H), 7.75 (td, J = 7.7, 1.7 Hz, 1H), 7.57 (d, J = 7.8 Hz, 1H), 7.37 (ddd, J = 7.6, 4.8, 1.2 Hz, 1H), 7.21−7.11 (m, 2H), 7.05 (td, J = 7.3, 1.6 Hz, 1H), 6.81 (d, J = 7.4 Hz, 1H), 6.59 (s, 1H), 5.20−5.02 (m, 1H), 3.66 (ddd, J = 10.3, 6.3, 3.8 Hz, 1H), 3.40 (dd, J = 20.2, 4.9 Hz, 1H), 2.28−2.18 (m, 1H), 1.80−1.72 (m, 1H), 1.39 (s, 9H), 0.84 (s, 9H), 0.02 (s, 3H), −0.00 (s, 3H). ¹³C{¹H} NMR (100 MHz, CDCl₃, ppm): δ 171.5, 154.2, 149.6, 149.0, 137.0, 134.6, 131.3, 127.6, 126.5, 126.0, 125.4, 125.1, 124.2, 118.2, 59.5, 56.5, 36.6, 35.1, 31.0, 26.1, 18.3, −5.2, −5.3. HR-MS (ESI-TOF) m/z: calcd for [M + H]⁺ C₂₇H₃₉N₂O₂Si, 451.2781; found, 451.2786. FT-IR (thin film, cm⁻¹) ν: 2955, 2857, 1653, 1098.

(1-(((tert-Butyldimethylsilyl)oxy)methyl)-3-cyclopropylisoquinolin-2(1H)-yl)(pyridin-2-yl)methanone (2ab). N-(2-((tert-Butyldimethylsilyl)oxy)-1-phenylethyl)picolinamide (178 mg, 0.50 mmol), cyclopropylacetylene (127 μL, 1.50 mmol, 3 equiv), Co(dpm)₂ (42.5 mg, 0.10 mmol, 20 mol %), NaOPiv (75 mg, 0.60 mmol, 1.2 equiv), Mn(OAc)₃·2H₂O (268 mg, 1.00 mmol, 2 equiv), and MeOH (5 mL) were mixed for 20 h at 80 °C under an O₂ atmosphere. After column chromatography (gradient petroleum ether/EtOAc from 6:1 to 4:1), 154 mg (73%) of a yellowish oil was obtained. R_f = 0.40 (petroleum ether/EtOAc 3:1). The product was isolated as a single regioisomer. The structure was confirmed by 2D-NMR (COSY, NOESY, see attached NMR data). ¹H NMR (400 MHz, CDCl₃, ppm): δ 8.61 (d, J = 4.3 Hz, 1H), 7.75 (td, J = 7.7, 1.7 Hz, 1H), 7.67 (d, J = 7.7 Hz, 1H), 7.33 (ddd, J = 7.4, 4.9, 1.1 Hz, 1H), 7.25−7.16 (m, 1H), 7.17−7.08 (m, 2H), 7.06 (d, J = 7.4 Hz, 1H), 5.98 (s, 1H), 5.85−5.35 (m, 1H), 3.85−3.67 (m, 1H), 3.61 (dd, J = 9.8, 7.1 Hz, 1H), 0.92−0.79 (m, 10H), 0.65−0.48 (m, 3H), 0.48−0.31 (m, 1H), −0.10 (s, 6H). ¹³C{¹H} NMR (100 MHz, CDCl₃, ppm): δ 168.1, 155.3, 148.8, 140.7, 136.7, 132.0, 131.4, 127.9, 127.3, 126.5, 124.9, 124.8, 124.4, 117.7, 62.8, 57.7, 25.9, 18.3, 16.3, 10.3, 7.8, −5.5, −5.6. HR-MS (ESI-TOF) m/z: calcd for [M + H]⁺ C₂₅H₃₃N₂O₂Si, 421.2311; found, 421.2315. FT-IR (thin film, cm⁻¹) ν: 2953, 2928, 2857, 1655, 1251, 1108.

(1-(((tert-Butyldimethylsilyl)oxy)methyl)-3,4-dimethylisoquinolin-2(1H)-yl)(pyridin-2-yl)methanone (2ac). N-(2-((tert-Butyldimethylsilyl)oxy)-1-phenylethyl)picolinamide (178 mg, 0.50 mmol), 2-butyne (60 μL, 0.75 mmol, 1.50 equiv), Co(dpm)₂ (42.5 mg, 0.10 mmol, 20 mol %), NaOPiv (75 mg, 0.60 mmol, 1.2 equiv), Mn(OAc)₃·2H₂O (268 mg, 1.00 mmol, 2 equiv), and MeOH (5 mL) were mixed for 16 h at 80 °C under an O₂ atmosphere. After column chromatography (gradient petroleum ether/EtOAc from 6:1 to 4:1), 142 mg (70%) of a yellowish oil was obtained. R_f = 0.25 (petroleum ether/EtOAc 4:1). Note! Because of restricted rotation about the amide bond, the signals observed in ¹NMR are broad and coupling resolution is low; some proton signals are split (see comparison of ¹H-NMR spectra at RT and 65 °C). Better quality ¹H NMR spectra were

obtained at 65 °C (due to the hardware limitations, 65 °C is the maximum temperature). ^{1}H NMR (400 MHz, C$_2$D$_2$Cl$_4$, 65 °C, ppm): δ 8.65 (d, J = 4.5 Hz, 1H), 7.80 (td, J = 7.7, 1.7 Hz, 1H), 7.68 (d, J = 7.7 Hz, 1H), 7.47–7.29 (m, 3H), 7.24–7.15 (m, 1H), 7.16–6.95 (m, 1H), 5.68–5.02 (m, 1H), 4.00–3.78 (m, 1H), 3.69 (dd, J = 9.7, 7.3 Hz, 1H), 2.12 (s, 3H), 1.96 (br s, 3H), 0.88 (s, 9H), −0.04 (s, 3H), −0.05 (s, 3H). ^{13}C{^{1}H} NMR (100 MHz, C$_2$D$_2$Cl$_4$, list of peaks given due to the split carbon signals caused by rotamers, ppm): δ 168.1, 166.4, 154.2, 153.5, 148.8, 136.8, 132.9, 132.6, 130.2, 128.5, 127.7, 126.9, 126.3, 124.8, 124.0, 122.7, 121.6, 120.2, 118.2, 62.3, 59.9, 56.1, 25.7, 21.0, 18.1, 17.7, 13.8, −5.6, −5.8. HR-MS (ESI-TOF) m/z: calcd for [M + H]$^+$ C$_{24}$H$_{33}$N$_2$O$_2$Si, 409.2311; found, 409.2315. FT-IR (thin film, cm^{-1}) ν: 2952, 2929, 2857, 1653, 1394, 1250, 1112.

(S)-(1-(((tert-Butyldimethylsilyl)oxy)methyl)-3,4-dimethylisoquinolin-2(1H)-yl)(pyridin-2-yl)methanone ((S)-2ac). (S)-N-(2-((tert-Butyldimethylsilyl)oxy)-1-phenylethyl)picolinamide (178 mg, 0.50 mmol), 2-butyne (118 μL, 1.50 mmol, 3 equiv), Co(dpm)$_2$ (42.5 mg, 0.10 mmol, 20 mol %), NaOPiv (75 mg, 0.60 mmol, 1.2 equiv), Mn(OAc)$_3$·2H$_2$O (268 mg, 1.00 mmol, 2 equiv), and MeOH (5 mL) were mixed for 16 h at 80 °C under an O$_2$ atmosphere. After column chromatography (gradient petroleum ether/EtOAc from 6:1 to 4:1), 142 mg (70%) of a yellowish oil was obtained. R$_f$ = 0.25 (petroleum ether/EtOAc 4:1). ee = >99% (see attached HPLC data). The NMR data matched that of racemate. $[\alpha]_D^{20}$ −429.2 (c = 0.917, CHCl$_3$).

(1-(((tert-Butyldimethylsilyl)oxy)methyl)-3,4-diethylisoquinolin-2(1H)-yl)(pyridin-2-yl)methanone (2ad). N-(2-((tert-Butyldimethylsilyl)oxy)-1-phenylethyl)picolinamide (178 mg, 0.50 mmol), hex-3-yne (169 μL, 1.50 mmol, 3 equiv), Co(dpm)$_2$ (42.5 mg, 0.10 mmol, 20 mol %), NaOPiv (75 mg, 0.60 mmol, 1.2 equiv), Mn(OAc)$_3$·2H$_2$O (268 mg, 1.00 mmol, 2 equiv), and MeOH (5 mL) were mixed for 16 h at 80 °C under an O$_2$ atmosphere. After column chromatography (gradient petroleum ether/EtOAc from 6:1 to 4:1), 167 mg (76%) of a yellowish oil was obtained. R$_f$ = 0.33 (petroleum ether/EtOAc 4:1). Note! Because of restricted rotation about the amide bond, the signals observed in ^{1}NMR are broad and coupling resolution is low; some proton signals are split (see comparison of ^{1}H NMR spectra at RT and 65 °C). Better quality ^{1}H NMR spectra were obtained at 65 °C (due to the hardware limitations, 65 °C is the maximum temperature). ^{1}H NMR (400 MHz, C$_2$D$_2$Cl$_4$, 65 °C, ppm): δ 8.65 (d, J = 4.4 Hz, 1H), 7.78 (td, J = 7.7, 1.5 Hz, 1H), 7.66 (d, J = 7.5 Hz, 1H), 7.42–7.29 (m, 3H), 7.18 (t, J = 7.2 Hz, 1H), 7.15–6.87 (m, 1H), 5.55–4.77 (m, 1H), 4.03–3.79 (m, 1H), 3.66 (dd, J = 9.5, 7.9 Hz, 1H), 3.19–1.73 (m, 4H), 1.19 (t, J = 7.5 Hz, 3H), 1.17–1.04 (m, 3H), 0.87 (s, 9H), 0.02––0.28 (m, 6H). ^{13}C{^{1}H} NMR (100 MHz, C$_2$D$_2$Cl$_4$, list of peaks given due to the split carbon signals caused by rotamers, ppm): δ 168.5, 166.9, 153.7, 148.9, 136.6, 135.7, 134.8, 133.3, 131.6, 127.7, 127.3, 127.2, 126.9, 126.2, 124.8, 124.1, 123.6, 122.7, 62.1, 59.6, 55.9, 25.7, 22.1, 20.6, 18.1, 14.0, 13.1, −5.6, −5.8. HR-MS (ESI-TOF) m/z: calcd for [M + H]$^+$ C$_{26}$H$_{37}$N$_2$O$_2$Si, 437.2624; found, 437.2629. FT-IR (thin film, cm^{-1}) ν: 2959, 2928, 2856, 1649, 1391, 1112.

(1-(((tert-Butyldimethylsilyl)oxy)methyl)-3,4-dipropylisoquinolin-2(1H)-yl)(pyridin-2-yl)methanone (2ae). N-(2-((tert-Butyldimethylsilyl)oxy)-1-phenylethyl)picolinamide (178 mg, 0.50 mmol), oct-4-yne (110 μL, 1.50 mmol, 3 equiv), Co(dpm)$_2$ (42.5 mg, 0.10 mmol, 20 mol %), NaOPiv (75 mg, 0.60 mmol, 1.2 equiv), Mn(OAc)$_3$·2H$_2$O (268 mg, 1.00 mmol, 2 equiv), and MeOH (5 mL) were mixed for 16 h at 80 °C under an O$_2$ atmosphere. After column chromatography (gradient petroleum ether/EtOAc from 6:1 to 4:1), 185 mg (80%) of a yellowish oil was obtained. R$_f$ = 0.36 (petroleum ether/EtOAc 4:1). Note! Because of restricted rotation about the amide bond, the signals observed in ^{1}NMR are broad and coupling resolution is low; some proton signals are split (see comparison of ^{1}H NMR spectra at RT and 65 °C). Better quality ^{1}H NMR spectra were obtained at 65 °C (due to the hardware limitations, 65 °C is the maximum temperature). ^{1}H NMR (400 MHz, C$_2$D$_2$Cl$_4$, 65 °C, ppm): δ 8.65 (d, J = 4.4 Hz, 1H), 7.78 (td, J = 7.7, 1.6 Hz, 1H), 7.64 (d, J = 7.4 Hz, 1H), 7.42–7.28 (m, 3H), 7.17 (t, J = 7.1 Hz, 1H), 7.14–6.88 (m, 1H), 5.46–4.85 (m, 1H), 4.04–3.85 (m, 1H), 3.70–3.57 (m, 1H), 2.68–2.46 (m, 3H), 1.75–1.39 (m, 5H), 1.06 (t, J = 7.3 Hz,

3H), 1.00–0.91 (m, 3H), 0.87 (s, 9H), 0.11––0.23 (m, 6H). ^{13}C{^{1}H} NMR (100 MHz, C$_2$D$_2$Cl$_4$, ppm): δ 168.5, 153.7, 148.9, 136.6, 135.1, 133.2, 131.9, 127.7, 127.2, 126.2, 124.9, 124.1, 123.4, 122.9, 62.1, 59.7, 56.0, 31.3, 29.6, 25.7, 22.6, 21.7, 18.1, 14.4, −5.7, −5.8. HR-MS (ESI-TOF) m/z: calcd for [M + H]$^+$ C$_{28}$H$_{41}$N$_2$O$_2$Si, 465.2937; found, 465.2946. FT-IR (thin film, cm^{-1}) ν: 2957, 2929, 2871, 1653, 1391, 1112.

(1-(((tert-Butyldimethylsilyl)oxy)methyl)-3-phenylisoquinolin-2(1H)-yl)(pyridin-2-yl)methanone (2af). N-(2-((tert-Butyldimethylsilyl)oxy)-1-phenylethyl)picolinamide (178 mg, 0.50 mmol), phenylacetylene (82 μL, 0.75 mmol, 1.5 equiv), Co(dpm)$_2$ (42.5 mg, 0.10 mmol, 20 mol %), NaOPiv (75 mg, 0.60 mmol, 1.2 equiv), Mn(OAc)$_3$·2H$_2$O (268 mg, 1.00 mmol, 2 equiv), and MeOH (5 mL) were mixed for 16 h at 80 °C under an O$_2$ atmosphere. After column chromatography (gradient petroleum ether/EtOAc from 6:1 to 4:1), 167 mg (73%) of a yellowish oil was obtained. R$_f$ = 0.27 (petroleum ether/EtOAc 4:1). The product was isolated as a single regioisomer. The structure was confirmed by 2D-NMR (COSY, NOESY, see attached NMR data). Note! Because of restricted rotation about the amide bond, the signals observed in ^{1}NMR are broad and coupling resolution is low; some proton signals are split (see 2D-NOESY NMR for crosspeaks). ^{1}H NMR spectra at 65 °C did not improve the coupling resolution quality (due to the hardware limitations, 65 °C is the maximum temperature). ^{1}H NMR (400 MHz, CDCl$_3$, ppm): δ 8.39–8.16 (m, 1H), 7.46–7.15 (m, 8H), 7.07–6.88 (m, 4H), 6.36–6.22 (m, 1H), 6.16–5.87 (m, 1H), 3.99–3.83 (m, 1H), 3.77 (dd, J = 10.1, 6.4 Hz, 1H), 0.89 (s, 9H), 0.08––0.10 (m, 6H). ^{13}C{^{1}H} NMR (100 MHz, C$_2$D$_2$Cl$_4$, ppm): δ 168.2, 154.3, 147.7, 138.9, 138.3, 136.0, 132.3, 131.3, 128.1, 127.9, 127.5, 127.3, 127.2, 126.8, 125.6, 124.2, 124.0, 114.5, 62.3, 56.7, 25.7, 18.0, −5.6, −5.7. HR-MS (ESI-TOF) m/z: calcd for [M + H]$^+$ C$_{28}$H$_{33}$N$_2$O$_2$Si, 457.2311; found, 457.2318. FT-IR (thin film, cm^{-1}) ν: 2957, 2928, 2856, 1661, 1653, 1363, 1111.

(S)-(1-(((tert-Butyldimethylsilyl)oxy)methyl)-3-phenylisoquinolin-2(1H)-yl)(pyridin-2-yl)methanone ((S)-2af). (S)-N-(2-((tert-Butyldimethylsilyl)oxy)-1-phenylethyl)picolinamide (178 mg, 0.50 mmol), phenylacetylene (82 μL, 0.75 mmol, 1.5 equiv), Co(dpm)$_2$ (42.5 mg, 0.10 mmol, 20 mol %), NaOPiv (75 mg, 0.60 mmol, 1.2 equiv), Mn(OAc)$_3$·2H$_2$O (268 mg, 1.00 mmol, 2 equiv), and MeOH (5 mL) were mixed for 16 h at 80 °C under an O$_2$ atmosphere. After column chromatography (gradient petroleum ether/EtOAc from 6:1 to 4:1), 160 mg (70%) of a yellowish oil was obtained. R$_f$ = 0.27 (petroleum ether/EtOAc 4:1). The product was isolated as a single regioisomer. ee = >99% (see attached HPLC data). The NMR data matched that of racemate. $[\alpha]_D^{20}$ −264.6 (c = 0.923, CHCl$_3$).

(1-(((tert-Butyldimethylsilyl)oxy)methyl)-3-(4-methoxyphenyl)-isoquinolin-2(1H)-yl)(pyridin-2-yl)methanone (2ag). N-(2-((tert-Butyldimethylsilyl)oxy)-1-phenylethyl)picolinamide (178 mg, 0.50 mmol), 4-methoxyphenylacetylene (97 μL, 0.75 mmol, 1.5 equiv), Co(dpm)$_2$ (42.5 mg, 0.10 mmol, 20 mol %), NaOPiv (75 mg, 0.60 mmol, 1.2 equiv), Mn(OAc)$_3$·2H$_2$O (268 mg, 1.00 mmol, 2 equiv), and MeOH (5 mL) were mixed for 17 h at 80 °C under an O$_2$ atmosphere. After column chromatography (gradient petroleum ether/EtOAc from 6:1 to 4:1, then 2:1), 215 mg (88%) of a yellowish oil was obtained. R$_f$ = 0.66 (petroleum ether/EtOAc 1:1). The product was isolated as a single regioisomer. The structure was confirmed by 2D-NMR (COSY, NOESY, see attached NMR data). Note! Because of restricted rotation about the amide bond, the signals observed in ^{1}NMR are broad and coupling resolution is low; some proton signals are split (see comparison of ^{1}H NMR spectra at RT and 65 °C and 2D-NOESY NMR for crosspeaks). ^{1}H NMR spectra at 65 °C did not improve the coupling resolution quality (due to the hardware limitations, 65 °C is the maximum temperature). ^{1}H NMR (400 MHz, C$_2$D$_2$Cl$_4$, ppm): δ 8.40–8.15 (m, 1H), 7.43–7.26 (m, 5H), 7.24–7.09 (m, 3H), 7.04–6.95 (m, 1H), 6.69–6.50 (m, 2H), 6.21 (s, 1H), 6.03–5.91 (m, 1H, overlapped with C$_2$D$_2$Cl$_4$), 3.94–3.83 (m, 1H), 3.78–3.62 (m, 4H), 0.92 (s, 9H), 0.03 (s, 3H), −0.03 (s, 3H). ^{13}C{^{1}H} NMR (100 MHz, C$_2$D$_2$Cl$_4$, ppm): δ 168.3, 158.7, 154.5, 149.8, 137.9, 135.9, 135.5, 132.3, 131.8, 131.5, 130.6, 128.2, 128.0, 127.3, 126.9, 125.4, 123.9, 113.2, 62.2, 56.7, 55.3, 25.8, 18.0,

−5.6, −5.7. HR-MS (ESI-TOF) m/z: calcd for $[M + H]^+$ $C_{29}H_{34}N_2O_3Si$, 487.2417; found, 487.2415. FT-IR (thin film, cm^{-1}) ν: 2954, 2929, 2856, 1653, 1507, 1249, 1180, 1111.

(1-(((tert-Butyldimethylsilyl)oxy)methyl)-3-(4-nitrophenyl)-isoquinolin-2(1H)-yl)(pyridin-2-yl)methanone (2ah). N-(2-((tert-Butyldimethylsilyl)oxy)-1-phenylethyl)picolinamide (178 mg, 0.50 mmol), 4-nitrophenylacetylene (110 mg, 0.75 mmol, 1.5 equiv), Co(dpm)$_2$ (42.5 mg, 0.10 mmol, 20 mol %), NaOPiv (75 mg, 0.60 mmol, 1.2 equiv), Mn(OAc)$_3$·2H$_2$O (268 mg, 1.00 mmol, 2 equiv), and MeOH (5 mL) were mixed for 16 h at 80 °C under an O$_2$ atmosphere. After column chromatography (gradient petroleum ether/EtOAc from 6:1 to 4:1, then 2:1), 125 mg (50%) of a yellow oil was obtained. R_f = 0.30 (petroleum ether/EtOAc 3:1). The product was isolated as a single regioisomer. The structure was confirmed by 2D-NMR (COSY, NOESY, see attached NMR data). Note! Because of restricted rotation about the amide bond, the signals observed in ^{1}NMR are broad and coupling resolution is low; some proton signals are split (see 2D-NOESY NMR for crosspeaks and comparison of ^{1}H NMR spectra at RT and 65 °C). ^{1}H NMR spectra at 65 °C did not improve the coupling resolution quality (due to the hardware limitations, 65 °C is the maximum temperature). ^{1}H NMR (400 MHz, C$_2$D$_2$Cl$_4$, 65 °C, ppm): δ 8.63−8.19 (m, 1H), 8.17−6.72 (m, 11H), 6.72−6.27 (m, 1H), 6.18−5.69 (m, 1H, overlapped with C$_2$D$_2$Cl$_4$), 4.24−3.86 (m, 1H), 3.89−3.72 (m, 1H), 0.92 (s, 9H), 0.25 to −0.25 (m, 6H). ^{13}C{^{1}H} NMR (100 MHz, C$_2$D$_2$Cl$_4$, ppm): δ 167.4, 153.6, 147.9, 146.1, 145.7, 136.5, 136.4, 132.5, 130.8, 129.3, 127.3, 127.0, 126.2, 126.1, 124.6, 123.8, 123.1, 117.5, 62.8, 56.7, 25.8, 18.0, −5.6, −5.7. HR-MS (ESI-TOF) m/z: calcd for $[M + H]^+$ $C_{28}H_{32}N_3O_4Si$, 502.2162; found, 502.2166. FT-IR (thin film, cm^{-1}) ν: 2954, 2929, 2856, 1662, 1595, 1520, 1343, 1108.

(E)-(1-(((tert-Butyldimethylsilyl)oxy)methyl)-3-(4-nitrophenyl)-8-(4-nitrostyryl)isoquinolin-2(1H)-yl)(pyridin-2-yl)methanone (2ah′). In addition to the major product described above, 52 mg (16%) of a minor product as a yellow oil was obtained. R_f = 0.20 (petroleum ether/EtOAc 3:1). Note! Because of restricted rotation about the amide bond, the signals observed in ^{1}NMR are broad and coupling resolution is low; some proton signals are split (see 2D-NOESY NMR for crosspeaks). ^{1}H NMR (400 MHz, C$_2$D$_2$Cl$_4$, ppm): δ 8.32−8.22 (m, 3H), 8.00−7.84 (m, 2H), 7.82−7.62 (m, 4H), 7.60−7.50 (m, 2H), 7.51−7.40 (m, 2H), 7.41−7.28 (m, 2H), 7.17 (d, J = 16.0 Hz, 1H), 7.11−6.99 (m, 1H), 6.58 (dd, J = 8.7, 5.1 Hz, 1H), 6.50 (s, 1H), 3.86 (t, J = 10.1 Hz, 1H), 3.74 (dd, J = 10.9, 4.9 Hz, 1H), 0.92 (s, 9H), 0.18−−0.22 (m, 6H). ^{13}C{^{1}H} NMR (100 MHz, C$_2$D$_2$Cl$_4$, ppm): δ 167.4, 153.5, 147.8, 146.8, 146.2, 145.5, 143.3, 142.0, 136.6, 133.9, 131.6, 130.7, 130.0, 128.7, 128.5, 127.4, 127.2, 126.8, 126.1, 124.8, 124.7, 124.1, 123.2, 117.5, 61.2, 53.1, 25.7, 18.0, −5.4, −5.6. HR-MS (ESI-TOF) m/z: calcd for $[M + H]^+$ $C_{36}H_{37}N_4O_6Si$, 649.2482; found, 649.2490. FT-IR (thin film, cm^{-1}) ν: 2965, 2828, 2847, 1595, 1519, 1341, 1109.

(1-(((tert-Butyldimethylsilyl)oxy)methyl)-3-(4-ethynylphenyl)-isoquinolin-2(1H)-yl)(pyridin-2-yl)methanone (2ai). N-(2-((tert-Butyldimethylsilyl)oxy)-1-phenylethyl)picolinamide (178 mg, 0.50 mmol), 1,4-diethynylbenzene (95 mg, 0.75 mmol, 1.5 equiv), Co(dpm)$_2$ (42.5 mg, 0.10 mmol, 20 mol %), NaOPiv (75 mg, 0.60 mmol, 1.2 equiv), Mn(OAc)$_3$·2H$_2$O (268 mg, 1.00 mmol, 2 equiv), and MeOH (5 mL) were mixed for 16 h at 80 °C under an O$_2$ atmosphere. After column chromatography (gradient petroleum ether/EtOAc from 6:1 to 4:1), 130 mg (54%) of a yellowish oil was obtained. R_f = 0.40 (petroleum ether/EtOAc 3:1). The product was isolated as a single regioisomer. The structure was confirmed by 2D-NMR (COSY, NOESY, see attached NMR data). Note! Because of restricted rotation about the amide bond, the signals observed in ^{1}NMR are broad and coupling resolution is low; some proton signals are split. ^{1}H NMR spectra at 65 °C did not improve the coupling resolution quality (due to the hardware limitations, 65 °C is the maximum temperature). ^{1}H NMR (400 MHz, C$_2$D$_2$Cl$_4$, 65 °C, ppm): δ 8.52−8.19 (m, 1H), 8.14−6.89 (m, 11H), 6.70−6.22 (m, 1H), 6.17−5.67 (m, 1H, overlapped with C$_2$D$_2$Cl$_4$), 4.25−3.85 (m, 1H), 3.79 (dd, J = 10.1, 6.2 Hz, 1H), 3.12 (s, 1H), 0.92 (s, 9H), 0.22−−0.31 (m, 6H). ^{13}C{^{1}H} NMR (100 MHz, C$_2$D$_2$Cl$_4$, ppm): δ 167.9,

154.1, 147.8, 139.5, 137.5, 136.2, 132.4, 131.6, 131.2, 128.1, 127.5, 127.1, 126.6, 125.8, 124.3, 124.2, 120.7, 115.3, 83.5, 78.1, 62.5, 56.7, 25.7, 18.0, −5.6, −5.7. HR-MS (ESI-TOF) m/z: calcd for $[M + H]^+$ $C_{30}H_{33}N_2O_2Si$, 481.2311; found, 481.2319. FT-IR (thin film, cm^{-1}) ν: 2955, 2930, 2857, 1653, 1363, 1111.

(1-(((tert-Butyldimethylsilyl)oxy)methyl)-3-(thiophen-3-yl)-isoquinolin-2(1H)-yl)(pyridin-2-yl)methanone (2aj). N-(2-((tert-Butyldimethylsilyl)oxy)-1-phenylethyl)picolinamide (178 mg, 0.50 mmol), 3-ethynylthiophene (149 μL, 1.50 mmol, 3 equiv), Co(dpm)$_2$ (42.5 mg, 0.10 mmol, 20 mol %), NaOPiv (75 mg, 0.60 mmol, 1.2 equiv), Mn(OAc)$_3$·2H$_2$O (268 mg, 1.00 mmol, 2 equiv), and MeOH (5 mL) were mixed for 16 h at 80 °C under an O$_2$ atmosphere. After column chromatography (gradient petroleum ether/EtOAc from 6:1 to 4:1), 150 mg (65%) of a yellowish oil was obtained. R_f = 0.55 (petroleum ether/EtOAc 2:1). The product was isolated as a single regioisomer. The structure was confirmed by 2D-NMR (COSY, NOESY, see attached NMR data). Note! Because of restricted rotation about the amide bond, the signals observed in ^{1}NMR are broad and coupling resolution is low; some proton signals are split. ^{1}H NMR spectra at 65 °C did not improve the coupling resolution quality (due to the hardware limitations, 65 °C is the maximum temperature). ^{1}H NMR (400 MHz, C$_2$D$_2$Cl$_4$, 65 °C, ppm): δ 8.55−8.26 (m, 1H), 7.62−7.49 (m, 1H), 7.45−7.22 (m, 5H), 7.23−6.84 (m, 4H), 6.54−6.25 (m, 1H), 6.05−5.62 (m, 1H, overlapped with C$_2$D$_2$Cl$_4$), 4.06−3.86 (m, 1H), 3.80 (dd, J = 10.0, 6.8 Hz, 1H), 0.91 (s, 9H), 0.19−−0.18 (m, 6H). ^{13}C{^{1}H} NMR (100 MHz, C$_2$D$_2$Cl$_4$, ppm): δ 168.0, 154.2, 147.9, 140.5, 136.0, 133.5, 132.5, 131.2, 128.0, 127.4, 127.1, 126.4, 125.5, 124.1, 123.8, 122.8, 113.4, 62.3, 56.8, 25.8, 18.1, −5.6, −5.7. HR-MS (ESI-TOF) m/z: calcd for $[M + H]^+$ $C_{26}H_{31}N_2O_2SiS$, 463.1876; found, 463.1877. FT-IR (thin film, cm^{-1}) ν: 2957, 2927, 2856, 1653, 1507, 1111.

(1-(((tert-Butyldimethylsilyl)oxy)methyl)-3,4-diphenylisoquinolin-2(1H)-yl)(pyridin-2-yl)methanone (2ak). N-(2-((tert-Butyldimethylsilyl)oxy)-1-phenylethyl)picolinamide (178 mg, 0.50 mmol), diphenylacetylene (134 mg, 0.75 mmol, 1.5 equiv), Co(dpm)$_2$ (42.5 mg, 0.10 mmol, 20 mol %), NaOPiv (75 mg, 0.60 mmol, 1.2 equiv), Mn(OAc)$_3$·2H$_2$O (268 mg, 1.00 mmol, 2 equiv), and MeOH (5 mL) were added for 16 h at 80 °C under an O$_2$ atmosphere. After column chromatography (gradient petroleum ether/EtOAc from 6:1 to 4:1), 205 mg (77%) of a yellowish oil was obtained. R_f = 0.25 (petroleum ether/EtOAc 4:1). Note! Because of restricted rotation about the amide bond,[3,5] some of the signals observed in ^{1}NMR are broad and coupling resolution is low; some proton signals are split (see 2D-NOESY NMR for crosspeaks). ^{1}H NMR (400 MHz, C$_2$D$_2$Cl$_4$, ppm): δ 8.34 (d, J = 4.0 Hz, 1H), 7.44−7.07 (m, 11H), 7.03−6.95 (m, 1H), 6.87−6.69 (m, 5H), 6.06−5.98 (m, 1H, overlapped with C$_2$D$_2$Cl$_4$), 4.23−4.05 (m, 1H), 3.93 (dd, J = 10.2, 6.3 Hz, 1H), 0.98 (s, 9H), 0.13 (s, 3H), 0.08 (s, 3H). ^{13}C{^{1}H} NMR (100 MHz, CDCl$_3$, ppm): δ 163.3, 155.4, 147.9, 138.8, 137.0, 136.1, 134.3, 133.2, 132.3, 131.2, 130.2, 128.2, 127.9, 127.3, 127.2, 127.0, 126.7, 126.6, 125.8, 123.9, 123.7, 63.2, 56.7, 26.1, 18.5, −5.2, −5.4. HR-MS (ESI-TOF) m/z: calcd for $[M + H]^+$ $C_{34}H_{37}N_2O_2Si$, 533.2624; found, 533.2632. FT-IR (thin film, cm^{-1}) ν: 2957, 2930, 2857, 1663, 1112.

(S)-(1-(((tert-Butyldimethylsilyl)oxy)methyl)-3,4-diphenylisoquinolin-2(1H)-yl)(pyridin-2-yl)methanone ((S)-2ak). (S)-N-(2-((tert-Butyldimethylsilyl)oxy)-1-phenylethyl)picolinamide (178 mg, 0.50 mmol), diphenylacetylene (134 mg, 0.75 mmol, 1.5 equiv), Co(dpm)$_2$ (42.5 mg, 0.10 mmol, 20 mol %), NaOPiv (75 mg, 0.60 mmol, 1.2 equiv), Mn(OAc)$_3$·2H$_2$O (268 mg, 1.00 mmol, 2 equiv), and MeOH (5 mL) were mixed for 16 h at 80 °C under an O$_2$ atmosphere. After column chromatography (gradient petroleum ether/EtOAc from 6:1 to 4:1), 177 mg (67%) of a yellowish oil was obtained. R_f = 0.25 (petroleum ether/EtOAc 4:1). ee = >99% (see attached HPLC data). The NMR data matched that of racemate. $[\alpha]_D^{20}$ −385.4 (c = 0.773, CHCl$_3$).

(3,4-Bis(4-bromophenyl)-1-(((tert-butyldimethylsilyl)oxy)-methyl)isoquinolin-2(1H)-yl)(pyri-din-2-yl)methanone (2al). N-(2-((tert-Butyldimethylsilyl)oxy)-1-phenylethyl)picolinamide (178 mg, 0.50 mmol), bis(4-bromophenyl)acetylene (252 mg, 0.75 mmol, 1.5

equiv), Co(dpm)₂ (42.5 mg, 0.10 mmol, 20 mol %), NaOPiv (75 mg, 0.60 mmol, 1.2 equiv), Mn(OAc)₃·2H₂O (268 mg, 1.00 mmol, 2 equiv), and MeOH (5 mL) were mixed for 16 h at 80 °C under an O₂ atmosphere. After column chromatography (gradient petroleum ether/EtOAc from 6:1 to 4:1), 261 mg (76%) of a white powder was obtained. R_f = 0.33 (petroleum ether/EtOAc 3:1). Note! Because of restricted rotation about the amide bond,[3,5] some of the signals observed in ¹NMR are broad and coupling resolution is low; some proton signals are split. ¹H NMR spectra at 65 °C did not improve the coupling resolution quality (due to the hardware limitations, 65 °C is the maximum temperature). ¹H NMR (400 MHz, C₂D₂Cl₄, ppm): δ 8.65–8.14 (m, 1H), 7.50–7.19 (m, 7H), 7.12–7.00 (m, 3H), 6.95–6.87 (m, 2H), 6.76–6.70 (m, 1H), 6.11–5.94 (m, 1H, overlapped with C₂D₂Cl₄), 4.17–3.96 (m, 1H), 3.93–3.82 (m, 1H), 0.97 (s, 9H), 0.17 (s, 3H), 0.10 (s, 3H). ¹³C{¹H} NMR (100 MHz, C₂D₂Cl₄, ppm): δ 168.6, 154.6, 147.6, 137.1, 136.3, 135.0, 133.5, 132.4, 132.1, 131.9, 131.5, 131.3, 130.1, 128.0, 127.7, 127.0, 125.4, 125.2, 124.1, 123.8, 121.1, 120.8, 62.9, 56.3, 25.8, 18.1, −5.4, −5.6. HR-MS (ESI-TOF) m/z: calcd for [M + H]⁺ C₃₄H₃₅N₂O₂SiBr₂, 689.0828; found, 689.0835. FT-IR (thin film, cm⁻¹) $ν$: 2955, 2929, 2857, 1668, 1389, 1108.

(1-(((tert-Butyldimethylsilyl)oxy)methyl)-4-methyl-3-phenylisoquinolin-2(1H)-yl)(pyridin-2-yl)methanone (2am). N-(2-((tert-Butyldimethylsilyl)oxy)-1-phenylethyl)picolinamide (178 mg, 0.50 mmol), 1-phenyl-1-propyne (94 μL, 0.75 mmol, 1.5 equiv), Co(dpm)₂ (42.5 mg, 0.10 mmol, 20 mol %), NaOPiv (75 mg, 0.60 mmol, 1.2 equiv), Mn(OAc)₃·2H₂O (268 mg, 1.00 mmol, 2 equiv), and MeOH (5 mL) were mixed for 16 h at 80 °C under an O₂ atmosphere. After column chromatography (gradient petroleum ether/EtOAc from 6:1 to 4:1), 171 mg (73%) of a yellowish oil was obtained. R_f = 0.22 (petroleum ether/EtOAc 4:1). The product was isolated as a single regioisomer. The structure was confirmed by 2D-NMR (COSY, NOESY, see attached NMR data). Note! Because of restricted rotation about the amide bond,[3,5] some of the signals observed in ¹NMR are broad and coupling resolution is low; some proton signals are split (see 2D-NOESY NMR for crosspeaks). ¹H NMR (400 MHz, C₂D₂Cl₄, ppm): δ 8.30 (d, J = 4.4 Hz, 1H), 7.48–7.17 (m, 6H), 7.08–6.98 (m, 5H), 6.81 (d, J = 7.7 Hz, 1H), 5.91 (t, J = 7.0 Hz, 1H), 4.01–3.89 (m, 1H), 3.81 (dd, J = 10.3, 6.1 Hz, 1H), 2.06 (s, 3H), 0.93 (s, 9H), 0.07 (s, 3H), 0.01 (s, 3H). ¹³C{¹H} NMR (100 MHz, C₂D₂Cl₄, ppm): δ 168.7, 155.1, 147.5, 138.4, 136.0, 133.8, 132.9, 132.6, 129.9, 128.0, 127.3, 127.2, 127.0, 126.8, 123.9, 123.6, 123.5, 118.7, 62.6, 56.0, 25.8, 18.0, 15.2, −5.6, −5.7. HR-MS (ESI-TOF) m/z: calcd for [M + H]⁺ C₂₉H₃₅N₂O₂Si, 471.2468; found, 471.2469. FT-IR (thin film, cm⁻¹) $ν$: 3060, 2954, 2929, 2857, 1653, 1388, 1363, 1117.

(1-(((tert-Butyldimethylsilyl)oxy)methyl)-3-(trimethylsilyl)-isoquinolin-2(1H)-yl)(pyridin-2-yl)methanone (2an). N-(2-((tert-Butyldimethylsilyl)oxy)-1-phenylethyl)picolinamide (178 mg, 0.50 mmol), trimethylsilylacetylene (213 μL, 1.50 mmol, 3 equiv), Co(dpm)₂ (42.5 mg, 0.10 mmol, 20 mol %), NaOPiv (75 mg, 0.60 mmol, 1.2 equiv), Mn(OAc)₃·2H₂O (268 mg, 1.00 mmol, 2 equiv), and MeOH (5 mL) were mixed for 16 h at 80 °C under an O₂ atmosphere. After column chromatography (gradient petroleum ether/EtOAc from 6:1 to 4:1), 160 mg (71%) of a yellowish oil was obtained. R_f = 0.80 (petroleum ether/EtOAc 2:1). The product was isolated as a single regioisomer. The structure was confirmed by 2D-NMR (COSY, NOESY, see attached NMR data).

Procedure for Gram-Scale Synthesis. A 100 mL pressure tube equipped with a magnetic stir bar was charged with N-(2-((tert-butyldimethylsilyl)oxy)-1-phenylethyl)picolinamide (1.00 g, 2.79 mmol), Co(dpm)₂ (238 mg, 0.56 mmol, 20 mol %), NaOPiv (415 mg, 3.35 mmol, 1.2 equiv), Mn(OAc)₃·2H₂O (1.50 g, 5.58 mmol, 2 equiv), and MeOH (28 mL). The reaction mixture was purged with O₂ for 30 s, then trimethylsilylacetylene (1.2 mL, 8.37 mmol, 3 equiv) was added, and the mixture was heated at 80 °C for 18 h. The reaction mixture was cooled to room temperature, and the solvent was evaporated. To the residue, potassium sodium tartrate (50 mL of 1 M aqueous solution) was added, and the mixture was extracted with EtOAc (3 × 50 mL). The combined organic phase was dried over

Na₂SO₄ and filtered, and the solvent was evaporated. After column chromatography (gradient petroleum ether/EtOAc from 6:1 to 4:1), 1.00 g (80%) of a yellowish oil was obtained. ¹H NMR (400 MHz, CDCl₃, ppm): δ 8.64 (ddd, J = 4.8, 1.7, 1.0 Hz, 1H), 7.84–7.71 (m, 2H), 7.42–7.33 (m, 1H), 7.25 (td, J = 7.5, 1.3 Hz, 1H), 7.20–7.12 (m, 2H), 7.00 (d, J = 7.3 Hz, 1H), 6.61 (s, 1H), 5.37 (t, J = 7.1 Hz, 1H), 3.89 (dd, J = 9.7, 7.9 Hz, 1H), 3.47 (dd, J = 9.7, 6.6 Hz, 1H), 0.78 (s, 9H), 0.33 (s, 9H), −0.11 (s, 3H), −0.16 (s, 3H). ¹³C{¹H} NMR (100 MHz, CDCl₃, ppm): δ 168.2, 154.2, 148.5, 142.0, 136.9, 132.2, 130.8, 128.2, 127.3, 128.1, 125.9, 125.2, 125.0, 124.8, 62.8, 59.5, 26.0, 18.4, 0.9, −5.49, −5.50. HR-MS (ESI-TOF) m/z: calcd for [M + H]⁺ C₂₅H₃₇N₂O₂Si₂, 453.2394; found, 453.2397. FT-IR (thin film, cm⁻¹) $ν$: 2952, 2929, 2857, 1647, 1405, 1246, 1118.

Synthesis of Tetrahydroisoquinolines (S,S)-3an and (S,S)-4an. *((1S,3S)-1-(((tert-Butyldimethylsilyl)oxy)methyl)-3-(trimethyl-silyl)-3,4-dihydroisoquinolin-2(1H)-yl)(pyridin-2-yl)methanone ((S,S)-3an).* Approximately 15−20 mL of ammonia was condensed in 50 mL flask equipped with a magnetic stir bar and cooled to −78 °C using an acetone/dry ice bath. Under an argon atmosphere, at −78 °C, (1-(((tert-butyldimethylsilyl)oxy)methyl)-3-(trimethyl-silyl)-isoquinolin-2(1H)-yl)(pyridin-2-yl)methanone (255 mg, 0.56 mmol) solution in THF (6 mL) was added followed by sodium (61 mg, 2.52 mmol, 4.5 equiv). The resulting mixture (dark blue) was stirred at −78 °C until complete conversion (TLC control). The resulting mixture was diluted with dist. H₂O (10 mL) and EtOAc (15 mL), allowed to warm to room temperature, and stirred with open cap until all liquid ammonia evaporated. The organic phase was separated, the aqueous phase was extracted with EtOAc (2 × 15 mL), dried over Na₂SO₄, filtered, and evaporated under reduced pressure. After column chromatography (petroleum ether/EtOAc 4:1), 175 mg (69%) of a yellowish oil was obtained. R_f = 0.50 (petroleum ether/EtOAc 4:1). Note! ¹H NMR analysis of the crude reaction mixture showed d.r. > 20/1. Only major diastereomer was collected. The structure of the major diastereomer was confirmed by 2D-NMR after directing group removal. ¹H NMR (400 MHz, CDCl₃, ppm): δ 8.61 (ddd, J = 4.8, 1.6, 0.9 Hz, 1H), 7.76 (td, J = 7.7, 1.8 Hz, 1H), 7.58 (dt, J = 7.8, 1.0 Hz, 1H), 7.33 (ddd, J = 7.6, 4.9, 1.2 Hz, 1H), 7.23−7.09 (m, 3H), 6.94 (d, J = 7.3 Hz, 1H), 5.04 (dd, J = 8.4, 6.1 Hz, 1H), 4.19 (dd, J = 9.5, 6.1 Hz, 1H), 3.96 (dd, J = 12.3, 7.2 Hz, 1H), 3.73 (dd, J = 9.4, 8.6 Hz, 1H), 3.08 (dd, J = 15.7, 12.4 Hz, 1H), 2.96 (dd, J = 15.9, 7.2 Hz, 1H), 0.75 (s, 9H), 0.20 (s, 9H), −0.14 (s, 3H), −0.18 (s, 3H). ¹³C{¹H} NMR (100 MHz, CDCl₃, ppm): δ 169.3, 155.5, 148.5, 136.9, 135.8, 135.6, 128.2, 127.8, 127.3, 126.0, 124.3, 124.1, 65.4, 60.8, 43.4, 29.5, 26.0, 18.4, −1.4, −5.5. HR-MS (ESI-TOF) m/z: calcd for [M + H]⁺ C₂₅H₃₉N₂O₂Si₂, 455.2550; found, 455.2564. FT-IR (thin film, cm⁻¹) $ν$: 2952, 2928, 2857, 1628, 1405, 1248, 1109. $[α]_D^{20}$ 66.5 (c = 1.140, CHCl₃).

(1S,3S)-1-(((tert-Butyldimethylsilyl)oxy)methyl)-3-(trimethylsilyl)-1,2,3,4-tetrahydroisoquinoline ((S,S)-4an). ((1S,3S)-1-(((tert-Butyldimethylsilyl)oxy)methyl)-3-(trimethylsilyl)-3,4-dihydroisoquinolin-2(1H)-yl)(pyridin-2-yl)methanone (147 mg, 0.32 mmol) was dissolved in THF (4 mL) under an argon atmosphere. The solution was cooled in a water/ice bath to 0 °C, and LiAlH₄ (18.4 mg, 0.48 mmol, 1.5 equiv) was added; then reaction mixture was stirred at 0 °C for 10 min (with incomplete conversion by TLC). The reaction was quenched with water (10 mL) and extracted with EtOAc (3 × 10 mL). The combined organic phase was dried over Na₂SO₄, filtered, and evaporated under reduced pressure to afford the crude product. After column chromatography (petroleum ether/EtOAc 10:1), 96 mg (86%) of a yellowish oil was obtained. R_f = 0.50 (petroleum ether/EtOAc 10:1). ee = >99% (see attached HPLC data; for ee determination compound was derivatized to N-benzoylderivative and TBS group was cleaved). ¹H NMR (400 MHz, CDCl₃, ppm): δ 7.19−7.01 (m, 4H), 4.18 (dd, J = 9.6, 3.6 Hz, 1H), 4.13−3.99 (m, 1H), 3.66 (dd, J = 9.4, 8.1 Hz, 1H), 2.86−2.76 (m, 1H), 2.62 (dd, J = 15.9, 2.8 Hz, 1H), 2.38 (dd, J = 12.6, 3.0 Hz, 1H), 1.80 (br s, 1H, overlapped with water), 0.88 (s, 9H), 0.10 (s, 9H), 0.07 (s, 3H), 0.02 (s, 3H). ¹³C{¹H} NMR (100 MHz, CDCl₃, ppm): δ 137.5, 136.5, 129.1, 126.1, 125.6, 125.1, 67.5, 59.1, 43.6, 31.8, 26.0, 18.4, −3.8, −5.1, −5.2. HR-MS (ESI-TOF) m/z: calcd for [M + H]⁺

$C_{19}H_{36}NOSi_2$, 350.2335; found, 350.2347. FT-IR (thin film, cm^{-1}) ν: 2954, 2929, 2857, 1472, 1249, 1100. $[\alpha]_D^{20}$ 58.3 (c = 1.080, CHCl$_3$).

■ ASSOCIATED CONTENT

ⓈI Supporting Information

The Supporting Information is available free of charge at https://pubs.acs.org/doi/10.1021/acs.joc.0c00207.

Optimization studies along with copies of the NMR spectra and HPLC chromatograms (PDF)

■ AUTHOR INFORMATION

Corresponding Author

Liene Grigorjeva − *Latvian Institute of Organic Synthesis LV-1006 Riga, Latvia;* ● orcid.org/0000-0003-3497-6776; Email: liene_grigorjeva@osi.lv

Authors

Jekaterina Bolsakova − *Latvian Institute of Organic Synthesis LV-1006 Riga, Latvia*

Lukass Lukasevics − *Latvian Institute of Organic Synthesis LV-1006 Riga, Latvia*

Complete contact information is available at:
https://pubs.acs.org/10.1021/acs.joc.0c00207

Notes

The authors declare no competing financial interest.

■ ACKNOWLEDGMENTS

■ REFERENCES

(1) Selected reviews on TM-catalyzed C−H functionatization: (a) Lyons, T. W.; Sanford, M. S. Palladium-Catalyzed Ligand-Directed C−H Functionalization Reactions. *Chem. Rev.* **2010**, *110*, 1147−1169. (b) Ackermann, L. Carboxylate-Assisted Transition-Metal-Catalyzed C−H Bond Functionalizations: Mechanism and Scope. *Chem. Rev.* **2011**, *111*, 1315−1345. (c) Chen, X.; Engle, K. M.; Wang, D.-H.; Yu, J.-Q. Palladium(II)-Catalyzed C−H Activation/C−C Cross-coupling Reactions: Versatility and Practicality. *Angew. Chem., Int. Ed.* **2009**, *48*, 5094−5115. (d) Baudoin, O. Transition Metal-Catalyzed Arylation of Unactivated C(sp^3)−H Bonds. *Chem. Soc. Rev.* **2011**, *40*, 4902−4911. (e) He, J.; Wasa, M.; Chan, K. S. L.; Shao, Q.; Yu, J.-Q. Palladium-Catalyzed Transformations of Alkyl C−H Bonds. *Chem. Rev.* **2017**, *117*, 8754−8786. (f) Ackermann, L. Carboxylate-Assisted Ruthenium-Catalyzed Alkyne Annulations by C−H/Het−H Bond Functionalizations. *Acc. Chem. Res.* **2014**, *47*, 281−295. (g) Baudoin, O. Ring Construction by Palladium(0)-Catalyzed C(sp^3)−H Activation. *Acc. Chem. Res.* **2017**, *50*, 1114−1123. (h) Colby, D. A.; Tsai, A. S.; Bergman, R. G.; Ellman, J. A. Rhodium Catalyzed Chelation-Assisted C−H Bond Functionalization Reactions. *Acc. Chem. Res.* **2012**, *45*, 814−825. (i) Gao, K.; Yoshikai, N. Low-Valent Cobalt Catalysis: New Opportunities for C−H Functionalization. *Acc. Chem. Res.* **2014**, *47*, 1208−1219. (j) Dwivedi, V.; Kalsi, D.; Sundararaju, B. Electrochemical-/ Photoredox Aspects of Transition Metal-Catalyzed Directed C−H Bond Activations. *ChemCatChem* **2019**, *11*, 5160−5187.

(2) Selected reviews on Co-catalyzed C−H functionatization: (a) Gandeepan, P.; Müller, T.; Zell, D.; Cera, G.; Warratz, S.; Ackermann, L. 3d Transition Metals for C−H Activation. *Chem. Rev.* **2019**, *119*, 2192−2452. (b) Ujwaldev, S. M.; Harry, N. A.; Divakar, M. A.; Anilkumar, G. Cobalt-Catalyzed C−H Activation: Recent Progress in Heterocyclic Chemistry. *Catal. Sci. Technol.* **2018**, *8*, 5983−6018. (c) Moselage, M.; Li, J.; Ackermann, L. Cobalt-Catalyzed

C-H Activation. *ACS Catal.* **2016**, *6*, 498−525. (d) Hyster, T. K. High-Valent Co(III)- and Ni(II)-Catalyzed C−H Activation. *Catal. Lett.* **2015**, *145*, 458−467. (e) Daugulis, O.; Roane, J.; Tran, L. D. Bidentate, Monoanionic Auxiliary-Directed Functionalization of Carbon-Hydrogen Bonds. *Acc. Chem. Res.* **2015**, *48*, 1053−1064. (f) Kommagalla, Y.; Chatani, N. Cobalt(II)-catalyzed C−H functionalization using an *N,N′*-bidentate directing group. *Coord. Chem. Rev.* **2017**, *350*, 117−135.

(3) Grigorjeva, L.; Daugulis, O. Cobalt-Catalyzed, Aminoquinoline-Directed C(sp^2)−H Bond Alkenylation by Alkynes. *Angew. Chem., Int. Ed.* **2014**, *53*, 10209−10212.

(4) Selected examples using Co(II) salts as pre-catalysts with bidentate directing group assistance: C−H functionalization with alkynes (a) Kalsi, D.; Dutta, S.; Barsu, N.; Rueping, M.; Sundararaju, B. Room-Temperature C−H Bond Functionalization by Merging Cobalt and Photoredox Catalysis. *ACS Catal.* **2018**, *8*, 8115−8120. (b) Nguyen, T. T.; Grigorjeva, L.; Daugulis, O. Cobalt-Catalyzed, Aminoquinoline-Directed Functionalization of Phosphinic Amide sp^2 C−H Bonds. *ACS Catal.* **2016**, *6*, 551−554. (c) Landge, V. G.; Midya, S. P.; Rana, J.; Shinde, D. R.; Balaraman, E. Expedient Cobalt-Catalyzed C−H Alkynylation of (Entantiopure) Benzylamines. *Org. Lett.* **2016**, *18*, 5252−5255. ; C−H functionalization with alkenes (d) Grigorjeva, L.; Daugulis, O. Cobalt-Catalyzed, Aminoquinoline-Directed Coupling of sp^2 C−H Bonds with Alkenes. *Org. Lett.* **2014**, *16*, 4684−4687. (e) Kalsi, D.; Barsu, N.; Chakrabarti, S.; Dahiya, P.; Rueping, M.; Sundararaju, B. C−H and N−H bond annulation of aryl amides with unactivated olefins by merging cobalt(III) and photo-redox catalysis. *Chem. Commun.* **2019**, *55*, 11626−11629. (f) Gandee-pan, P.; Rajamalli, P.; Cheng, C.-H. Diastereoselective [3+2] Annulation of Aromatic/Vinylic Amides with Bicyclic Alkenes through Cobalt-Catalyzed C−H Activation and Intramolecular Nucleophilic Addition. *Angew. Chem., Int. Ed.* **2016**, *55*, 4308−4311. ; C−H functionalization with allenes (g) Thrimurtulu, N.; Dey, A.; Maiti, D.; Volla, C. M. R. Cobalt-Catalyzed sp^2-C-H Activation: Intermolecular Heterocyclization with Allenes at Room Temperature. *Angew. Chem., Int. Ed.* **2016**, *55*, 12361−12365. (h) Thrimurtulu, N.; Nallagonda, R.; Volla, C. M. R. Cobalt-Catalyzed Aryl C−H Activation and Highly Regioselective Intermolecular Annulation of Sulfonamides with Allenes. *Chem. Commun.* **2017**, *53*, 1872−1875. ; C-H functionalization with isonitriles (i) Kalsi, D.; Barsu, N.; Sundararaju, B. CoIII-Catalyzed Isonitrile Insertion/Acyl Group Migration Between C−H and N−H bonds of Arylamides. *Chem.— Eur. J.* **2018**, *24*, 2360−2364. ; C−H functionalization CO or CO-surrogates (j) Grigorjeva, L.; Daugulis, O. Cobalt-Catalyzed Direct Carbonylation of Aminoquinoline Benzamides. *Org. Lett.* **2014**, *16*, 4688−4690. (k) Ni, J.; Li, J.; Fan, Z.; Zhang, A. Cobalt-Catalyzed Carbonylation of C(sp^2)−H Bonds with Azodicarboxylate as the Carbonyl Source. *Org. Lett.* **2016**, *18*, 5960−5963. (l) Nguyen, T. T.; Grigorjeva, L.; Daugulis, O. Aminoquinoline-Directed, Cobalt-Catalyzed Carbonylation of Sulfonamide sp^2 C−H Bonds. *Chem. Commun.* **2017**, *53*, 5136−5138.

(5) Cobalt-catalyzed, picolinamide directed benzamide reactions with alkynes: (a) Martínez, Á. M.; Rodríguez, N.; Gómez-Arrayás, R.; Carretero, J. C. Cobalt-Catalyzed *ortho*-C−H Functionalization/ Alkyne Annulation of Benzylamine Derivatives: Access to Dihydroisoquinolines. *Chem.—Eur. J.* **2017**, *23*, 11669−11676. (b) Kuai, C.; Wang, L.; Li, B.; Yang, Z.; Cui, X. Cobalt-Catalyzed Selective Synthesis of Isoquinolines Using Picolinamide as a Traceless Directing Group. *Org. Lett.* **2017**, *19*, 2102−2105. (c) Yao, Y.; Lin, Q.; Yang, W.; Yang, W.; Gu, F.; Guo, W.; Yang, D. Cobalt(II)-Catalyzed [4 + 2] Annulation of Picolinamides with Alkynes via C−H Bond Activation. *Chem.—Eur. J.* **2020**, DOI: 10.1002/chem.202000411.

(6) We tested the reported reaction conditions (refs[3,5a,b]) for cobalt catalyzed benzamide sp^2 C−H alkenylation with alkynes using our model substrate — *N*-(2-((tert-butyldimethylsilyl)oxy)-1-phenylethyl)picolinamide. Low reaction conversion was observed. See the Supporting Information for details.

(7) Scott, J. D.; Williams, R. M. Chemistry and Biology of the Tetrahydroisoquinoline Antitumor Antibiotics. *Chem. Rev.* **2002**, *102*, 1669−1730.

(8) Selected reviews on asymmetric synthesis of isoquinoline alkaloids: (a) Chrzanowska, M.; Rozwadowska, M. D. Asymmetric Synthesis of Isoquinoline Alkaloids. *Chem. Rev.* **2004**, *104*, 3341−3370. (b) Liu, W.; Liu, S.; Jin, R.; Guo, H.; Zhao, J. Novel Strategies for Catalytic Asymmetric Synthesis of C1-Chiral 1,2,3,4-Tetrahydroisoquinolines and 3,4-Dihydrotetrahydroisoquinolines. *Org. Chem. Front.* **2015**, *2*, 288−299. (c) Chrzanowska, M.; Grajewska, A.; Rozwadowska, M. D. Asymmetric Synthesis of Isoquinoline Alkaloids: 2004−2015. *Chem. Rev.* **2016**, *116*, 12369−12465.

(9) See the Supporting Information for details.

(10) Planas, O.; Whiteoak, C. J.; Martin-Diaconescu, V.; Gamba, I.; Luis, J. M.; Parella, T.; Company, A.; Ribas, X. Isolation of Key Organometallic Aryl-Co(III) Intermediates in Cobalt-Catalyzed $C(sp^2)$−H Functionalizations and New Insights into Alkyne Annulation Reaction Mechanisms. *J. Am. Chem. Soc.* **2016**, *138*, 14388−14397.

(11) Zeng, W.; Nukeyeva, M.; Wang, Q.; Jiang, C. Synthesis of unnatural α-amino acid derivatives *via* selective *o*-C-H functionalization. *Org. Biomol. Chem.* **2018**, *16*, 598−608.

(12) Yuan, J.; Liu, C.; Chen, Y.; Zhang, Z.; Yan, D.; Zhang, W. Rhodium-Catalyzed Intramolecular Hydroacylation of 1,2-Disubstituted Alkenes for the Synthesis of 2-Substituted Indanones. *Tetrahedron* **2019**, *75*, 269−277.

(13) Malkov, A. V.; Gouriou, L.; Lloyd-Jones, G. C.; Starý, I.; Langer, V.; Spoor, P.; Vinader, V.; Kočovský, P. Asymmetric Allylic Substitution Catalyzed by C_1-Symmetrical Complexes of Molybdenum: Structural Requirements of the Ligand and the Stereochemical Course of the Reaction. *Chem.—Eur. J.* **2006**, *12*, 6910−6929.

(14) Xu, Q.; Xie, H.; Zhang, E.-L.; Ma, X.; Chen, J.; Yu, X.-C.; Li, H. Selective Catalytic Hofmann *N*-Alkylation of Poor Nucleophilic Amines and Amides with Catalytic Amounts of Alkyl Halides. *Green Chem.* **2016**, *18*, 3940−3944.

Lukasevics, L.; Cizikovs, A.; Grigorjeva, L. Synthesis of 3-Hydroxymethyl Isoindolinones via Cobalt-Catalyzed C(sp^2)–H Carbonylation of Phenylglycinol Derivatives. *Org. Lett.* **2020**, *22* (7), 2720-2723.

Synthesis of 3-Hydroxymethyl Isoindolinones via Cobalt-Catalyzed C(sp²)−H Carbonylation of Phenylglycinol Derivatives

Lukass Lukasevics,[†] Aleksandrs Cizikovs,[†] and Liene Grigorjeva*

Read Online

ACCESS | 📊 Metrics & More | 📖 Article Recommendations | 🆂 Supporting Information

ABSTRACT: An efficient method for the synthesis of 3-hydroxymethyl isoindolinones via cobalt-catalyzed C(sp²)−H carbonylation of phenylglycinol derivatives using picolinamide as a traceless directing group is demonstrated. The reaction proceeds in the presence of a commercially available cobalt(II) tetramethylheptanedionate catalyst and employs DIAD as a "CO" surrogate. This synthetic route offers a broad substrate scope, excellent regioselectivity, and full preservation of the original stereochemistry. Besides, the developed method provides a pathway for accessing valuable enantiopure 3-substituted isoindolinone derivatives.

☐ 19 examples, yield up to 96%   ☐ good functional group tolerance
☐ picolinamide as a traceless DG   ☐ full preservation of original stereochemistry
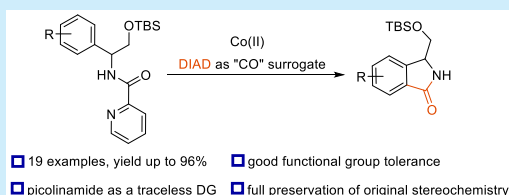
The 3-substituted isoindolinone motif is a common fragment present in naturally occurring alkaloids as well as various biologically active compounds (Figure 1).[1] Therefore,
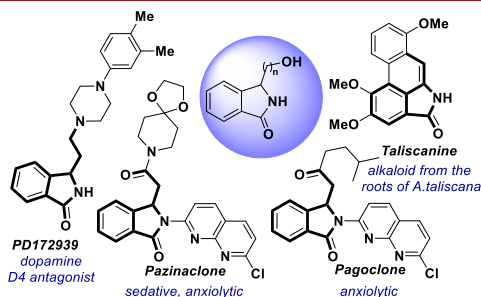
Figure 1. 3-Hydroxymethyl isoindolinone and examples of biologically active 3-substituted isoindolinone compounds.

the development of novel methodologies toward 3-substituted isoindolinone derivatives is of great interest. Although there are numerous methods for the synthesis of racemic 3-substituted isoindolinones, only a few approaches toward enantiopure 3-substituted isoindolinone derivatives have been reported.[2] 3-Hydroxymethyl and 3-hydroxyethyl isoindolinones (Figure 1) are highly functional building blocks that are commonly used for the preparation of diverse biologically active compounds.[3] A straightforward method to access 3-hydroxymethyl isoindolinones would be C−H carbonylation of readily accessible phenylglycinol derivatives. Nevertheless, only a limited number of examples of such a route have been reported. In 2017 the Shi group reported an example of ruthenium-catalyzed carbonylation of phenylglycinol derivative (Scheme 1).[4a] In their 2018

Scheme 1. C−H Carbonylation of Phenylglycinol Derivatives
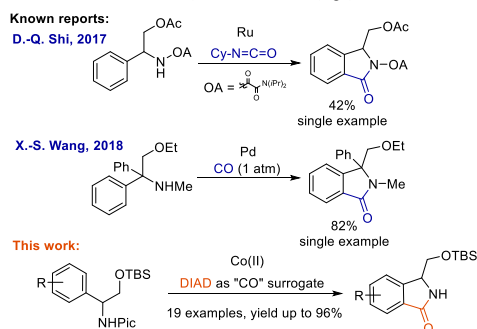
report, the Wang group included a challenging example of palladium-catalyzed carbonylation of a quaternary phenylglycinol derivative (Scheme 1).[4b] Although there are relatively many reports on C−H carbonylation of benzylamines,[5] unfortunately the developed methodology cannot be successfully transferred to phenylglycinols.[6] That might be related to steric effects of phenylglycinol substrate and/or the ability of the phenylglycinol hydroxyl group to coordinate to the transition metal (TM), thereby deactivating the catalyst.

C−H functionalization using cobalt(II) salts in combination with bidentate directing groups has attracted enormous interest in past few years.[7] Since the initial report by Daugulis in 2014,[8] where Co(II) salts in combination with an aminoquinoline directing group were used as high-valent cobalt(III) precursors, a large number of other C−H functionalization reactions based on this approach have been reported, showing the potential of this methodology.[9] In 2017 Cui reported that picolinamide can be used as a traceless directing group under cobalt catalysis, thus saving effort for directing group cleavage afterward.[10]
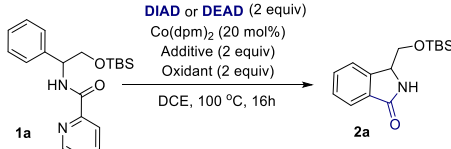
Herein we report an efficient method for the synthesis of 3-substituted isoindolinones via cobalt-catalyzed C−H carbonylation of phenylglycinol derivatives using DIAD as a "CO" surrogate and picolinamide as a traceless directing group.

For optimization studies, phenylglycinol derivative **1a** was chosen as a model substrate with diethyl azodicarboxylate (DEAD) (Table 1, entries 1−7) or diisopropyl azodicarboxylate

Table 1. Optimization of the Reaction Conditions[a]

entry	oxidant	additive	1a:2a	yield (%)[b]
1[c]	Mn(OAc)$_3$·2H$_2$O	NaOPiv	4:1	20
2[c]	AgOAc	NaOPiv	19:1	<5
3[c]	air	NaOPiv	5.7:1	15
4[c]	Ag$_2$CO$_3$	NaOPiv	1.1:1	45
5[c]	Ag$_2$CO$_3$	NaOAc	1.7:1	35
6[c]	Ag$_2$CO$_3$	AcOH	4.3:1	15
7[c]	Ag$_2$CO$_3$	PivOH	1:3	75
8[d]	**Ag$_2$CO$_3$**	**PivOH**	**1:49**	**98**
9[e]	Ag$_2$CO$_3$	PivOH	1.6:1	25
10[f]	Ag$_2$CO$_3$	PivOH	>19:1	<5
11[g]	Ag$_2$CO$_3$	PivOH	3.5:1	18
12[h]	Ag$_2$CO$_3$	PivOH	1:0	0

[a]Reaction conditions: **1a** (0.1 mmol), DIAD (0.2 mmol, 2 equiv), Co(dpm)$_2$ (0.02 mmol, 20 mol %), additive (0.1−0.2 mmol, 1−2 equiv), oxidant (0.2 mmol, 2 equiv), DCE (1 mL), 100 °C. Co(dpm)$_2$ = bis(2,2,6,6-tetramethyl-3,5-heptanedionato)cobalt(II) (CAS no. 13986-53-3). [b]NMR yields using triphenylmethane as an internal standard. [c]DEAD (0.2 mmol, 2 equiv) was used as the "CO" surrogate. [d]PivOH (0.1 mmol, 1 equiv). [e]Toluene was used as the solvent. [f]CF$_3$CH$_2$OH was used as the solvent. [g]Co(OAc)$_2$·2H$_2$O was used as the catalyst. [h]Without catalyst.

(DIAD) (entries 8−12) as the "CO" surrogate. During the optimization studies, a range of cobalt catalysts, oxidants, base/acid additives, and reaction solvents were evaluated. The reaction of **1a** with DEAD in the presence of Co(dpm)$_2$ as the catalyst, Mn(OAc)$_3$·2H$_2$O, and NaOPiv as the base in DCE at 100 °C afforded the carbonylation product **2a** in 20% yield (entry 1). Oxidant screening (entries 2−4) showed that the yield of product **2a** can be increased to 45% using Ag$_2$CO$_3$. The effect of the additive on the product yield was studied next. With NaOAc as the base, the yield of isoindolinone **2a** slightly decreased to 35% (entry 5). Addition of AcOH gave the product in 15% yield (entry 6). A crucial increase in the product yield to 75% was observed using PivOH (entry 7). The product yield

additionally was increased when DEAD was replaced with DIAD (entry 8). Alternative solvents, e.g., toluene (entry 9) or CF$_3$CH$_2$OH (entry 10), gave poorer results. Catalyst screening revealed that Co(dpm)$_2$ is the catalyst of choice (entry 8 vs entry 11). A control experiment excluding the catalyst (entry 12) showed no formation of product **2a**.

With the optimized conditions in hand, we next examined substrate scope (Scheme 2). Unfortunately, *O*-unprotected phenylglycinol **1b** did not give corresponding product **2b**. Using a TBS protecting group, we obtained the corresponding isoindolinone **2a** in a very good yield (84%). Phenylglycinol derivatives **1c** and **1d** with *O*-PMB and *O*-MOM protection were less successful substrates and yielded corresponding

Scheme 2. Substrate Scope[a]

[a]Reaction conditions: **1** (0.5 mmol), DIAD (1.0 mmol, 2 equiv), Co(dpm)$_2$ (0.10 mmol, 20 mol %), PivOH (0.5 mmol, 1 equiv), Ag$_2$CO$_3$ (1.0 mmol, 2 equiv), DCE (5 mL), 100 °C. [b]Standard conditions, 1 mmol scale. [c]Co(dpm)$_2$ (30 mol %). [d]Synthesized from *N*-((1*R*,2*S*)-2-((*tert*-butyldimethylsilyl)oxy)-1,2-diphenyl-ethyl)-picolinamide and isolated as a single diastereomer. [e]After 24 h, additional Co(dpm)$_2$ (30 mol %) and Ag$_2$CO$_3$ (2 equiv) were added.
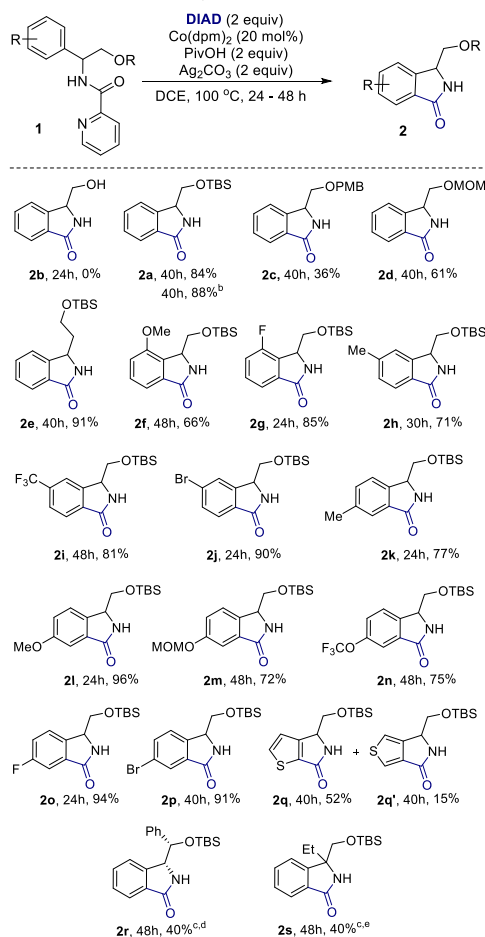
carbonylation products **2c** and **2d** in lower isolated yields of 36% and 61%, respectively. β-Phenylalaninol derivative **1e** was a competent substrate and gave isoindolinone **2e** in excellent yield (91%). Phenylglycinol derivatives with various functional groups on the benzene ring were investigated. We observed that the reactions using phenylglycinol derivatives **1** with *para*, *meta*, and *ortho* substitution patterns were successful. Using *meta*-substituted substrates **1h−j**, we observed excellent regioselectivity and obtained carbonylation products that formed by reaction of the less hindered C−H bond, which is consistent with literature examples.[8]

Diverse functionalities were tolerated under the reaction conditions, including electron-donating groups, such as alkyl (products **2h** and **2k**), methoxy (**2f** and **2l**), and methoxymethyl ether (**2m**), as well as electron-withdrawing groups, such as trifluoromethyl (**2i**) and trifluoromethoxy (**2n**). Halogenated phenylglycinol derivatives **1g**, **1j**, **1o**, and **1p** gave the corresponding isoindolinones **2g**, **2j**, **2o**, and **2p** in excellent yields (85−94%). Interestingly, thiophene amino alcohol derivative **1q** was a competent substrate for carbonylation. In this case the reaction was not selective, and both regioisomers **2q** (52%) and **2q′** (15%) were isolated. Sterically hindered amide **1r** yielded carbonylation product **2r** in 40% yield. In addition, we demonstrated that quaternary amino alcohol **1s** can be transformed to the corresponding product **2s** in an acceptable yield. In this case additional amounts of catalyst and oxidant were required after 24 h.

We used enantiopure (*S*)-phenylglycinol derivative (*S*)-**1a** in order to determine whether the stereochemical integrity of the substrate's α-position is preserved (Scheme 3). We observed that under the carbonylation conditions this stereocenter was preserved completely, and no loss of enantiopurity was detected for the product (*S*)-**2a**.

Scheme 3. Preservation of Stereochemistry
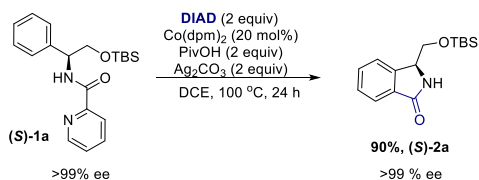
In conclusion, we have developed an efficient method for the synthesis of 3-hydroxymethyl isoindolinones via cobalt-catalyzed C(sp^2)−H carbonylation of phenylglycinol derivatives using picolinamide as a traceless directing group. The reaction proceeds in the presence of a commercially available cobalt(II) tetramethylheptanedionate catalyst and employs DIAD as a "CO" surrogate. This synthetic route offers a broad substrate scope, excellent regioselectivity, and full preservation of the original stereochemistry. Besides, the developed method provides a pathway for accessing valuable enantiopure 3-substituted isoindolinone derivatives.

ASSOCIATED CONTENT

Supporting Information

The Supporting Information is available free of charge at https://pubs.acs.org/doi/10.1021/acs.orglett.0c00672.

Experimental procedures and characterization data for all new compounds along with copies of the NMR spectra and HPLC chromatograms (PDF)

AUTHOR INFORMATION

Corresponding Author

Liene Grigorjeva − *Latvian Institute of Organic Synthesis LV-1006 Riga, Latvia;* orcid.org/0000-0003-3497-6776; Email: liene_grigorjeva@osi.lv

Authors

Lukass Lukasevics − *Latvian Institute of Organic Synthesis LV-1006 Riga, Latvia*

Aleksandrs Cizikovs − *Latvian Institute of Organic Synthesis LV-1006 Riga, Latvia*

Complete contact information is available at:
https://pubs.acs.org/10.1021/acs.orglett.0c00672

Author Contributions

[†]L.L. and A.C. contributed equally.

Notes

The authors declare no competing financial interest.

REFERENCES

(1) (a) Speck, K.; Magauer, T. *Beilstein J. Org. Chem.* **2013**, *9*, 2048−2078. (b) Belliotti, T. R.; Brink, W. A.; Kesten, S. R.; Rubin, J. R.; Wustrow, D. J.; Zoski, K. T.; Whetzel, S. Z.; Corbin, A. E.; Pugsley, T. A.; Heffner, T. G.; Wise, L. D. *Bioorg. Med. Chem. Lett.* **1998**, *8*, 1499−1502. (c) Takahashi, I.; Kawakami, T.; Hirano, E.; Yokota, H.; Kitajima, H. *Synlett* **1996**, *1996*, 353−355. (d) Stuk, T. L.; Assink, B. K.; Bates, R. C., Jr.; Erdman, D. T.; Fedij, V.; Jennings, S. M.; Lassig, J. A.; Smith, R. J.; Smith, T. L. *Org. Process Res. Dev.* **2003**, *7*, 851−855. (e) Petronzi, C.; Collarile, S.; Croce, G.; Filosa, R.; De Caprariis, P.; Peduto, A.; Palombi, L.; Intintoli, V.; Di Mola, A.; Massa, A. *Eur. J. Org. Chem.* **2012**, *2012*, 5357−5365.

(2) (a) Di Mola, A.; Palombi, L.; Massa, A. *Targets Heterocycl. Syst.* **2014**, *18*, 113−140 and references therein. (b) Comins, D. L.; Schilling, S.; Zhang, Y. *Org. Lett.* **2005**, *7*, 95−98 and references therein. (c) Zhou, W.; Zhang, Y.-X.; Nie, X.-D.; Si, C.-M.; Sun, X.; Wei, B.-G. *J. Org. Chem.* **2018**, *83*, 9879−9889 and references therein.

(3) (a) Royo, S.; Chapman, R. S. L.; Sim, A. M.; Peacock, L. R.; Bull, S. D. *Org. Lett.* **2016**, *18*, 1146−1149. (b) Patel, B. H.; Mason, A. M.; Patel, H.; Coombes, R. C.; Ali, S.; Barrett, A. G. M. *J. Org. Chem.* **2011**, *76*, 6209−6217. (c) Berdini, V.; Buck, I. M.; Day, J. E. H.; Griffiths-Jones, C. M.; Heightman, T. D.; Howard, S.; Murray, C. W.; Norton, D.; O'Reilly, M.; Woolford, A. J. A.; Cooke, M. L.; Cousin, D.; Onions, S. T.; Shannon, J. M.; Watts, J. P. WO 2017068412, 2017. (d) Ray, S. K.; Sadhu, M. M.; Biswas, R. G.; Unhale, R. A.; Singh, V. K. *Org. Lett.* **2019**, *21*, 417−422.

(4) (a) Han, J.; Wang, N.; Huang, Z.-B.; Zhao, Y.; Shi, D.-Q. *J. Org. Chem.* **2017**, *82*, 6831−6839. (b) Cheng, X.-F.; Wang, T.; Li, Y.; Wu, Y.; Sheng, J.; Wang, R.; Li, C.; Bian, K.-J.; Wang, X.-S. *Org. Lett.* **2018**, *20*, 6530−6533.

(5) Examples of TM-catalyzed carbonylation of benzylamines: Cobalt: (a) Ling, F.; Ai, C.; Lv, Y.; Zhong, W. *Adv. Synth. Catal.* **2017**, *359*, 3707−3712. Palladium: (b) Zhang, C.; Ding, Y.; Gao, Y.; Li, S.; Li, G. *Org. Lett.* **2018**, *20* (9), 2595−2598. (c) Fu, L.-Y.; Ying, J.; Qi, X.; Peng, J.-B.; Wu, X.-F. *J. Org. Chem.* **2019**, *84* (3), 1421−1429.

(6) Under the cobalt-catalyzed carbonylation conditions reported in ref 5a, carbonylation of phenylglycinol derivative **1a** gave a 13% yield of product **2a**. For details, see the Supporting Information.

(7) Selected reviews on Co-catalyzed C−H functionatization: (a) Hyster, T. K. *Catal. Lett.* **2015**, *145*, 458−467. (b) Daugulis, O.; Roane, J.; Tran, L. D. *Acc. Chem. Res.* **2015**, *48*, 1053−1064. (c) Moselage, M.; Li, J.; Ackermann, L. *ACS Catal.* **2016**, *6*, 498−525. (d) Kommagalla, Y.; Chatani, N. *Coord. Chem. Rev.* **2017**, *350*, 117−135. (e) Ujwaldev, S. M.; Harry, N. A.; Divakar, M. A.; Anilkumar, G. *Catal. Sci. Technol.* **2018**, *8*, 5983−6018. (f) Gandeepan, P.; Müller, T.; Zell, D.; Cera, G.; Warratz, S.; Ackermann, L. *Chem. Rev.* **2019**, *119*, 2192−2452.

(8) Grigorjeva, L.; Daugulis, O. *Angew. Chem., Int. Ed.* **2014**, *53*, 10209−10212.

(9) Selected examples using cobalt catalysis: C−H functionalization with alkynes: (a) Planas, O.; Whiteoak, C. J.; Company, A.; Ribas, X. *Adv. Synth. Catal.* **2015**, *357*, 4003−4012. (b) Kalsi, D.; Sundararaju, B. *Org. Lett.* **2015**, *17*, 6118−6121. (c) Zhang, J.; Chen, H.; Lin, C.; Liu, Z.; Wang, C.; Zhang, Y. *J. Am. Chem. Soc.* **2015**, *137*, 12990−12996. (d) Nguyen, T. T.; Grigorjeva, L.; Daugulis, O. *ACS Catal.* **2016**, *6*, 551−554. (e) Landge, V. G.; Midya, S. P.; Rana, J.; Shinde, D. R.; Balaraman, E. *Org. Lett.* **2016**, *18*, 5252−5255. C−H functionalization with alkenes: (f) Grigorjeva, L.; Daugulis, O. *Org. Lett.* **2014**, *16*, 4684−4687. (g) Ma, W.; Ackermann, L. *ACS Catal.* **2015**, *5*, 2822−2825. (h) Gandeepan, P.; Rajamalli, P.; Cheng, C.-H. *Angew. Chem., Int. Ed.* **2016**, *55*, 4308−4311. C−H functionalization with allenes: (i) Thrimurtulu, N.; Dey, A.; Maiti, D.; Volla, C. M. R. *Angew. Chem., Int. Ed.* **2016**, *55*, 12361−12365. (j) Thrimurtulu, N.; Nallagonda, R.; Volla, C. M. R. *Chem. Commun.* **2017**, *53*, 1872−1875. (k) Li, T.; Zhang, C.; Tan, Y.; Pan, W.; Rao, Y. *Org. Chem. Front.* **2017**, *4*, 204−209. C−H functionalization with CO or CO surrogates: (l) Grigorjeva, L.; Daugulis, O. *Org. Lett.* **2014**, *16*, 4688−4690. (m) Ni, J.; Li, J.; Fan, Z.; Zhang, A. *Org. Lett.* **2016**, *18*, 5960−5963. (n) Nguyen, T. T.; Grigorjeva, L.; Daugulis, O. *Chem. Commun.* **2017**, *53*, 5136−5138. (o) Zeng, L.; Tang, S.; Wang, D.; Deng, Y.; Chen, J.-L.; Lee, J.-F.; Lei, A. *Org. Lett.* **2017**, *19*, 2170−2173. (p) Sau, S. C.; Mei, R.; Struwe, J.; Ackermann, L. *ChemSusChem* **2019**, *12*, 3023−3027.

(10) Picolinamide as a traceless directing group: Kuai, C.; Wang, L.; Li, B.; Yang, Z.; Cui, X. *Org. Lett.* **2017**, *19*, 2102−2105.

Lukasevics, L.; Grigorjeva, L. Cobalt-catalyzed carbonylation of the C–H bond. *Org. Biomol. Chem.*, **2020**, 18, 7460-7466.

REVIEW

Cobalt-catalyzed carbonylation of the C–H bond

Lukass Lukasevics and Liene Grigorjeva [ID] *

Direct carbonylation of the C–H bond is a great tool for installing a carbonyl group in a wide variety of substrates. This review summarizes the C–H bond carbonylation methodologies using the cobalt-catalyzed C–H bond functionalization approach. Despite the fact that cobalt-catalyzed carbonylation methodologies have been known since Murahashi's report in 1955, this area is still underdeveloped, particularly carbonylation of the C(sp³)–H bond.

Introduction

One of the most important transformations in organic chemistry is the formation of C–C bonds due to their importance in the construction of complex molecules and natural products. CO can be used as a readily available and cheap C(1) source and reactions with carbon monoxide have been intensively investigated by chemists as it is one of the most straightforward and efficient paths to carbonyl-containing products.[1] Depending on the reaction conditions, four main carbonylation mechanisms could be envisioned: (1) cationic carbonylation arising from the activation of the CO molecule with strong Brønsted or Lewis acids; (2) anionic carbonylation *via* direct nucleophilic attack on carbon monoxide by carbon bases to form reactive acyl anion species; (3) carbonylation of carbon-centered radicals to form acyl radical species; and (4) metal-mediated carbonylation *via* a migratory insertion step in the metal–carbon bond.[2] The majority of carbonylation reactions are based on the transition metal catalysis approach.[1,2] These methodologies often require the starting material to be pre-functionalized, which leads to the use of additional synthetic steps or protecting group manipulations. On the other hand, a different and more promising path for the construction of such C–C bonds is direct C–H carbonylation. Typically, C–H bonds are relatively stable under the reaction conditions due to their high BDEs compared to other types of atom linkages, which is why reorganization of C–H bonds *via* direct functionalization is a highly challenging task. Since the discovery of transition metal-catalyzed C–H functionalization reactions, chemists around the world have used this methodology to selectively construct not only C–C bonds but also C–O, C–N, C–S, and C–Hal bonds. This unique pathway has been utilized

Latvian Institute of Organic Synthesis, Aizkraukles 21, LV-1006 Riga, Latvia.
E-mail: liene_grigorjeva@osi.lv
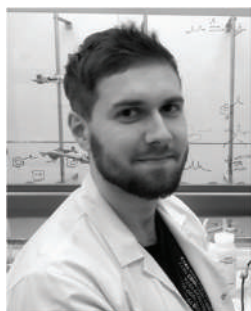
Lukass Lukasevics

Lukass Lukasevics completed his Master's degree in 2019 at Riga Technical University, Latvia. Currently, he is working on his Ph.D. thesis under the supervision of Dr Chem. Liene Grigorjeva at the Latvian Institute of Organic Synthesis, Riga, Latvia. His research interests are focused on the development of new methodologies for cobalt-catalyzed C–H bond functionalization reactions.

Liene Grigorjeva

Liene Grigorjeva received her Ph. D. degree from Riga Technical University (Latvia) in 2013, under the supervision of Prof. Aigars Jirgensons. Then she joined the group of Prof. Daugulis at the University of Houston (USA) as a postdoctoral researcher (2013–2016). Currently, she is a principal researcher at the Latvian Institute of Organic Synthesis and Assistant Professor at Riga Technical University. Her research interests are focused on the development of novel methodologies based on C–H bond functionalization under cobalt catalysis.

immensely both in the development of new methodologies and in the industrial production of building blocks for organic synthesis. Most of the results have been achieved with noble metal catalysts, although recently the first-row transition metals have emerged as an attractive alternative.[3] In particular, cobalt(II) salts in combination with monodentate or bidentate directing groups and oxidants have received exponential attention from synthetic organic chemists since the published methodology of benzamide alkenylation by Daugulis and Grigorjeva in 2014.[4]

Cobalt-catalyzed carbonylation of the C–H bond

Since the discovery of C–H functionalization reactions, most of the results have been achieved using low-valent cobalt catalysis. The first example of carbonylation dates back to 1955 when Murahashi demonstrated the synthesis of isoindolinones 2a–d (Scheme 1).[5] In this work, the Co$_2$(CO)$_8$ catalyst was used together with CO gas to selectively introduce a carbonyl group in Schiff bases 1a–d with good yields (70–96%). Although this reaction was synthetically useful, the reaction conditions required high pressure and temperature.

Murahashi's methodology was expanded later in 2006 (Scheme 2). Sen and co-workers reported the carbonylation of Schiff bases 3a–c in the presence of Co(I) and Co(0) catalysts to readily form isoindolinones 4a–c. The formation of the product was proposed to occur via the C–H activation step followed by migratory insertion of the CO molecule and reductive elimination. In contrast to Murahashi's work, Sen showed that this transformation can be achieved under milder reaction conditions with lower catalyst loadings.[6]

In 2014, Daugulis and Grigorjeva reported the first example of high-valent Co-catalyzed carbonylation of benzamide derivatives 5 (Scheme 3a).[7] The reaction proceeded in the presence of the Co(acac)$_2$ catalyst, Mn(OAc)$_3$·2H$_2$O and O$_2$ oxidants, and TFE solvent under a CO atmosphere at room temperature. The authors used the 8-aminoquinoline directing group to selectively obtain phthalimide derivatives 6 in good yields. These mild reaction conditions were compatible with halogen, cyano,

Scheme 2 Cobalt-catalyzed carbonylation of imines 3.
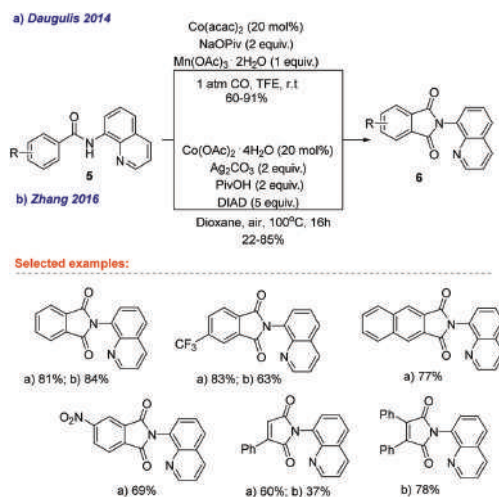
Scheme 3 Cobalt-catalyzed C–H carbonylation of benzamide 5 derivatives.

ester, nitro, and other functionalities. Additionally, the authors showed that the directing group can be easily removed by treatment with ammonia in methanol to obtain the phthalimide derivative in a good yield. These findings inspired Zhang and co-workers to extend Daugulis' work two years later (Scheme 3b). In their work, the authors used the Co (OAc)$_2$·4H$_2$O and Ag$_2$CO$_3$ catalytic system to carbonylate benzamides 5 to obtain phthalimide derivatives 6 with good yields and excellent functional group tolerance. Their approach was the first example of the use of dialkylazadicarboxylates as a non-toxic carbon monoxide source. Although Zhang's method utilizes a relatively safer way for CO generation, the reaction conditions require two equivalents of the silver oxidant and a temperature of 100 °C. Additionally, the method unfortunately lacks site selectivity if 3-substituted benzamide substrates 5 are used, giving a mixture of the products.[8]

Based on Zhang's mechanism studies and previous literature reports, the authors proposed a possible catalytic cycle (Scheme 4). According to the proposal, initially Co(II) is oxidized to Co(III) followed by the coordination and C–H acti-

Scheme 1 An early example of low-valent cobalt-catalyzed carbonylation of Schiff base 1.
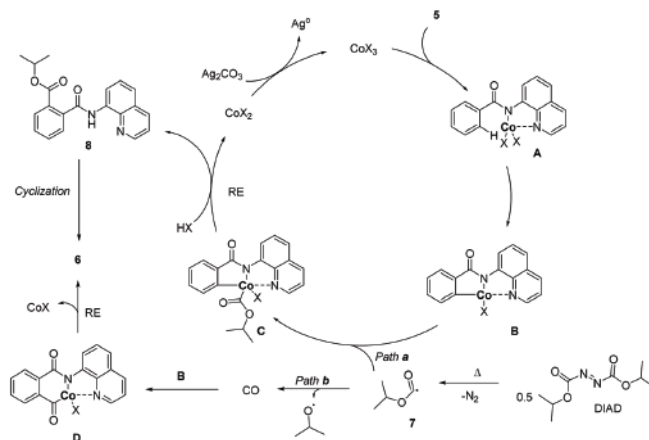
Scheme 4 The catalytic cycle for carbonylation of benzamides **5**.

vation of substrate **A** forming complex **B**. Thermal decomposition of DIAD leads to the formation of radical **7** which attacks Co complex **B** and gives intermediate **C** (path a). Reductive elimination gives ester **8** and returns Co(II) to the catalytic cycle. Intramolecular nucleophilic cyclization gives phthalimide **6**. Alternatively, CO is generated from radical **7**, which after migratory insertion forms acyl cobalt **D**. The phthalimide **6** product is generated by reductive elimination, releasing Co(I) species which are reoxidized to Co(III).

High-valent cobalt catalysis in C–H carbonylation was further explored by Wang and co-workers in 2015.[9] In their work, the Cp*Co(CO)I₂ catalyst was used in combination with Cu(OAc)₂·H₂O and Ag₂CO₃ oxidants with the PivOH additive under a CO atmosphere to transform vinyl phenols **9** into cumarin derivatives **10** (Scheme 5). The mild reaction conditions ensured good compatibility with alkyl, alkoxy, halogen and nitro substituents in the benzene ring moiety giving products in good yields. The introduction of a substituent next to the vinyl group resulted in a diminished yield probably due to steric factors, thus limiting R² substituents to Me, Et, homobenzyl and aryl.

In 2017, Daugulis reported a method for the C–H carbonylation of sulfonamides **11** using DIAD as the CO source (Scheme 6). In contrast to Zhang's work published a year earlier, the authors were able to substitute silver salts with the Mn(OAc)₂ co-oxidant and air as the terminal oxidant, although batch-wise addition of DIAD and a higher catalyst loading were necessary. This report demonstrates a wide substrate scope, good functional group tolerance and moderate to good yields. Additionally, the 8-aminoquinoline directing
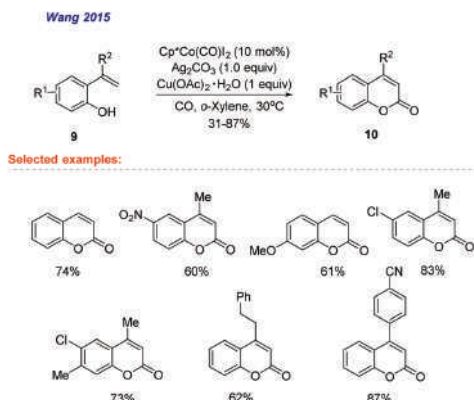
Scheme 5 Synthesis of cumarin **10** derivatives *via* Co-catalyzed C–H carbonylation.
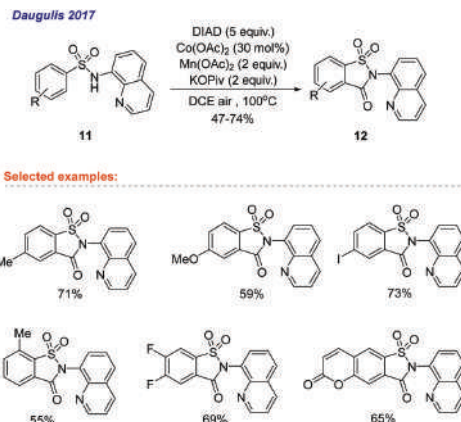
Scheme 6 Carbonylation of sulfonamides **11**.

group can be removed in the presence of BBr_3 and $PhI(TFA)_2$ to obtain saccharin derivatives.[10]

In contrast to the relatively large number of Co-catalyzed C(sp²)–H carbonylation methodologies, C–H activation and functionalization of the C(sp³)–H bond is a highly difficult task, and until 2017, there were no reports documented. In 2017, Sundararaju,[11] Gaunt[12] and Lei[13] independently discovered the cobalt-catalyzed carbonylation of the C(sp³)–H bond. In their research, 1°, 2° and 3° carbons in pivaloyl amides **13** were carbonylated in the presence of the bidentate 8-amino-quinoline directing group to obtain succinimide derivatives **14** (Scheme 7). Gaunt, Lei and Sundararaju developed similar catalytic systems, which allowed the use of a variety of substituents at the α-center – alkyl, cycloalkyl, phenyl, benzyl, ester, amino, trifluoromethyl, *etc*. – with good yields. Interestingly, Sundararaju demonstrated that when competing C(sp²)–H and C(sp³)–H bonds were carbonylated, the unactivated C(sp³)–H bond showed a higher reactivity over the C(sp²)–H bond, which typically is more reactive in C–H functionalization reactions.

Based on the experimental results and mechanistic studies, Lei reported a plausible reaction mechanism (Scheme 8).[13] Using XAS spectroscopy, the authors confirmed that the oxidation of Co(II) species to Co(III) occurs after the binding of Co(II) to the substrate and ligand exchange. According to the proposed mechanism, the Co(II) complex first coordinates with the pivaloyl amide **13** and forms Co(II) complex **E**, which is
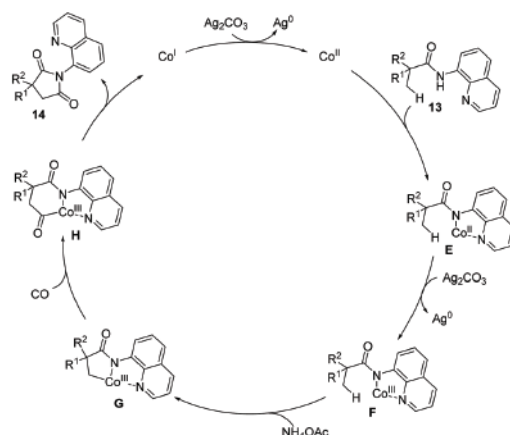
Scheme 8 The proposed mechanism for cobalt-catalyzed C(sp³)–H carbonylation of pivaloyl amide **13**.

then oxidized by Ag_2CO_3 to give Co(III) complex **F**. Next, using NH_4OAc, the activation of the C(sp³)–H bond takes place and forms intermediate **G**. Insertion of CO generates cyclic acyl Co(III) complex **H**, which undergoes reductive elimination and forms Co(I) species and liberates succinimide **14**. Finally, the Co(I) species are oxidized by Ag_2CO_3 to regenerate Co(II).

In the same year, Zhong was the first to report cobalt-catalyzed carbonylation of benzylamines **15** using picolinamide as a traceless directing group to obtain isoindolinone derivatives **16** (Scheme 9).[14] In his work, the following were used: DIAD as the CO source, $Co(OAc)_2 \cdot 4H_2O$ as the catalyst, Ag_2CO_3 as the oxidant, and pivaloic acid additive in TFE solvent. The developed method has a wide substrate scope; alkyl, alkoxy, halogen, aryl, and other substituents in the benzene ring moiety were tolerated under the reaction conditions, although the method is limited to H, Me, and Et substituents in the
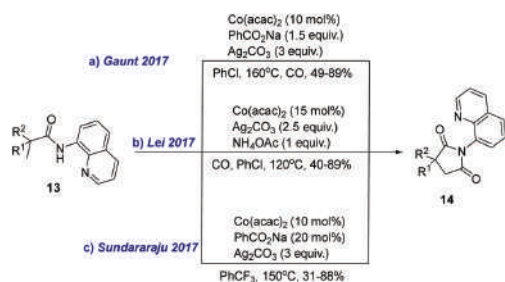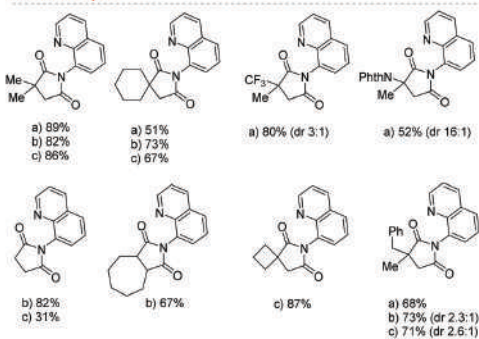
Scheme 7 Cobalt-catalyzed carbonylation of the C(sp³)–H bond in pivaloyl amide **13**.
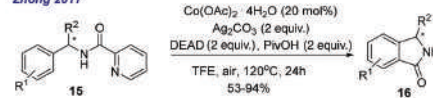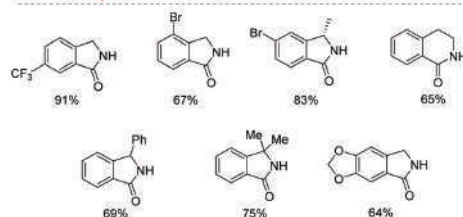
Scheme 9 Benzylamine **15** carbonylation using picolinamide as a traceless directing group.

benzylic position (R^2 = H, Me, Et). Additionally, the authors demonstrated that under the reaction conditions, no racemization of the starting material was observed.

In 2018, Lei and co-workers demonstrated that cobalt-catalyzed C–H carbonylation can be achieved in an electrochemical manner.[15] The authors successfully substituted chemical oxidants with electrical energy by employing the $Co(OAc)_2 \cdot 4H_2O$ catalyst together with RVC/Ni electrodes to carbonylate benzamides **17** under a CO atmosphere to obtain phthalimide derivatives **18a** in good yields (Scheme 10a). No degradation of the starting material was observed under the reaction conditions, which are compatible with a variety of alkyl, halogen, aryl, and heteroaryl substituents. Additionally, the authors showed that by changing the catalytic system, it is possible to successfully use benzamides **17** for the cobalt-catalyzed carboamidation of the C–H bond to obtain amides **18b** (Scheme 10b). In this transformation, a large variety of both cyclic and acyclic amines are reactive.

In the same year, Sundararaju and co-workers developed a protocol for the generation of CO by the reduction of CO_2 in a 2-chamber system which can be successfully applied to the Co-catalyzed C–H carbonylation of benzamides, sulfonamides and pivaloyl amides (Scheme 11).[16] The CO gas is generated in chamber **A** from disilane **19** and CO_2 where it is deoxygenated and transferred to chamber **B**, where C–H functionalization takes place. Employing the $Co(acac)_2$ catalyst, $PhCO_2Na$ additive and Ag_2CO_3 oxidant in trifluorotoluene at 100 °C, the authors were able to carbonylate benzamides **5** and sulfonamides **11** with moderate yields. By slightly modifying the catalytic system,

Scheme 11 Carbonylation of benzamides **5**, sulfonamides **11** and pivaloyl amides **13**.

the authors additionally demonstrated the applicability of their 2-chamber protocol to achieve the carbonylation of C(sp³)–H bonds in pivaloyl amides **13** with moderate to good yields.

The traceless picolinamide group assisted cobalt-catalyzed C–H carbonylation methodology was further explored by Zhong and co-workers in 2018.[17] The authors used the $CoCl_2$ catalyst in the presence of the NaOPiv base and DIAD as a CO source to carbonylate aryl anilines **20** obtaining phenanthridinones **21** in excellent yields (Scheme 12). This transformation has good functional group tolerance and does not require an additional oxidant employing O_2 as the sole oxidant.

In the same year, Zhai introduced the easily cleavable bidentate 2-(1-methylhydrazinyl)pyridine directing group for the carbonylation of benzamide derivatives **22** (Scheme 13a).

In their work, the authors showed a large scope of benzamide substrates that can be converted into phthalimides **23** with good to excellent yields in the presence of the Co

Scheme 10 Cobalt-catalyzed electrochemical carbonylation and carboamidation of benzamide **17**.
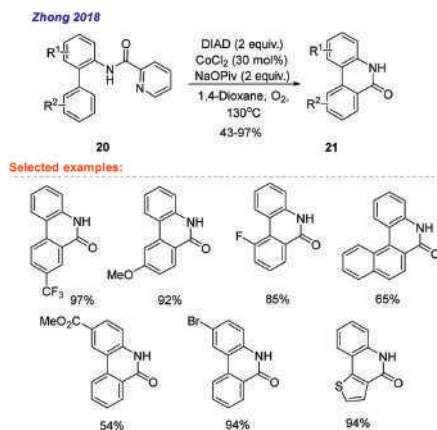
Scheme 12 Carbonylation of aryl aniline **20**.
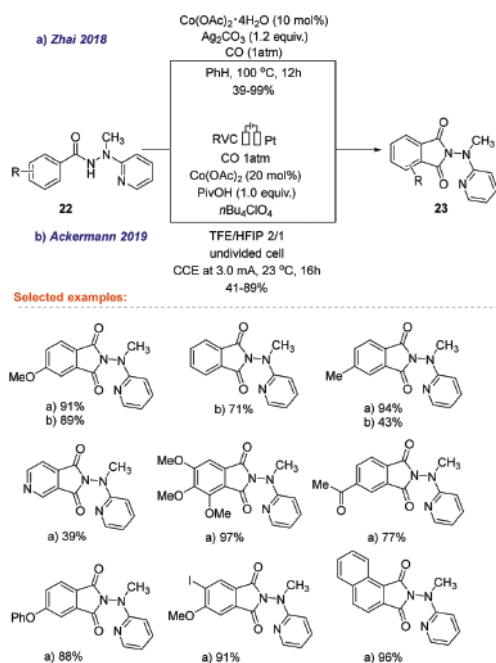
Scheme 13 C–H carbonylation of benzamide **22**.

(OAc)$_2$·4H$_2$O catalyst, the Ag$_2$CO$_3$ oxidant and a CO atmosphere. The directing group can be easily cleaved under hydrogenolytic conditions.[18] The next year, the Ackermann group demonstrated that this transformation is achievable under cobalt electrocatalytic conditions (Scheme 13b), where phthalimides **23** were obtainable under mild conditions, although only limited to 5 examples.[19]
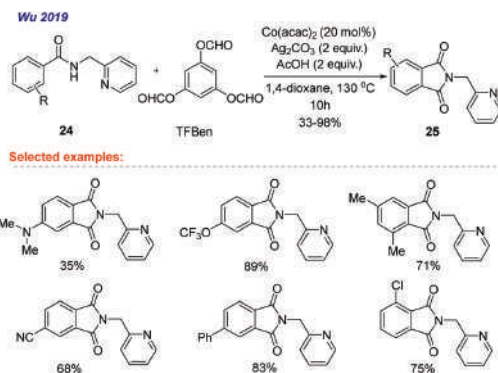
Scheme 14 Cobalt-catalyzed carbonylation of benzamides **24** using TFBen as a "CO" source.

In 2019, Wu and colleagues reported the synthesis of phthalimide derivatives **25** *via* cobalt-catalyzed C–H carbonylation of benzamides **24** using picolinamide as a directing group, the Co(acac)$_2$ catalyst, the Ag$_2$CO$_3$ oxidant and the AcOH additive (Scheme 14). For the generation of CO *in situ*, the authors used TFBen, which had not been used in cobalt-catalyzed carbonylation reactions before. The reaction conditions were compatible with alkyl, aryl, heteroaryl, alkoxy, halogen, nitro, ester, and amine functionalities, giving phthalimide derivatives **25** in good to excellent yields. Additionally, the authors illustrated the synthetic utility of their catalytic system by performing the gram-scale synthesis of **25** with a very good yield.[20]

In 2020, Grigorjeva and co-workers reported the cobalt-catalyzed traceless picolinamide directing group assisted C–H carbonylation of phenylglycinol derivatives **26** (Scheme 15).[21]

In their study, DIAD served as a "CO" source in the presence of the Co(dpm)$_2$ catalyst, the Ag$_2$CO$_3$ oxidant and the PivOH additive to obtain isoindolinones **27** in good to excel-
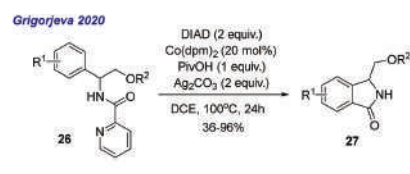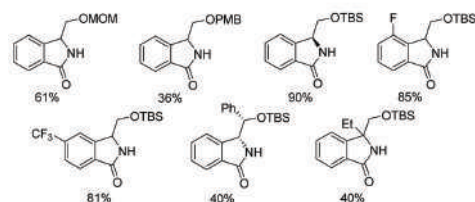
Scheme 15 C–H carbonylation of phenylglycinol derivative **26**.

lent yields. The reaction conditions are compatible with alkyl, heteroaryl, and halogen functionalities and different alcohol protecting groups. In addition, complete stereo integrity is preserved under the reaction conditions.[21]

Conclusions

C–H activation and functionalization have been intensively studied over the last couple of decades; however, most of the achievements in this field have been obtained using precious metals. This short review illustrates the utility of high-valent cobalt catalysis in C–H carbonylation reactions. Typically, a strong chelating bidentate directing group in combination with an oxidant is necessary for successful transformation. Benzamides, sulphonamides, benzylamines, aryl anilines, phenols and amino alcohols can be suitable substrates along with aminoquinoline, picolinamide, picolinamine and hydrazinyl pyridine directing groups to obtain highly valuable products with potential applications in medicinal chemistry. In contrast to the reported achievements in C(sp^2)–H carbonylation, the development of C(sp^3)–H bond carbonylation methodologies is a highly challenging task and still remains underdeveloped.

Conflicts of interest

There are no conflicts to declare.

Acknowledgements

Notes and references

1 Selected reviews on transition metal catalyzed carbonylation: (*a*) J.-B. Peng, F.-P. Wu and X.-F. Wu, *Chem. Rev.*, 2019, **119**, 2090; (*b*) X.-F. Wu, X. Fang, L. Wu, R. Jackstell, H. Neumann and M. Beller, *Acc. Chem. Res.*, 2014, **47**, 1041; (*c*) Y. Li, Y. Hu and X.-F. Wu, *Chem. Soc. Rev.*, 2018, **47**, 172; (*d*) J.-B. Peng, X. Qi and X.-F. Wu, *Synlett*, 2017, **28**, 175; (*e*) N. Rajesh, N. Barsu and B. Sundararaju, *Tetrahedron Lett.*, 2018, **59**, 862.

2 (*a*) M. Beller, *Catalytic Carbonylation Reactions*, Springer, Berlin, 2006; (*b*) M. Beller and X.-F. Wu, *Transition Metal Catalyzed Carbonylation Reactions: Carbonylative Activation of C-X Bonds*, Springer, Amsterdam, 2013; (*c*) L. Kollär, *Modern Carbonylation Methods*, Wiley-VCH, Weinheim, 2008.

3 Selected reviews on Co-catalyzed C–H functionalization: (*a*) T. K. Hyster, *Catal. Lett.*, 2015, **145**, 458; (*b*) O. Daugulis, J. Roane and L. D. Tran, *Acc. Chem. Res.*, 2015, **48**, 1053; (*c*) M. Moselage, J. Li and L. Ackermann, *ACS Catal.*, 2016, **6**, 498; (*d*) Y. Kommagalla and N. Chatani, *Coord. Chem. Rev.*, 2017, **350**, 117; (*e*) S. M. Ujwaldev, N. A. Harry, M. A. Divakar and G. Anilkumar, *Catal. Sci. Technol.*, 2018, **8**, 5983; (*f*) P. Gandeepan, T. Müller, D. Zell, G. Cera, S. Warratz and L. Ackermann, *Chem. Rev.*, 2019, **119**, 2192; (*g*) A. Baccalini, S. Vergure, P. Dolui, G. Zanoni and D. Maiti, *Org. Biomol. Chem.*, 2019, **17**, 10119.

4 L. Grigorjeva and O. Daugulis, *Angew. Chem., Int. Ed.*, 2014, **53**, 10209.

5 S. Murahashi, *J. Am. Chem. Soc.*, 1955, **77**, 6403.

6 J. K. Funk, H. Yennawar and A. Sen, *Helv. Chim. Acta*, 2006, **89**, 1687.

7 L. Grigorjeva and O. Daugulis, *Org. Lett.*, 2014, **16**, 4688.

8 J. Ni, J. Li, Z. Fan and A. Zhang, *Org. Lett.*, 2016, **18**, 5960.

9 X.-G. Liu, S.-S. Zhang, C.-Y. Jiang, J.-Q. Wu, Q. Li and H. Wang, *Org. Lett.*, 2015, **17**, 5404.

10 T. T. Nguyen, L. Grigorjeva and O. Daugulis, *Chem. Commun.*, 2017, **53**, 5136.

11 N. Barsu, S. K. Bolli and B. Sundararaju, *Chem. Sci.*, 2017, **8**, 2431.

12 P. Williamson, A. Galván and M. J. Gaunt, *Chem. Sci.*, 2017, **8**, 2588.

13 L. Zeng, S. Tang, D. Wang, Y. Deng, J.-L. Chen, J.-F. Lee and A. Lei, *Org. Lett.*, 2017, **19**, 2170.

14 F. Ling, C. Ai, Y. Lv and W. Zhong, *Adv. Synth. Catal.*, 2017, **359**, 3675.

15 L. Zeng, H. Li, S. Tang, X. Gao, Y. Deng, G. Zhang, C.-W. Pao, J.-L. Chen, J.-F. Lee and A. Lei, *ACS Catal.*, 2018, **8**, 5448.

16 N. Barsu, D. Kalsi and B. Sundararaju, *Catal. Sci. Technol.*, 2018, **8**, 5963.

17 F. Ling, C. Zhang, C. Ai, Y. Lv and W. Zhong, *J. Org. Chem.*, 2018, **83**, 5698.

18 S. Qiu, S. Zhai, H. Wang, C. Tao, H. Zhao and H. Zhai, *Adv. Synth. Catal.*, 2018, **360**, 3271.

19 S. C. Sau, R. Mei, J. Struwe and L. Ackermann, *ChemSusChem*, 2018, **12**, 3023.

20 L.-Y. Fu, J. Ying and X. F. Wu, *J. Org. Chem.*, 2019, **84**, 12648.

21 L. Lukasevics, A. Cizikovs and L. Grigorjeva, *Org. Lett.*, 2020, **22**, 2720.

Lukasevics, L.; Cizikovs, A.; Grigorjeva, L. Cobalt-Catalyzed C(sp^2)–H Carbonylation of Amino Acids Using Picolinamide as a Traceless Directing Group. *Org. Lett.* 2021 *23* (7), 2748-2753.

Letter

Cobalt-Catalyzed C(sp^2)−H Carbonylation of Amino Acids Using Picolinamide as a Traceless Directing Group

Lukass Lukasevics, Aleksandrs Cizikovs, and Liene Grigorjeva*

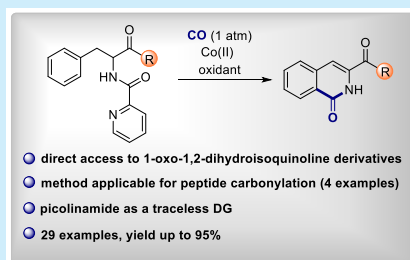Cite This: *Org. Lett.* 2021, 23, 2748−2753

Read Online

ACCESS | Metrics & More | Article Recommendations | Supporting Information

ABSTRACT: Herein we report an efficient protocol for the C(sp^2)−H carbonylation of amino acid derivatives based on an inexpensive cobalt(II) salt catalyst. Carbonylation was accomplished using picolinamide as a traceless directing group, CO (1 atm) as the carbonyl source, and Co(dpm)$_2$ as the catalyst. A broad range of phenylalanine derivatives bearing diverse functional groups were tolerated. Moreover, the method can be successfully applied for the C(sp^2)−H carbonylation of short peptides thereby allowing access for peptide late-stage carbonylation.

- direct access to 1-oxo-1,2-dihydroisoquinoline derivatives
- method applicable for peptide carbonylation (4 examples)
- picolinamide as a traceless DG
- 29 examples, yield up to 95%

Amino acids and peptides play an essential role in medicinal chemistry, synthetic organic chemistry, and biotechnology; therefore, direct functionalization of amino acid derivatives and peptides via C−H bond activation has attracted immense interest during the past decade.[1] In addition, the late-stage modification of peptides has a tremendous potential to promote the development of innovative peptide drugs.[2] Progress on direct C−H bond functionalization of amino acid derivatives has been achieved mainly using late transition metal catalysis.[1] The functionalization of amino acid C(sp^3)−H bonds is relatively well-developed allowing installation of various functional groups both in the α-position[3] and on the amino acid side chain.[1e] However, methods for amino acid side chain C(sp^2)−H bond functionalization are less explored, particularly for phenylalanine derivatives.[4] Therefore, the development of new synthetic methods for the site selective modification of phenylalanine derivatives is of great interest.

In the past decade, notable progress has been achieved with the development of C−H functionalization methodology using cobalt as an alternative to precious transition metal catalysts.[5] The use of cobalt(II) salt catalysts in combination with bidentate directing groups has been proven to be an effective strategy for various C−H bond transformations.[6] Despite the progress made so far, substrate diversity that can be used for C−H functionalization under cobalt catalysis is still under-developed when compared to noble transition metal catalysis.[5] To the best of our knowledge, only two examples of the cobalt-catalyzed C−H functionalization of amino acids or peptides have been reported so far. In 2017, Correa and co-workers demonstrated cobalt-catalyzed selective arylation of glycine esters and peptides through a radical pathway.[7] In 2019, the Ackermann group reported the first example of cobalt(III)-

catalyzed C−H allylation of a tryptophan moiety in structurally complex peptides (Scheme 1a).[8]

C−H bond carbonylation using transition metal (TM) catalysis is an efficient tool to introduce a carbonyl group, and it gives access to various valuable compounds. In recent years, a number of carbonylation methods have been developed using cobalt catalysis.[9] However, most of them can only be applied to aliphatic amide or benzamide type substrates. To date, there are no literature examples for direct carbonylation of phenylalanine type substrates using first-row TM catalysis. So far, there have been only two reports for phenylalanine carbonylation, both exploiting palladium metal. In 2007, the Vicente group showed a stoichiometric example of *ortho*-palladation of a phenylalanine ester and a subsequent reaction of the formed complex with CO gas (Scheme 1b).[10] In 2011, Garcia, Granell, and co-workers demonstrated palladium-catalyzed carbonylation of quaternary amino acids (Scheme 1c).[11]
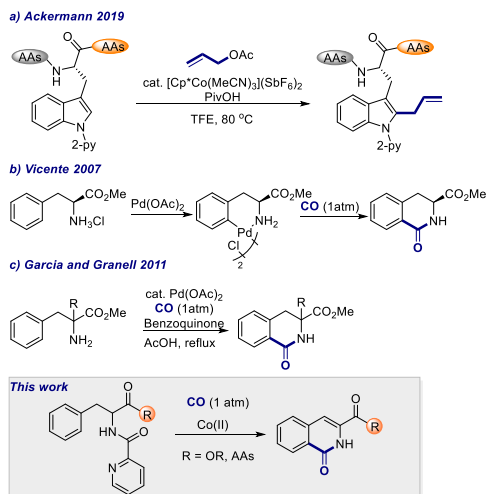
Herein we report an efficient method for the synthesis of 1,2-dihydroisoquinolinolones via C(sp^2)−H carbonylation of phenylalanine derivatives. Methyl picolinoylphenylalaninate **1aa** was chosen as a model substrate for amino acid C(sp^2)−H carbonylation. A picolinamide directing group (DG) was introduced by Daugulis in 2005[12] and has been extensively used for a large diversity of transformations

Scheme 1. Selected Examples on C−H Functionalization of Amino Acids

Table 1. Optimization of Reaction Conditions[a]

entry	change from above conditions	yield, %[b]
1	oxidant: Ag$_2$CO$_3$ (3 equiv)	37
2	oxidant: Mn(OAc)$_3$·2H$_2$O (3 equiv)	56
3	none	70
4	oxidant: air	0
5	NaOPiv (2 equiv) instead of PivOH	27
6	catalyst: Co(OAc)$_2$ (20 mol %)	24
7	catalyst: Co(acac)$_3$ (20 mol %)	30
8	catalyst: Co(dpm)$_2$ (30 mol %)	94
9	without catalyst	0
10	solvent: DCE, 100 °C	50
11	solvent: toluene, 100 °C	50
12	"CO" surrogate: DIAD	32
13	"CO" surrogate: DEAD	30

[a]Reaction conditions: **1aa** (0.1 mmol), CO (1 atm), Co(dpm)$_2$ (0.02 mmol), PivOH (0.2 mmol), oxidant (0.15−0.3 mmol), PhCl (1 mL), 120 °C. [b]NMR yields using triphenylmethane as an internal standard. Co(dpm)$_2$ = bis(2,2,6,6-tetramethyl-3,5-heptanedionato)cobalt(II) (CAS 13986-53-3); DEAD = diethyl azodicarboxylate; DIAD = diisopropyl azodicarboxylate.

catalyzed by various TMs.[13] In 2017, Cui demonstrated picolinamide as a traceless DG;[14] since then, a number of reports for picolinamide as a traceless DG have been reported.[15] For optimization studies, conditions similar to those reported previously for the carbonylation of amino alcohol derivatives were employed.[15b] Using Co(dpm)$_2$ catalyst in combination with Ag$_2$CO$_3$ as the oxidant and PivOH as the additive under 1 atm of CO, we observed the formation of 1,2-dihydroisoquinolinolone **2aa** in 37% yield (Table 1, entry 1).

Oxidant screening (entries 1−4) revealed that the yield of **2aa** can be increased to 70% using a combination of Ag$_2$CO$_3$ and Mn(OAc)$_3$·2H$_2$O (entry 3). Control experiments excluding the oxidant or the catalyst showed no formation of **2aa** (entries 4, 9). Changing the acid additive to NaOPiv decreased the yield of **2aa** to 27% (entry 5). Other catalysts, such as Co(OAc)$_2$ (entry 6) or Co(acac)$_3$ (entry 7), formed **2aa** in lower yield.[16] The final conditions were found when the product yield additionally was increased to 94% using a higher catalyst loading, 30 mol % (entry 8). We speculate that the high catalyst loading is required due to the coordination of 2-picolinic acid that is released during the reaction to the metal, which may reduce the catalytic activity of cobalt catalyst.[14,17] Indeed, we observed that the product **2aa** yield decreased with an increase in the amount of added 2-picolinic acid.[16] Subsequently, other reaction solvents were screened, such as DCE (entry 10) and toluene (entry 11); however, none of them gave a better yield. Other CO sources such as DIAD (entry 12) or DEAD (entry 13) were less effective. It is worth mentioning that during the optimization we did not observe formation of either products arising from the radical reaction at α-center of phenylalanine, nor oxidation or decarboxylation of **1aa**. It should be noted that, in comparison with Pd catalysis, we did not observe the formation of indoline or indole byproducts resulting from intramolecular C(sp^2)−H amination.[18]

With the optimized conditions in hand, we next examined the reaction scope with respect to phenylalanine esters (Scheme 2). The reaction of substrate **1aa** bearing a methyl ester functionality with CO gave product **2aa** in excellent yield,

Scheme 2. Carbonylation of Phenylalanine Derivatives 1[a]

[a]Reaction conditions: **1** (0.5 mmol), CO (1 atm), Co(dpm)$_2$ (0.15 mmol, 30 mol %), PivOH (1.0 mmol, 2 equiv), Ag$_2$CO$_3$ (0.75 mmol, 1.5 equiv), Mn(OAc)$_3$·2H$_2$O (1.0 mmol, 2 equiv), PhCl (5 mL), 120 °C, isolated yields. [b]Reaction in 1.7 mmol scale, 13 h.

94%; upscaling the reaction to a 1.7 mmol scale gave product **2aa** in 75% yield. At the same time, phenylalanine ethyl, *t*-butyl, and benzyl esters **1ba−da** gave very good yields (70−83%). We found that allyl ester **1ea** was a competent substrate as well and gave product **2ea** in an acceptable yield, 50%.

We next investigated the scope of the C(sp^2)−H carbonylation method with respect to the amino acid derivative **1** (Scheme 3). Gratifyingly, a wide substrate scope with an *ortho*,

Scheme 3. Scope for C(sp²)−H Carbonylation of Amino Acid Derivatives 1[a]
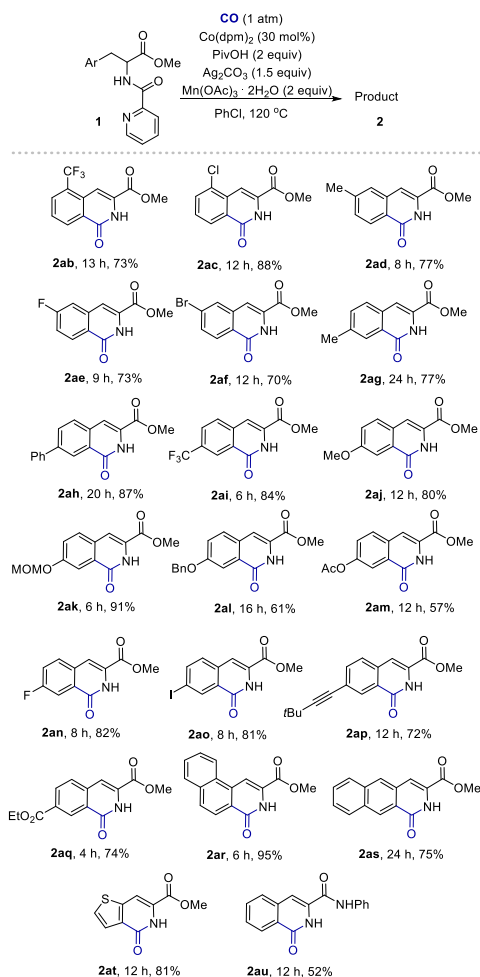
2ab, 13 h, 73%   **2ac**, 12 h, 88%   **2ad**, 8 h, 77%

2ae, 9 h, 73%   **2af**, 12 h, 70%   **2ag**, 24 h, 77%

2ah, 20 h, 87%   **2ai**, 6 h, 84%   **2aj**, 12 h, 80%

2ak, 6 h, 91%   **2al**, 16 h, 61%   **2am**, 12 h, 57%

2an, 8 h, 82%   **2ao**, 8 h, 81%   **2ap**, 12 h, 72%

2aq, 4 h, 74%   **2ar**, 6 h, 95%   **2as**, 24 h, 75%

2at, 12 h, 81%   **2au**, 12 h, 52%

[a]Reaction conditions: **1** (0.5 mmol), CO (1 atm), Co(dpm)₂ (0.15 mmol, 30 mol %), PivOH (1.0 mmol, 2 equiv), Ag₂CO₃ (0.75 mmol, 1.5 equiv), Mn(OAc)₃·2H₂O (1.0 mmol, 2 equiv), PhCl (5 mL), 120 °C, isolated yields.

meta, and *para* substitution pattern gave the corresponding carbonylation products in moderate to excellent yields. Using *meta*-substituted phenylalanine derivatives **1ad−af**, excellent regioselectivity was observed, and we selectively obtained only carbonylation products arising from reaction of less hindered C−H bond, even using *meta*-fluoro-substituted phenylalanine derivative **1ae**.[19]

Importantly, diverse functionalities were tolerated under the reaction conditions, such as alkyl (products **2ad**, **2ag**), halide (**2ac**, **2ae**, **2af**, **2an**, **2ao**), trifluoromethyl (**2ab**, **2ai**), phenyl (**2ah**), ethyl ester (**2aq**), methoxy (**2aj**), methoxymethyl ether (**2ak**), and benzyl ether (**2al**). *O*-Acetyl tyrosine derivative **1am** was less successful and gave a carbonylation product in

moderate yield (57%). During the reaction, we observed partial cleavage of the acetyl group under the reaction conditions. We were pleased to find that phenylalanine derivative **1ap** bearing the *t*-butylacetylenyl substituent was a competent substrate and gave product **2ap** in 72% yield. Both naphthyl amino acids **1ar** and **1as** reacted smoothly and formed 1,2-dihydroisoquinolinone derivatives **2ar** and **2as** in excellent yield. Moreover, the thiophene amino acid derivative **1at** was compatible with the reaction conditions and formed the corresponding product **2at** in a good yield. Furthermore, we determined that even challenging amide derivative **1au**, which potenialy could deactivate the catalyst by coordination, gave carbonylation product **2au** in acceptable yield, 52%.

Investigating the reaction scope, we found some limitations (Scheme 4). Substrate **3a** was unreactive, suggesting that the

Scheme 4. Unsuccessful Substrates
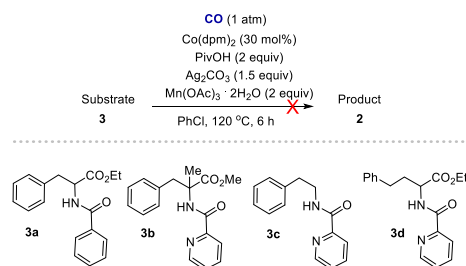
picolinamide directing group has an essential role for C−H carbonylation. Quaternary amino acid **3b**, homobenzyl amide **3c**, and homophenylalanine derivative **3d** did not give carbonylation products, suggesting that both the geometry of substrate as well as the ester functionality at α-carbon are crucial for successful transformation.

Encouraged by the result that amide **1au** underwent carbonylation, we decided to apply the method for more challenging substrates: short peptides. It is known that amide bonds within peptide can chelate metal ions thereby deactivating the reaction catalyst. We were pleased to find that under standard reaction conditions product formation was observed, albeit a large amount of decomposition byproducts were detected by NMR that could be related to the fact that peptides are prone to undergo oxidative cleavage. Excluding Mn(OAc)₃·2H₂O and increasing the Ag₂CO₃ equivalents improved the product yield. Gratifyingly, dipeptides **4a−c** and tripeptide **4d** underwent carbonylation and formed products **5a−d** in acceptable to good yields (Scheme 5). Unfortunately, under the reaction conditions, partial racemization was observed. Product **5a** was obtained with 86% ee, and **5c** with 93% ee. Notably, in the carbonylation of enantiopure **4d**, partial racemization most likely occurred, but purification led to the isolation of the pure major diastereoisomer in 46% yield.

To understand the reaction mechanism, several additional experiments were conducted (Scheme 6).

We synthesized unsaturated phenylalanine derivative **6** and found that carbonylation under standard conditions yielded product **2aa** in 91% yield, suggesting that **6** might be an intermediate for the formation of **2aa**. Interestingly, we found that addition of radical scavenger TEMPO significantly suppressed the carbonylation reaction of **1aa** but only slightly

Scheme 5. Carbonylation of Peptides 4a–d[a]
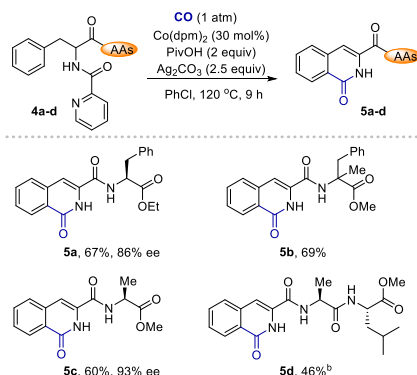
[a]Reaction conditions: **4** (0.2 mmol), CO (1 atm), Co(dpm)$_2$ (0.06 mmol, 30 mol %), PivOH (0.4 mmol, 2 equiv), Ag$_2$CO$_3$ (0.5 mmol, 2.5 equiv), PhCl (1 mL), 120 °C, isolated yields. [b]Yield for pure diastereomer.

Scheme 6. Mechanistic Studies
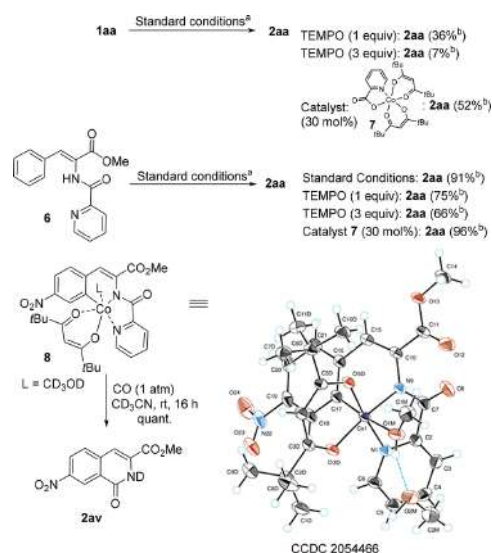
[a]Standard reaction conditions: **1aa** or **6** (0.1 mmol), CO (1 atm), Co(dpm)$_2$ (0.03 mmol, 30 mol %), PivOH (0.2 mmol, 2 equiv), Ag$_2$CO$_3$ (0.15 mmol, 1.5 equiv), Mn(OAc)$_3$·2H$_2$O (0.2 mmol, 2 equiv), PhCl (1 mL), 120 °C, 16 h. [b]NMR yield using triphenyl-methane as an internal standard.

affected carbonylation of **6**, indicating that the radical reaction pathway could be involved for the synthesis of unsaturated intermediate **6**. Moreover, under standard conditions by TLC, we observed the formation of cobalt complex **7** which was isolated, and its structure was confirmed by NMR. Exploiting complex **7** as the reaction catalyst for substrate **1aa** gave product **2aa** in only 52% yield. Interestingly, substrate **6** carbonylation using catalyst **7** resulted in product **2aa** in 96% yield, suggesting that complex **7** is not as efficient catalyst as

Co(dpm)$_2$ for the formation of **6**. Our attempts to isolate the C−H activated complex **8** were successful. The structure of complex **8** was confirmed by X-ray crystallography. We were pleased to find that under CO (1 atm) at room temperature complex **8** quantitatively formed product **2av** which was determined by NMR.

On the basis of the control experiments, isolated intermediates, and previous literature reports,[20] we propose the plausible mechanism (Scheme 7).

Scheme 7. Proposed Mechanism for the Cobalt-Catalyzed Carbonylation of Phenylalanine Derivatives 1
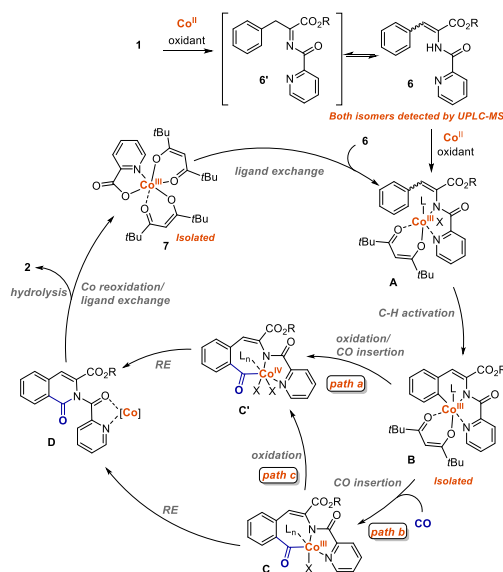
Initially, the phenylalanine derivative **1** using Co(II) catalyst under oxidative conditions is oxidized to the corresponding imine intermediate **6′** which then tautomerizes to the corresponding enamine **6**[3,7] (both double bond isomers were detected by TLC and UPLC-MS). Next, Co(II) salt coordinates with **6** and is oxidized to Co(III) intermediate **A**[20e] followed by the C(sp^2)−H bond cobaltation to form complex **B**. Complex **B** may be oxidized to the Co(IV) species followed by CO coordination and insertion to form Co(IV) complex **C′**, which then undergoes a reductive elimination step to form **D** (path a). Alternatively, complex **B** will undergo CO coordination and insertion to form Co(III) complex **C** which gives intermediate **D** after reductive elimination (path b). Path c may also be operative according to which intermediate **C** is oxidized to **C′**. Next, the directing group in intermediate **D** is hydrolyzed to liberate **2**, and cobalt is reoxidized to Co(III) to form complex **7**, which we observed by TLC in all carbonylation reactions. The catalytic cycle restarts with ligand exchange in complex **7** to form intermediate **A**. At this point of study, it is hard to distinguish between possible pathways, but according to control experiments, we believe that, in our case, path b may be more favorable over path a or c, as stoichiometric complex **8** formed **2av** without addition of oxidant.

In summary, we have developed an efficient protocol for the $C(sp^2)-H$ carbonylation of amino acid derivatives based on the inexpensive $Co(dpm)_2$ catalyst. A broad range of phenylalanine derivatives bearing diverse functional groups were tolerated. Carbonylation of the amino acid $C(sp^2)-H$ bond was accomplished using picolinamide as a traceless directing group and carbon monoxide (1 atm) as the carbonyl source. In addition, the developed method can be successfully applied to the $C(sp^2)-H$ carbonylation of short peptides thereby offering opportunity for peptide late-stage carbonylation.

■ ASSOCIATED CONTENT

Ⓢ Supporting Information

The Supporting Information is available free of charge at https://pubs.acs.org/doi/10.1021/acs.orglett.1c00660.

> Experimental procedures and characterization data for all new compounds along with copies of the NMR spectra and HPLC chromatograms (PDF)
> Crystallographic data (PDF)

Accession Codes

CCDC 2054466 contains the supplementary crystallographic data for this paper. These data can be obtained free of charge via www.ccdc.cam.ac.uk/data_request/cif, or by emailing data_request@ccdc.cam.ac.uk, or by contacting The Cambridge Crystallographic Data Centre, 12 Union Road, Cambridge CB2 1EZ, UK; fax: +44 1223 336033.

■ AUTHOR INFORMATION

Corresponding Author

Liene Grigorjeva − *Latvian Institute of Organic Synthesis, Riga LV-1006, Latvia;* ⊙ orcid.org/0000-0003-3497-6776; Email: liene_grigorjeva@osi.lv

Authors

Lukass Lukasevics − *Latvian Institute of Organic Synthesis, Riga LV-1006, Latvia*

Aleksandrs Cizikovs − *Latvian Institute of Organic Synthesis, Riga LV-1006, Latvia*

Complete contact information is available at:
https://pubs.acs.org/10.1021/acs.orglett.1c00660

Author Contributions

The manuscript was written through contributions of all authors. All authors have given approval to the final version of the manuscript.

Notes

The authors declare no competing financial interest.

■ REFERENCES

(1) Selected reviews: (a) Mondal, S.; Chowdhury, S. *Adv. Synth. Catal.* **2018**, *360*, 1884−1912. (b) Zhan, B.-B.; Jiang, M.-X.; Shi, B.-F. *Chem. Commun.* **2020**, *56*, 13950−13958. (c) Wang, W.; Lorion, M. M.; Shah, J.; Kapdi, A. R.; Ackermann, L. *Angew. Chem., Int. Ed.* **2018**, *57*, 14700−14717. (d) Brandhofer, T.; García Mancheño, O. *Eur. J. Org. Chem.* **2018**, *2018*, 6050−6067. (e) Zhang, M.; Zhong, S.; Peng, Y.; Jiang, J.; Zhao, Y.; Wan, C.; Zhang, Z.; Zhang, R.; Zhang, A. Q. *Org. Chem. Front.* **2021**, *8*, 133−168.

(2) Lee, A. C.-L.; Harris, J. L.; Khanna, K. K.; Hong, J.-H. *Int. J. Mol. Sci.* **2019**, *20*, 2383−2404.

(3) San Segundo, M.; Correa, A. *Synthesis* **2018**, *50*, 2853−2866.

(4) Review: (a) Li, X.; Xiong, W.; Ding, Q. *Chinese J. Org. Chem.* **2019**, *39*, 1867−1874. Selected key references: (b) Terrey, M. J.; Perry, C. C.; Cross, W. B. *Org. Lett.* **2019**, *21*, 104−108. (c) San Segundo, M.; Correa, A. *Chem. Sci.* **2019**, *10*, 8872−8879. (d) Zheng, Y.; Song, W. *Org. Lett.* **2019**, *21*, 3257−3260. (e) Ding, Q.; Ye, S.; Cheng, G.; Wang, P.; Farmer, M. E.; Yu, J.-Q. *J. Am. Chem. Soc.* **2017**, *139*, 417−425. (f) Bai, C.; Cai, C.; Yu, Z.; Wang, H. *Angew. Chem., Int. Ed.* **2018**, *57*, 13912−13916.

(5) Selected reviews: (a) Gandeepan, P.; Müller, T.; Zell, D.; Cera, G.; Warratz, S.; Ackermann, L. *Chem. Rev.* **2019**, *119*, 2192−2452. (b) Moselage, M.; Li, J.; Ackermann, L. *ACS Catal.* **2016**, *6*, 498−525. (c) Kommagalla, Y.; Chatani, N. *Coord. Chem. Rev.* **2017**, *350*, 117−135. (d) Daugulis, O.; Roane, J.; Tran, L. D. *Acc. Chem. Res.* **2015**, *48*, 1053−1064. (e) Hyster, T. K. *Catal. Lett.* **2015**, *145*, 458−467.

(6) Selected examples: (a) Grigorjeva, L.; Daugulis, O. *Angew. Chem., Int. Ed.* **2014**, *53*, 10209−10212. (b) Kalsi, D.; Sundararaju, B. *Org. Lett.* **2015**, *17*, 6118−6121. (c) Nguyen, T. T.; Grigorjeva, L.; Daugulis, O. *Chem. Commun.* **2017**, *53*, 5136−5138. (d) Sau, S. C.; Mei, R.; Struwe, J.; Ackermann, L. *ChemSusChem* **2019**, *12*, 3023−3027. (e) Thrimurtulu, N.; Dey, A.; Maiti, D.; Volla, C. M. R. *Angew. Chem., Int. Ed.* **2016**, *55*, 12361−12365.

(7) Cobalt-catalyzed arylation of glycine esters and peptides through a radical pathway: (a) San Segundo, M.; Guerrero, I.; Correa, A. *Org. Lett.* **2017**, *19*, 5288−5291. (b) Andrade-Sampedro, P.; Correa, A.; Matxain, J. M. *J. Org. Chem.* **2020**, *85*, 13133−13140.

(8) Lorion, M. M.; Kaplaneris, N.; Son, J.; Kuniyil, R.; Ackermann, L. *Angew. Chem., Int. Ed.* **2019**, *58*, 1684−1688.

(9) Selected reviews: (a) Lukasevics, L.; Grigorjeva, L. *Org. Biomol. Chem.* **2020**, *18*, 7460−7466. (b) Peng, J.-B.; Wu, F.-P.; Wu, X.-F. *Chem. Rev.* **2019**, *119*, 2090−2127. (c) Rajesh, N.; Barsu, N.; Sundararaju, B. *Tetrahedron Lett.* **2018**, *59*, 862−868. (d) Li, Y.; Hu, Y.; Wu, X.-F. *Chem. Soc. Rev.* **2018**, *47*, 172−194.

(10) Vicente, J.; Saura-Llamas, I.; García-López, J.-A.; Calmuschi-Cula, B.; Bautista, D. *Organometallics* **2007**, *26*, 2768−2776.

(11) López, B.; Rodríguez, A.; Santos, D.; Albert, J.; Ariza, X.; Garcia, J.; Granell, J. *Chem. Commun.* **2011**, *47*, 1054−1056.

(12) Zaitsev, V. G.; Shabashov, D.; Daugulis, O. *J. Am. Chem. Soc.* **2005**, *127*, 13154−13155.

(13) Selected examples for C−H functionalization using picolinamide DG: (a) Nadres, E. T.; Daugulis, O. *J. Am. Chem. Soc.* **2012**, *134*, 7−10. (b) Schreib, B. S.; Carreira, E. M. *J. Am. Chem. Soc.* **2019**, *141*, 8758−8763. (c) Bolsakova, J.; Lukasevics, L.; Grigorjeva, L. *J. Org. Chem.* **2020**, *85*, 4482−4499. (d) Rej, S.; Chatani, N. *ACS Catal.* **2018**, *8*, 6699−6706. (e) Martínez, Á. M.; Rodríguez, N.; Arrayás, R. G.; Carretero, J. C. *Chem. Commun.* **2014**, *50*, 2801−2803.

(14) Kuai, C.; Wang, L.; Li, B.; Yang, Z.; Cui, X. *Org. Lett.* **2017**, *19*, 2102−2105.

(15) Picolinamide as a traceless DG: (a) Ling, F.; Ai, C.; Lv, Y.; Zhong, W. *Adv. Synth. Catal.* **2017**, *359*, 3707−3712. (b) Lukasevics, L.; Cizikovs, A.; Grigorjeva, L. *Org. Lett.* **2020**, *22*, 2720−2723. (c) Ling, F.; Zhang, C.; Ai, C.; Lv, Y.; Zhong, W. *J. Org. Chem.* **2018**, *83*, 5698−5706.

(16) Please see the Supporting Information for details.

(17) (a) Gandeepan, P.; Rajamalli, P.; Cheng, C.-H. *Angew. Chem., Int. Ed.* **2016**, *55*, 4308−4311. (b) Ying, J.; Fu, L.-Y.; Zhong, G.; Wu, X.-F. *Org. Lett.* **2019**, *21*, 5694−5698. (c) Gao, Q.; Lu, J.-M.; Yao, L.; Wang, S.; Ying, J.; Wu, X.-F. *Org. Lett.* **2021**, *23*, 178−182.

(18) (a) Mei, T.-S.; Leow, D.; Xiao, H.; Laforteza, B. N.; Yu, J.-Q. *Org. Lett.* **2013**, *15*, 3058−3061. (b) He, G.; Zhao, Y.; Zhang, S.; Lu, C.; Chen, G. *J. Am. Chem. Soc.* **2012**, *134*, 3−6.

(19) Sun, B.; Yoshino, T.; Kanai, M.; Matsunaga, S. *Angew. Chem., Int. Ed.* **2015**, *54*, 12968−12972.

(20) (a) Ni, J.; Li, J.; Fan, Z.; Zhang, A. *Org. Lett.* **2016**, *18*, 5960−5963. (b) Barsu, N.; Bolli, S. K.; Sundararaju, B. *Chem. Sci.* **2017**, *8*, 2431−2435. (c) Landge, V. G.; Jaiswal, G.; Balaraman, E. *Org. Lett.* **2016**, *18*, 812−815. (d) Hao, X.-Q.; Du, C.; Zhu, X.; Li, P.-X.; Zhang, J.-H.; Niu, J.-L.; Song, M.-P. *Org. Lett.* **2016**, *18*, 3610−3613. (e) Zeng, L.; Tang, S.; Wang, D.; Deng, Y.; Chen, J.-L.; Lee, J.-F.; Lei, A. *Org. Lett.* **2017**, *19*, 2170−2173.

Lukasevics, L.; Cizikovs, A.; Grigorjeva, L. C–H bond functionalization by high-valent cobalt catalysis: current progress, challenges and future perspectives. *Chem. Commun.*, **2021**, 57, 10827-10841.

Check for updates

C–H bond functionalization by high-valent cobalt catalysis: current progress, challenges and future perspectives

Lukass Lukasevics, Aleksandrs Cizikovs and Liene Grigorjeva ID *

Over the last decade, high-valent cobalt catalysis has earned a place in the spotlight as a valuable tool for C–H activation and functionalization. Since the discovery of its unique reactivity, more and more attention has been directed towards the utilization of cobalt as an alternative to noble metal catalysts. In particular, Cp*Co(III) complexes, as well as simple Co(II) and Co(III) salts in combination with bidentate chelation assistance, have been extensively used for the development of novel transformations. In this review, we have demonstrated the existing trends in the C–H functionalization methodology using high-valent cobalt catalysis and highlighted the main challenges to overcome, as well as perspective directions, which need to be further developed in the future.

1. Introduction

Transition metal-catalyzed direct functionalization of relatively inert C–H bonds has become an essential organic synthesis tool, which allows the simplification of synthetic schemes and allows the use of simpler starting materials for the construction of various complex targets like natural products, amino acids and peptides, diverse pharmaceuticals, *etc.*[1] Outstanding progress has been made using precious transition metal catalysis, despite the low natural abundance, toxicity and expensiveness.[1] Nowadays, a great emphasis is placed on the development of sustainable step and atom-economic, environmentally friendly C–H functionalization methods.[2] Despite that, only relatively recently earth-abundant 3d transition metals have attracted increased interest and had been explored for catalytic purposes.[3] Development of C–H functionalization methods using first-row transition metals is still a growing field with a lot of challenges ahead and we can expect some important discoveries in the near future. Among the other 3d elements, cobalt is considered as a sustainable metal due to its biorelevance, earth abundance, lower toxicity and price.[4] Since 2010, there has been enormous interest and rapid progress in the development of C–H bond activation and functionalization methods using cobalt catalysis, therefore cobalt could be considered as a rising star in homogenous catalysis and one of the most promising 3d metals for C–H functionalization.[3–5]

Herein, we summarize the progress made in the development of C–H bond functionalization methods under high-valent

cobalt catalysis, highlighting the key achievements and current challenges of this topic.

2. Historical background

Methods for C–H bond activation and functionalization using cobalt are divided into two main categories depending on the reaction conditions and cobalt catalyst used for cobaltation (Scheme 1): (1) low-valent cobalt catalysis – Co(0), Co(I) or Co(II) species provide C–H cobaltation, reactions typically are performed under reductive conditions; (2) high-valent cobalt catalysis – C–H cobaltation is achieved using well-defined Co(III) species, or *in situ* prepared Co(III) species from a Co(II) or Co(III) precatalyst under oxidative or non-reductive conditions.[4b]

The origin of C–H bond activation and functionalization using cobalt dates back to 1955 when Murahashi reported the first example of low-valent cobalt-catalyzed C–H bond carbonylation of a Schiff base for the synthesis of isoindolinones (Scheme 2a).[6a] After a long period of silence, in 1994, Kisch and co-workers reported the $CoH_3(PPh_3)_3$ or $CoH(N_2)(PPh_3)_3$ catalyzed alkenylation of azobenzenes with diphenylacetylene (Scheme 2b).[6b] Later, in 1997, Lenges and Brookhart demonstrated the Cp*Co(I) complex catalyzed intra- and intermolecular hydroacylation of vinylsilane

*Latvian Institute of Organic Synthesis, Aizkraukles 21, LV-1006 Riga, Latvia.
E-mail: Liene_grigorjeva@osi.lv*
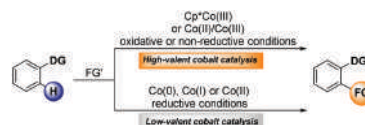
Scheme 1 Categories for cobalt-catalyzed C–H functionalization.
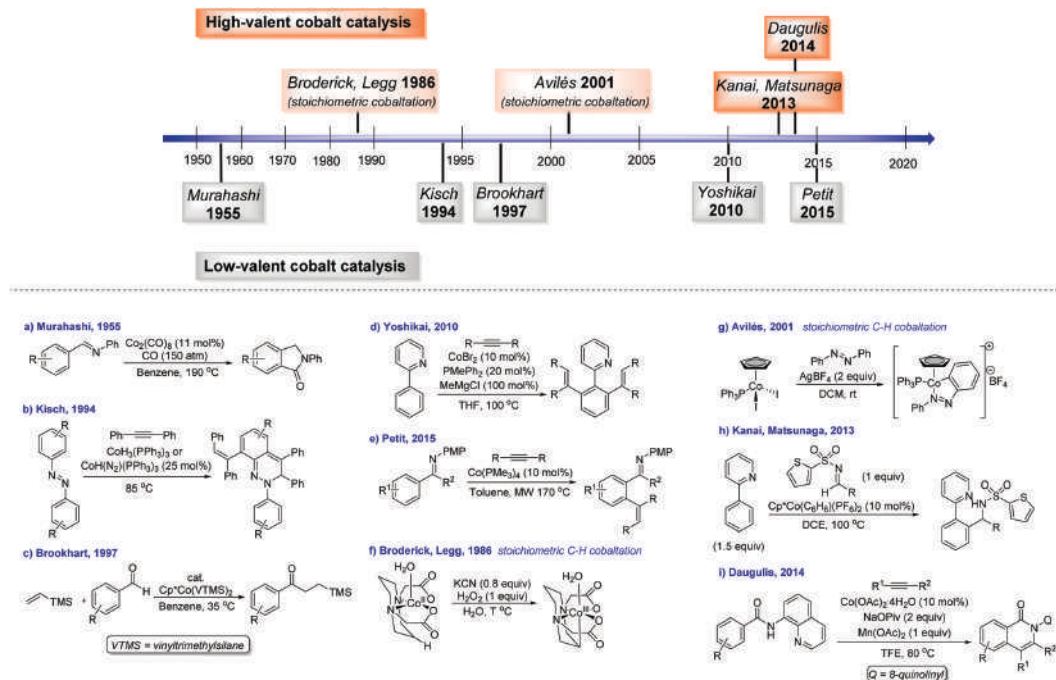
Scheme 2 Timeline of the development of C–H bond activation and functionalization methods using cobalt catalysis.

with aromatic aldehydes (Scheme 2c).[6c] A turning point for low-valent cobalt catalysis was achieved in 2010, when Yoshikai and co-workers demonstrated an elegant method for the chelation-assisted alkenylation of aryl pyridines with internal alkynes. The developed method was based on the employment of an *in situ* generated low-valent cobalt catalyst, which was generated from a simple Co(II) salt in the presence of a ligand using a Grignard reagent as the reductant (Scheme 2d).[6d]

Since its discovery, this approach has been extensively used for a large diversity of transformations.[7] Low-valent cobalt catalysis was explored later by Petit and co-workers. In 2015, Petit's group demonstrated C(sp²)–H bond alkenylation with internal alkynes using a simple, well-defined low-valent cobalt catalyst (Scheme 2e).[6e] Contrary to the method developed by Yoshikai, in this case, reducing agents or additives were unnecessary for the successful transformation. Although the use of low-valent cobalt catalysis for C–H bond activation and functionalization gave a relatively wide scope of methods, typically they suffer from low functional group tolerance under the reaction conditions.

Broderick, Legg and co-workers, in 1986, reported initial studies on intramolecular C–H bond activation with high-valent cobalt species to form a stable Co(III)-alkyl complex (Scheme 2f).[6f] In 2001, Avilés and co-workers were first to demonstrate that the CpCo(III) complex is able to activate the *ortho*-C–H bond in azobenzene in the presence of AgBF₄ to form an *ortho*-metalated Co(III) complex (Scheme 2g).[6g] The turning point for C–H bond functionalization

using high-valent cobalt catalysis was reached in 2013, when Kanai, Matsunaga and co-workers reported the first example of the Cp*Co(III) catalyzed directed addition reaction of the C(sp²)–H bond to polar electrophiles (Scheme 2h).[6h] This pioneering work served as a base for the discovery of dozens of new transformations. A year later, in 2014, Daugulis and co-workers demonstrated the cobalt-catalyzed aminoquinoline-directed benzamide alkenylation/annulation reaction with terminal and internal alkynes (Scheme 2i).[6i] Thus, it is shown for the first time that cheap and earth-abundant Co(II) salts in combination with bidentate directing group assistance can be efficiently exploited for C–H functionalization as high-valent cobalt(III) precursors. This strategy, as well, served as a basis for a large number of discoveries. Further progress made in the development of C–H bond functionalization methods using either Cp*Co(III) catalysts or bidentate chelation assisted cobalt catalysis is discussed below.

3. High-valent cobalt catalysis: Cp*Co(III) catalysis

3.1. Directing group

Inspired by the successful use of cationic Cp*Rh(III) complexes for C–H bond functionalization, Kanai, Matsunaga and co-workers developed an economically and environmentally advantageous alternative – Cp*Co(III) complexes.[6h] Being homologous with

rhodium, cationic high-valent cobalt complexes not only exhibited the ability to promote C–H bond functionalization, but also demonstrated the same unique and versatile reactivity and selectivity as Cp*Rh(III) complexes.

A directing group plays an important role in cobalt-catalyzed C–H bond activation – it helps in bringing cobalt in close proximity to the target C–H bond and facilitates the formation of a cobaltacycle with which the second reaction component reacts.[1f] A directing group also controls the reaction regioselectivity. Great progress has been achieved using Cp*Co(III) catalysis; however, the developed C–H bond functionalization methods mainly rely on the use of strongly coordinating directing groups such as pyridyl, pyrimidyl, purinyl and pyrazolyl.[8] Using strongly coordinating group assistance, C(sp²)–H bond functionalization with alkynes,[9a,b] alkenes,[9c] acrylates,[9d] maleimides,[9e,f] maleate esters,[9e] allenes,[9g] sulfonyl imines,[6h,9h] aldehydes,[9i,j] ketenimines,[9k] isocyanates,[9l,m] "allyl" sources,[9n–p] carbamates,[9q] diazo compounds,[9r] "CN" sources,[9s,t] organic azides,[9u,v] etc. has been developed (Scheme 3).[9]

Nevertheless, compounds containing strongly coordinating directing groups, such as aryl or heteroaryl pyridine, pyrazine, purine and pyrazole analogues, are of biological and pharmaceutical interest; however, these directing groups are difficult to manipulate in further synthetic transformations, which significantly reduces the applicability of the developed method. On the other hand, it is a great tool for demonstrating and proving new discoveries. Despite the wide applicability of the directing group approach for C–H functionalization, the removal of the directing group is an important drawback as it often requires harsh reaction conditions and/or multiple-step synthesis, thereby reducing the step-economical nature of the C–H activation strategy. Recently, several approaches have emerged to overcome these drawbacks. One of the approaches is the use of the traceless directing group strategy. Traceless directing groups are a novel class of directing groups that assist in performing two steps in one pot: (1) chelation assisted C–H bond functionalization; (2) DG cleavage (Scheme 4).[10] The second alternative is the use of a transient directing group, which is installed and removed in situ. Typically, a transient directing group is generated from a weakly coordinating directing group by the reaction with co-catalytic or stoichiometric amounts of a modifier, which endows the weakly coordinating directing group with better σ-donor functionality and is released after C–H functionalization.[11] Another alternative is the direct use of the existing functional group
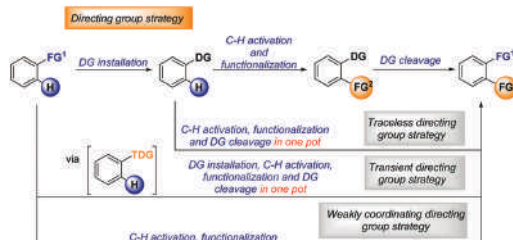
Scheme 4 Directing group strategies for C–H bond activation and functionalization.

(e.g. carboxylic acids, ketones, esters, ethers, amides, etc.) as a weakly coordinating directing group for C–H activation and functionalization. Although this approach seems to be the most attractive one, especially for the late-stage synthesis, it is also the most challenging one due to the poor reactivity towards C–H functionalization and low thermodynamical stability of the resulting metalacycle.[12]

To highlight directing group strategies applied under Cp*Co(III) catalysis and emphasize their importance in the development of sustainable transformations, representative examples are given below.

3.1.1. Traceless directing groups. The first two reports on traceless directing group application for Cp*Co(III) catalyzed C–H bond functionalization date back to 2014, when Kanai and co-workers reported the indole C–H bond alkenylation/annulation sequence. In this report, morpholine amide was used as a directing group (Scheme 5a).[13a] In the same year, Ellman and co-workers demonstrated furan synthesis via aldehyde addition to alkenyl oxime C–H bonds. A traceless oxime directing group was used for this transformation (Scheme 5b).[13b]

Since the development of this synthetic approach in 2014, several traceless directing groups have been designed and applied for C–H bond functionalization of aniline-type derivatives, as well as for benzamides and other compounds. Using traceless directing group assistance, C(sp²)–H bond functionalization with alkynes,[14] alkenes,[15] maleimides,[16] aldehydes,[13b] and dioxazolones[17] has been developed (Scheme 6).

Most of the monodentate traceless directing groups used for Cp*Co(III) catalyzed C–H bond transformation (amide, ester, hydrazine, ester, nitroso, etc.) have a dual role – to control the
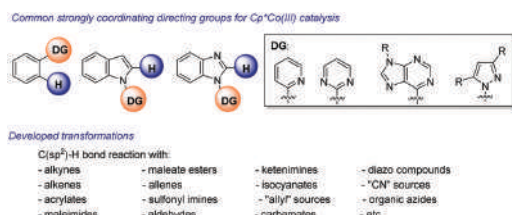
Scheme 3 Strongly coordinating directing groups for Cp*Co(III) catalysis and developed transformations.
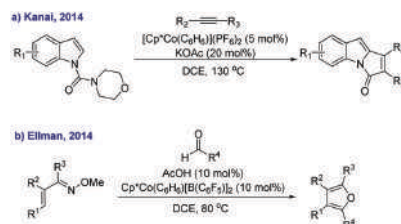
Scheme 5 First examples of traceless directing group application for Cp*Co(III) catalyzed C–H bond functionalization.
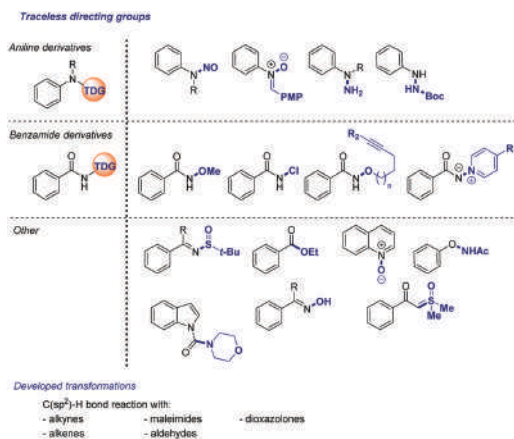
Scheme 6 Common traceless directing groups for Cp*Co(III) catalyzed C–H bond functionalization.

Scheme 7 Cp*Co(III) catalyzed *ortho*-amidation of benzaldehydes.

site selectivity for the C–H activation step and, at the same time, to serve as an internal oxidant to reoxidize Co(I) to Co(III) species and regenerate the catalytic cycle. Despite the fact that the traceless directing group strategy has stood out as an attractive alternative to the classic directing group approach (step economy), more efforts still need to be applied to develop this direction further. Currently, the most important drawback of this approach is the limited transformation range. For example, C–H bond functionalization reactions with alkynes are relatively well studied using a wide range of substrates, while there are only a limited number of reports on C–H functionalization using other C–H functionalization reagents.

3.1.2. Transient directing groups. The transient directing group strategy has gained a lot of attention in recent years from a cost-effective and sustainable point of view and has been assessed as a promising tool for C–H functionalization. However, at present, this approach mainly relies on the use of 4d transition metal catalysts such as ruthenium, palladium and rhodium.[18]

The first examples of the use of the transient directing group strategy for cobalt catalyzed C–H bond activation and functionalization were reported in 2019 by Li and co-workers[19a] and Sundararaju's group.[19b] Both groups independently reported the *ortho*-amidation of various benzaldehydes with dioxazolones using Cp*Co(III) catalysts (Scheme 7a and b). In their work, anilines were employed to enhance the coordination ability of the aldehyde by forming an imine functional group *in situ*, which could serve as a monodentate directing group and be cleaved either after the reaction during workup or in the reaction mixture.

Thus far, *ortho*-amidation is the only known transformation that employs the transient directing group strategy. The lack of reports on this topic clearly indicates that this approach is a highly challenging task and most likely will become a hot topic in the near future, as there is an urgent need for new C–H functionalization methods based on the 3d transition metal catalyzed transient directing group strategy.
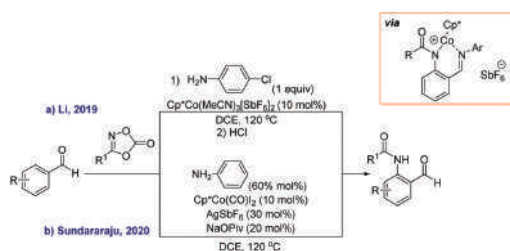
3.1.3. Weakly coordinating directing groups. Utilizing substrates with weakly coordinating directing groups for C–H bond activation and functionalization is beneficial and a powerful approach for developing new sustainable transformations. Compared to the approaches described above, the weakly coordinating directing group approach has the most step- and atom-economical nature. It employs useful functional motifs as directing groups, therefore, no extra steps are required for directing group installation and removal. Despite this fact, the development of such methodology is highly desirable and still a challenging task due to the low reactivity and thermodynamical stability of the key metalacycle. However, several successful C–H bond functionalization reactions have been developed. Representative examples are given below.

In 2014, Glorius and co-workers demonstrated the first example of selective *mono*-iodination of the *ortho*-C–H bond exploiting N-alkyl benzamide as a substrate (Scheme 8a).[20a] Since then, N-alkyl amides, as well as N-alkyl thioamides, were exploited as weakly coordinating directing groups under Cp*Co(III) catalysis for a variety of transformations.[20] Another elegant example of the weakly coordinating directing group approach was published in 2017 by Sundararaju and co-workers (Scheme 8b).[21] The authors demonstrated a benzoic acid annulation reaction with internal alkynes, which was the first example exploiting carboxylic acid as a directing group under Cp*Co(III) catalysis. In 2018, Maji and co-workers published the first example of the weakly coordinating ketone directed regioselective *mono*-C–H allylation reaction (Scheme 8c).[22] An interesting example was reported by Anbarasan's group in 2016. They reported an intramolecular dehydrogenative C–H/X–H coupling as an efficient approach for the synthesis of indoles and benzofurans, thus demonstrating that the current approach is not limited to intermolecular transformations (Scheme 8d).[23] The range of intramolecular C–H functionalization reactions was further expanded in 2020 by Lete and co-workers, who realized the N-alkyl amide directed synthesis of dihydrobenzofurans (Scheme 8e).[24]

Although this direction is evolving, new discoveries and studies are needed. The C–H functionalization methodology scope needs to be expanded.

3.2. C(sp³)–H bond activation and functionalization

Due to the lower acidity and lack of π-electrons in sp³ hybridized carbon, $C(sp^3)$–H bond activation is a more challenging task. Over the last decade, many reports on $C(sp^2)$–H bond
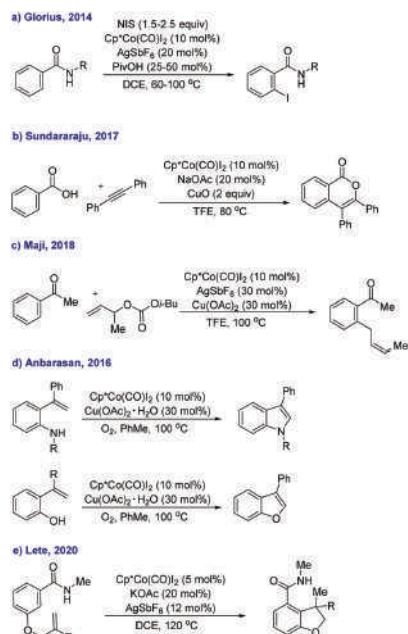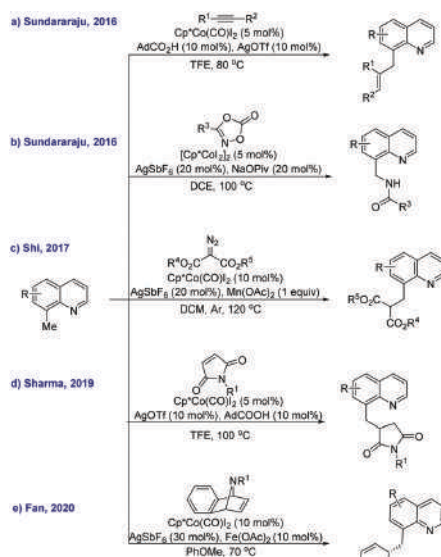
Scheme 8 Representative examples of Cp*Co(III) catalyzed C–H bond functionalization using the weakly coordinating directing group approach.

Scheme 9 Cp*Co(III) catalyzed C(sp³)–H bond functionalization of 8-methylquinoline.

functionalization have been published whereas the development of novel C(sp³)–H bond functionalization methodology seems to be lagging behind. Despite its great potential in the construction of complex biologically active compounds, even with several tetrahedral centres, only a dozen new reports were published over 5 years. Nevertheless, some progress has been achieved in this field.

The first report on C(sp³)–H bond activation and functionalization using a high-valent Cp*Co(III) catalyst was published in 2016 by Sundararaju and co-workers. They demonstrated that under Cp*Co(III) catalysis, the alkenylation of 8-methylquinolines can be achieved (Scheme 9a).[25a] Among the diverse C(sp³)–H bond functionalization substrates, 8-methylquinolines have been proved to be excellent substrates for a large number of C–H bond transformations using various transition metal catalysts. Shortly after the first publication, the same group reported the 8-methylquinoline amidation reaction using oxazoline as the amidating reagent (Scheme 9b).[25b] In 2017, Shi and co-workers extended the scope for 8-methylquinoline C(sp³)–H bond functionalization and reported the alkylation reaction with diazo carbonyl compounds (Scheme 9c).[25c] Sharma and co-workers demonstrated the alkylation reaction with maleimides (Scheme 9d).[25d] Recently, in 2020, Fan and co-workers revealed the coupling of 8-methylquinoline with azabicyclic alkenes via C(sp³)–H bond functionalization (Scheme 9e).[25e]

Besides 8-methylquinoline substrates, several reports on C(sp³)–H functionalization of aliphatic thioamides have been published. In 2017, Seayad reported an amidation protocol

using dioxazolones (Scheme 10a).[26a] In 2019, Loh developed a C–N bond formation methodology using anthranils to obtain aniline derivatives (Scheme 10b).[26b] Similar work was reported by Li and co-workers in 2020, where the amination of thioamides with anthranils to obtain various aniline derivatives was demonstrated (Scheme 10c).[26c]

Nevertheless, C(sp³)–H bond functionalization reactions using Cp*Co(III) catalysis are still limited to two substrate types: 8-methylquinolines and aliphatic thioamides. This is a perspective direction for new discoveries and breakthroughs. The development of more reactive catalysts, application of diverse directing groups or different strategies might be required to overcome this challenge.[27]
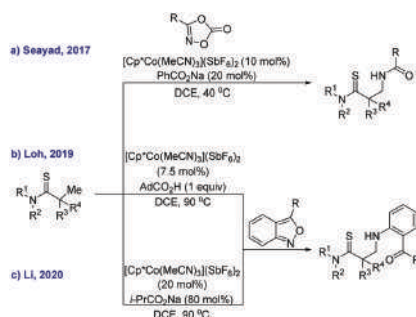
Scheme 10 Cp*Co(III) catalyzed C(sp³)–H bond functionalization of thioamides.

3.3. Late-stage C–H functionalization

The late-stage functionalization strategy enables the construction and modification of complex molecules by introducing functional groups in the molecule in the very last step of the synthesis in the presence of other functional groups.[28] Such an approach is especially advantageous when it gives access to diverse functionalized molecules which would be more difficult to obtain via conventional chemical pathways. This strategy has immense potential in drug discovery as it allows for much faster synthesis of drug analogues with increased structural complexity, as well as the diversification of natural products. C–H bond activation and functionalization are excellent candidates for the late-stage functionalization toolkit, because transition metal catalysts often allow selective C–H bond cleavage and have good functional group tolerance.[28] Recently, great effort has been made to substitute noble metal catalysts with 3d metals to further increase the cost-effectiveness and environmental friendliness of this strategy.

There is only a limited number of examples of the late-stage C–H functionalization strategy using Cp*Co(III) catalysis.[29] The first example of Cp*Co(III) catalyzed late-stage C–H functionalization was demonstrated by Ackermann's group in 2019. In their work, they developed Cp*Co(III) catalyzed C–H allylation of a tryptophan moiety in structurally complex peptides (Scheme 11).[29a] The developed methodology displayed a very good functional group tolerance and reactivity even with β-amino acids.

In 2019, Ellman and co-workers reported the Cp*Co(III) catalyzed late-stage functionalization of the natural product thiostrepton with various dioxazolones (Scheme 12).[29b] The reaction conditions were mild and tolerated the delicate structure of the natural product, yielding a predominantly mono-amidated product, even though in the majority of cases, the formation of di-amidated products was also observed. They found that the terminal dehydroalanine (Dha1) position is preferred, resulting in product mixtures with a regioisomeric ratio ranging from 3.3:1 to 24:1 with complete Z-selectivity.

Recently, in 2020, Ackerman and co-workers developed a versatile and elegant late-stage C–H bond methylation methodology for complex drug molecules under Cp*Co(III) catalysis. The designed catalytic system was applicable to a large variety of drug molecules with inherently different directing groups (heterocyclic monodentate directing groups, amides, ketones, aldehydes, phenols, amines, etc.). They demonstrated the versatility of the developed protocol to several biologically active structures and marketed drug molecules to produce methylated analogues. The selected example is depicted in Scheme 13 – the late-stage C–H functionalization of paclitaxel, which the authors were able to successfully methylate in 32% yield.[29c]
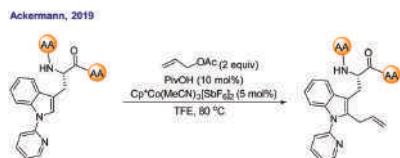
Scheme 11   Cp*Co(III) catalyzed late-stage functionalization of peptides.
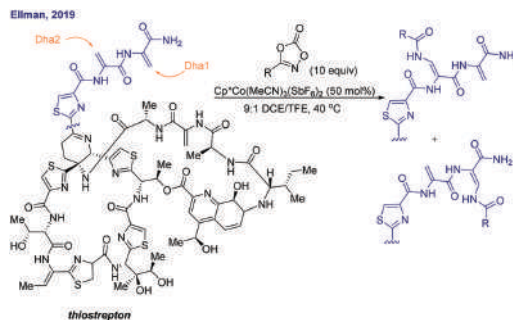
Scheme 12   Cp*Co(III) catalyzed late-stage functionalization of peptides.
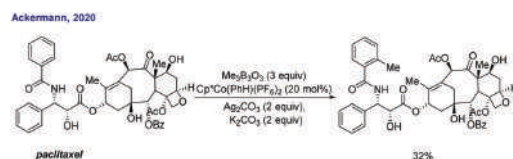
Scheme 13   Late-stage C–H methylation of paclitaxel.

Natural product and drug diversification is essential in drug discovery, therefore, the development of novel methods using the late-stage functionalization strategy is of great interest and in high demand.

3.4. Multi-component addition to C–H bonds

From the perspective of atom- and step-economy, multicomponent reactions could potentially be one of the promising directions towards sustainable and green chemistry. They allow the construction of diverse complex structures from simple precursors given the large number of possible combinations of coupling partners.[30]

In 2016, Ellman and co-workers disclosed the first example of Cp*Co(III)-catalyzed asymmetric C–H bond functionalization using three-component addition cascades. In the reported work, a 1-pyrazole directing group ensured selective C–H activation, followed by the insertion of alkyl enone and diastereoselective addition to aldehyde to generate aldol products (Scheme 14a).[31a] The phenyl pyrazole substrate was further used in multicomponent cascade addition reactions three years later by the same group. In this report, the authors demonstrated C–H bond functionalization with substituted dienes and aldehydes/ketones to obtain secondary or tertiary homoallyl alcohols in a highly diastereoselective fashion (Scheme 14b).[31b] Recently, in 2021, Ellman and co-workers published the three-component cyanation of phenyl pyrazole with substituted dienes and N-cyano succinimide to construct a quaternary C(sp³)–CN centre (Scheme 14c).[31c]

In addition to phenyl pyrazole multi-component C–H functionalization, Ellman's group explored the possibilities of the construction of complex structures using various N,N-dialkyl benzamides with different coupling partners. In 2017, they described the Cp*Co(III)-catalyzed three-component C–H coupling reaction, where
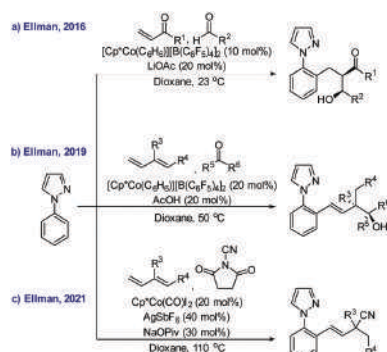
Scheme 14 Multi-component C–H functionalization of phenyl pyrazole *via* Cp*Co(III) catalysis.
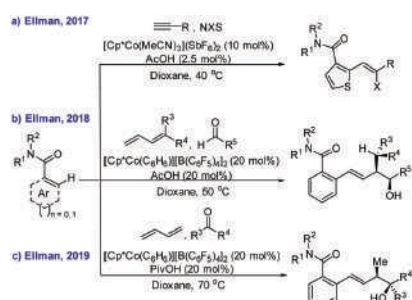

Scheme 15 Multi-component C–H functionalization of benzamides *via* Cp*Co(III) catalysis.

benzamides were first added to the terminal alkyne followed by halogenation to furnish alkenyl halides (Scheme 15a).[32a] A year after, in 2018, Ellman and co-workers reported the three-component transformation of *N,N*-dialkyl benzamides with dienes and aldehydes to form two new C–C bonds and several stereocenters with good diastereoselectivity in the corresponding reaction products (Scheme 15b).[32b] In 2019, they published similar work, which described the three-component diastereoselective addition of *N,N*-dialkyl benzamides with butadiene and various symmetrical and non-symmetrical ketones to obtain homoallyl alcohols (Scheme 15c).[32c]

At this point, Ellman and co-workers are the only pioneers for this topic. Therefore, it is highly desirable for other groups to join this valuable field with new ideas, to make faster progress.

3.5. Enantioselective C–H bond functionalization

Shortly after the discovery of high-valent cobalt catalysis, not much attention was directed towards enantioselective C–H functionalization, where the main progress was achieved using noble transition metal catalysis.[33] Since the first example of cobalt catalyzed enantioselective C–H functionalization in 2018, decent progress has been also achieved in this field, although it is still at its infancy stage, as the only reported examples are
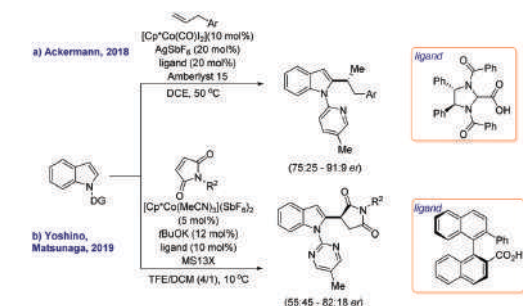
Scheme 16 Cp*Co(III) catalyzed enantioselective C–H functionalization of indoles.

solely catalyzed by Cp*Co(III) complexes. Two main strategies employed for chirality induction are either the use of chiral ligands or Cp^xCo(III) catalysts.

In 2018, Ackerman's group reported the first Cp*Co(III)-catalyzed enantioselective C–H alkylation protocol for indole derivatives and alkenes (Scheme 16a).[34a] In their work, the Cp*Co(III) catalyst, AgSbF₆ and amberlyst 15 additives in combination with the chiral carboxylic acid ligand were used to achieve a high level of enantiocontrol and a moderate reactivity. In 2019, Yoshino, Matsunaga and co-workers demonstrated the enantioselective version of Cp*Co(III) catalyzed 1,4-addition of indoles to maleimides *via* C–H activation (Scheme 16b).[34b] In the reported protocol, the authors speculated that within the catalytic cycle, the migratory insertion step is reversible and a chiral carboxylic acid could assist in selective protodemetalation to furnish predominantly one stereoisomer.

In 2018, Yoshino, Matsunaga and co-workers developed a methodology for the asymmetric C(sp³)–H amidation of thio-amides with dioxazolones (Scheme 17a).[35a] Mechanistic studies showed that the C–H activation step is irreversible in nature, thereby indicating that the carboxylic acid plays an important role in the C–H activation step and not in the later stages of the reaction. Expanding their previous work, one year later, in 2019, Yoshino, Matsunaga and co-workers published their results on the cobalt-catalyzed C(sp³)–H amidation of thioamides with
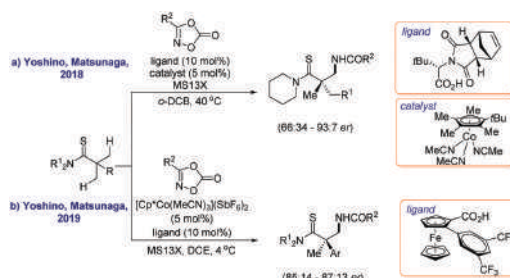
Scheme 17 Cp*Co(III)-catalyzed enantioselective C–H functionalization of thioamides.
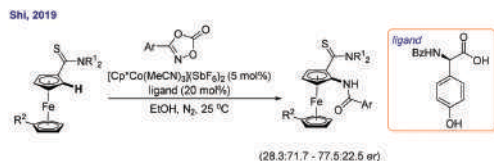
Scheme 18 Cp*Co(III)-catalyzed enantioselective C–H functionalization of ferrocenes.

dioxazolones (Scheme 17b).[35b] The concept of the reported methodology remained the same – the addition of a chiral carboxylic acid to the reaction mixture, which would promote the enantioselective C–H activation step.

In 2019, Shi developed a methodology for the Cp*Co(III)-catalyzed, thioamide-directed enantioselective C–H bond amidation of ferrocenes with dioxazolones (Scheme 18).[36]

In the same year, in 2019, Cramer's group reported the enantioselective C–H bond annulation protocol of *N*-chloroamides with olefins to obtain cyclic amides (Scheme 19a).[37a] Enantioselectivity was attained using a chiral Cp*Co(III) catalyst, which is an analogue to the chiral Cp[x]Rh(III) complex, developed by Cramer in 2018.[37b] To understand the ligand geometry–selectivity relationship, they generated steric maps of the binding pocket and concluded that the naphthyl backbone is responsible for the orientation and alignment of the metalacycle, whereas the *t*-butyl group in the Cp[x] moiety is responsible for the specific orientation of the olefin, minimizing the steric interaction. Expanding the use of chiral Cp[x]Co(III) catalysts, in 2021, Cramer and co-workers published a methodology for the synthesis of L-isotyrosine *via* C–H activation and functionalization (Scheme 19b).[37c] In this study, they used a chiral Cp[x]Co(III) catalyst (R = i-Pr) for the enantioselective carboamination of acrylates with *N*-phenoxyamides. The developed catalytic system was very efficient and delivered L-isotyrosines in a highly enantioselective fashion (most of the examples were >99:1 er) in moderate to very good yields. Additionally, they applied the methodology to other olefins – bicyclic alkenes (Scheme 19c).[37c] They found that the bulkier *t*-Bu-group in the Cp[x] moiety in the catalyst was more efficient to
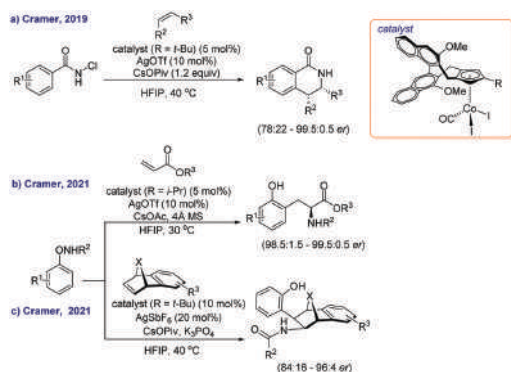
deliver carboamination products. These reaction conditions were mild and no significant limitations were found during the reaction scope studies, yielding products in predominantly excellent yields and high enantioselectivities (mostly >92:8 er).

4. High-valent cobalt catalysis: bidentate chelation assisted cobalt catalysis

4.1. Directing groups

After the pioneering work by Daugulis and co-workers in 2014, bidentate chelation assisted cobalt-catalyzed C–H bond functionalization was proved as an efficient and versatile tool for a large number of various functionalization reactions showing the potential of this methodology.[6i] In such cases, substrates can act as tridentate pincer-type ligands that are able to stabilize high-valent cobalt intermediates. The combination of bidentate directing groups and simple cobalt salts has enabled both C(sp[2])–H and C(sp[3])–H bond functionalization. At present, most of the discovered methods, where simple Co(II) and Co(III) salts are used as catalysts, heavily rely on the use of *N*-based bidentate directing groups such as quinolinoyl, picolinoyl, pyridinyl *N*-oxide, *etc.*, and on the use of stoichiometric oxidants.[3,5f] Using bidentate strongly coordinating group assistance, C(sp[2])–H bond functionalization with alkynes,[38a–e] alkenes,[38f–h] acrylates,[38i] maleimides,[38j] alkanes,[38k] allenes,[38l–n] arylboronic acids,[38o] "CO" sources,[38p–s] amines,[38t,u] alcohols,[38v] "allyl" sources,[38w–z] isonitriles,[39a,b] carboxylic acids,[39a–e] alkylidene cyclopropanes,[39f] heteroarenes,[39g] *etc.* has been developed (Scheme 20).

C–H bond functionalization under bidentate chelation assisted cobalt catalysis is highly efficient; however, it requires prior installation and then the removal of the directing group. Similar to Cp*Co(III) catalysis, bidentate chelation assisted cobalt catalysis is also being developed towards more sustainable chemistry. Several alternative methods to the classical directing group strategy have been developed (traceless directing group strategy, the use of weakly coordinating directing groups; as far as we know, the transient directing group strategy has not been applied for bidentate-chelation assisted cobalt catalysis).

a) Cramer, 2019

b) Cramer, 2021

c) Cramer, 2021

Scheme 19 Cp[x]Co(III)-catalyzed enantioselective C–H functionalization.
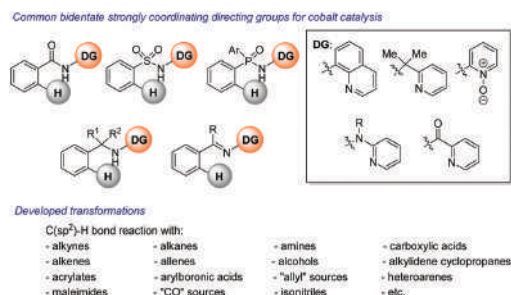
Scheme 20 Bidentate strongly coordinating directing groups for cobalt catalysis and developed transformations.
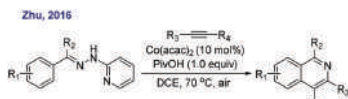
Scheme 21 The first example of bidentate traceless directing group enabled C–H functionalization.
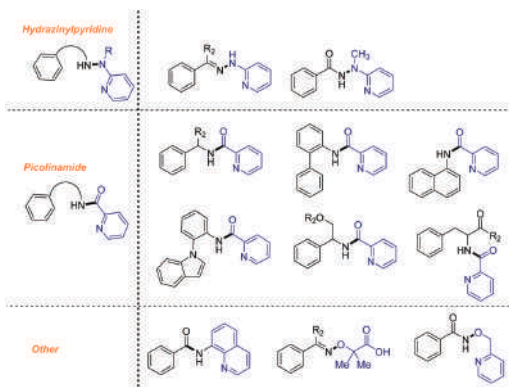
4.1.1. Traceless directing groups.

The first report on bidentate chelation-assisted cobalt-catalyzed C–H functionalization using traceless directing groups was published in 2016 by Zhu and co-workers (Scheme 21).[40] In the reported work, they demonstrated the application of the 2-hydrazinylpyridine bidentate directing group in combination with a simple Co(acac)$_2$ catalyst for C–H annulation with alkynes to obtain isoquinoline derivatives.

Since then, several diverse bidentate traceless directing groups have been introduced and employed for C–H functionalization with alkynes,[41a–e] alkenes[41f,g] and ''CO'' sources[38s,41h–l] (Scheme 22).

Although substantial progress in this area has been achieved, it still lacks the diversity of coupling partners and directing groups compatible with the requirements for the traceless nature of the transformation.

4.1.2. Weakly coordinating directing groups.

Analogous to Cp*Co(III) catalysts, simple Co(II) salts can also be employed as catalysts for C–H functionalization using monodentate weakly coordinating directing groups. Unfortunately, it is not as easily achievable due to the thermodynamic instability arising from the lack of coordination of the directing group. Nevertheless, this C–H functionalization approach is highly valuable as it does not require the installation and removal of the directing group, and it allows the use of simpler and cheaper catalysts. So far, a single report has been published using this strategy. In 2018, the Daugulis group successfully employed benzoic acid for the C–H/OH annulation with alkynes and alkenes (Scheme 23).[42]

The use of weakly coordinating directing groups in combination with simple Co(II) salt catalysts holds great potential and

Scheme 23 Example of the cobalt-catalyzed C–H functionalization using weakly coordinating directing groups.

more progress in the future, involving different directing groups and coupling partners, is highly desirable.

4.2. C(sp^3)–H bond activation and functionalization

Bidentate chelation assisted cobalt catalysis has enabled not only C(sp^2)–H bond functionalization, but also C(sp^3)–H bond activation and functionalization. Thus, in 2015, Li, Ge and co-workers first reported the 8-aminoquinline directed, Co(OAc)$_2$ catalyzed intramolecular amidation of aliphatic amides yielding lactams (Scheme 24a).[43a] Additionally, they showed that intermolecular amidation is possible. The same year, Zhang and co-workers demonstrated that by using the aminoquinoline directing group under cobalt catalysis, aliphatic amides can be functionalized with terminal alkynes to obtain cyclic amides (Scheme 24b).[43b] In 2016, Xu and co-workers demonstrated a single example of aminoquinoline directed C–H alkylation of an aliphatic amide with AlMe$_3$ enabled via Co(acac)$_3$ catalysis (Scheme 24c).[43c]

Later, in 2017, Sundararaju,[44a] Gaunt[44b] and Lei[44c] independently developed an aminoquinoline directed C(sp^3)–H carbonylation methodology for aliphatic amides to obtain succinimides (Scheme 25a–c).[44] In 2017, Shi and co-workers published multiple C–H activation strategies to obtain cyclopropane moieties (Scheme 25d).[44d]

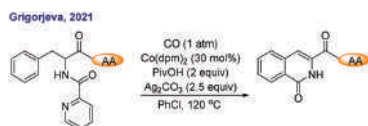### 4.3. Late-stage functionalization

In contrast to Cp*Co(III) catalysis, methods for the late-stage C–H bond functionalization of natural products or drug compounds are not developed using bidentate chelation assisted

Scheme 22 Common traceless directing groups for cobalt catalyzed C–H bond functionalization.
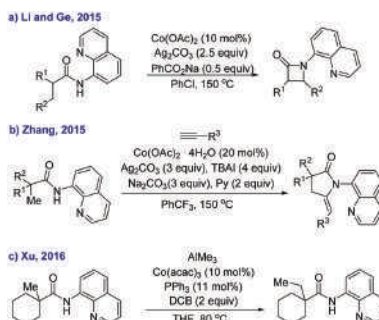
Scheme 24 Bidentate chelation assisted cobalt catalyzed C(sp^3)–H bond functionalization.
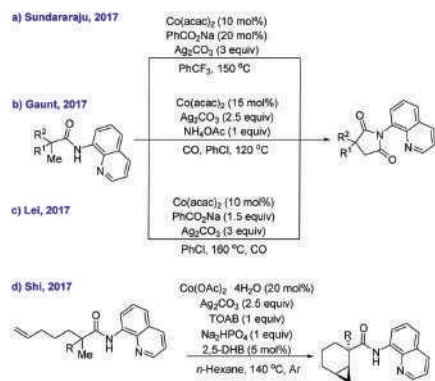
Scheme 25 Bidentate chelation assisted cobalt catalyzed C(sp^3)−H bond carbonylation (a−c) and intramolecular cyclization (d).

Scheme 26 Cobalt catalyzed C−H bond carbonylation of Phe containing short peptides.

cobalt catalysis. In 2021, Grigorjeva and co-workers reported the closest example to late-stage functionalization. They developed the cobalt catalyzed C−H carbonylation of phenylalanine derivatives using CO as the carbonyl source and picolinamide as the traceless directing group (Scheme 26).[41l] Additionally, they demonstrated that the developed carbonylation method can also be applied to dipeptides and tripeptides, albeit with minor erosion of enantiopurity of the stereocenter in the adjacent amino acid.

Similar to Cp*Co(III) catalysis, the development of novel methods using the late-stage functionalization strategy is of great interest and is in high demand, especially using simple Co(II) salts as catalysts.

4.4. Multi component addition to C−H bonds

In the literature, there is a single example of the multi-component addition to C−H bonds using bidentate chelation assisted cobalt catalysis. Recently, in 2021, Niu, Yang and co-workers have demonstrated the three-component coupling reaction of benzamides, diazo compounds and TBHP that allowed the construction of new C−C and C−O bonds.[45] In contrast to Ellman's work, they employed the bidentate 8-aminoquinoline directing group that allowed the use of the cheap Co(II) catalyst (Scheme 27).[45]

4.5. Electrochemical oxidation

In the last few decades, more and more attention has been directed towards sustainable and green chemistry.[2] Chemists have actively been trying to develop a novel methodology that would comply with the principles of green chemistry. Reaction conditions, which require lower reaction temperatures, avoid
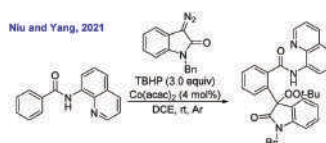
Scheme 27 Aminoquinoline-directed cobalt-catalyzed multicomponent addition to C−H bonds.

non-renewable solvents and use selective catalysts, are very desirable.[46] Even though C−H activation is a step in the right direction by eliminating the necessity for pre-functionalization, it often requires harsh reaction conditions and stoichiometric amounts of chemical oxidants, thus partially outweighing the advantages that it provides. Nevertheless, in recent years, cobalt catalyzed C−H activation protocols, that partially solve these issues, have been developed by employing biomass-derived solvents,[47] reducing reaction temperatures and substituting chemical oxidants with air or electricity. Using air as an oxidant in C−H functionalization reactions is optimal, but unfortunately, often additional stoichiometric or catalytic amounts of co-oxidants are necessary for successful transformation.

The first example of cobalt-catalyzed electrochemical C−H functionalization was reported by Ackermann and co-workers in 2017 (Scheme 28a).[48a] They demonstrated that electric energy can be successfully employed to replace chemical oxidants, which are often required in stoichiometric amounts for the re-oxidation of a cobalt catalyst. The single-cell setup in the presented work employed the RVC–Pt electrodes, pyridine-N-oxide directing group and Co(OAc)$_2$ catalyst, along with the NaOPiv additive in an alcohol solvent to obtain benzamide ortho-alkoxylation products. Using a similar setup, one year later, in 2018, Ackermann and co-workers discovered that benzamides can participate in the C–H/N–H annulation reaction with alkynes (Scheme 28b).[48b] In contrast to previously reported methodology, C–H functionalization with alkynes was achieved in a more atom-economical fashion, requiring close to equimolar amounts of alkynes, whereas alkoxylation required 240 equivalents. In the same year, Ackermann
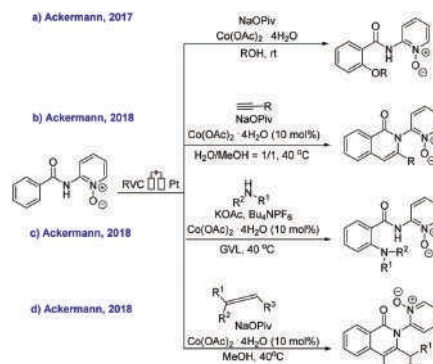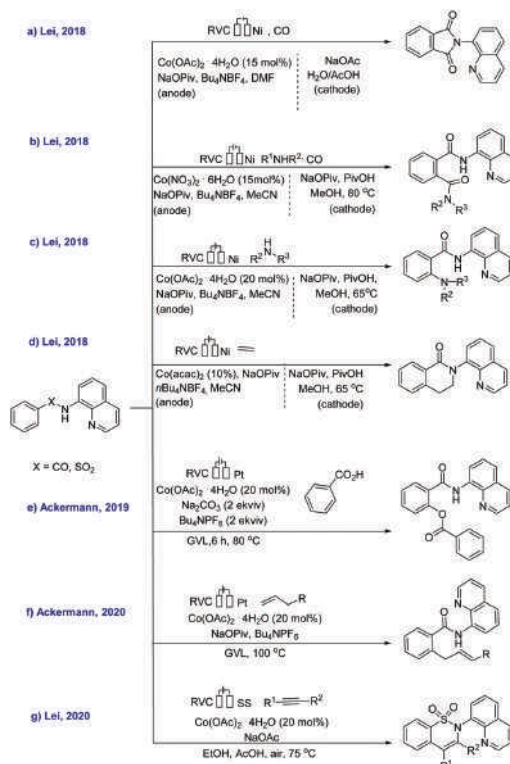

Scheme 28 Cobalt catalyzed electrochemical C−H functionalization of benzamides.
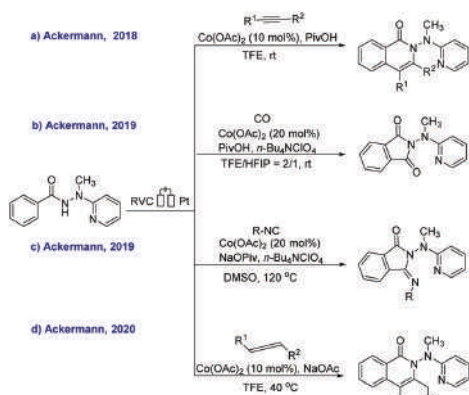
and co-workers reported an unprecedented electrochemical C–H amination with disubstituted amines using a cheap Co(II) catalyst under very mild reaction conditions. An additional advantage of the reported protocol was the use of the biomass-derived renewable GVL solvent (Scheme 28c).[48c] In 2018, Ackermann and co-workers employed the same substrate in the electrochemical C–H annulation with allenes (Scheme 28d).[48d] In the reported work, the catalytic system and electrochemical setup were very similar to the alkoxylation protocol and delivered cyclization products in moderate to excellent yields in a highly regioselective fashion.

In the following years, Ackermann and co-workers continued to explore the viable transformations and developed several methodologies for the cobalt catalyzed electrochemical C–H functionalization of benzhydrazides.[49] In 2018, they demonstrated the first example of electrochemical C–H/N–H annulation that was applicable to internal alkynes and provided isoquinolinones with high regioselectivity (Scheme 29a).[49a] In 2019, Ackermann and co-workers published a methodology for the cobalt catalyzed C–H carbonylation of benzamides using CO as a carbonyl source to obtain phthalimides (Scheme 29b).[49b] Interestingly, the same methodology could be applied for C–H functionalization with isocyanides by slightly changing the reaction conditions to obtain the corresponding insertion products (Scheme 29c).[49b] The next year, in 2020, Ackermann and co-workers reported a method for the C–H/N–H annulation of benzhydrazides with allenes to obtain cyclic products, using a similar setup that was used for the annulation with internal alkynes in 2018 (Scheme 29d).[49c]

Several methodologies for the cobalt-catalyzed electrochemical C–H functionalization of aminoquinoline benzamides have been developed. In 2018, Lei and co-workers reported a C–H bond carbonylation protocol using CO as the carbonyl source to deliver phthalimides (Scheme 30a).[50a] In contrast to Ackerman's previous protocols, a divided cell setup with RVC/Ni electrodes was used. The report also demonstrated a protocol for the carboamidation of thiophene derivatives to yield the corresponding amides in good and moderate yields with a slight change in the catalytic system (Scheme 30b).[50a] The same year,

Scheme 30 Cobalt-catalyzed electrochemical C–H functionalization of benzamides and sulfonamides.

in 2018, Lei and co-workers showed that a similar catalytic system was additionally applicable for the C–H amination of benzamide derivatives, if the carbonyl source was excluded from the reaction mixture (Scheme 30c).[50b] Additionally, in 2018, Lei and co-workers demonstrated that ethylene or acetylene can be employed for electrochemical functionalization to obtain C–H/N–H annulation products mostly in very good yields (Scheme 30d).[50c] After a year, in 2019, Ackermann and co-workers disclosed the first example of cobalt-catalyzed C–H acyloxylation via electrocatalysis using a single-cell setup with RVC/Pt electrodes and GVL as a renewable solvent (Scheme 30e).[50d] In 2020, Ackermann and co-workers used the same catalytic system and setup to achieve the first cobalt-catalyzed electrocatalytic C–H allylation with non-activated alkenes (Scheme 30f).[50e] The same year, in 2020, Lei's group disclosed the C–H/N–H annulation of sulphonamides with alkynes to obtain sultams using a single-cell setup with cheap RVC/SS (stainless steel) electrodes (Scheme 30g).[50f]

5. Conclusions and outlook

The ultimate goal of synthetic organic chemistry is the ability to construct complex molecules from readily available starting

Scheme 29 Cobalt catalyzed electrochemical C–H functionalization of benzhydrazides.

materials in the shortest and easiest sequence possible. Ideally, green chemistry principles should be involved in the developed methodology, which would ensure sustainability and renewability and reduce the ecological footprint. Thus, the development of an ideal transformation, which avoids the generation of waste, reduces the consumption of non-renewable resources and is efficient as well as economically friendly, is highly desirable. During the last decade, high-valent cobalt catalyzed C–H bond activation and functionalization have become a part of the essential toolkit for synthetic chemists due to their numerous advantages over classical synthetic methodologies. In this review, we have summarized the overall current progress in high-valent cobalt catalyzed C–H functionalization and evaluated the possible directions that might potentially be a hot topic in the future.

The reactivity of cobalt catalysis can drastically change depending on the catalyst used, thus the high-valent cobalt catalysis should be distinguished in two separate categories: C–H functionalization reactions catalyzed by Cp*Co(III) complexes and C–H functionalization reactions catalyzed by Co(II) salts that can be oxidized to Co(III) *in situ*. In terms of reactivity, the Cp* ligand coordination mode enables the Cp*Co(III) catalyst to resemble its Cp*Rh analogues and in certain aspects has an advantage over simple Co(II) salt catalysis. This is clearly visible from the perspective of compatibility with the directing groups used in the C–H functionalization reactions. The increased stability of the C–H activation Cp*Co intermediates allows the use of weaker and more simple directing groups, which rarely is possible with Co(II) salts that more often require bidentate *N*-chelation. On the other hand, Cp*Co(III) catalysts are more expensive and should be synthesized in the lab.

To ensure the selectivity of C–H functionalization, directing groups are exploited that can chelate the metal and bring it in proximity to the C–H bond. The directing groups can also be devised in separate categories, based on their step-economy and the nature of their coordination ability. Monodentate strongly coordinating directing groups are typically used in Cp*Co(III) catalyzed reactions and are very often not removable. This is a minor drawback as it potentially limits the possible uses for the obtained products. However, monodentate weakly coordinating directing groups can be considered as one of the most desirable types of directing groups due to their step-economical nature that does not require additional installation and removal steps. Unfortunately, the progress in this field has been slow and is still underdeveloped. Since the first report in 2014, there have been 6 published examples using Cp*Co(III) catalysis, and 2 using Co(II) salts and more work is required.

Bidentate directing groups are commonly used with Co(II) salts under oxidative conditions. These directing groups, especially 8-aminoquinoline and picolinamide, have been extensively exploited in C–H functionalization reactions and a wide range of transformations have been developed.

Traceless directing groups can be monodentate or bidentate and offer advantages over the classical directing group approach as they are removed *in situ* under the reaction conditions, thus increasing the step-economy. Additionally, in Cp*Co(III) catalyzed reactions, traceless directing groups often serve as an internal oxidant and remove the necessity for additional oxidants. Thus far, decent progress in this field has been achieved both in Cp*Co(III) and bidentate chelation assisted Co(II) catalyzed reactions and many examples can be found in the literature exploiting a variety of directing groups. However, unfortunately, most of the reported transformations are limited to carbonylation and annulation reactions with alkynes, diynes and alkenes. Higher diversity in compatible coupling partners is needed.

Transient directing groups are installed and removed under the reaction conditions *in situ*. They are relatively recent additions to the field of cobalt catalysis and previously had been only used for noble metal catalyzed C–H functionalization. Despite their offered advantages in step-economy, very little progress has been achieved in this field, having only two examples reported in the literature, catalyzed by Cp*Co(III), whereas reactions exploiting simple Co(II) salts as catalysts are not known at all. More development on the diversity of transient directing groups and C–H functionalization coupling partners is expected in the future.

One of the most challenging but highly valuable directions is C(sp^3)–H bond functionalization. Since the first report in 2015, several research groups have contributed to this field and developed novel transformations both in Cp*Co(III) and bidentate chelation assisted Co(II) catalyzed reactions. Nonetheless, the overall progress in this direction is relatively slow and lacks diversity in exploitable directing groups as well as coupling partners when compared to the overall state of the art in the cobalt catalyzed C–H functionalization field.

The enantioselective C–H functionalization field has tremendous potential in drug discovery and medicinal chemistry for its ability to construct chiral carbon centres directly. Two general chirality induction strategies are exploited. First, the use of chiral carboxylic acids, which can either enantioselectively protodemetalate the cobalt-alkyl intermediate, resulting in a chiral tertiary carbon centre, or serve as a chiral additive, which promotes the enantioselective C–H activation step. The second chirality induction strategy involves the use of Cp^{x}Co(III) catalysts with the chiral Cp^x backbone, which promotes the enantioselective C–H functionalization step. So far, only a handful of examples catalyzed by Cp^{x}Co(III) catalysts have been reported and more progress is expected in the future involving more viable directing groups and transformations. A very promising strategy for enantioselective C–H functionalization could be the use of chiral transient groups, which so far have not been introduced in cobalt catalysis.

Multi-component C–H functionalization reactions are a very convenient pathway to obtain complex structures in a single step from simpler starting materials. Over the last 6 years, a clear contribution to this field has been made by Ellman's group who developed a variety of novel transformations catalyzed by Cp*Co(III) catalysts. On the other hand, bidentate chelation-assisted Co(II)-catalyzed multi-component C–H functionalization reactions remain underdeveloped having only one example published this year. Given the number of possible combinations of coupling partners and obtainable products, as well as the green nature of this field, rapid progress is expected in the future.

Late-stage functionalization has relatively recently emerged as one of the cobalt catalysis "branches", having the first reported example in 2019. This field holds potential for being a very useful approach in drug discovery as it gives access to rapid diversification of natural products and synthesis of drug analogues. So far, only few methodologies have been reported, three of them being catalyzed by Cp*Co(III) and a single example performed under bidentate chelation assisted Co(II) catalysis.

Another step in the right direction is the development of electrochemical oxidation for C–H functionalization protocols. Electrochemical anodic oxidation of Co catalysts is an excellent way to substitute chemical oxidants and make reaction conditions milder and reduce the produced waste. Since the first published example in 2017 by Ackermann, a steady progress has been achieved in this field allowing to obtain various products in an environmentally friendly way. However, there is still some space to improve the discovered methodology in terms of directing group diversity, as the majority of the C–H functionalization protocols exploit only three types of directing groups. Additionally, more methods where cheaper metal electrodes could be used are highly desirable.

Finally, all of the reported cobalt catalyzed C–H functionalization reactions are only *ortho*-selective. Successful *meta*- or *para*-oriented C–H functionalization reactions are a huge challenge for chemists even using noble metal catalysis. Novel directing groups for *meta*- or *para*-C–H functionalization under cobalt catalysis very likely will be an enormous breakthrough for cobalt catalysis.

Conflicts of interest

There are no conflicts to declare.

Acknowledgements

Notes and references

1 Selected reviews on transition metal-catalyzed C–H bond functionalization: (a) S. Rej, A. Das and N. Chatani, *Coord. Chem. Rev.*, 2021, **431**, 213683; (b) Y. Wu, C. Pi, Y. Wu and X. Cui, *Chem. Soc. Rev.*, 2021, **50**, 3677; (c) T. Naveen, *Tetrahedron*, 2021, **84**, 132025; (d) V. Dwivedi, D. Kalsi and B. Sundararaju, *ChemCatChem*, 2019, **11**, 5160; (e) D. J. Abrams, P. A. Provencher and E. J. Sorensen, *Chem. Soc. Rev.*, 2018, **47**, 8925; (f) J. He, M. Wasa, K. S. L. Chan, Q. Shao and J.-Q. Yu, *Chem. Rev.*, 2017, **117**, 8754; (g) H. M. Davies and D. Morton, *J. Org. Chem.*, 2016, **81**, 343; (h) T. Gensch, M. N. Hopkinson, F. Glorius and J. Wencel-Delord, *Chem. Soc. Rev.*, 2016, **45**, 2900; (i) C. Sambiagio, D. Schönbauer, R. Blieck, T. Dao-Huy, G. Pototschnig, P. Schaaf, T. Wiesinger, M. F. Zia, J. Wencel-Delord, T. Besset, B. U. W. Maes and M. Schnürch, *Chem. Soc. Rev.*, 2018, **47**, 6603; (j) A. Correa, *Eur. J. Inorg. Chem.*, 2021, 2928; (k) D. Maiti and S. Guin, *Remote C-H Bond Functionalizations: Methods and Strategies in Organic Synthesis*, WILEY-VCH, Weinheim, 2021; (l) S. Dutta, T. Bhattacharya, D. B. Werz and D. Maiti, *Chem*, 2021, **7**, 555; (m) J. Das, S. Guin and D. Maiti, *Chem. Sci.*, 2020, **11**, 10887; (n) J. Das, D. K. Mal, S. Maji and D. Maiti, *ACS Catal.*,

2021, **11**, 4205; (o) U. Dutta, S. Maiti, T. Bhattacharya and D. Maiti, *Science*, 2021, **372**, 701; (p) R. L. Carvalho, G. G. Dias, C. L. M. Pereira, P. Ghosh, D. Maiti and E. N. da Silva Júnior, *J. Braz. Chem. Soc.*, 2021, **32**, 917; (q) A. Baccalini, G. Faita, G. Zanoni and D. Maiti, *Chem. – Eur. J.*, 2020, **26**, 9749; (r) W. Ali, G. Prakash and D. Maiti, *Chem. Sci.*, 2021, **12**, 2735; (s) S. Basak, J. P. Biswas and D. Maiti, *Synthesis*, 2021, 3151; (t) R. L. Carvalho, R. G. Almeida, K. Murali, L. A. Machado, L. F. Pedrosa, P. Dolui, D. Maiti and E. N. da Silva Júnior, *Org. Biomol. Chem.*, 2021, **19**, 525.
2 T. Dalton, T. Faber and F. Glorius, *ACS Cent. Sci.*, 2021, **7**, 245.
3 P. Gandeepan, T. Müller, D. Zell, G. Cera, S. Warratz and L. Ackermann, *Chem. Rev.*, 2019, **119**, 2192.
4 (a) M. Hapke and G. Hilt, *Cobalt Catalysis in Organic Synthesis: Methods and Reactions*, WILEY-VCH, Weinheim, 2020; (b) T. Yoshino and S. Matsunaga, *Adv. Organomet. Chem.*, 2017, **68**, 197.
5 Selected reviews on cobalt-catalyzed C–H bond functionalization: (a) S. K. Banjare, T. Nanda, B. V. Pati, P. Biswal and P. C. Ravikumar, *Chem. Commun.*, 2021, **57**, 3630; (b) R. Mei, U. Dhawa, R. C. Samanta, W. Ma, J. Wencel-Delord and L. Ackermann, *ChemSusChem*, 2020, **13**, 3306; (c) L. Lukasevics and L. Grigorjeva, *Org. Biomol. Chem.*, 2020, **18**, 7460; (d) A. Baccalini, S. Vergura, P. Dolui, G. Zanoni and D. Maiti, *Org. Biomol. Chem.*, 2019, **17**, 10119; (e) Y. Kommagalla and N. Chatani, *Coord. Chem. Rev.*, 2017, **350**, 117; (f) O. Daugulis, J. Roane and L. D. Tran, *Acc. Chem. Res.*, 2015, **48**, 1053; (g) D. Wei, X. Zhu, J.-L. Niu and M.-P. Song, *ChemCatChem*, 2016, **8**, 1242; (h) T. Yoshino and S. Matsunaga, *Asian J. Org. Chem.*, 2018, **7**, 1193.
6 (a) S. Murahashi, *J. Am. Chem. Soc.*, 1955, **77**, 6403; (b) G. Halbritter, F. Knoch, A. Wolski and H. Kisch, *Angew. Chem., Int. Ed. Engl.*, 1994, **33**, 1603; (c) C. P. Lenges and M. Brookhart, *J. Am. Chem. Soc.*, 1997, **119**, 3165; (d) K. Gao, P.-S. Lee, T. Fujita and N. Yoshikai, *J. Am. Chem. Soc.*, 2010, **132**, 12249; (e) B. J. Fallon, E. Derat, M. Amatore, C. Aubert, F. Chemla, F. Ferreira, A. Perez-Luna and M. Petit, *J. Am. Chem. Soc.*, 2015, **137**, 2448; (f) K. Kanamori, W. E. Broderick, R. F. Jordan, R. D. Willett and J. I. Legg, *J. Am. Chem. Soc.*, 1986, **108**, 7122; (g) T. Avilés, A. Dinis, M. J. Calhorda, P. Pinto, V. Félix and M. G. B. Drew, *J. Organomet. Chem.*, 2001, **625**, 186; (h) T. Yoshino, H. Ikemoto, S. Matsunaga and M. Kanai, *Angew. Chem., Int. Ed.*, 2013, **52**, 2207; (i) L. Grigorjeva and O. Daugulis, *Angew. Chem., Int. Ed.*, 2014, **53**, 10209.
7 (a) K. Gao and N. Yoshikai, *Acc. Chem. Res.*, 2014, **47**, 1208; (b) N. Yoshikai, *Bull. Chem. Soc. Jpn.*, 2014, **87**, 843; (c) L. Ackermann, *J. Org. Chem.*, 2014, **79**, 8948.
8 S. Wang, S.-Y. Chen and X.-Q. Yu, *Chem. Commun.*, 2017, **53**, 3165.
9 Selected examples using Cp*Co(III) catalysis: C–H bond functionalization with alkynes – (a) S. Wang, J.-T. Hou, M.-L. Feng, X.-Z. Zhang, S.-Y. Chen and X.-Q. Yu, *Chem. Commun.*, 2016, **52**, 2709; (b) M. Sen, N. Rajesh, B. Emayavaramban, J. R. Premkumar and B. Sundararaju, *Chem. – Eur. J.*, 2018, **24**, 342; C–H bond functionalization with alkenes – ; (c) D. Zell, M. Bursch, V. Müller, S. Grimme and L. Ackermann, *Angew. Chem. Int. Ed.*, 2017, **56**, 10378; C–H bond functionalization with acrylates – ; (d) N. Barsu, B. Emayavaramban and B. Sundararaju, *Eur. J. Org. Chem.*, 2017, 4370; C–H bond functionalization with maleimides – ; (e) Z. Zhang, S. Han, M. Tang, L. Ackermann and J. Li, *Org. Lett.*, 2017, **19**, 3315; (f) N. Muniraj and K. R. Prabhu, *ACS Omega*, 2017, **2**, 4470; C–H bond functionalization with allenes–; (g) S. Nakanowatari, R. Mei, M. Feldt and L. Ackermann, *ACS Catal.*, 2017, **7**, 2511; C–H bond functionalization with sulfonyl imines – ; (h) T. Yoshino, H. Ikemoto, S. Matsunaga and M. Kanai, *Chem. – Eur. J.*, 2013, **19**, 9142; C–H bond functionalization with aldehydes – ; (i) J. Li, Z. Zhang, W. Ma, M. Tang, D. Wang and L.-H. Zou, *Adv. Synth. Catal.*, 2017, **359**, 1717; (j) X. Chen, X. Hu, Y. Deng, H. Jiang and W. A. Zeng, *Org. Lett.*, 2016, **18**, 4742; C–H bond functionalization with keteamines – ; (k) X. Zhou, Z. Fan, Z. Zhang, P. Lu and Y. Wang, *Org. Lett.*, 2016, **18**, 4706; C–H bond functionalization with isocyanates – ; (l) J. Li and L. Ackermann, *Angew. Chem., Int. Ed.*, 2015, **54**, 8551; (m) J. R. Hummel and J. A. Ellman, *Org. Lett.*, 2015, **17**, 2400; C–H bond allylation – ; (n) D.-G. Yu, T. Gensch, F. de Azambuja, S. Vásquez-Céspedes and F. Glorius, *J. Am. Chem. Soc.*, 2014, **136**, 17722; (o) T. Gensch, S. Vásquez-Céspedes, D.-G. Yu and F. Glorius, *Org. Lett.*, 2015, **17**, 3714; (p) Y. Suzuki, B. Sun, K. Sakata, T. Yoshino, S. Matsunaga and M. Kanai, *Angew. Chem., Int. Ed.*, 2015, **54**, 9944; C–H bond functionalization with carbamates – ; (q) P. Patel and S. Chang, *ACS Catal.*, 2015, **5**, 853; C–H bond functionalization with diazo compounds – ; (r) D. Zhao, J. H. Kim, L. Stegemann,

C. A. Strassert and F. Glorius, *Angew. Chem., Int. Ed.*, 2015, **54**, 4508; C–H bond cyanation – ; (*s*) J. Li and L. Ackermann, *Angew. Chem., Int. Ed.*, 2015, **54**, 3635; (*t*) A. B. Pawar and S. Chang, *Org. Lett.*, 2015, **17**, 660; C–H bond functionalization with organic azides – ; (*u*) B. Sun, T. Yoshino, S. Matsunaga and M. Kanai, *Chem. Commun.*, 2015, **51**, 4659; (*v*) B. Sun, T. Yoshino, S. Matsunaga and M. Kanai, *Adv. Synth. Catal.*, 2014, **356**, 1491.

10 (*a*) A. Cizikovs, L. Lukasevics and L. Grigorjeva, *Tetrahedron*, 2021, **93**, 132307; (*b*) G. Rani, V. Luxami and K. Paul, *Chem. Commun.*, 2020, **56**, 12479; (*c*) A. Zarkadoulas, I. Zgouleta, N. V. Tzouras and G. C. Vougioukalakis, *Catalysts*, 2021, **11**, 554.

11 (*a*) P. Gandeepan and L. Ackermann, *Chem*, 2018, **4**, 199; (*b*) Q. Zhao, T. Pannecoucke and L. Besset, *Synthesis*, 2017, 4808; (*c*) S. St. John-Campbell and J. A. Bull, *Org. Biomol. Chem.*, 2018, **16**, 4582; (*d*) J. I. Higham and J. A. Bull, *Org. Biomol. Chem.*, 2020, **18**, 7291; (*e*) N. Goswami, T. Bhattacharya and D. Maiti, *Nat. Rev. Chem.*, 2021, **5**, 646.

12 (*a*) K. M. Engle, T.-S. Mei, M. Wasa and J.-Q. Yu, *Acc. Chem. Res.*, 2012, **45**, 788; (*b*) S. De Sarkar, W. Liu, S. I. Kozhushkov and L. Ackermann, *Adv. Synth. Catal.*, 2014, **356**, 1461; (*c*) R. Thakur, Y. Jaiswal and A. Kumar, *Tetrahedron*, 2021, **93**, 132313.

13 (*a*) H. Ikemoto, T. Yoshino, K. Sakata, S. Matsunaga and M. Kanai, *J. Am. Chem. Soc.*, 2014, **136**, 5424; (*b*) J. R. Hummel and J. A. Ellman, *J. Am. Chem. Soc.*, 2015, **137**, 490.

14 Traceless directing group strategy application under Cp*Co(III) catalysis for C–H bond functionalization with alkynes: (*a*) H. Ikemoto, R. Tanaka, K. Sakata, M. Kanai, T. Yoshino and S. Matsunaga, *Angew. Chem., Int. Ed.*, 2017, **56**, 7156; (*b*) A. Lerchen, S. Vásquez-Céspedes and F. Glorius, *Angew. Chem., Int. Ed.*, 2016, **55**, 3208; (*c*) Z. Shou, J. Wang, L. Wang, K. Chen, C. Song and J. Zhu, *Org. Lett.*, 2016, **18**, 3806; (*d*) L. Kong, X. Yang, X. Zhou, S. Yu and X. Li, *Org. Chem. Front.*, 2016, **3**, 813; (*e*) N. Barsu, M. Sen, J. R. Premkumar and B. Sundararaju, *Chem. Commun.*, 2016, **52**, 1338; (*f*) Y. Liang and N. Jiao, *Angew. Chem., Int. Ed.*, 2016, **55**, 4035; (*g*) H. Wang, M. Moselage, M. J. González and L. Ackermann, *ACS Catal.*, 2016, **6**, 2705; (*h*) G. Sivakumar, A. Vijeta and M. Jeganmohan, *Chem. – Eur. J.*, 2016, **22**, 5899; (*i*) M. Sen, R. Mandal, A. Das, D. Kalsi and B. Sundararaju, *Chem. – Eur. J.*, 2017, **23**, 17454; (*j*) L. N. Chavan, K. K. Gollapelli, R. Chegondi and A. B. Pawar, *Org. Lett.*, 2017, **19**, 2186; (*k*) A. Lerchen, T. Knecht, M. Koy, C. G. Daniliuc and F. Glorius, *Chem. – Eur. J.*, 2017, **23**, 12149; (*l*) M. Sen, D. Kalsi and B. Sundararaju, *Chem. – Eur. J.*, 2015, **21**, 15529; (*m*) K. Muralirajan, R. Kuppusamy, S. Prakash and C. H. Cheng, *Adv. Synth. Catal.*, 2016, **358**, 774; (*n*) F. Wang, Q. Wang, M. Bao and X. Li, *Chin. J. Catal.*, 2016, **37**, 1423; (*o*) Y. Yu, Q. Wu, D. Liu, L. Yu, Z. Tan and G. Zhu, *Org. Chem. Front.*, 2019, **6**, 3868; (*p*) X. Yu, K. Chen, S. Guo, P. Shi, C. Song and J. Zhu, *Org. Lett.*, 2017, **19**, 5348; (*q*) S. H. Kwak and O. Daugulis, *Chem. Commun.*, 2020, **56**, 11070.

15 Traceless directing group strategy application under Cp*Co(III) catalysis for C–H bond functionalization with alkenes: (*a*) A. Dey, A. Rathi and C. M. R. Volla, *Asian J. Org. Chem.*, 2018, **7**, 1362; (*b*) A. Lerchen, T. Knecht, C. G. Daniliuc and F. Glorius, *Angew. Chem., Int. Ed.*, 2016, **55**, 15166; (*c*) X. Yu, K. Chen, Q. Wang, W. Zhang and J. Zhu, *Org. Chem. Front.*, 2018, **5**, 994.

16 N. Muniraj and K. R. Prabhu, *Org. Lett.*, 2019, **21**, 1068.

17 F. Wang, H. Wang, Q. Wang, S. Yu and X. Li, *Org. Lett.*, 2016, **18**, 1306.

18 T. Bhattacharya, S. Pimparkar and D. Maiti, *RSC Adv.*, 2018, **8**, 19456.

19 (*a*) J. Huang, J. Ding, T.-M. Ding, S. Zhang, Y. Wang, F. Sha, S.-Y. Zhang, X.-Y. Wu and Q. Li, *Org. Lett.*, 2019, **21**, 7342; (*b*) B. Khan, V. Dwivedi and B. Sundararaju, *Adv. Synth. Catal.*, 2020, **362**, 1195.

20 Selected examples: (*a*) D.-G. Yu, T. Gensch, F. de Azambuja, S. Vásquez-Céspedes and F. Glorius, *J. Am. Chem. Soc.*, 2014, **136**, 17722; (*b*) T. Gensch, S. Vásquez-Céspedes, D.-G. Yu and F. Glorius, *Org. Lett.*, 2015, **17**, 3714; (*c*) Y. Bunno, N. Murakami, Y. Suzuki, M. Kanai, T. Yoshino and S. Matsunaga, *Org. Lett.*, 2016, **18**, 2216; (*d*) T. Li, C. Shen, Y. Sun, J. Zhang, P. Xiang, X. Lu and G. Zhong, *Org. Lett.*, 2019, **21**, 7772; (*e*) X. Li, T. Huang, Y. Song, Y. Qi, L. Li, Q. Xiao and Y. Zhang, *Org. Lett.*, 2020, **22**, 5925; (*f*) Z.-Z. Zhang, G. Liao, H.-M. Chen and B.-F. Shi, *Org. Lett.*, 2021, **23**, 2626.

21 R. Mandal and B. Sundararaju, *Org. Lett.*, 2017, **19**, 2544.

22 M. R. Sk, S. S. Bera and M. S. Maji, *Org. Lett.*, 2018, **20**, 134.

23 J. Ghorai, A. C. S. Reddy and P. Anbarasan, *Chem. – Eur. J.*, 2016, **22**, 16042.

24 A. Carral-Menoyo, N. Sotomayor and E. Lete, *J. Org. Chem.*, 2020, **85**, 10261.

25 (*a*) M. Sen, B. Emayavaramban, N. Barsu, J. R. Premkumar and B. Sundararaju, *ACS Catal.*, 2016, **6**, 2792; (*b*) N. Barsu, M. A. Rahman, M. Sen and B. Sundararaju, *Chem. – Eur. J.*, 2016, **22**, 9135; (*c*) S.-Y. Yan, P.-X. Ling and B.-F. Shi, *Adv. Synth. Catal.*, 2017, **359**, 2912; (*d*) R. Kumar, R. Kumar, D. Chandra and U. Sharma, *J. Org. Chem.*, 2019, **84**, 1542; (*e*) H. Tan, R. Khan, D. Xu, Y. Zhou, X. Zhang, G. Shi and B. Fan, *Chem. Commun.*, 2020, **56**, 12570.

26 (*a*) P. W. Tan, A. M. Mak, M. B. Sullivan, D. J. Dixon and J. Seayad, *Angew. Chem., Int. Ed.*, 2017, **56**, 16550; (*b*) R.-H. Liu, Q.-C. Shan, X.-H. Hu and T.-P. Loh, *Chem. Commun.*, 2019, **55**, 5519; (*c*) L. Liu, Z. Zhang, Y. Wang, Y. Zhang and J. Li, *Synthesis*, 2020, 3881.

27 T. Yoshino and S. Matsunaga, *Adv. Synth. Catal.*, 2017, **359**, 1245.

28 Selected reviews on late-stage C–H functionalization: (*a*) L. Guillemard, N. Kaplaneris, L. Ackermann and M. J. Johansson, *Nat. Rev. Chem.*, 2021, **5**, 522; (*b*) B. Hong, T. Luo and X. Lei, *ACS Cent. Sci.*, 2020, **6**, 622; (*c*) M. Moir, J. J. Danon, T. A. Reekie and M. Kassiou, *Expert Opin. Drug Discovery*, 2019, **14**, 1137.

29 (*a*) M. M. Lorion, N. Kaplaneris, J. Son, R. Kuniyil and L. Ackermann, *Angew. Chem., Int. Ed.*, 2019, **58**, 1684; (*b*) R. J. Scamp, E. deRamon, E. K. Paulson, S. J. Miller and J. A. Ellman, *Angew. Chem., Int. Ed.*, 2019, **59**, 890; (*c*) S. D. Friis, M. J. Johansson and L. Ackermann, *Nat. Chem.*, 2020, **12**, 511.

30 J.-P. Wan, L. Gan and Y. Liu, *Org. Biomol. Chem.*, 2017, **15**, 9031.

31 (*a*) J. A. Boerth, J. R. Hummel and J. A. Ellman, *Angew. Chem., Int. Ed.*, 2016, **55**, 12650; (*b*) S. Dongbang, Z. Shen and J. A. Ellman, *Angew. Chem., Int. Ed.*, 2019, **58**, 12590; (*c*) S. Dongbang and J. A. Ellman, *Angew. Chem., Int. Ed.*, 2021, **60**, 2135.

32 (*a*) J. A. Boerth and J. A. Ellman, *Angew. Chem., Int. Ed.*, 2017, **56**, 9976; (*b*) J. A. Boerth, S. Maity, S. K. Williams, B. Q. Mercado and J. A. Ellman, *Nat. Catal.*, 2018, **1**, 673; (*c*) Z. Shen, C. Li, B. Q. Mercado and J. A. Ellman, *Synthesis*, 2020, 1239.

33 T. K. Achar, S. Maiti, S. Jana and D. Maiti, *ACS Catal.*, 2020, **10**, 13748.

34 (*a*) F. Pesciaioli, U. Dhawa, J. C. A. Oliveira, R. Yin, M. John and L. Ackermann, *Angew. Chem., Int. Ed.*, 2018, **57**, 15425; (*b*) T. Kurihara, M. Kojima, T. Yoshino and S. Matsunaga, *Asian J. Org. Chem.*, 2020, **9**, 368.

35 (*a*) S. Fukagawa, Y. Kato, R. Tanaka, M. Kojima, T. Yoshino and S. Matsunaga, *Angew. Chem., Int. Ed.*, 2019, **58**, 1153; (*b*) D. Sekine, K. Ikeda, S. Fukagawa, M. Kojima, T. Yoshino and S. Matsunaga, *Organometallics*, 2019, **38**, 3921.

36 Y.-H. Liu, P.-X. Li, Q.-J. Yao, Z.-Z. Zhang, D.-Y. Huang, M. D. Le, H. Song, L. Liu and B.-F. Shi, *Org. Lett.*, 2019, **21**, 1895.

37 (*a*) K. Ozols, Y.-S. Jang and N. Cramer, *J. Am. Chem. Soc.*, 2019, **141**, 5675; (*b*) S.-G. Wang, S. H. Park and N. Cramer, *Angew. Chem., Int. Ed.*, 2018, **57**, 5459; (*c*) K. Ozols, S. Onodera, Ł. Woźniak and N. Cramer, *Angew. Chem., Int. Ed.*, 2021, **60**, 655.

38 Selected examples using bidentate chelation assisted cobalt catalysis: C–H bond functionalization with alkynes – (*a*) D. Kalsi, S. Dutta, N. Barsu, M. Rueping and B. Sundararaju, *ACS Catal.*, 2018, **8**, 8115; (*b*) J. Bolsakova, L. Lukasevics and L. Grigorjeva, *J. Org. Chem.*, 2020, **85**, 4482; (*c*) T. T. Nguyen, L. Grigorjeva and O. Daugulis, *ACS Catal.*, 2016, **6**, 551; (*d*) O. Planas, C. J. Whiteoak, A. Company and X. Ribas, *Adv. Synth. Catal.*, 2015, **357**, 4003; (*e*) P. A. Zagorska, L. Grigorjeva and J. Bolsakova, *Chem. Heterocycl. Compd.*, 2021, **57**, 159; C–H bond functionalization with alkenes – ; (*f*) L. Grigorjeva and O. Daugulis, *Org. Lett.*, 2014, **16**, 4684; (*g*) P. Gandeepan, P. Rajamalli and C.-H. Cheng, *Angew. Chem., Int. Ed.*, 2016, **55**, 4308; (*h*) R. Nallagonda, N. Thrimurtulu and C. M. R. Volla, *Adv. Synth. Catal.*, 2018, **360**, 255; C–H bond functionalization with acrylates – ; (*i*) W. Ma and L. Ackermann, *ACS Catal.*, 2015, **5**, 2822; C–H bond functionalization with maleimides–; (*j*) R. Manoharan and M. Jeganmohan, *Org. Lett.*, 2017, **19**, 5884C–H bond functionalization with alkenes – ; (*k*) Q. Li, W. Hu, R. Hu, H. Lu and G. Li, *Org. Lett.*, 2017, **19**, 4676; C–H bond functionalization with allenes – ; (*l*) N. Thrimurtulu, A. Dey, D. Maiti and C. M. R. Volla, *Angew. Chem., Int. Ed.*, 2016, **55**, 12361; (*m*) N. Thrimurtulu, R. Nallagonda and C. M. R. Volla, *Chem. Commun.*, 2017, **53**, 1872; (*n*) T. Li, C. Zhang, Y. Tan, W. Pan and Y. Rao, *Org. Chem. Front.*, 2017, **4**, 204; C–H bond functionalization with arylboronic acids – ; (*o*) L. Hu, Q. Gui, X. Chen, Z. Tan and G. Zhu, *Org. Biomol. Chem.*, 2016, **14**, 11070; C–H bond functionalization with "CO" sources – ; (*p*) L. Grigorjeva and O. Daugulis, *Org. Lett.*, 2014, **16**, 4688; (*q*) T. T. Nguyen, L. Grigorjeva and O. Daugulis, *Chem.*

Commun., 2017, **53**, 5136; (*r*) J. Ni, J. Li, Z. Fan and A. Zhang, *Org. Lett.*, 2016, **18**, 5960; (*s*) L. Lukasevics, A. Cizikovs and L. Grigorjeva, *Org. Lett.*, 2020, **22**, 2720; C–H bond functionalization with amines – ; (*t*) L.-B. Zhang, S.-K. Zhang, D. Wei, X. Zhu, X.-Q. Hao, J.-H. Su, J.-L. Niu and M.-P. Song, *Org. Lett.*, 2016, **18**, 1318; (*u*) Q. Yan, T. Xiao, Z. Liu and Y. Zhang, *Adv. Synth. Catal.*, 2016, **358**, 2707; C–H bond functionalization with alcohols – ; (*v*) L.-B. Zhang, X.-Q. Hao, S.-K. Zhang, Z.-J. Liu, J.-F. Gong, J.-L. Niu and M.-P. Song, *Angew. Chem., Int. Ed.*, 2015, **54**, 272; C–H bond functionalization with "allyl" sources – ; (*w*) T. Yamaguchi, Y. Kommagalla, Y. Aihara and N. Chatani, *Chem. Commun.*, 2016, **52**, 10129; (*x*) S. Maity, R. Kancherla, U. Dhawa, E. Hoque, S. Pimparkar and D. Maiti, *ACS Catal.*, 2016, **6**, 5493; (*y*) A. Baccalini, S. Vergura, P. Dolui, S. Maiti, S. Dutta, S. Maity, F. F. Khan, G. K. Lahiri, G. Zanoni and D. Maiti, *Org. Lett.*, 2019, **21**, 8842; (*z*) S. Maity, P. Dolui, R. Kancherla and D. Maiti, *Chem. Sci.*, 2017, **8**, 5181.

39 Selected examples using bidentate chelation assisted cobalt catalysis: C–H bond functionalization with isonitriles – (*a*) Z.-Y. Gu, C.-G. Liu, S.-Y. Wang and S.-J. Ji, *J. Org. Chem.*, 2017, **82**, 2223; (*b*) D. Kalsi, N. Barsu, P. Dahiya and B. Sundararaju, *Synthesis*, 2017, 3937; C–H bond functionalization with carboxylic acids – ; (*c*) J. Lan, H. Xie, X. Lu, Y. Deng, H. Jiang and W. Zeng, *Org. Lett.*, 2017, **19**, 4279; (*d*) R. Ueno, S. Natsui and N. Chatani, *Org. Lett.*, 2018, **20**, 1062; (*e*) C. Lin, Z. Chen, Z. Liu and Y. Zhang, *Adv. Synth. Catal.*, 2018, **360**, 519; C–H bond functionalization with alkylidene cyclopropanes – ; (*f*) M. Li and F. Y. Kwong, *Angew. Chem., Int. Ed.*, 2018, **57**, 6512; C–H bond functionalization with heteroarenes – ; (*g*) G. Tan, S. He, X. Huang, X. Liao, Y. Cheng and J. You, *Angew. Chem., Int. Ed.*, 2016, **55**, 10414.

40 S. Zhou, M. Wang, L. Wang, K. Chen, J. Wang, C. Song and J. Zhu, *Org. Lett.*, 2016, **18**, 5632.

41 Traceless directing group strategy application under bidentate chelation assisted cobalt catalysis for C–H bond functionalization with alkynes: (*a*) A. Dey and C. M. R. Volla, *Org. Lett.*, 2020, **22**, 7480; (*b*) X.-C. Li, C. Du, H. Zhang, J.-L. Niu and M.-P. Song, *Org. Lett.*, 2019, **21**, 2863; (*c*) M. Liu, J.-L. Niu, D. Yang and M.-P. Song, *J. Org. Chem.*, 2020, **85**, 4067; (*d*) C. Kuai, L. Wang, B. Li, Z. Yang and X. Cui, *Org. Lett.*, 2017, **19**, 2102; (*e*) F. Ling, Z. Xie, J. Chen, C. Ai, H. Shen, Z. Wang, X. Yi and W. Zhong, *Adv. Synth. Catal.*, 2019, **361**, 3094; C–H bond functionalization with alkenes: (*f*) P. Gandeepan, P. Rajamalli and C. H. Cheng, *Angew. Chem., Int. Ed.*, 2016, **55**, 4308; (*g*) S. Qiu, S. Zhai, H. Wang, X. Chen and H. Zhai, *Chem. Commun.*, 2019, **55**, 4206; C–H bond carbonylation: (*h*) F. Ling, C. Ai,

Y. Lv and W. Zhong, *Adv. Synth. Catal.*, 2017, **359**, 3707; (*i*) F. Ling, C. Zhang, C. Ai, Y. Lv and W. Zhong, *J. Org. Chem.*, 2018, **83**, 5698; (*j*) J. Ying, L.-Y. Fu, G. Zhong and X.-F. Wu, *Org. Lett.*, 2019, **21**, 5694; (*k*) Q. Gao, J.-M. Lu, L. Yao, S. Wang, J. Ying and X.-F. Wu, *Org. Lett.*, 2021, **23**, 178; (*l*) L. Lukasevics, A. Cizikovs and L. Grigorjeva, *Org. Lett.*, 2021, **23**, 2748.

42 T. T. Nguyen, L. Grigorjeva and O. Daugulis, *Angew. Chem., Int. Ed.*, 2018, **57**, 1688.

43 (*a*) X. Wu, K. Yang, Y. Zhao, H. Sun, G. Li and H. Ge, *Nat. Commun.*, 2015, **6**, 6462; (*b*) J. Zhang, H. Chen, C. Lin, Z. Liu, C. Wang and Y. Zhang, *J. Am. Chem. Soc.*, 2015, **137**, 12990; (*c*) H. Wang, S. Zhang, Z. Wang, M. He and K. Xu, *Org. Lett.*, 2016, **18**, 5628.

44 (*a*) N. Barsu, S. K. Bolli and B. Sundararaju, *Chem. Sci.*, 2017, **8**, 2431; (*b*) P. Williamson, A. Galván and M. J. Gaunt, *Chem. Sci.*, 2017, **8**, 2588; (*c*) L. Zeng, S. Tang, D. Wang, Y. Deng, J.-L. Chen, J.-F. Lee and A. Lei, *Org. Lett.*, 2017, **19**, 2170; (*d*) Z.-Z. Zhang, Y.-Q. Han, B.-B. Zhan, S. Wang and B.-F. Shi, *Angew. Chem., Int. Ed.*, 2017, **56**, 13145.

45 M.-H. Li, X.-J. Si, H. Zhang, D. Yang, J.-L. Niu and M.-P. Song, *Org. Lett.*, 2021, **23**, 914.

46 R. C. Samanta, T. H. Meyer, I. Siewert and L. Ackermann, *Chem. Sci.*, 2020, **11**, 8657.

47 P. Gandeepan, N. Kaplaneris, S. Santoro, L. Vaccaro and L. Ackermann, *ACS Sustainable Chem. Eng.*, 2019, **7**, 8023.

48 (*a*) N. Sauermann, T. H. Meyer, C. Tian and L. Ackermann, *J. Am. Chem. Soc.*, 2017, **139**, 18452; (*b*) C. Tian, L. Massignan, T. H. Meyer and L. Ackermann, *Angew. Chem., Int. Ed.*, 2018, **57**, 2383; (*c*) N. Sauermann, R. Mei and L. Ackermann, *Angew. Chem., Int. Ed.*, 2018, **57**, 5090; (*d*) T. H. Meyer, J. C. A. Oliveira, S. C. Sau, N. W. J. Ang and L. Ackermann, *ACS Catal.*, 2018, **8**, 9140.

49 (*a*) R. Mei, N. Sauermann, J. C. A. Oliveira and L. Ackermann, *J. Am. Chem. Soc.*, 2018, **140**, 7913; (*b*) S. C. Sau, R. Mei, J. Struwe and L. Ackermann, *ChemSusChem*, 2019, **12**, 3023; (*c*) R. Mei, X. Fang, L. He, J. Sun, L. Zou, W. Ma and L. Ackermann, *Chem. Commun.*, 2020, **56**, 1393.

50 (*a*) L. Zeng, H. Li, S. Tang, X. Gao, Y. Deng, G. Zhang, C.-W. Pao, J.-L. Chen, J.-F. Lee and A. Lei, *ACS Catal.*, 2018, **8**, 5448; (*b*) X. Gao, P. Wang, L. Zeng, S. Tang and A. Lei, *J. Am. Chem. Soc.*, 2018, **140**, 4195; (*c*) S. Tang, D. Wang, Y. Liu, L. Zeng and A. Lei, *Nat. Commun.*, 2018, **9**, 798; (*d*) C. Tian, U. Dhawa, J. Struwe and L. Ackermann, *Chin. J. Chem.*, 2019, **37**, 552; (*e*) U. Dhawa, C. Tian, W. Li and L. Ackermann, *ACS Catal.*, 2020, **10**, 6457; (*f*) Y. Cao, Y. Yuan, Y. Lin, X. Jiang, Y. Weng, T. Wang, F. Bu, L. Zeng and A. Lei, *Green Chem.*, 2020, **22**, 1548.

Cizikovs, A.; <u>Lukasevics, L.</u>; Grigorjeva, L. Cobalt-catalyzed C–H bond functionalization using traceless directing group. *Tetrahedron* **2021**, *93*, 132307.

Reprinted with the permission from Elsevier

Cobalt-catalyzed C−H bond functionalization using traceless directing group

Aleksandrs Cizikovs, Lukass Lukasevics, Liene Grigorjeva*

Organic Synthesis Methodology Group, Latvian Institute of Organic Synthesis, Aizkraukles Street 21, Riga, LV-1006, Latvia

A B S T R A C T

Available online-Transition metal-catalyzed C−H bond functionalization using traceless directing group (TDG) strategy has recently emerged as an attractive tool for the site selective and atom-economic construction of C−C and C-Heteroatom bonds. In this review we present the developed methodology using TDG strategy under high valent cobalt catalysis.

© 2021 Elsevier Ltd. All rights reserved.

1. Introduction

Transition metal-catalyzed C−H bond activation and functionalization represents an attractive strategy for the construction of C−C and C-Heteroatom bonds. Most of successfully developed methods of transition metal-catalyzed C−H bond activation and functionalization use precious transition metal catalysts [1]. Recently, there has been a push to replace noble metal catalysts to first-row transition metals as they are earth abundant, less toxic and inexpensive. In the past decade, cobalt has emerged as an attractive alternative to noble metals for its unique reactivity, low cost and environmentally friendly properties [2]. One of the major challenges using C−H activation strategy is to achieve the desired regioselectivity. Intrinsic reactivity differences of C−H bonds in arenes are less pronounced compared to heteroaromatic compounds, thus selective cleavage of specific C−H bond is difficult to achieve [1,2]. To overcome this selectivity issue in the metal-catalyzed C−H activation, specific ligands or substrate modification with a directing group (DG) are used. DG contains functional group that can coordinate metal center in the close proximity to the desired C−H bond. Nowadays there are designed DGs that allow achieving selective C−H functionalization in *ortho-*, *meta-* and even, few examples, in *para-*position of arenes [1−3]. The use of

DGs over the years has become an essential approach for designing new transformations for C−C and C-heteroatom bond formation. The ability to control selectivity enables pharmaceutical industry to use the newly developed methodologies for the new drug development [4]. Despite the high utility of DG approach for the C−H functionalization, there are some drawbacks: 1) often it is difficult to remove a DG; a multiple step synthesis and/or harsh reaction conditions are required; 2) installation and removal of the strongly coordinating DG add additional reaction steps, thus reducing the step-economical nature of C−H bond activation strategy [4]. One of the approaches to overcome these drawbacks is the use of traceless directing group strategy. Traceless directing groups (TDGs) are a novel class of DG that assist in performing two steps in one pot: 1) chelation assisted C−H bond functionalization; 2) DG cleavage (Scheme 1) [5].

The use of TDG strategy for the C−H functionalization has a great potential and further developments in this field are highly desirable. This review covers both, monodentate TDGs (can act as an internal oxidant) and bidentate TDGs.

2. Traceless directing groups

2.1. Monodentate traceless directing groups

High valent Cp*Co(III) catalyst pioneered by Kanai and Matsunaga [6] has received enormous attention due to the high and unique reactivity shown towards C−H activation and

---

* Corresponding author.
E-mail address: liene_grigorjeva@osi.lv (L. Grigorjeva).

Scheme 1. TDG strategy.
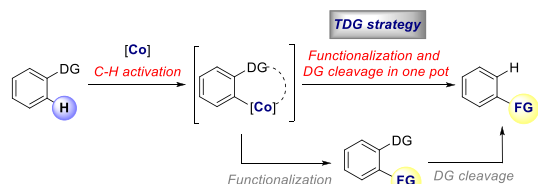
functionalization using monodentate DGs. A numerous methods have been developed based on this approach [2a,7], including the TDG strategy methods.

In 2014, Kanai and co-workers reported cobalt-catalyzed indole **1** C−H bond alkenylation/annulation sequence (Scheme 2) [8]. The reaction proceeds in the presence of [Cp*Co(C₆H₆)](PF₆)₂ catalyst, KOAc additive at 130 °C temperature. Morpholine amide was used as a DG to selectively obtain pyrrolo[1,2-α]indolone derivatives **2** in moderate to good yields. Other directing groups, such as *N, N*-alkyl disubstituted amides, formed a mixture of non-cyclic alkenylation product and the desired pyrroloindolone **2**. The optimal reaction conditions were compatible with a variety of substituents at the benzene ring, such as alkyl, halogen, alkoxy and ester groups. The alkenylation/annulation sequence was successful using various disubstituted alkynes, although terminal alkynes led to the formation of non-cyclic alkenylation products under the reaction conditions. With unsymmetrical aryl/alkyl alkynes reaction products were obtained with excellent regioselectively (mostly as single regioisomers), however the use of unsymmetrical diaryl alkynes led to the product formation in poor regioisomeric ratio.

Based on mechanistic experiments and DFT calculations, the authors postulated a possible reaction mechanism (Scheme 3) [8]. First, thermal dissociation of benzene and ligand exchange to acetate generates catalytically active cobalt complex **3**, which co-ordinates to the carbamoyl group of indole **1** forming complex **4**. Next, C−H activation takes place via concerted metalation-deprotonation mechanism affording indolyl-Co species **5**. Alkyne coordination followed by insertion generates alkenyl-Co intermediate **6**. Nucleophilic addition to carbonyl group leads to complex **7**,
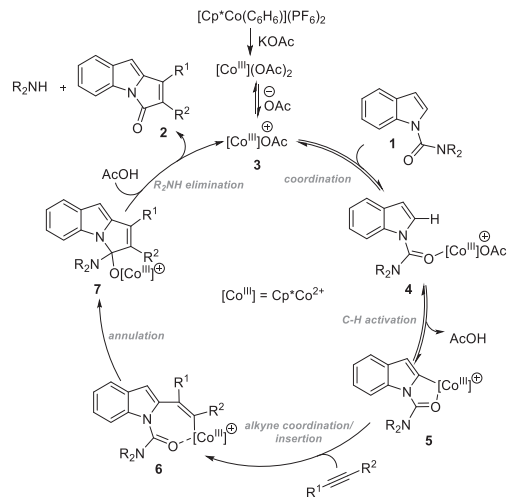
subsequent elimination of morpholine delivers product **2** and re-generates the active cobalt species **3**.

Later, in 2017, Yoshino, Matsunaga and co-workers reported further study on C−H alkenylation of indoles **8**. Authors discovered that tetrasubstituted alkenes **9** form as a kinetically controlled product by directing group migration (Scheme 4) [9]. Under carefully optimized conditions, both electron-donating as well as electron-withdrawing substituents were compatible and gave 4- and 5-substituted indoles **9** in moderate to excellent yields. Unfortunately, terminal alkynes did not provide corresponding indoles **9**.

In 2016, Glorius group developed a high valent Co-catalyzed direct synthesis of *N*-unprotected indoles **11**. For the reaction of hydrazine derivatives **10** with alkynes the *t*-butyloxycarbonyl (Boc)

Scheme 3. Plausible mechanism for the synthesis of pyrroloindolones **2**.
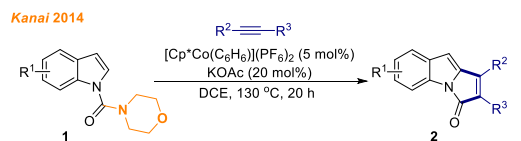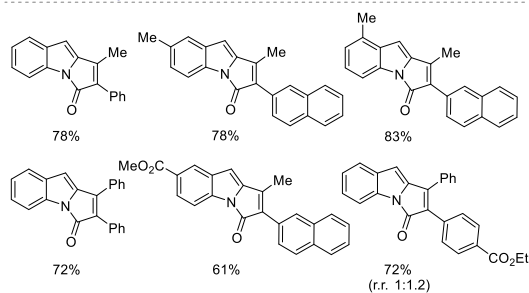
Scheme 2. Cp*Co-catalyzed synthesis of pyrroloindolones **2**.
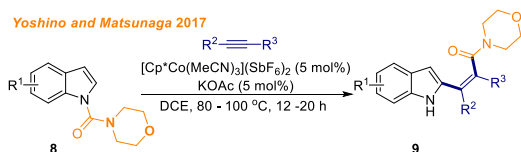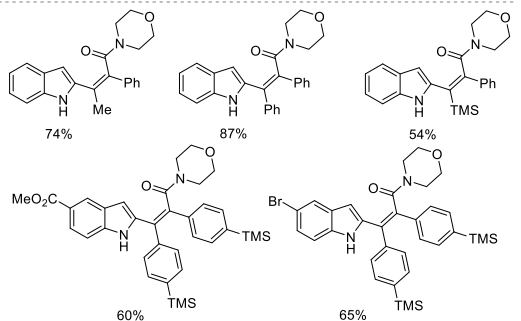
Scheme 4. Cp*Co-catalyzed synthesis of indoles **9**.

protecting group was used as an internal oxidant (Scheme 5) [10]. In this work Cp*Co(CO)I$_2$ catalyst, AgSbF$_6$ and KOAc additives were found to be the best for the synthesis of indoles **11**. The reported method did not require any external oxidant due to the presence of N−N bond in substrates, which can be oxidatively cleaved by the cobalt catalyst. The developed method showed a wide substrate scope; various electron-donating and electron-withdrawing functional groups at the *para*-position on the benzene moiety were well-tolerated under the reaction conditions. Whereas only a few examples of *ortho*- and *meta*-substituents were presented. Different symmetrical disubstituted diaryl alkynes led to the formation of indoles in good yields and, in addition, unsymmetrical alkynes led to the formation of a single regioisomer.

The product formation was explained in the proposed reaction mechanism based on preliminary mechanistic studies and reported literature precedents (Scheme 6) [10]. First, catalytically active cobalt species **3** are generated. Next, substrate **10** coordination, followed by C−H activation takes place to form cobaltacycle **12**, which is presumably additionally stabilized by the Boc-group. The 7-membered intermediate **13** forms via alkyne coordination and subsequent migratory insertion. Then, *N*-ligand shift takes place to form a six-membered cobaltacycle **14**. Intermediate **15** forms via reductive elimination step, followed by oxidative addition of N−N bond to cobalt to form complex **16**. Alternatively, concerted fragmentation of cobaltacycle **14** to produce complex **16** is also included as a possible pathway. Finally, intermediate **16** protonation by acetic acid leads to the formation of the desired indole **11**, release of Boc-DG and regeneration of the active cobalt species **3**.

Zhu and co-workers demonstrated a Cp*Co-catalyzed methodology for the synthesis of indoles **18** and **19** from phenylhydrazines **17** using *N*-amino group as a TDG (Scheme 7) [11]. For the synthesis of indoles **18**, phenylhydrazines **17** reacted with disubstituted alkynes using [Cp*CoI$_2$]$_2$ catalyst, AgSbF$_6$ and Zn(OTf)$_2$ additives. Authors were able to ensure good functional group tolerance under the reaction conditions, respectively, alkoxy, alkyl, halogen and ester substituents at the benzene ring yielded corresponding products in moderate to very good yields. The investigation of the alkyne scope using aryl/alkyl disubstituted alkynes gave indoles **18** as a single regioisomers. By the slight modification of the reaction conditions, authors demonstrated that terminal alkynes can be successfully exploited for C−H bond functionalization, which typically is a challenging task due to competing reaction pathways. The reaction of phenylhydrazines **17** with terminal alkynes

Scheme 6. Plausible mechanism for the synthesis of indoles **11**.

Scheme 7. Cp*Co-catalyzed synthesis of indoles **18** and **19**.

required the use of [Cp*Co(MeCN)$_3$](SbF$_6$)$_2$ complex in combination with Zn(OTf)$_2$ and resulted in the formation of indoles **19** as single regioisomers.

In 2016, Li group developed a Cp*Co catalyzed C(sp^2)-H bond annulation methodology using simple benzoate esters **20** and symmetric diaryl alkynes (Scheme 8) [12]. The reported protocol employs Cp*Co(CO)I$_2$ catalyst, AgNTf$_2$ and Zn(OAc)$_2$ additives, and HFIP as the reaction solvent to yield indenones **21** in good yields. The optimized reaction conditions were compatible with substrates **20** containing alkyl, alkoxy and aryl groups, giving indenones **21** in good to excellent yields, although halogen substituted substrates **20** displayed lower reactivity. Additionally, two parallel experiments were performed with the substrates containing *o*-methyl and *o*-chloro functionalities. Interestingly, the product ratio after

Scheme 5. Cp*Co-catalyzed synthesis of indoles **11**.
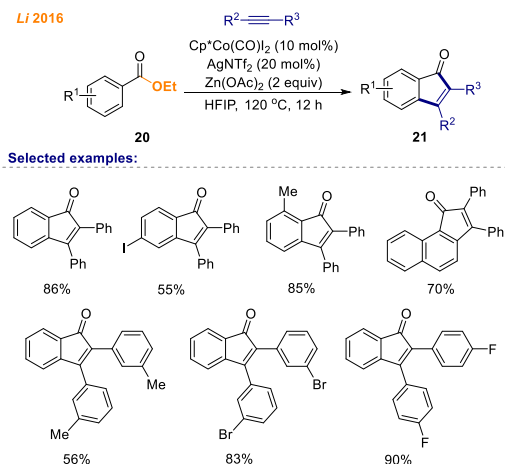
Scheme 8. Cp*Co-catalyzed synthesis of indenones **21**.

6 h of reaction was 2.3:1 in favor of the methyl substituted product, which demonstrated a preferred reactivity of electron-rich benzoates.

Plausible mechanism is given in Scheme 9 [12]. First, the generation of the active catalyst takes place. Next, the active catalyst coordination to ethyl benzoate **20**, followed by C—H activation step generates a five-member cyclic intermediate **22** with a release of acetic acid. Afterwards, alkyne coordination and migratory insertion gives 7-member cobaltacycle **23** followed by the nucleophilic attack of alkenyl group on carbonyl creating Co(III) alkoxide species **24**. Finally, after protonation of complex **24** by acetic acid, ethanol is eliminated, desired product **21** is formed and the active catalyst is returned to the catalytic cycle. Authors propose that the additional role of Zn(OAc)$_2$ is enhancing the electrophilicity of the ester group by coordination with Zn(II), which facilitates insertion of the vinyl-Co bond into the carbonyl group to form complex **24**.

Sundararaju and co-workers in 2015 reported an interesting

cobalt-catalyzed annulation of quinoline-*N*-oxides **25** with internal alkynes via C—H activation and oxygen atom transfer reaction (Scheme 10) [13]. This protocol does not require any external oxidant due to the presence of N—O bond in the substrate which serves as an internal oxidant and a TDG. Authors used Cp*Co(CO)I$_2$ catalyst in combination with NaOPiv additive in TFE to synthetize 8-substituted quinoline derivatives **26**. The reported method has a broad substrate scope - aryl, alkyl, acyl, alkoxy, nitro, and amino substituents at the quinoline withstood the reaction conditions. Symmetrical and unsymmetrical aryl/alkyl substituted alkynes were found to be competent reactants under the reaction conditions giving products with a good regioselectivity.

Based on preliminary mechanistic experiments, DFT calculations and previous literature reports, the plausible reaction mechanism is shown in Scheme 11 [13]. Initially, the catalytically active cationic cobalt complex **27** is generated. Next, coordination to quinoline *N*-oxide **25** takes place followed by C—H activation to form 5-membered cobaltacycle **29**. Then, alkyne coordination, followed by migratory insertion occurs leading to the formation of 7-membered cobalt complex **30**, which can further undergo reductive elimination delivering Co(I) intermediate **31**. Finally, oxidative addition of Co(I) to N—O bond leads to the formation of 7-membered cobaltacycle **32** followed by protodemetalation to form desired product **26** and regenerate the catalytically active cationic cobalt species **27**.

A year later, in 2016, Jiao and co-workers demonstrated a cobalt-catalyzed *N*-substituted indole **34** synthesis from *N*-nitrosoanilines **33** and disubstituted alkynes (Scheme 12) [14]. The reaction proceeded in the presence of [Cp*Co(MeCN)$_3$](SbF$_6$)$_2$ catalyst and Cu(OAc)$_2$ additive. Interestingly, addition of Zn(OAc)$_2$ and Fe(OAc)$_2$ furnished the desired indoles **34** in moderate yields, which is convincing that this reaction does not require any external oxidant and nitroso-DG served as an internal oxidant, while copper acetate acts as a base. Alkyl, alkoxy, halogen and ester functionalities along with cyano group as the substituent on benzene in *meta*- and *para*-positions reacted well under the reaction conditions, although *ortho*-substituent retarded the reaction. Different internal alkyl/
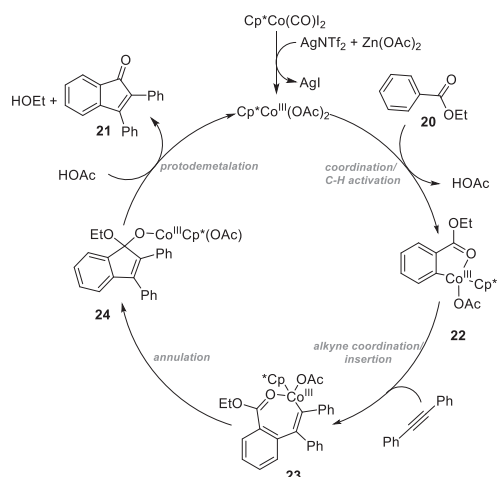
Scheme 9. Plausible mechanism for the synthesis of indenones **21**.
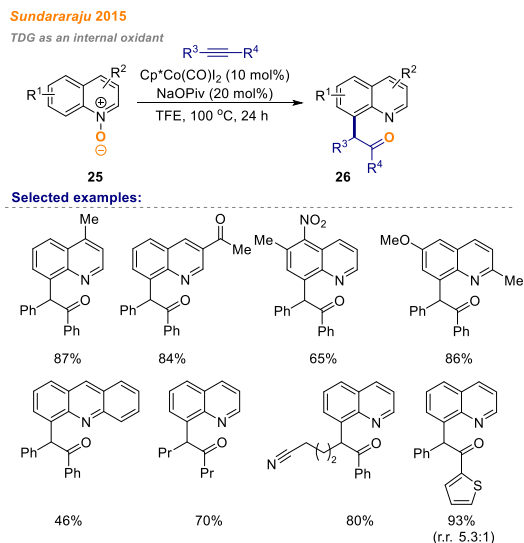
Scheme 10. Cp*Co-catalyzed synthesis of quinolines **26**.
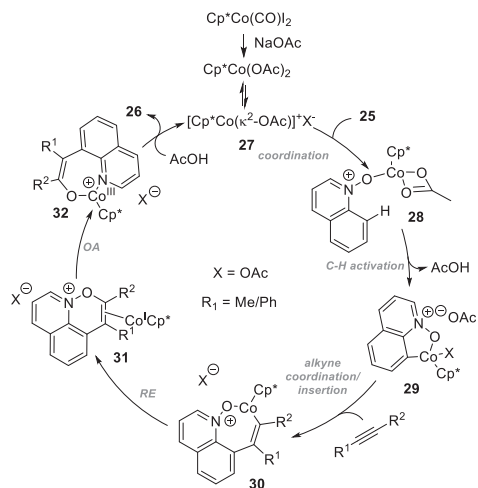
Scheme 11. Plausible mechanism for the synthesis of quinolines **26**.

Scheme 12. Cp*Co-catalyzed synthesis of indoles **34**.

Scheme 13. Cp*Co-catalyzed synthesis of indoles **36**.

Scheme 14. Plausible mechanism for the synthesis of indoles **36**.

aryl disubstituted symmetrical and unsymmetrical alkynes gave corresponding indoles **34** in reasonable yields with moderate to excellent regioselectivity.

In the same year, Ackermann group disclosed a Cp*Co-catalyzed method for the synthesis of 2,3-substituted *N*-unprotected indoles **36** from arylnitrones **35** (Scheme 13) [15]. Cp*Co(CO)I₂ catalyst, AgSbF₆ together with NaOAc additive in HFIP were found to be the best catalytic system. Electron-donating and electron withdrawing functional groups in *para*- and *meta*-positions, such as halogen, alkyl and heteroaryl were well-tolerated under the reaction conditions providing indoles in good to excellent yields with a high level of regioselectivity. Additionally, this synthetic approach may be upscaled with no significant loss of the product yield.

Based on the control experiments, authors proposed the plausible catalytic cycle for this transformation (Scheme 14) [15]. Firstly,

generated active Co-catalyst coordinates to the substrate **35**. Metalacycle **37** is generated during C—H cobaltation, which was found to be the rate-determining step of the reaction (KIE studies by independent reaction). The subsequent alkyne coordination and insertion into C—Co bond generates cobalt intermediate **38,** which then undergoes *N*—O cleavage along with a new C—O bond formation. Then, protodemetalation of complex **39** in presence of acetic acid regenerates active cobalt cationic complex, leading to the formation of *ortho*-protected amino ketone **40**, which upon hydrolysis and intramolecular condensation forms the desired product **36**.

In 2016, Jeganmohan group reported a cobalt-catalyzed cyclization of substituted *N*-methoxy benzamides **41** with alkynes, yielding isoquinolinones **42** in good to excellent yields and high regioselectivity (Scheme 15, a)) [16]. In the reported method, Cp*Co(CO)I₂ catalyst in combination with NaOAc additive in TFE solution were used exploiting *N*-methoxy TDG as an internal
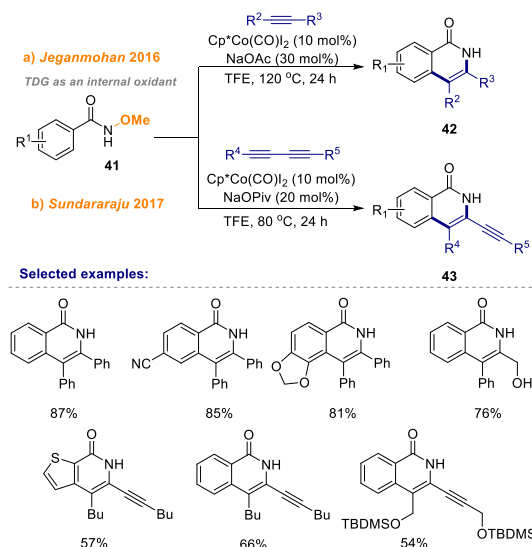
Scheme 15. Cp*Co-catalyzed synthesis of isoquinolinones **42** and **43**.

Scheme 16. Cp*Co-catalyzed synthesis of indolizidines **45**.

oxidant. The developed reaction conditions were mild and tolerated sensitive functionalities on benzene, such as halogen, cyano and nitro group, as well as various substitution patterns in alkyne component. The next year, Sundararaju group demonstrated similar approach towards the cyclization of benzamide derivatives **41** in annulation reaction with symmetrical 1,3-diynes (Scheme 15, b)) [17]. Similarly to Jeganmohan's work, a wide variety of benzene *meta*- and *para*-position substituents including alkyl, alkoxy, halogen, nitro and thioether were tolerated well under reaction conditions and displayed excellent regioselectivity. Although diynes displayed similar reactivity compared to alkynes, this protocol allowed to perform annulation reaction at lower temperature.

The reactivity of traceless *N*-methoxy DG was further explored by Pawar and co-workers in 2017. They developed a novel method for the synthesis of indolizidines **45** from benzamides **44** and substituted alkynediones (Scheme 16) [18]. A Cp*Co(CO)I₂ catalyst and NaOAc additive in TFE solution were found to be the most suitable catalytic system for the developed transformation, leading to the formation of desired products in moderate to good yields. A broad functional group tolerance was displayed including electron-donating, as well as electron-withdrawing groups in benzene *meta*- and *para*-positions. However, *ortho*-substituted benzamides **44** were not suitable substrates, which were attributed to the steric effect. Good reactivity was also achieved using electronically different alkynediones, although terminal alkynedione was not compatible with the reaction conditions.

Authors proposed the plausible mechanistic pathway for this transformation, based on performed experimental studies and previous literature reports (Scheme 17) [18]. According to the proposed catalytic cycle, first, generation of the active Co-species takes place. Then, coordination to benzamide **44** and C—H cobaltation results in the formation of complex **46**. Five-membered cobaltacycle **46** formation was found to be irreversible and the rate-determining step of the catalytic cycle. Afterwards, alkyne coordination followed by migratory insertion into Co—C bond forms seven-member intermediate **47**. Noteworthy, the weak co-ordination of alkynedione to cobalt center is responsible for the
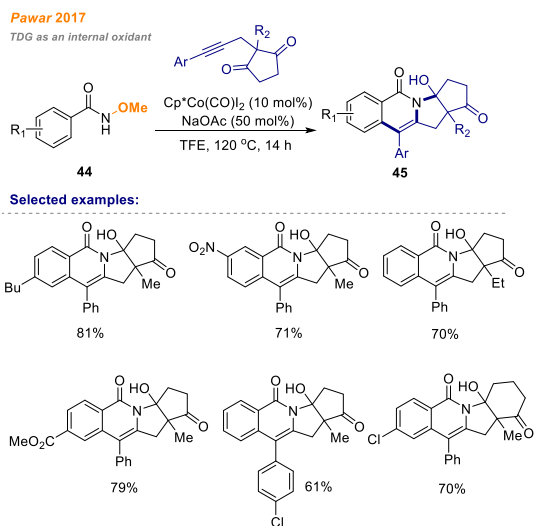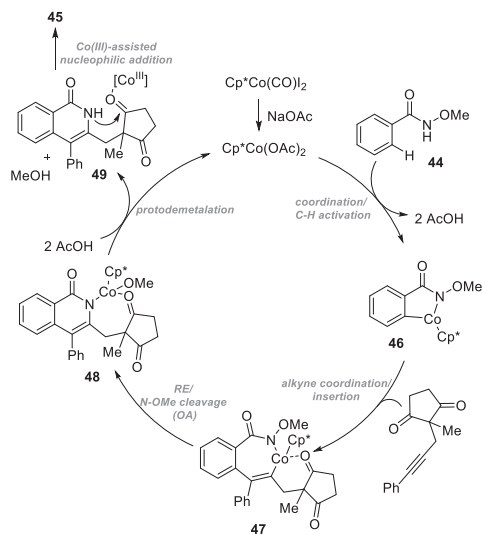
Scheme 17. Plausible mechanism for the synthesis of indolizidines **45**.

opposite regioselectivity of alkyne insertion. Next, reductive elimination takes place, followed by N—OMe bond cleavage leading to the formation of intermediate **48**, which after protodemetalation furnishes isoquinolinone **49** and releases catalytically active cobalt species. Additionally, this step involves elimination of methanol as a byproduct which indicates the traceless nature of *N*-methoxy DG. Eventually, nucleophilic attack of amide N—H of intermediate **49** to the carbonyl group delivers the desired product **45**.

Volla and co-workers in 2018 reported a method for the C—H bond activation in *N*-methoxy benzylamides **50** and their annulation reaction with 7-oxabenzonorbornadienes (Scheme 18) [19].
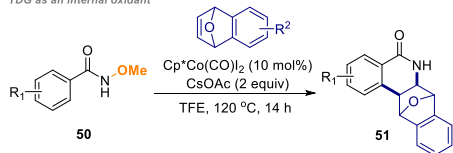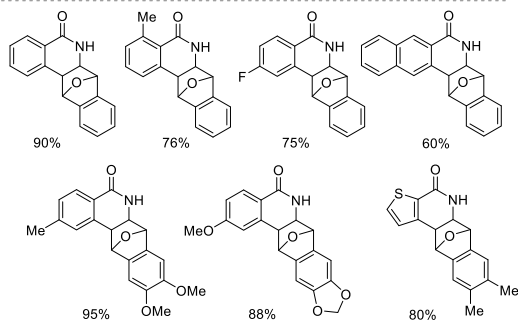
Scheme 18. Cp*Co-catalyzed synthesis of annulation products **51**.

Scheme 19. Plausible mechanism for the synthesis of **51**.

Authors found that the optimal reaction conditions included the use of Cp*Co(CO)I$_2$ catalyst, CsOAc base in TFE. With the optimized reaction conditions in hand, authors demonstrated possible substrate scope of *N*-methoxybenzamides **50**, as well as 7-oxabenzonorbornadienes, which included various *N*-methoxybenzamides **50** with electron-donating groups in *ortho*-, *meta*- or *para*-position of arene yielding products **51** in good to excellent yields. *N*-methoxybenzamides **50** containing electron-withdrawing groups in different position of the arene were also well-tolerated under the optimized conditions giving corresponding products in good yields. Authors showed that the reaction is highly regioselective, *meta*-substituted *N*-methoxybenzamides **50** gave the only regioisomer with sterically less hindered C—H bond activation. Next, authors explored the scope of various 7-oxabenzonorbornadienes, and found that 6,7-dimethoxy, 6,7dimethyl or dioxalone derived substrates yielded products **51** in good yields.

Based on experimental observations and previous literature reports, authors proposed the plausible catalytic cycle for the cobalt-catalyzed *N*-methoxybenzamide **50** annulation with 7-oxabenzonorbornadienes (Scheme 19) [19]. The active cobalt complex, which is generated from Cp*Co(CO)I$_2$ and CsOAc, co-ordinates to *N*-methoxybenzamide **50**, followed by C—H activation via concerted metalation-deprotonation mechanism to form cobaltacycle **52**. Next, alkene coordination and migratory insertion take place to form cobalt complex **53**. Facile reductive elimination forms Co(I), which undergoes oxidation by N—OMe yielding intermediate **54**. Further protodemetalation with AcOH results in annulation product **51** and Co(III) species, which are returned to the catalytic cycle.

A novel Cp*Co(III)-catalyzed method for the synthesis of *N*-acetyl phenylalanines **56** from phenoxyacetamides **55** was reported by the Glorious group in 2016. Monodentate O-NHAc TDG in combination with Cp*Co(CO)I$_2$ catalyst and AgSbF$_6$, CsOAc, K$_3$PO$_4$ additives (Scheme 20) were found to be the best catalytic system for successful carboamination of alkenes [20]. The mild reaction conditions were compatible with a broad substrate scope, various electron-donating and electron-withdrawing substituents
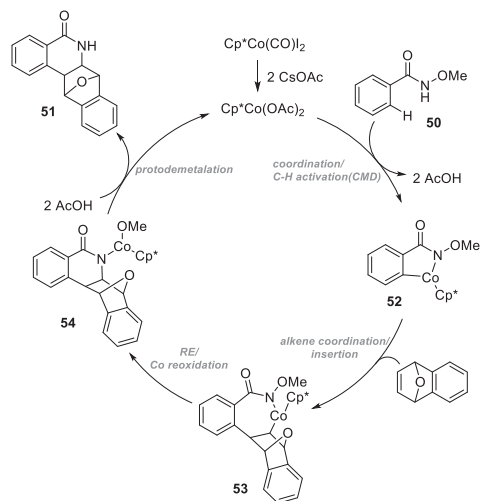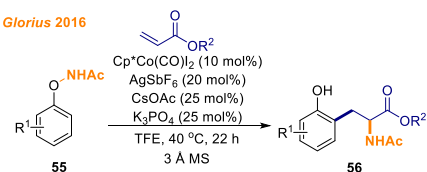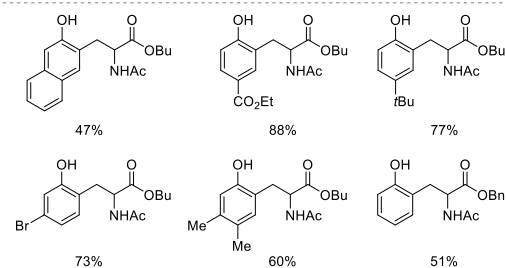
Scheme 20. Cp*Co-catalyzed synthesis of phenylalanines **56**.

containing phenoxyacetamides **55** performed well and gave the corresponding product **56** in good yield. However, the majority of given examples is with *meta*- and/or *para*-substitution patterns. The only *ortho*-methyl substituted product was obtained in acceptable yield, which authors explained with the steric demand of Cp*Co catalyst.

The mechanistic studies support the proposed catalytic cycle (Scheme 21) [20]. Initially, the active cobalt complex is formed, followed by the C—H activation to give the five-member cobaltacycle **57** via elimination of acetic acid. Cobalt complex **57** then undergoes olefin coordination and migratory insertion into Co—C bond leading to the formation of seven-membered intermediate **58**. Afterwards, reductive elimination results in the formation of complex **59**. Then N—O bond oxidatively adds to the Co(I) to give the intermediate **60**. Protodemetalation by acetic acid delivers the
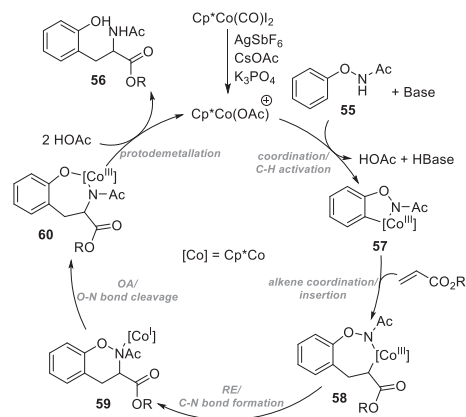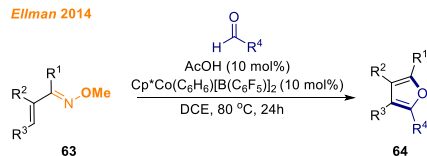
Scheme 21. Plausible mechanism for the synthesis of phenylalanines **56**.

Scheme 23. Cp*Co-catalyzed synthesis of furanes **64**.

desired product **56** and regenerates the active cobalt(III) species.
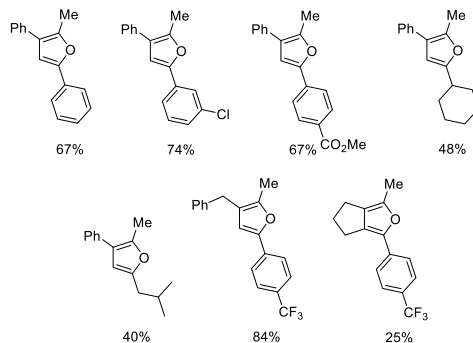
In 2017, Glorius and co-workers developed a protocol for the intramolecular C−H annulation concept of *N*-substituted amides **61** with alkynes. Alkyne-tethered hydroxamic esters as a DG and an internal oxidant in combination with Cp*Co(CO)I$_2$ catalyst and AgSbF$_6$, CsOPiv, PivOH additives were found to be the catalytic system of choice for the synthesis of isoquinolinones **62** in moderate to excellent yields (Scheme 22) [21]. Both electron-donating as well as electron-withdrawing substituents at *ortho*-, *meta*- and *para*-positions on the aromatic system were compatible with the reaction conditions. Additionally, authors found that reaction is not limited to a specific of the alkyne tether; butyne-, hexyne- and heptyne-tether successfully yielded the corresponding isoquinolinone products **62**.

In 2014, Ellman and co-workers reported the first example of the furan **64** synthesis via cobalt-catalyzed aldehyde addition to alkenyl C−H bond of substrates **63** (Scheme 23) [22]. In the developed method, cationic Cp*Co(III) catalyst was used in

combination with a traceless oxime directing group, which had not been used in cobalt catalyzed C−H functionalization reactions before. The substrate scope was explored using several α,β-unsaturated oxime methyl ethers **63** and different aldehydes. It was found that disubstituted oximes gave reaction products in higher yields compared to tri-substituted substrates. A broad aromatic and aliphatic aldehyde scope with halogen, alkyl and ester functionalities was compatible with the reaction conditions and formed furanes **64** in moderate to very good yields.

A year later, in 2015, Sundararaju and co-workers published a methodology for the cobalt-catalyzed annulation of oximes with alkynes (Scheme 24) [23]. As a result from the optimization studies,
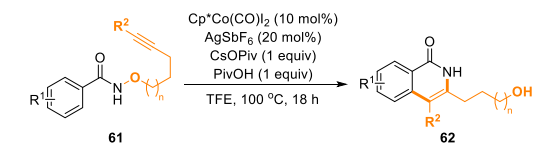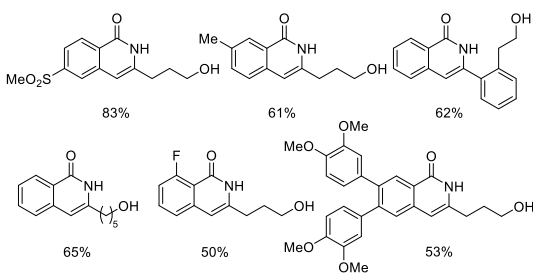
Scheme 22. Cp*Co-catalyzed synthesis of isoquinolinones **62**.
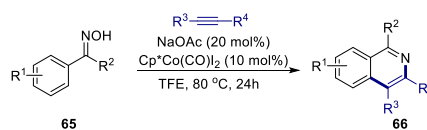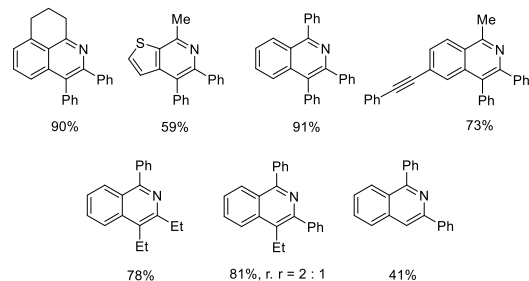
Scheme 24. Cp*Co-catalyzed synthesis of isoquinolines **66**.

Cp*Co(CO)I₂ catalyst and NaOAc additive in TFE together with oxime TDG at 80 °C temperature were found to be the best catalytic system for the successful transformation. The annulation process went smoothly for a broad scope of substrates bearing different functional groups in *para*-, *ortho*- or *meta*-positions, giving isoquinolines **66** in very good yields. Additionally, both symmetrical and unsymmetrical, aryl and alkyl disubstituted alkynes were efficiently employed as a coupling partners and provided corresponding products **66** in good to very good yields. Products **66** were obtained as a mixture of regioisomers (ranging from 1.5:1 to 4:1) if unsymmetrical alkynes were used. Terminal alkynes were also tested, they displayed lower reactivity and gave products in low and moderate yields, although the reaction regioselectivity was excellent.

Cheng and co-workers in 2016 expanded the methodology to access 1-aminoisoquinolines **68**. Authors demonstrated that *N*′-hydroxyimidamide functional group also can be used both as TDG and an internal oxidant for C−H functionalization with alkynes to obtain isoquinoline derivatives **68** under similar reaction conditions that was reported before by Sundararaju (Scheme 25) [24]. Generally, most of the tested *N*′-hydroxybenzimidamides **67** reacted smoothly and provided corresponding 1-aminoisoquinolines **68** in moderate to high yields. Substituents such as alkyl, halogen, nitro, alkoxy at *N*′-hydroxybenzimidamide **67** aromatic moiety were compatible with the reaction conditions, although substrates containing electron-withdrawing functional groups tended to give products in better yields than substrates containing electron-donating ones. The effect of amino protecting group was tested, and it was found that sterically hindered amino group was necessary for the reaction to proceeded successfully. Authors explained, that protecting groups like Bn or *n*-Bu allowed free NH from amino group to coordinate with cobalt complex, which did not lead to the C−H activation. Additionally, various alkynes were tested for the compatibility with the reaction conditions. Symmetrical aryl and alkyl alkynes reacted smoothly and formed products **68** in good yields, whereas unsymmetrical alkynes gave mixture of regioisomers (ranging from 1.5:1 to 2.3:1).

The proposed reaction mechanism is depicted in Scheme 26 [24]. The reaction is initiated by the reaction of Cp*Co(CO)I₂ with
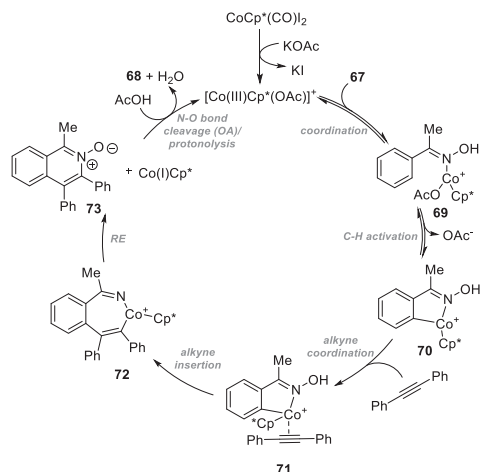
Scheme 26. Plausible mechanism for the synthesis of isoquinolines **68**.

KOAc to generate the active Co(III) species. Next, coordination of the active Co(III) catalyst to substrate **67** forms cobalt complex **69**, which undergoes reversible C−H cobaltation to give intermediate **70**. Subsequent alkyne coordination forms intermediate **71**, next migratory insertion takes place and leads to **72**. Subsequent reductive elimination gives *N*-oxide **73** and Co(I) species. Finally, cleavage of the N−O bond by Co(I) releases isoquinoline **68** and Co(III) species, which returns to the catalytic cycle.
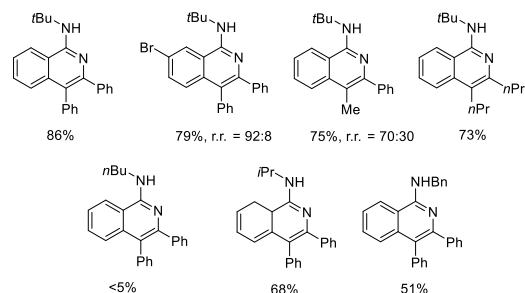
Li and co-workers in 2016 disclosed a novel method for the synthesis of quinazoline derivatives **75** via C−H functionalization pathway (Scheme 27, a)) [25]. Under the Cp*Co(CO)I₂ catalysis conditions in the presence of AgNTf₂ additive in DCE *N*-sulfinylimine derivatives **74** reacted with dioxazolones and formed
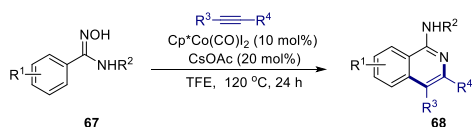
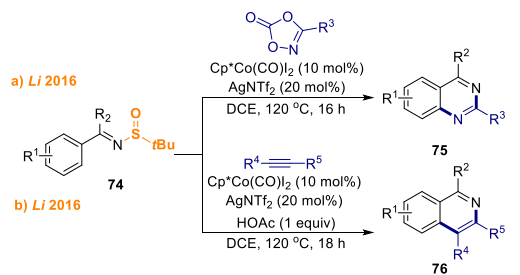**Scheme 25.** Cp*Co-catalyzed synthesis of isoquinolines **68**.
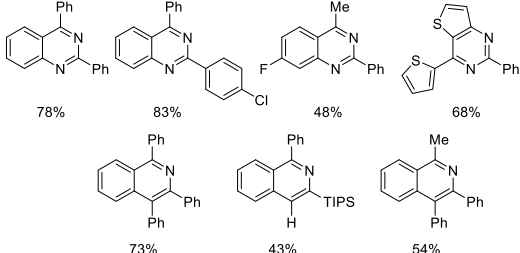
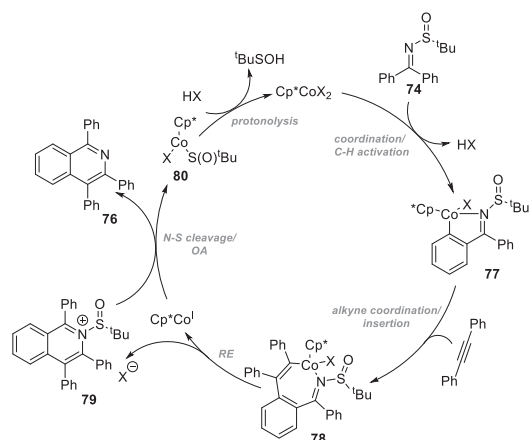**Scheme 27.** Cp*Co-catalyzed synthesis of quinazolines **75** and isoquinolines **76**.

quinazolines **75** in moderate to excellent yields. In developed method *N*-sulfinyl group served as a TDG, and N–S bond as an internal oxidant. Symmetrical *N*-sulfinylimines **74** reacted smoothly, however, it was observed that the reaction of unsymmetrical *N*-sulfinylimines **74** containing different aryl substituents in some cases was not selective due to electronic bias of the substituents.

Additionally, in the same year, Li used similar reaction conditions to demonstrate the application of *N*-sulfinyl group for the synthesis of isoquinolines **76**. Under the cobalt catalysis *N*-sulfinylimines **74** reacted with alkynes to form isoquinoline derivatives **76** (Scheme 27, b)) [26]. Symmetrical and unsymmetrical diaryl/dialkyl substituted alkynes tolerated the reaction conditions, however in case of terminal alkynes the reaction yields were generally lower.

The proposed reaction mechanism is shown in Scheme 28 [26]. First, C–H activation of *N*-sulfinylimine **74** gives a metalacycle **77**. Then, alkyne coordinates and inserts into C–Co bond forming seven-membered cobaltacycle **78**. Next, reductive elimination takes place yielding isoquinolinium salt **79** and Cp*Co(I) species. The N–S bond is proposed to oxidatively add to Co(I) species yielding the desired product **76** and Co(III) complex **80**, which undergoes protonolysis to regenerate the active cobalt catalyst by the elimination of *t*-BuSOH as a byproduct.

In 2019 Zhu and co-workers reported a novel procedure for the synthesis of 1-naphthols **82** with alkynes (Scheme 29) [27]. In their work, authors employed sulfoxonium ylide as a TDG and an internal oxidant in combination with Cp*Co(CO)I₂ catalyst, AgOTf and KOAc additives in DCE solution at 140 °C temperature. Both electron-withdrawing and electron-donating groups on benzene were well tolerated giving products predominantly in very good yields. Substituents in *ortho*-position were reactive, albeit giving products in slightly lower yields, which authors attributed to the steric hindrance. In the case of *meta*-substituted substrates, the reaction proceeded in a highly regioselective fashion, where functionalization was observed only at more sterically accessible C–H bond. Alkyne scope studies showed that both symmetrical and unsymmetrical aryl alkynes were compatible with the reaction conditions and gave products in moderate to excellent yields, whereas dialkyl alkynes did not display any reactivity.

A synthetic approach towards isoquinolinones **84** using *N*-

Scheme 29. Cp*Co-catalyzed synthesis of 1-naphthols **82**.

chloroamide TDG as an internal oxidant was demonstrated by Zhu and co-workers in 2017 (Scheme 30, a)) [28]. In the presence of Cp*Co(CO)I₂ catalyst and KOAc, AgOAc additives *N*-chlorobenzamides **83** reacted with alkynes to produce isoquinolinones **84** in moderate to good yields. Various electron-donating and electron-withdrawing substituents at *para*-position of aryl moiety gave products in high yields. *Meta*-substituted *N*-chlorobenzamides **83** gave products in good yields, but the regioselectivity varied depending on substituents. However, *ortho*-substituted *N*-chlorobenzamides **83** yielded products in lower yields, especially for bulkier substituents. Good reactivity was also achieved using different symmetrical and terminal alkynes, which predominantly
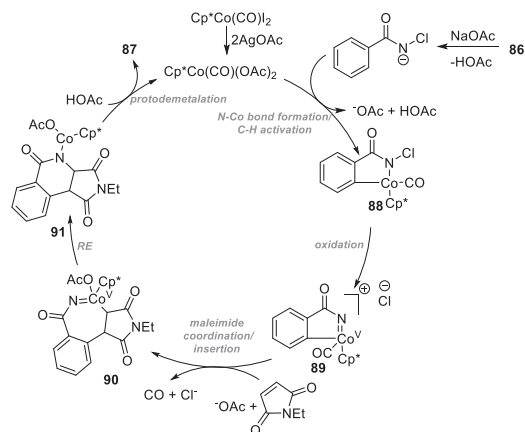

Scheme 28. Plausible mechanism for the synthesis of isoquinolines **76**.
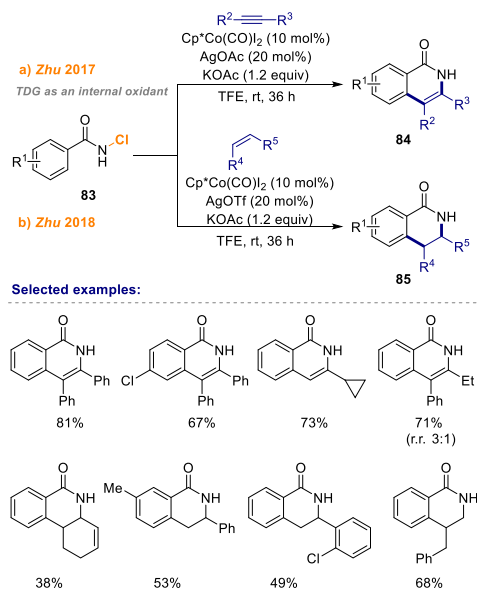
Scheme 30. Cp*Co-catalyzed *N*-chlorobenzamide **83** reaction with alkynes and alkenes.

yielded products as a single regioisomer, while unsymmetrical internal alkynes gave a mixture of regioisomers. Additionally, authors were able to synthesize and characterize stable five-membered cobaltacycle via direct C−H activation using stoichiometric amounts of catalyst and silver salt.

One year later, Zhu group demonstrated cobalt-catalyzed cyclization of *N*-chlorobenzamides **83** with alkenes (Scheme 30, b)) [29]. The optimization studies showed that combination of AgOTf and KOAc is the most suitable for the transformation along with the same catalyst as in previous group's report. Likewise no external oxidant is required due to the presence of N−Cl bond which serves as an internal oxidant in this protocol. Both electron-donating and electron-withdrawing amides **83** were successfully applied to yield the corresponding 3, 4-dihydroisoquinolinones **85** in moderate to good yields. Different alkyl/aryl substituted alkenes were compatible with the reaction conditions and showed superior regioselectivity for the transformation. Interestingly, *N*-chlorobenzamide reaction with allyl benzene as a functionalization reagent showed the completely opposite regioselectivity.

In 2019, Prabhu and co-workers reported a strategy for the cyclization of *N*-chlorobenzamides **86** through cobalt-catalyzed [4 + 2] annulation reaction with maleimides (Scheme 31) [30]. Authors used Cp*Co(CO)I₂ catalyst, AgOAc and NaOAc additives in the TFE solution at room temperature. Mild reaction conditions were tolerable wide variety of substituents at *meta-* and *para*-positions on benzene as well as *N*-alkyl and *N*-aryl substituents of the maleimide counterpart. The scope for *N*-chlorobenzamides **86** includes a single example of 2-fluoro substituted benzamide, but under the reaction conditions it formed product in low yield. Interestingly, unprotected maleimide, maleic acid and maleic acid anhydride do not participate in this reaction.

According to the plausible reaction mechanism (Scheme 32) [30], the reaction between in situ generated cobalt species with anionic form of **86** leads to the formation of five-membered cobaltacycle **88**. Next, *N*-chloro-DG assisted Co(III) oxidation to Co(V) delivers intermediate **89**. Insertion of maleimide into Co−C bond forms cyclic 7-membered cobalt intermediate **90**, which upon reductive elimination leads to the formation of Co(III) intermediate **91**. Protodemetalation of **91** produces the target product **87**.

Scheme 32. Plausible mechanism for the Cp*Co-catalyzed [4 + 2] annulation reaction.

and regenerates the active Co(III) species. Noteworthy, the carbonyl ligand is bound to cobalt only in the first catalytic cycle, and the most likely is replaced with solvent molecule onwards.

## 2.2. Bidentate traceless directing groups

Bidentate DG is one of the most efficient tools for the selective C−H bond functionalization [31]. In 2005 Daugulis introduced quinolinamide and picolinamide directing groups [32], and in 2014 demonstrated that cheap and earth-abundant Co(II) salts in combination with bidentate DG assistance can be efficiently exploited for C−H functionalization as high-valent cobalt(III) precursors [33]. Since then, a large number of methods have been developed based on this strategy [34]. The major drawback using bidentate DG is the step economy (requires installation prior and removal after the C−H functionalization). Besides, the removal of bidentate DG often requires harsh conditions that gives only average product yields. One of the tools to solve this problem is the use of a TDG strategy.

In 2016, Zhu group developed the first bidentate-directing enabled traceless synthesis of isoquinoline **93** derivatives. In contrast to monodentate directing groups, 2-hydrazinylpyridine-DG allowed the use of low-cost Co(acac)₂ catalyst while ensuring good reactivity of starting materials and terminal alkynes. The reaction conditions were mild and provided products in generally good yields, tolerating wide range of substituents at *meta-* and *para*-positions on the benzene ring, whereas the *ortho*-substitution significantly diminished the product yield (Scheme 33) [35]. Both terminal and internal aryl alkynes with diverse substitution patterns were reactive, yielding products **93** in good yields and with remarkable regioselectivity. Interestingly, only trace amount of the product was observed under inert atmosphere, which indicates the crucial role of air for maintaining the reaction, however, mechanistic studies also showed that 2-hydrazinylpyridine-DG could serve as an internal co-oxidant.

Later, Volla and co-workers demonstrated cobalt-catalyzed synthesis of 3-alkynylated isoquinolines **95** (Scheme 34) [36]. Optimization studies showed that catalytic amount of cobalt(II) acetate in combination with KPF₆ additive in polyethylene glycol solution open-air at 100 °C was the best catalytic system for the transformation, although other combinations were also appropriate. They found that bidentate chelation of 2-hydrazinylpyridine-DG was crucial for the successful
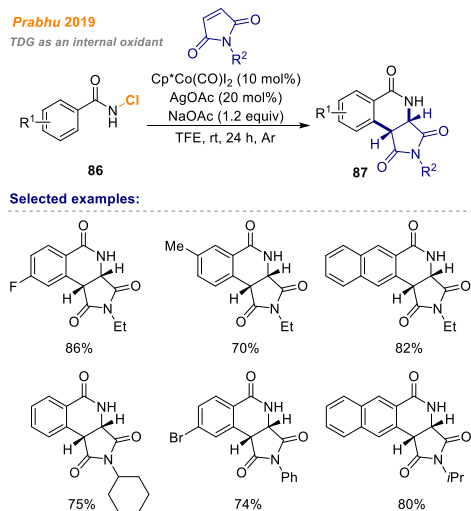
Scheme 31. Cp*Co-catalyzed synthesis of [4 + 2] annulated product **87**.
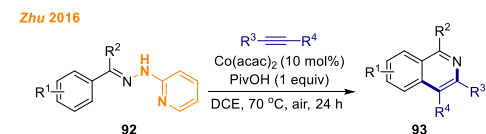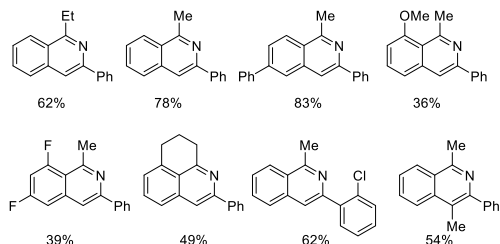
Scheme 33. Co(II)-catalyzed synthesis of isoquinolines **93**.
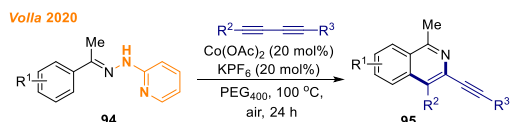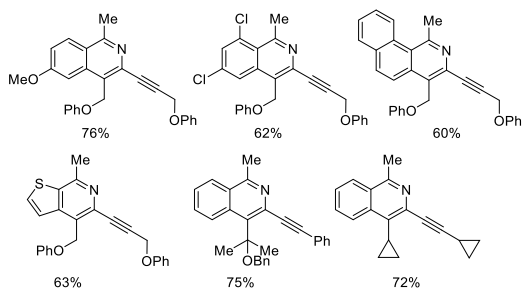
Scheme 34. Co(II)-catalyzed hydrazone **94** reaction with 1,3-diynes.
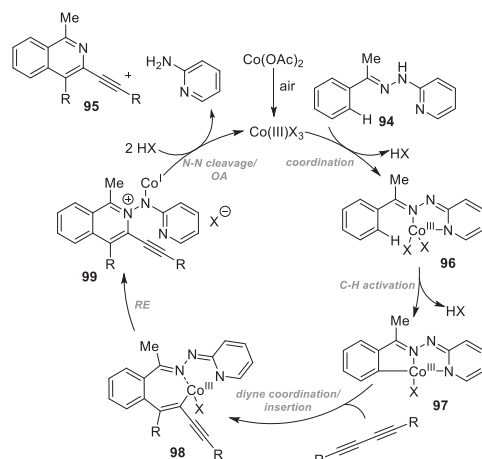
Scheme 35. Plausible mechanism for the synthesis of isoquinolines **95**.
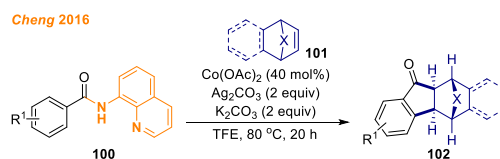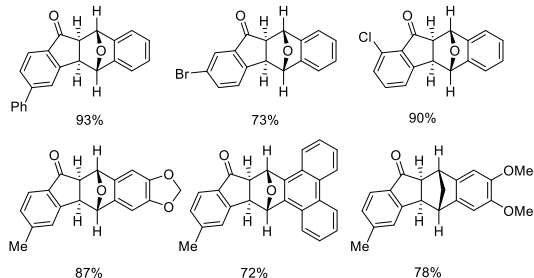
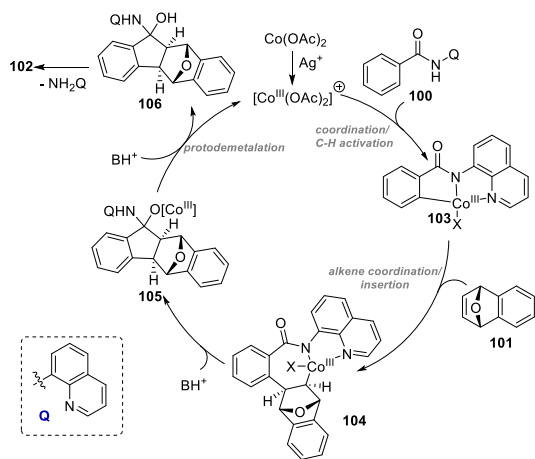**Scheme 36.** Co(II)-catalyzed synthesis of [3 + 2] formal cycloaddition product **102**.

transformation. Electron-donating and electron-withdrawing substituents at different positions on benzene tolerated well.

Preliminary mechanistic studies showed that the plausible mechanism (Scheme 35) [36] involves coordination of Co(III) with hydrazinylpyridine **94**, followed by ligand exchange to form intermediate **96**, which then undergoes C—H bond activation delivering cobaltacycle **97**. After diyne coordination and regioselective migratory insertion, intermediate **98** is formed. Reductive elimination with subsequent N—N bond cleavage leads to the annulation product **95**, 2-aminopyridine and regenerates Co(III) species.

A novel cobalt-catalyzed C—H [3 + 2] formal cycloaddition of benzamides **100** and bicyclic alkenes **101** employing 8-aminoquinoline as a bidentate TDG was disclosed by Cheng and co-workers in 2016 (Scheme 36) [37]. Optimization studies revealed that Cp*Co(III) catalyst can be substituted with simple Co(OAc)$_2$ salt in combination with K$_2$CO$_3$ additive in TFE solution at 80 °C temperature, although additional 2 equivalents of external Ag$_2$CO$_3$ oxidant were required for the successful transformation. A variety of alkyl, alkoxy and halogen functionalities on the benzene tolerated well the reaction conditions, even substitution at *ortho*-

position gave products in impressively high yields. Norbornene, norbornadiene and benzonorbornadienes were appropriate reaction partners and gave the desired products **102** in good yields, whereas azabicyclic alkene failed to give the corresponding annulation product under the reaction conditions.

The proposed reaction mechanism is shown in Scheme 37 [37]. At the beginning, Co(II) is oxidized to Co(III) by Ag$_2$CO$_3$. Then, benzamide **100** is coordinated to the active cobalt catalyst, followed by C—H activation providing intermediate **103**. Subsequent alkene coordination to cobalt center and migratory insertion into C—Co bond delivers seven-membered cobaltacycle **104**. Next, intramolecular nucleophilic addition of the C—Co to the amide carbonyl group takes place forming intermediate **105**. As the last step of the transformation, protodemetalation of **105** and elimination of 8-aminoquinoline provides the final ketone **102** and regenerates catalytically active Co(III) species.

Scheme 37. Plausible mechanism for the synthesis of [3 + 2] formal cycloaddition product **102**.

also served as an internal oxidant (Scheme 39) [39]. The main advantage of the developed transformation was the use of cheap Co(acac)$_3$ salt instead of Cp*Co(III) catalyst. Despite the replacement of the catalyst, great reactivity was observed towards a large variety of symmetrical/unsymmetrical, alkyl and aryl substituted internal and terminal alkynes in a very selective fashion. Substrates with a wide range of electron-withdrawing and electron-donating groups at different positions on the benzene successfully afforded the final isoquinolines **110** predominantly in excellent yields.

One year later, in 2020, Song and co-workers developed a new TDG, which was used for the cobalt(II) catalyzed synthesis of 3,4-disubstituted isoquinolinones **112** from benzamides **111** (Scheme 40) [40]. 2-Hydroxymethyl pyridine was used as a TDG for this transformation in combination with Co(OAc)$_2$·4H$_2$O catalyst, AgOAc oxidant and PivOH additive in TFE solution. The reaction presented good functional group tolerance: alkyl, alkoxy, halogen, ester and thiophene functionalities containing *N*-(pyridine-2-ylmethoxy)benzamides **111** were competent substrates under the reaction conditions. Although, the developed method was limited mostly to disubstituted symmetrical alkynes. The use of unsymmetrical alkynes gave mixture of regioisomers, however terminal alkynes did not lead to the product **112** formation.

Cui and co-workers in 2017 introduced a cobalt-catalyzed benzylamine **113** C−H functionalization with alkynes exploiting picolinamide for the first time as a TDG (Scheme 41, a)) [41]. Different functionalities on the benzene ring were successfully tolerated under this protocol and gave the desired isoquinolines **114** in moderate to very good yields, although benzylamines **113** with electron-withdrawing groups gave somewhat lower yields than those with electron-donating groups. Subsequent alkyne scope study showed that various disubstituted aryl and alkyl alkynes displayed good reactivity and gave products **114** in moderate to excellent yields, although unsymmetrical alkynes were mostly unselective and gave products as regioisomer mixtures ranging from 1:1 to 8:1. An advantage of this protocol was the use of oxygen as a terminal oxidant, as no other external oxidants were necessary.

In the same year, Zhong group reported picolinamide assisted cobalt-catalyzed C−H carbonylation of benzylamines **113** (Scheme 41, b)) [42]. In their study diethyl azadicarboxylate (DEAD) was used as a CO surrogate, Co(OAc)$_2$·4H$_2$O as a catalyst, Ag$_2$CO$_3$ as an

In 2019, Zhai and co-workers developed a one-pot synthesis of benzofluorenones **108** (Scheme 38) [38]. Optimization of the reaction of *N′*-methyl-*N′*-(2-pyridinyl)benzohydrazide **107** with 1,4-epoxydihydronaphthalene demonstrated that the highest product **108** yield was achieved using Co(OAc)$_2$ catalyst, Cs$_2$CO$_3$ base under oxygen atmosphere in TFE. *Ortho*-, *meta*- and *para*-substituted benzoyl hydrazides **107** bearing an electron-withdrawing group or electron-donating group reacted smoothly giving products **108** in moderate to very good yields. In addition, high regioselectivity was achieved if *meta*-substituted benzoyl hydrazides **107** were used. Authors demonstrated that 7-oxabenzonorbornadienes containing electron-donating groups at different positions of the arene moiety were suitable for the reaction and provided benzofluorenones **108** in good yields.

In 2019, Song reported a new approach for the synthesis of isoquinolines **110** exploiting L,X-type α-imino-oxy acid TDG, that
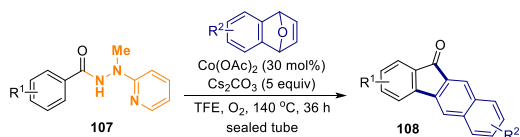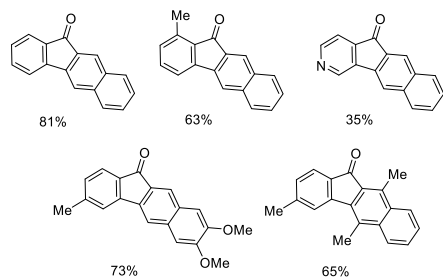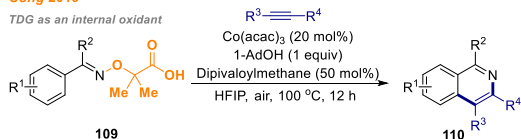

Scheme 38. Cobalt-catalyzed synthesis of benzofluorenones **108**.
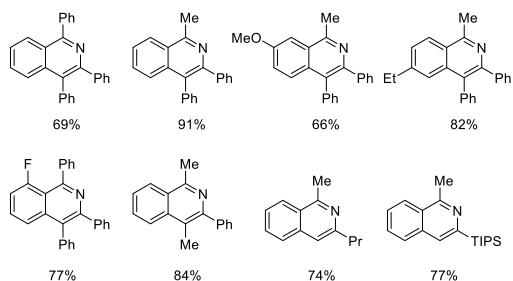
Scheme 39. Co(III)-catalyzed synthesis of isoquinolines **110**.

Song 2020

111

Selected examples:

60% 86% 46% 56%

83% 44% 94%, r.r. = 2:1
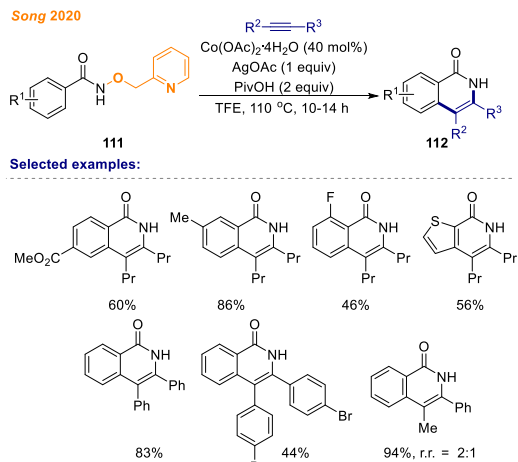
Scheme 40. Co(II)-catalyzed synthesis of isoquinolinones **112**.

a) *Cui* 2017

b) *Zhong* 2017

113

114

115

Selected examples:

75% 72% 68% 58%

76% 53% 69% 83%
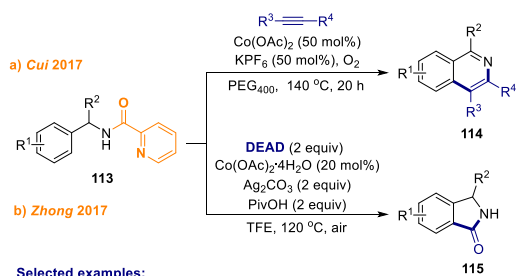
Scheme 41. Co(II)-catalyzed C−H bond functionalization of benzylamines **113**.

oxidant and pivalic acid as an additive in TFE solution, yielding a variety of *N*-unprotected isoindolinones **115** in moderate to excellent yields. Substrates **113** bearing electron-withdrawing group showed slightly better reactivity compared to electron-donating groups. Authors found, that *ortho*- and *meta*-substituted benzylamines **113** formed products **115** in lower yields than those with *para*-substituents. Noteworthy, *meta*-substituted benzylamines **113** gave corresponding products as a single regioisomer. Additional experiments demonstrated that reaction conditions were mild and no erosion of enantiopurity was observed under the reaction conditions using enantioenriched substrates.

Based on Zhong's mechanism studies and literature reports proposed reaction mechanism is depicted in Scheme 42 [42].
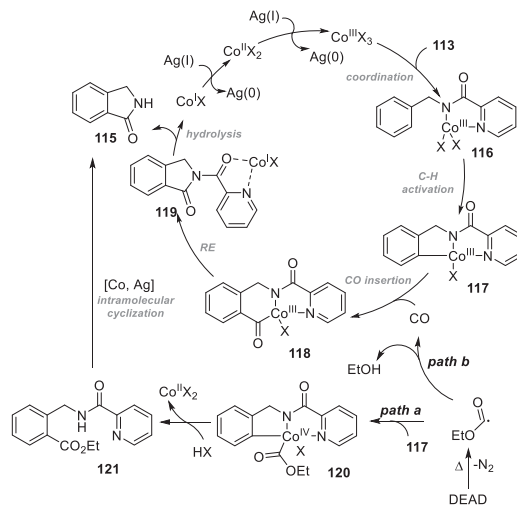
Scheme 42. Plausible mechanism for the synthesis of isoindolinones **115**.

Initially, Co(II) species are oxidized to catalytically active Co(III), which then coordinates to benzylamines **113** forming complex **116**, followed by C(sp^2)-H bond activation leading to the formation of cobaltacycle **117**. Thermal decomposition of DEAD generates the esteric radical enclosing two possible pathways. The esteric radical could attack the intermediate **117** with subsequent reductive elimination resulting in intermediate **121** with the release of Co(II) species (path a). Intramolecular cyclization of **121** and hydrolysis of picolinamide afford the desired isoindolinones **115** along with the elimination of ethanol and picolinic acid. Alternatively, esteric radical generates the CO gas which could migratory insert into C−Co bond forming cobaltacycle **118** (path b). Afterwards, reductive elimination delivers intermediate **119** that under hydrolysis forms the desired product **115**. Co(I) salts are subsequently reoxidized to Co(III) and returned to the catalytic cycle.

Inspired by their previous work, Zhong and co-workers further explored picolinamide directing group assisted C−H carbonylation and in 2018 reported a new approach for the phenanthridinone **123** synthesis (Scheme 43) [43]. The protocol employs DIAD as the CO surrogate, CoCl$_2$ catalyst, NaOPiv additive and oxygen as the sole oxidant. Substrate scope studies revealed that the reaction conditions were tolerated by a very broad functional group diversity in both aryl rings, and majority of products were obtained in excellent yields, although authors mentioned, that reactions were less effective for *ortho*-substitutes substrates **122**.

In 2019, Zhong and co-workers reported a one pot procedure that allowed to obtain dibenzoazepine derivatives **125** from *ortho*-phenylanilines **124** via cobalt-catalyzed C−H annulation followed by the directing group cleavage (Scheme 44) [44]. The devloped catalytic system employed CoCl$_2$ catalyst, NaOPiv additive and Mn(OAc)$_2$/O$_2$ oxidant system in TFE at 120 °C temperature. The substrate scope studies showed that electron-rich substrates displayed better reactivity compared to electron-poor substrates and gave the products mostly in moderate yields. Also, authors demonstrated that the reaction conditions are compatible with symmetrical and unsymmetrical diaryl internal alkynes as well as terminal alkynes. Interestingly, in case of terminal alkynes, complete regioselectivity of alkyne addition was attained, whereas unsymmetric internal alkynes gave regioisomeric mixture in 1:1.2

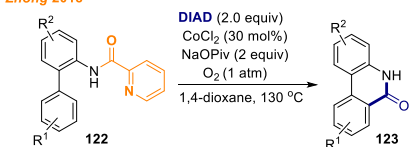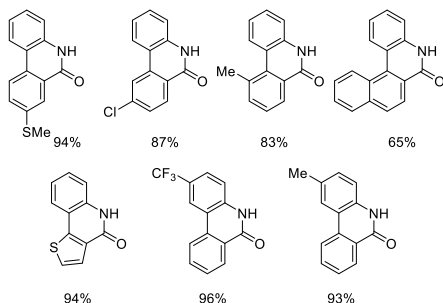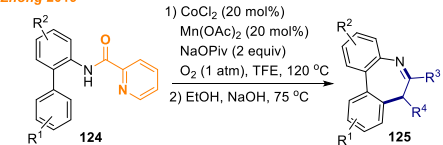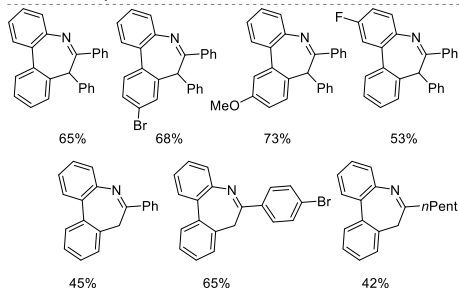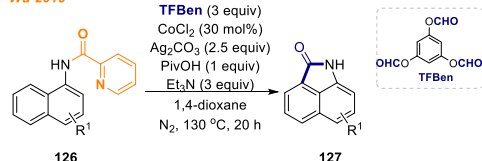**Scheme 43.** Co(II)-catalyzed synthesis of phenanthridinones **123**.

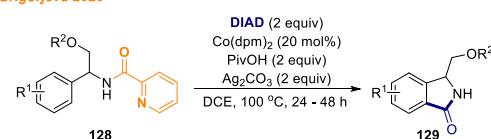**Scheme 44.** Co(II)-catalyzed synthesis of dibenzoazepines **125**.
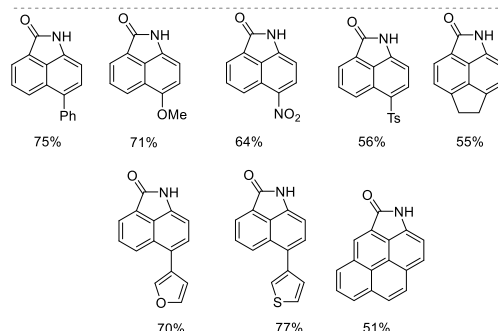
Scheme 45. Co(II)-catalyzed synthesis of benzoindolones **127**.
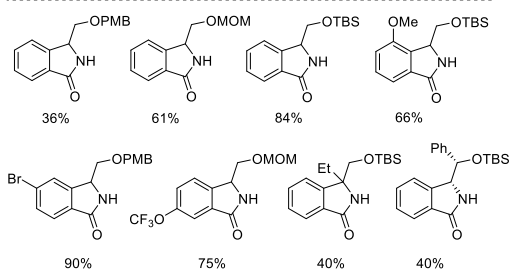
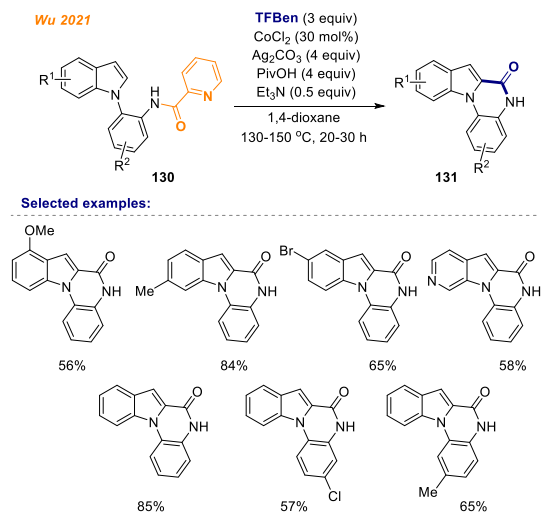**Scheme 46.** Co(II)-catalyzed synthesis of isoindolinones **129**.

ratio.

Wu group in 2019 developed an interesting traceless picolinamide directed strategy for the synthesis of benzoindolones **127** (Scheme 45) [45]. In contrast to the previous reports, authors substituted DIAD with solid benzene-1,3,5-triyl triformate (TFBen) for the generation of CO gas in situ. Different electron-donating and electron-withdrawing substituents, such as alkyl, alkoxy, nitro and ester groups at naphthylamide **126** C(4) position afforded smoothly the desired products in good yields. However, a substrate bearing methyl group in C(2) position gave only a trace amount of the target product, which authors attributed to the steric effect.

In 2020, Grigorjeva and co-workers demonstrated a traceless picolinamide DG assisted cobalt(II) catalyzed C–H carbonylation of phenylglycinol derivatives **128** (Scheme 46) [46]. Optimization studies revealed that this protocol requires Co(dpm)$_2$ catalyst,

PivOH additive, AgOAc oxidant and DIAD as a CO source to afford the desired isoindolinones **129** in moderate to excellent yields. A variety of electron poor and rich substrates were well-tolerated under the reaction conditions. Quaternary amino alcohols were found to be suitable substrates for the carbonylation reaction as well. Additionally, authors showed that this transformation proceeds with a full preservation of substrate original stereochemistry.

Recently, in 2021, Wu group reported a traceless picolinamide DG assisted C–H carbonylation for the synthesis of *N*-indoloquinoxalinone **131** (Scheme 47) [47]. For the transformation authors used similar reaction conditions as in their previous report in 2019 [45] – CoCl$_2$ catalyst, Ag$_2$CO$_3$ oxidant, PivOH and Et$_3$N additives in combination with TFBen as CO source in 1,4-dioxane. Different substituents on the indole **130** were well-tolerated under the

Wu 2021

TFBen (3 equiv)
CoCl₂ (30 mol%)
Ag₂CO₃ (4 equiv)
PivOH (4 equiv)
Et₃N (0.5 equiv)

1,4-dioxane
130-150 °C, 20-30 h

130 → **131**

Selected examples:

56%   84%   65%   58%

85%   57%   65%

Scheme 47. Co(II)-catalyzed carbonylation of *N*-substituted indoles **130**.

reaction conditions, yielding products in moderate to very good yields. Compounds bearing electron-donating and electron-withdrawing groups at C(4) and C(5) positions of the benzene ring were compatible with reaction conditions, whereas methyl group in C(6) position retarded the reaction due to steric effects.

Recently, Grigorjeva and co-workers reported an approach towards the C−H carbonylation of amino acids using picolinamide as a TDG (Scheme 48) [48]. In their study, catalytic system employed Co(dpm)₂ catalyst, PivOH additive and Ag₂CO₃, Mn(OAc)₃·2H₂O oxidants in PhCl solution under CO atmosphere at 120 °C to deliver isoquinolinones **133**. Both electron-donating and electron-withdrawing groups on the benzene moiety tolerated well the reaction conditions, moreover in case of *ortho*-substituents reaction yield was not affected by the steric effect. In addition, authors
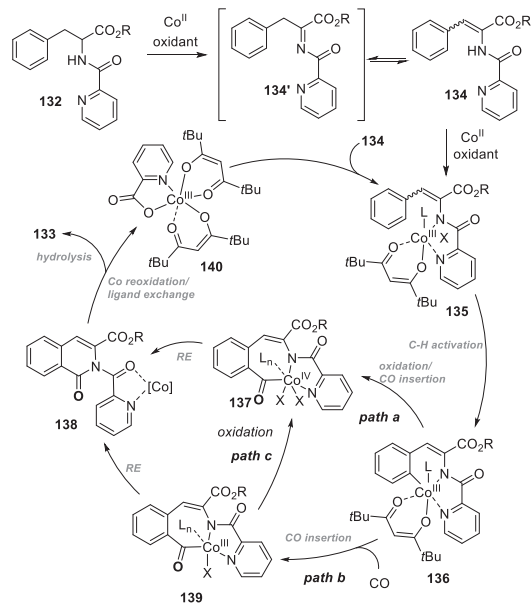
Grigorjeva 2021

CO (1 atm)
Co(dpm)₂ (30 mol%)
PivOH (2 equiv)
Ag₂CO₃ (1.5 equiv)
Mn(OAc)₃·2H₂O (2 equiv)

PhCl, 120 °C, 9-16 h

132 → **133**

Selected examples:

88%   73%   52%

69%   60%, 93% ee
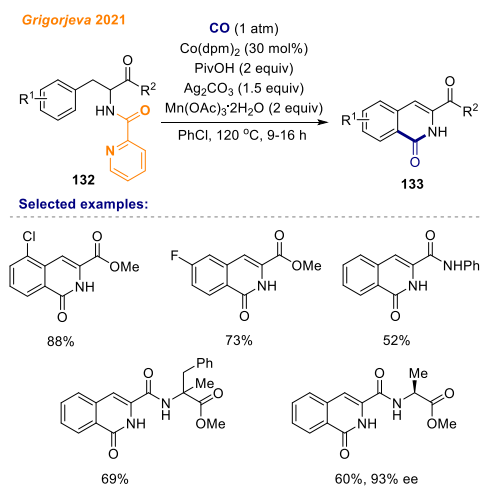
Scheme 48. Co(II)-catalyzed carbonylation of phenylalanines **132**.

showed, that the methodology may be applicable to a late-stage functionalization of short peptides.

Based on the control experiments and literature precedents, authors proposed a plausible reaction mechanism (Scheme 49) [48]. Initially phenylalanine **132** is converted to imine **134′** under oxidative conditions in the presence of Co(II) catalyst. Next, imine **134'** tautomerizes to corresponding enamine **134**, which then coordinates to Co(II) and is oxidized to Co(III) complex **135**, followed by C−H activation to deliver complex **136**. Further three possible pathways could be envisioned. According to path a, Co(III) complex is oxidized to Co(IV), followed by CO coordination and insertion, to give intermediate **137**, that after reductive elimination step forms **138**. Alternatively, formation of **138** could occur via coordination and migratory insertion of CO in complex **139**, followed by reductive elimination (path b). Similarly, path c also could be possible according to which, CO coordination and migratory insertion in complex **116** takes place to furnish intermediate **139**, followed by oxidation to Co(IV) complex **137**. Finally, after hydrolysis of **138,** product **133** is formed and upon oxidation of Co to complex **140**, catalytic cycle is restarted.

3. Conclusions

High valent cobalt-catalyzed C−H bond activation and functionalization represents an attractive strategy for the construction of C−C and C-heteroatom bonds. The use of DGs over the years has become an essential approach for designing new selective transformations via C−H functionalization. The ability to control selectivity enables the practical application of developed synthesis methods. Recently, TDG strategy has branched out as an attractive alternative to classic DG approach, thus potentially providing an advantage from the economical point of view (step and atom-economy). This review has covered the utility of TDG strategy for C−H functionalization using a high valent cobalt catalysis. TDGs like amide, hydrazine, ester, nitroso, oxime etc. have demonstrated

132 → **134'** ⇌ **134**

140   **135**

133   **137**   **136**

138   **139**

path a, path b, path c

C-H activation / oxidation / CO insertion
CO insertion
oxidation
hydrolysis
Co reoxidation/ ligand exchange
RE

Scheme 49. Plausible mechanism for the carbonylation of phenylalanines **132**.

their dual role to serve as a powerful tool for dictation of the C—H activation's step site selectivity while being able to serve as an internal oxidant and reoxidize Co(I) to Co(III) species to regenerate the catalytic cycle. To date, most of the Co(III)-catalyzed TDG directed C—H bond functionalization methods are limited to C(sp^2)-H bond annulation and carbonylation. Besides, cobalt catalyzed C(sp^3)-H bond functionalization using TDG strategy is yet underdeveloped. Exploration of other electrophilic reaction partners maintaining the traceless nature of directing group is highly desirable as it could lead to different synthetic transformations and products. Considering the advantages of TDGs and low cost of cobalt, we believe that further progress in Co-catalyzed C—H functionalization field is expected in the nearest future.

Declaration of competing interest

The authors declare that they have no known competing financial interests or personal relationships that could have appeared to influence the work reported in this paper.

Acknowledgments

References

[1] Selected reviews on TM catalyzed C-H functionalization: a) S. Rej, A. Das, N. Chatani, Coord. Chem. Rev. 431 (2021) 213683;
b) Y. Wu, C. Pi, Y. Wu, X. Cui, Chem. Soc. Rev. 50 (2021) 3677;
c) V. Dwivedi, D. Kalsi, B. Sundararaju, ChemCatChem 11 (2019) 5160;
d) J. He, M. Wasa, K.S.L. Chan, Q. Shao, J.-Q. Yu, Chem. Rev. 117 (2017) 8754;
e) H.M.L. Davies, D. Morton, J. Org. Chem 81 (2016) 343;
f) K. Gao, N. Yoshikai, Acc. Chem. Res. 47 (2014) 1208;
g) T. Gensch, M.N. Hopkinson, F. Glorius, J. Wencel-Delord, Chem. Soc. Rev. 45 (2016) 2900;
h) T. Naveen, Tetrahedron 84 (2021) 132025.
[2] Selected reviews on cobalt-catalyzed C-H functionalization: a) P. Gandeepan, T. Müller, D. Zell, G. Cera, S. Warratz, L. Ackermann, Chem. Rev. 119 (2019) 2192;
b) Y. Kommagalla, N. Chatani, Coord. Chem. Rev. 350 (2017) 117;
c) S.K. Banjare, T. Nanda, B.V. Pati, P. Biswal, P.C. Ravikumar, Chem. Commun. 57 (2021) 3630;
d) L. Lukasevics, L. Grigorjeva, Org. Biomol. Chem. 18 (2020) 7460;
e) S.M. Ujwaldev, N.A. Harry, M.A. Divakar, G. Anilkumar, Catal. Sci. Technol. 8 (2018) 5983.
[3] a) R.J. Phipps, M.J. Gaunt, Science 323 (2009) 1593;
b) Y.-H. Zhang, B.-F. Shi, J.-Q. Yu, J. Am. Chem. Soc. 131 (2009) 5072;
c) S. Lee, H. Lee, K.L. Tan, J. Am. Chem. Soc. 135 (2013) 18778;
d) G. Li, L. Wan, G. Zhang, D. Leow, J. Spangler, Yu, J.-Q. J. Am. Chem. Soc. 137 (2015), 4391;
e) A. Dey, S.K. Sinha, T.K. Achar, D. Maiti, Angew. Chem. Int. Ed. 58 (2019) 10820;
f) D. Maiti, S. Guin, Remote C-H Bond Functionalizations: Methods and Strategies in Organic Synthesis, WILEY-VCH, Weinheim, 2021, p. 438.
[4] C. Sambiagio, D. Schönbauer, R. Blieck, T. Dao-Huy, G. Pototschnig, P. Schaaf, T. Wiesinger, M.F. Zia, J. Wencel-Delord, T. Besset, B.U.W. Maes, M. Schnürch, Chem. Soc. Rev. 47 (2018) 6603.
[5] Selected reviews on C-H functionalization using TDG strategy a) G. Rani, V. Luxami, K. Paul, Chem. Commun. 56 (2020) 12479;
b) A. Zarkadoulas, I. Zgouleta, N.V. Tzouras, G.C. Vougioukalakis, Catalysts 11 (2021) 554;
c) F. Zhang, D.R. Spring, Chem. Soc. Rev. 43 (2014) 6906.
[6] T. Yoshino, H. Ikemoto, S. Matsunaga, M. Kanai, Angew. Chem. Int. Ed. 52 (2013) 2207.
[7] T. Yoshino, S. Matsunaga, Adv. Synth. Catal. 359 (2017) 1245.
[8] H. Ikemoto, T. Yoshino, K. Sakata, S. Matsunaga, M. Kanai, J. Am. Chem. Soc. 136 (2014) 5424.
[9] H. Ikemoto, R. Tanaka, K. Sakata, M. Kanai, T. Yoshino, S. Matsunaga, Angew. Chem. Int. Ed. 56 (2017) 7156.
[10] A. Lerchen, S. Vásquez-Céspedes, F. Glorius, Angew. Chem. Int. Ed. 55 (2016) 3208.
[11] S. Zhou, J. Wang, L. Wang, K. Chen, C. Song, J. Zhu, Org. Lett. 18 (2016) 3806.
[12] L. Kong, X. Yang, X. Zhou, S. Yu, X. Li, Org. Chem. Front. 3 (2016) 813.
[13] N. Barsu, M. Sen, J.R. Premkumar, B. Sundararaju, Chem. Commun. 52 (2016) 1338.
[14] Y. Liang, N. Jiao, Angew. Chem. Int. Ed. 55 (2016) 4035.
[15] H. Wang, M. Moselage, M.J. González, L. Ackermann, ACS Catal. 6 (2016) 2705.
[16] G. Sivakumar, A. Vijeta, M. Jeganmohan, Chem. Eur J. 22 (2016) 5899.
[17] M. Sen, R. Mandal, A. Das, D. Kalsi, B. Sundararaju, Chem. Eur. J. 23 (2017) 17454.
[18] L.N. Chavan, K.K. Gollapelli, R. Chegondi, A.B. Pawar, Org. Lett. 19 (2017) 2186.
[19] A. Dey, A. Rathi, C.M.R. Volla, Asian J. Org. Chem. 7 (2018) 1362.
[20] A. Lerchen, T. Knecht, C.G. Daniliuc, F. Glorius, Angew. Chem. Int. Ed. 55 (2016) 15166.
[21] A. Lerchen, T. Knecht, M. Koy, C.G. Daniliuc, F. Glorius, Chem. Eur J. 23 (2017) 12149.
[22] J.R. Hummel, J.A. Ellman, J. Am. Chem. Soc. 137 (2015) 490.
[23] M. Sen, D. Kalsi, B. Sundararaju, Chem. Eur J. 21 (2015) 15529.
[24] K. Muralirajan, R. Kuppusamy, S. Prakash, C.-H. Cheng, Adv. Synth. Catal. 358 (2016) 774.
[25] F. Wang, H. Wang, Q. Wang, S. Yu, X. Li, Org. Lett. 18 (2016) 1306.
[26] F. Wang, Q. Wang, M. Bao, X. Li, Chin. J. Catal. 37 (2016) 1423.
[27] Y. Yu, Q. Wu, D. Liu, L. Yu, Z. Tan, G. Zhu, Org. Chem. Front. 6 (2019) 3868.
[28] X. Yu, K. Chen, S. Guo, P. Shi, C. Song, J. Zhu, Org. Lett. 19 (2017) 5348.
[29] X. Yu, K. Chen, Q. Wang, W. Zhang, J. Zhu, Org. Chem. Front. 5 (2018) 994.
[30] N. Muniraj, K.R. Prabhu, Org. Lett. 21 (2019) 1068.
[31] Selected reviews a) S. Rej, Y. Ano, N. Chatani, Chem. Rev. 120 (2020) 1788;
b) H. Tang, X.-R. Huang, J. Yao, H. Chen, J. Org. Chem. 80 (2015) 4672.
[32] V.G. Zaitsev, D. Shabashov, O. Daugulis, J. Am. Chem. Soc. 127 (2005) 13154.
[33] L. Grigorjeva, O. Daugulis, Angew. Chem. Int. Ed. 53 (2014) 10209.
[34] Recent examples a) J. Bolsakova, L. Lukasevics, L. Grigorjeva, J. Org. Chem. 85 (2020) 4482;
b) A. Baccalini, S. Vergura, P. Dolui, S. Maiti, S. Dutta, S. Maity, F.F. Khan, G.K. Lahiri, Gi Zanoni, D. Maiti, Org. Lett. 21 (2019) 8842;
c) T.T. Nguyen, LV. Le, H.H. Pham, D.H. Nguyen, N.T.S. Phan, H.V. Le, A.N. Phan, Q. RSC Adv. 11 (2021) 12348;
d) P.A. Zagorska, L. Grigorjeva, J. Bolsakova, Chem. Heterocycl. Compd. 57 (2021) 159;
e) M.-H. Li, X.-J. Si, H. Zhang, D. Yang, J.-L. Niu, M.-P. Song, Org. Lett. 23 (2021) 914.
[35] S. Zhou, M. Wang, L. Wang, K. Chen, J. Wang, C. Song, J. Zhu, Org. Lett. 18 (2016) 5632.
[36] A. Dey, C.M.R. Volla, Org. Lett. 22 (2020) 7480.
[37] P. Gandeepan, P. Rajamalli, C.H. Cheng, Angew. Chem. Int. Ed. 55 (2016) 4308.
[38] S. Qiu, S. Zhai, H. Wang, X. Chen, H. Zhai, Chem. Commun. 55 (2019) 4206.
[39] X.-C. Li, C. Du, H. Zhang, J.-L. Niu, M.-P. Song, Org. Lett. 21 (2019) 2863.
[40] M. Liu, J.-L. Niu, D. Yang, M.-P. Song, J. Org. Chem. 85 (2020) 4067.
[41] C. Kuai, L. Wang, B. Li, Z. Yang, X. Cui, Org. Lett. 19 (2017) 2102.
[42] F. Ling, C. Ai, Y. Lv, W. Zhong, Adv. Synth. Catal. 359 (2017) 3707.
[43] F. Ling, C. Zhang, C. Ai, Y. Lv, W. Zhong, J. Org. Chem. 83 (2018) 5698.
[44] F. Ling, Z. Xie, J. Chen, C. Ai, H. Shen, Z. Wang, X. Yi, W. Zhong, Adv. Synth. Catal. 361 (2019) 3094.
[45] J. Ying, L.-Y. Fu, G. Zhong, X.-F. Wu, Org. Lett. 21 (2019) 5694.
[46] L. Lukasevics, A. Cizikovs, L. Grigorjeva, Org. Lett. 22 (2020) 2720.
[47] Q. Gao, J.-M. Lu, L. Yao, S. Wang, J. Ying, X.-F. Wu, Org. Lett. 23 (2021) 178.
[48] L. Lukasevics, A. Cizikovs, L. Grigorjeva, Org. Lett. 23 (2021) 2748.

Lukasevics, L.; Cizikovs, A.; Grigorjeva, L. Synthesis of 1-Aminoisoquinolines via Cobalt-Catalyzed C(sp^2)-H Bond Imination of Phenylalanine Derivatives. *Submitted manuscript*

Synthesis of 1-Aminoisoquinolines via Cobalt-Catalyzed C(sp²)-H Bond Imination of Phenylalanine Derivatives

Lukass Lukasevics, Aleksandrs Cizikovs, Liene Grigorjeva*

Latvian Institute of Organic Synthesis, Aizkraukles 21, Riga LV-1006, Latvia

Supporting Information Placeholder
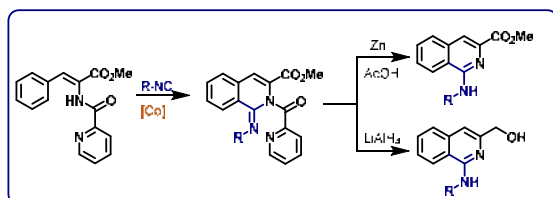
ABSTRACT: Herein we report the first example of cobalt-catalyzed, picolinamide-directed C-H bond imination protocol of phenylalanine derivatives using Co(dpm)₂ as a catalyst. The obtained imine products can easily be transformed to 1-aminoisoquinoline derivatives under reductive conditions, providing an attractive alternative to already existing methodologies. A wide range of functional groups were tolerated under the reaction conditions.

1-Aminoisoquinolines are important class of compounds due to their potential application in medicinal chemistry.[1] For example, 1-aminoisoquinoline fragment is found in various biologically active molecules (Fig 1.), that possess antitumor,[1a,b] antimalarial,[1c] antioxidant[1d] and pain relief[1e-g] activities. Accordingly, the development of novel methodologies for the synthesis of such moiety is of great interest among organic chemists.[2]
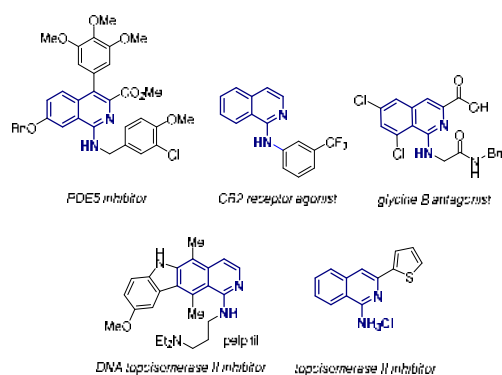

Figure 1. Selected examples of biologically active molecules with 1-aminoisoquinoline skeleton

In the last few decades transition metal-catalyzed direct C-H bond functionalization has served as a valuable tool for the construction of complex molecules from more simple starting materials, mainly due to its atom- and step-economical nature.[3] Nowadays, a great emphasis is placed on green and sustainable chemistry, therefore development of novel methodologies employing simpler, cheaper catalysts is desirable.[4] Third row transition metals (Fe, Co, Ni) have displayed a rapid increase in applicability in C-H bond functionalization reactions, having similar or even better reactivity than precious metal catalysts. In 2014, Daugulis demonstrated that simple Co(II) salts in combination with oxidant and bidentate directing group can be used as Co(III) precatalysts.[5] Since the initial report, the field of Co-catalyzed C-H functionalization has grown tremendously, having a large number of transformations reported based on this approach. Direct C-H functionalization has proven to be very effective approach to obtain 1-aminoisoquinolines in a very step-economical fashion. Several research groups have demonstrated the application of Rh,[6] Ru,[7] Mn[8] catalysts for the C-H/N-H annulation reactions with alkynes or alkenes. Similar methodologies have also been reported using Cp*Co(III) catalysis.[9-12] In 2016, Cheng and co-workers published the first example of Cp*Co(III)-catalyzed C-H/N-H annulation of N'-hydroxybenzimidamides with alkynes (Scheme 1, a)).[9] Over the following years, additional methodologies have been developed for amidine, oxadiazole and azadiazolone substrates by Ackermann,[10] Zhu,[11] Wang[12] (Scheme 1, b-d)). Apart from Ackermann's example, the isoquinoline cycle is constructed via migratory insertion of alkyne or diyne into C-Co bond, followed by reductive elimination step. Recently our group published a methodology for C-H carbonylation of phenylalanine derivatives to obtain isoquinolinones (Scheme 1, e).[13] In our initial report control experiments revealed that formation of carbonylation product occurred via unsaturated enamine intermediate which resulted most likely via SET oxidation of the α-centre on the substrate. As a continuation to our previous study, we extended the C-H

bond functionalization methodology using isocyanides. Although cobalt catalyzed C-H imination is known in arylamine[14] and benzamide[15] substrates, to the best of our knowledge, C-H bond imination of phenylalanine derivatives is unprecedented. Herein we report cobalt-catalyzed C-H bond functionalization of unsaturated phenyl alanine derivatives 1 with isocyanides to obtain products 2.

Scheme 1. 1-Aminoisoquinoline synthesis via cobalt-catalyzed C-H bond functionalization
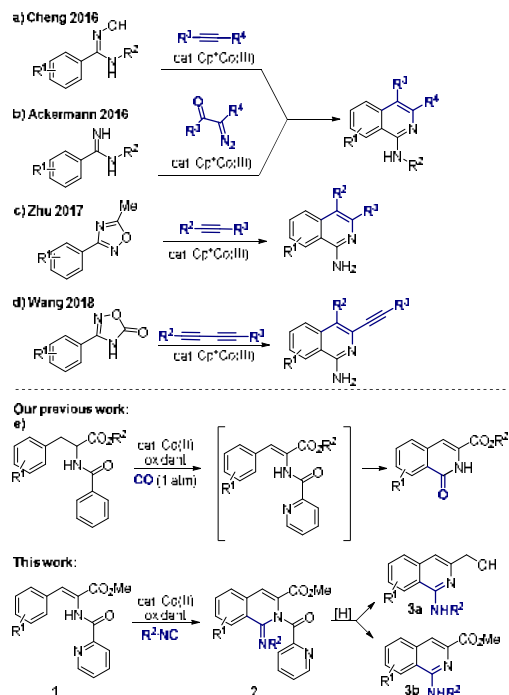
Unsaturated phenylalanine 1aa was chosen as a model substrate for the C-H bond imination with isocyanides. We began optimization of the reaction conditions by employing similar catalytic system that had shown good reactivity in our previous studies.[13] Using Co(dpm)$_2$ catalyst in combination with Ag$_2$CO$_3$ oxidant and NaOPiv additive with 2 equivalents of *t*-butyl isocyanide, we observed the formation of product 2aa in 75% yield (Table 1, entry 1). Oxidant screening showed that Ag^I or Mn^{III} oxidants were less effective, delivering product in significantly lower yield (entries 2, 3). In the control experiments where oxidant or catalyst were excluded, no formation of product 2aa was observed (entries 4, 12). Decreasing the loading of NaOPiv or substitution with LiOPiv or PivOH additives did not improve the product 2aa yield (entries 5-8). Similarly, lowering the catalyst loading or substituting to other Co(II) salts did not prove to be effective (entries 9-11). Other solvents like THF, MeCN, toluene or EtOAc showed good compatibility with the catalytic system, delivering product 2aa in similar or higher yields (entries 13, 15-17). The final reaction conditions were found by the addition of 4Å molecular sieves in THF, delivering the product 2aa in 92% yield.

With the optimized reaction conditions in hand, we next examined the isocyanide scope for C-H bond imination of unsaturated phenylalanine ester derivative 1aa (Scheme 2). Substrate 1aa in C-H bond imination with *t*-butyl isocyanide gave corresponding dihydroisoquinoline 2aa in very good yield - 86%. To show the utility of the developed methodology, we performed reaction upscaling to 1.8 mmol and obtained product 2aa in 72% yield.

Table 1. Optimization of the reaction conditions[a]

entry	changes from the above conditions	yield, (%)[b]
1	None	75
2	oxidant: AgOAc	36
3	oxidant: Mn(OAc)$_3$·2H$_2$O	0
4	oxidant: air	0
5	additive: LiOPiv	57
6	additive: NaOPiv (1.5 equiv)	58
7	additive: PivOH	71
8	without additive	0
9	catalyst: Co(dpm)$_2$ (15 mol%)	58
10	catalyst: Co(acac)$_2$	21
11	catalyst: Co(OAc)$_2$·4H$_2$O	16
12	without catalyst	0
13	solvent: THF	84
14	solvent: THF + 4Å MS	92
15	solvent: MeCN	73
16	solvent: toluene	66
17	solvent: EtOAc	79

[a]Reaction conditions: 1aa (0.1 mmol), *t*BuNC (0.2 mmol, 2.0 equiv), Co(dpm)$_2$ (0.02 mmol, 20 mol%), NaOPiv (0.2 mmol, 2 equiv), Ag$_2$CO$_3$ (0.15 mmol, 1.5 equiv), PhCl (1 mL), 100 °C. [b]NMR yields using triphenylmethane as an internal standard.

Similarly cyclohexyl isocyanide proved to be very reactive and gave the product 2ba in excellent 96% yield. *n*-Pentyl isocyanide and phenylethyl isocyanide were also compatible with the optimized reaction conditions and gave the corresponding products 2ca,da in very good yields – 79% and 80% respectively.

Scheme 2. Isocyanide scope for C(sp^2)-H bond imination of 1aa[a]
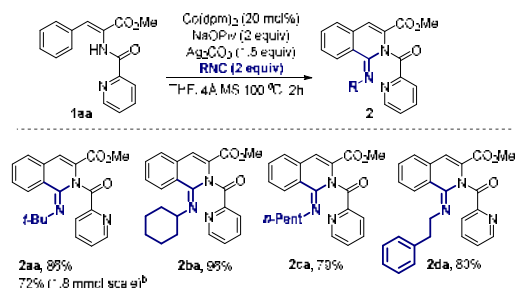
[a]Reaction conditions: 1aa (0.5 mmol), isocyanide (1.0 mmol, 2 equiv), Co(dpm)$_2$ (0.1 mmol, 20 mol%), NaOPiv (1.0 mmol, 2 equiv), Ag$_2$CO$_3$ (0.75 mmol, 1.5 equiv), THF (5 mL), 100 °C, 1.5g 4 Å MS, isolated yields. [b] Reaction time 4h.

Next, we examined the scope for unsaturated phenylalanine esters **1ab-ar** as illustrated in the Scheme 3. Electron donating Me-, OMe-, OAc- and Ar- groups in *ortho*-, *meta*- and *para*-positions were well tolerated and gave products **2ab-ag** in good and very good yields. Interestingly, 4-OAc substituted substrate **1af** underwent transacylation in addition to C-H imination under the reaction conditions and gave 4-OPiv product **2af** in 74% yield. Boc- and Phth-protected amino functional groups were also compatible with the catalytic system, providing products **2ai,aj** in 84% and 83% yields respectively. It should be noted that *meta*-substituted phenylalanine derivatives gave products as a single regioisomers, reacting exclusively in the less sterically hindered *ortho*-position. Various halogen substitution patterns in the benzene ring moiety in phenylalanines **1aj-am** were tolerated under the reaction conditions, furnishing products in 63-65% yields. Substrates containing ether moiety **1an,ao** gave products in good yields – 61% and 66%. Morover, thiophenyl-, naphthyl and furanyl amino acid derivatives reacted smoothly and desired products **2ap,aq,ar** were obtained in acceptable and good yields.

**Scheme 3. Substrate scope for C(sp²)-H bond imination of 1[a]**
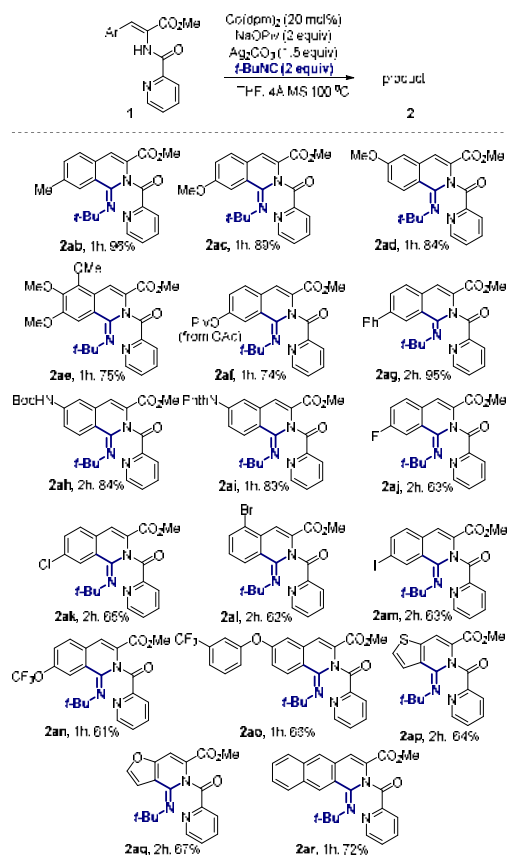
[a]Reaction conditions: **1** (0.5 mmol), *t*-BuNC (1.0 mmol, 2 equiv), Co(dpm)₂ (0.1 mmol, 20 mol%), NaOPiv (1.0 mmol, 2 equiv), Ag₂CO₃ (0.75 mmol, 1.5 equiv), THF (5 mL), 100 °C, 1.5g 4Å MS, isolated yields.

Next, we demonstrated the utility of the obtained products by the synthesis of 1-aminoisoquinolines (Scheme 4). We found that picolinamide can be easily cleaved under reductive conditions by employing LiAlH₄ to obtain product **3a** in excellent yield, although with complete reduction of ester moiety. Alternatively, when Zn/AcOH mixture was used, methyl ester **3b** was obtained in good yield. We were pleased by this result as it demonstrated that our developed protocol enables access to substituted 1-aminoisoquinoline building block in 3 steps from benzaldehydes in a very efficient fashion.[16] In order to gain insight into the reaction mechanism, we performed series of control experiments (Scheme 5.).

Scheme 4. Cleavage of the picolinamide directing group
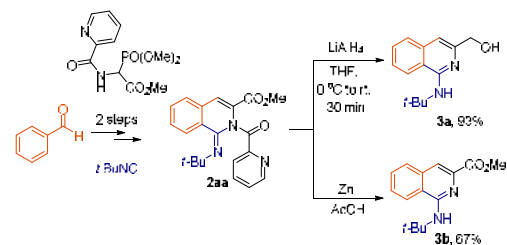
Scheme 5. Control experiments
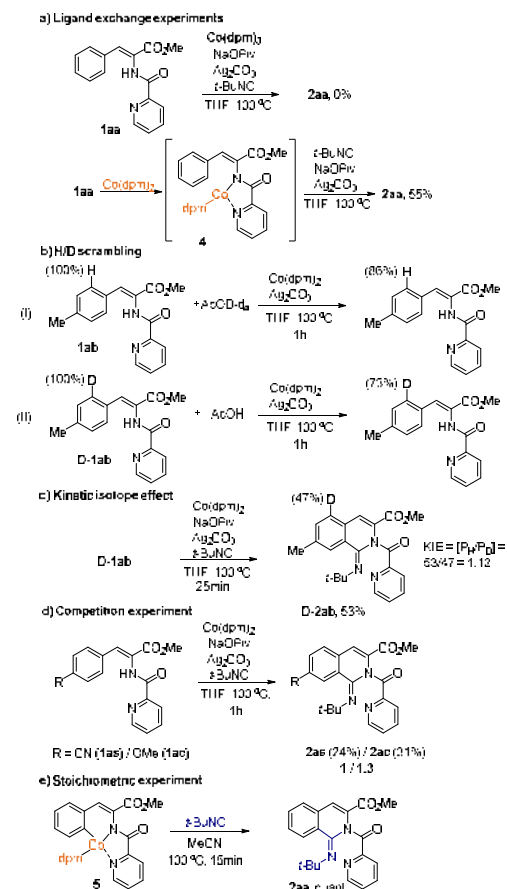
First, unsaturated phenylalanine derivative **1aa** under standard reaction conditions was unreactive if Co(dpm)$_2$ was substituted with Co(dpm)$_3$ (Scheme 5, a)). Such a result indicated that first step of the catalytic cycle is coordination of Co(dpm)$_2$ catalyst to the substrate and not the oxidation of Co(II) to Co(III). This was further supported by a stoichiometric experiment where Co(II)-substrate complex **4** underwent C-H functionalization under reaction conditions and delivered product **2aa** in 55% yield. H/D scrambling experiments were also conducted (Scheme 5, b)). By employing AcOD as a co-solvent, we observed 14% H/D scrambling in the *ortho*-position of the substrate **1ab** under the reaction conditions. Similar result was obtained using D-labeled substrate **D-1ab** and AcOH co-solvent. Additionally, the competition reaction gave KIE value of 1.12 (Scheme 5, c)). The obtained results from H/D scrambling experiments suggested that most likely C-H bond activation step is reversible and not involved in the RDS of the reaction. Further competition experiments, in which equimolar amounts of electron-poor and electron-rich substrates **1as**, **ac** were subjected to the standard reaction conditions in one pot, a slight preference for electron rich substrate **1ac** was observed in a NMR analysis (Scheme 5, d)). Such a result suggests that C-H activation likely occurs via electrophilic pathway.[17] Next, we performed stoichiometric experiment with Co(III)-substrate C-H activation complex **5** (Scheme 5, e)). Interestingly, complex **5** in reaction with *t*-butyl isocyanide in absence of external oxidant underwent C-H functionalization smoothly and gave product **2aa** in quantitative NMR yield, indicating that **5** is a very likely intermediate of the catalytic cycle. Based on the mechanistic considerations and literature precedents, the plausible catalytic cycle is depicted in the Scheme 6. The catalytic cycle is initiated by the coordination of Co(dpm)$_2$ to the substrate, followed by ligand exchange. Co(II) complex **A** is then oxidized by Ag$_2$CO$_3$ furnishing Co(III) complex **B**, which then undergoes C-H activation via S$_E$Ar or BIES mechanism to form complex **C**. Subsequent coordination and migratory insertion of the isocyanide provides iminoyl-Co complex **D**, which reductively eliminates final product **2aa** and Co(I). Alternative pathways involving Co(IV) intermediates are not likely, as the complex **5** was readily converted to the product **2aa** in presence of *t*-butyl isocyanide and absence of external oxidant during the control experiments. Finally Co(I) is reoxidized to Co(II) and returned to the catalytic cycle.

Scheme 6. Plausible reaction mechanism
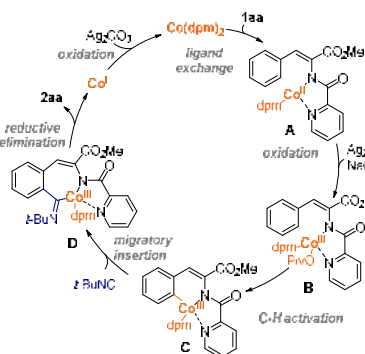
In summary, we have developed the first example of Co-catalyzed C-H imination protocol of phenylalanine derivatives. This novel methodology enables to exploit isocyanides as C1 synthon and obtain substituted 1-aminoisoquinolines providing convenient alternative to already existing synthetic methods. The mild reaction conditions allowed to obtain products in high yields with high selectivity whilst tolerating wide range of functional groups. The mechanistic experiments support electrophilic C-H activation mechanism followed by migratory insertion/reductive elimination as key steps in the formation of the product.

ASSOCIATED CONTENT

The Supporting Information is available free of charge at http://pubs.acs.org.
Experimental procedures and characterization data for all new compounds along with copies of the NMR spectra.

AUTHOR INFORMATION

Corresponding Author

* Liene Grigorjeva - Latvian Institute of Organic Synthesis LV-1006 Riga, Latvia; orcid.org/0000-0003-3497-6776; Email: liene_grigorjeva@osi.lv

Authors

Lukass Lukasevics - Latvian Institute of Organic Synthesis, Riga LV-1006, Latvia
Aleksandrs Cizikovs - Latvian Institute of Organic Synthesis, Riga LV-1006, Latvia

Author Contributions

The manuscript was written through contributions of all authors. All authors have given approval to the final version of the manuscript.

Notes

The authors declare no competing financial interest.

REFERENCES

(1) Selected examples: (a) Smith, A. L.; DeMorin, F. F.; Paras, N. A.; Huang, Q.; Petkus, J. K.; Doherty, E. M.; Nixey, T.; Kim, J. L.; Whittington, D. A.; Epstein, L. F.; Lee, M. R.; Rose, M. J.; Babij, C.; Fernando, M.; Hess, K.; Le, Q.; Beltran, P.; Carnahan, J. *J. Med. Chem.* **2009**, *52* (20), 6189-6192; (b) Kim, K.-E.; Cho, W.-J.; Chang, S.-J.; Yong, C.-S.; Lee, C.-H.; Kim, D.-D. *Int. J. Pharm.* **2001**, *217*, 101-110; (c) Gutteridge, C. E.; Hoffman, M. M.; Bhattacharjee, A. K.; Milhous, W. K.; Gerena, L. *Bioorganic Med. Chem. Lett.* **2011**, *21* (2), 786-789; (d) Ghosh, B.; Antonio, T.; Zhen, J.; Kharkar, P.; Reith, M. E. A.; Dutta, A. K. *J. Med. Chem.* **2010**, *53* (3), 1023-1037; (e) Sakamoto, T.; Koga, Y.; Hikota, M.; Matsuki, K.; Murakami, M.; Kikkawa, K.; Fujishige, K.; Kotera, J.; Omori, K.; Morimoto, H.; Yamada, K. *Bioorganic Med. Chem. Lett.* **2014**, *24* (22), 5175-5180; (f) Prchalová, E.; Hin, N.; Thomas, A. G.; Veeravalli, V.; Ng, J.; Alt, J.; Rais, R.; Rojas, C.; Li, Z.; Hihara, H.; Aoki, M.; Yoshizawa, K.; Nishioka, T.; Suzuki, S.; Kopajtic, T.; Chatrath, S.; Liu, Q.; Dong, X.; Slusher, B. S.; Tsukamoto, T. *J. Med. Chem.* **2019**, *62* (18), 8631-

8641; (g) Saari, R.; Törmä, J. C.; Nevalainen, T. *Bioorg. Med. Chem.* **2011**, *19* (2), 939-950;

(2) Gujjarappa, R.; Vodnala, N.; Malakar, C. C. *Adv. Synth. Catal.* **2020**, *362*, 4896-4990.

(3) Selected reviews: (a) Gandeepan, P.; Müller, T.; Zell, D.; Cera, G.; Warratz, S.; Ackermann, L. *Chem. Rev.* **2019**, *119*, 2192-2452; (b) Moselage, M.; Li, J.; Ackermann, L. *ACS Catal.* **2016**, *6*, 498-525; (c) Kommagalla, Y.; Chatani, N. *Coord. Chem. Rev.* **2017**, *350*, 117-135; (d) Daugulis, O.; Roane, J.; Tran, L. D. *Acc. Chem. Res*. **2015**, *48*, 1053-1064. (e) Hyster, T. K. *Catal. Lett*. **2015**, *145*, 458-467; (f) Lukasevics, L.; Cizikovs, A.; Grigorjeva, L. *Chem. Commun.* **2021**, *57*, 10827-10841.

(4) (a) Dalton, T.; Faber, T.; Glorius, F. *ACS Cent. Sci.*, **2021**, *7*, 245-261; (b) Samanta, R. C.; Meyer, T. H.; Siewert, I.; Ackermann, L. *Chem. Sci.*, **2020**, *11*, 8657-8670.

(5) Grigorjeva, L; Daugulis, O. *Angew. Chem., Int. Ed.* **2014**, *53*, 10209-10212.

(6) (a) Zuo, Y.; He, X.; Yi Ning, Y. W.; Shang, Y. *J. Org. Chem.* **2018**, *83*, 13463-13472; (b) Huang, X.; Xu, Y.; Li, J.; Lai, R.; Luo, Y.; Wang, Q.; Yang, Z.; Wu, Y. *Chin. Chem. Lett.* **2021**, *32* (11), 3518-3521; (c) Yang, Q.; Wu, C.; Zhou, J.; He, G.; Liu, H.; Zhou, Y. *Org. Chem. Front.* **2019**, *6* (3), 393–398; (d) Zheng, G.; Tian, M.; Xu, Y.; Chen, X.; Li, X. *Org. Chem. Front.* **2018**, *5* (*6*), 998-1002; (e) Li, J.; Zhang, Z.; Tang, M.; Zhang, X.; Jin, J. *Org. Lett.* **2016**, *18* (15), 3898-3901; (f) Li, C.; Xu, H. B.; Zhang, J.; Liu, M.; Dong, L. *Org. Biomol. Chem.* **2020**, *18* (7), 1412–1416; (g) Zhou, Y.; Hua, R. *J. Org. Chem.* **2021**, *86* (13), 8862-8872; (h) Wei, X.; Zhao, M.; Du, Z.; Li, X. *Org. Lett.* **2011**, *13* (17), 4636-4639.

(7) (a) Li, J.; John, M.; Ackermann, L. *Chem. Eur. J.* **2014**, *20* (18), 5403–5408; (b) Kaishap, P. P.; Duarah, G.; Chetia, D.; Gogoi, S. *Org. Biomol. Chem.* **2017**, *15* (16), 3491–3498; (c) Wu, C.; Zhou, J.; He, G.; Li, H.; Yang, Q.; Wang, R.; Zhou, Y.; Liu, H. *Org. Chem. Front.* **2019**, *6* (8), 1183-1188.

(8) Li, Y.; Wang, H.; Li, Y.; Li, Y.; Sun, Y.; Xia, C.; Li, Y. *J. Org. Chem.* **2021** *86* (24), 18204-18210.

(9) Muralirajan, K.; Kuppusamy, R.; Prakash, S.; Cheng, C. H. *Adv. Synth. Catal.* **2016**, *358* (5), 774-783.

(10) Li, J.; Tang, M.; Zang, L.; Zhang, X.; Zhang, Z.; Ackermann, L. *Org. Lett.* **2016**, *18* (11), 2742-2745.

(11) Yang, F.; Yu, J.; Liu, Y.; Zhu, J. *Org. Lett.* **2017**, *19* (11), 2885-2888.

(12) Zhang, W.; Li, H.; Wang, L. *Adv. Synth. Catal.* **2019**, *361* (12), 2885-2896.

(13) Lukasevics, L.; Cizikovs, A.; Grigorjeva, L. *Org. Lett.* **2021**, *23* (7), 2748-2753.

(14) Zhu, T. H.; Wang, S. Y.; Tao, Y. Q.; Wei, T. Q.; Ji, S. J. *Org. Lett.* **2014**, *16* (4), 1260-1263.

(15) (a) Gu, Z. Y.; Liu, C. G.; Wang, S. Y.; Ji, S. J. *J. Org. Chem.* **2017**, *82* (4), 2223-2230; (b) Kalsi, D.; Barsu, N.; Dahiya, P.; Sundararaju, B. *Synthesis* **2017**, *49* (17), 3937-3944; (c) Zou, F.; Chen, X.; Hao, W. *Tetrahedron* **2017**, *73* (6), 758-763; (d) Kalsi, D.; Barsu, N.; Sundararaju, B. *Chem. Eur. J.* **2018**, *24* (10), 2360-2364; (e) Chen, J.; Jin, L.; Zhou, J.; Jiang, X.; Yu, C. *Tetrahedron Lett.* **2019**, *60* (31), 2054-2058; (f) Sau, S. C.; Mei, R.; Struwe, J.; Ackermann, L. *ChemSusChem.* **2019**, *12* (13), 3023–3027; (g) Kalsi, D.; Barsu, N.; Sundararaju, B. *Chem. Eur. J.* **2018**, *24* (10), 2360-2364.

(16) See Supporting Information for details.

(17) (a) Tian, C.; Massignan, L.; Meyer, T. H.; Ackermann, L. *Angew. Chem., Int. Ed.* **2018**, *57* (9), 2383-2387; (b) Mei, R; Sauermann, N.; Oliveira, J. C. A.; Ackermann, L. *J. Am. Chem. Soc.* **2018**, *140*, 7913-7921; (c) Zell, D.; Bursch, M.; Müller, V.; Grimme, S.; Ackermann, L. *Angew. Chem., Int. Ed.* **2017**, *56* (35), 10378-10382.

Lukasevics, L.; Grigorjeva, L. Cobalt-Catalyzed Picolinamide-Directed Synthesis of Heterocycles *Targets Heterocycl. Syst. (book series)* **2021**, *25,* 144-161.

COBALT-CATALYZED PICOLINAMIDE-DIRECTED SYNTHESIS OF HETEROCYCLES

Lukass Lukasevics, Liene Grigorjeva*
Latvian Institute of Organic Synthesis, Aizkraukles Street 21, Riga, LV-1006, Latvia
(E-mail: liene_grigorjeva@osi.lv)

Abstract. *Transition metal catalyzed C-H activation and functionalization methodology has made tremendous advancement in the past few decades. Significant progress for C-H bond functionalization has been achieved using second row transition metal catalysts. In the past decade, C-H functionalization using cobalt catalysts have emerged as an attractive alternative due to its low cost and environmentally friendly properties. The replacement of expensive noble metal catalysts with readily available alternatives is beneficial to achieve more sustainable C-H functionalization methods with the application in the synthesis and in the production of relevant chemical compounds. Herein we describe the developed cobalt-catalyzed, picolinamide-directed methods for the synthesis of heterocyclic compounds.*

Contents
1. Introduction
2. C-H functionalization with alkynes
3. C-H functionalization with CO or CO surrogates
4. C-H functionalization with heteroarenes
5. Conclusions
Acknowledgement
References

1. Introduction

In the past few decades, transition metal catalyzed direct functionalization of ubiquitous C-H bonds has experienced outstanding progress. Developed C-H bond functionalization methodology has emerged as an important tool that allows simplification of synthetic schemes, thereby making synthetic pathway more economical and environmentally beneficial.[1] Most of the discovered methods are based on directed C-H activation to achieve regioselective transformation. The directing group used for C-H activation contains a functional group that can coordinate metal centre in the close proximity to the desired C-H bond thus providing highly selective C-H activation. Among the various directing groups used, bidentate directing groups have been demonstrated as one of the most efficient tools for the selective C-H functionalization.[2] The efficiency of bidentate directing groups in C-H activation and functionalization reactions can be explained by the ability to stabilize high-valent transition-metal intermediates. The quinolinamide and picolinamide directing groups were introduced in 2005 by Daugulis group.[3] Later, in 2014, Daugulis group demonstrated that Co(II) salts in combination with bidentate directing group assistance can be exploited as a high valent Co(III) precursors for the C-H activation and functionalization.[4] Cobalt is a highly desirable alternative to noble metals due to its low cost and environmentally friendly properties; therefore, the discovery of the bidentate directing group-assisted high valent cobalt-catalyzed C-H functionalization inspired researchers from other groups to contribute to this area.[5] Using this approach, a number of methods have been developed for the synthesis of diverse relevant heterocyclic targets, e.g. sultams,[6a-c] saccharines,[6d] phthalimides,[6e,f] isoquinolines,[6g] isoquinolones,[6h, i] phosphaquinolones[6j,k] *etc*.

Since the pioneering work by Daugulis,[3] picolinamide directing group has extensively been used for a large diversity of C-H bond functionalization reactions catalyzed by various transition metals.[7] The wide application of the picolinamide directing group is due to the provided *ortho*-selectivity of C-H activation step. Furthermore, picolinoyl group is easy to introduce on an amine-type substrate, as well as after reaction it is easy to remove from the products.[8]

Herein we summarize the developed C-H functionalization methodology for the synthesis of various heterocycles under cobalt-catalysis using picolinamide as directing group.
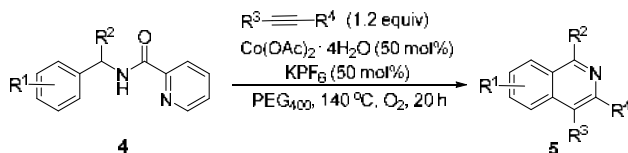
2. C-H functionalization with alkynes

In 2014, Daugulis and Grigorjeva reported the first example of cobalt-catalyzed, picolinamide-directed C-H activation and functionalization (Scheme 1).[4] Although the focus of their research was on the use of 8-aminoquinoline for C-H functionalization of benzamides with alkynes, they additionally demonstrated that picolinamide can be successfully used as a bidentate directing group to achieve selective C-H activation. They showed that 1-methylbenzylamine derived picolinamide **1** in the presence of readily available Co(OAc)$_2$·4H$_2$O catalyst, NaOPiv additive and Mn(OAc)$_2$ oxidant, can be annulated with 2-butyne to yield 1,2-dihydroisoquinoline derivative **2**. The authors demonstrated that the picolinamide directing group could be easily removed under base hydrolysis conditions to afford isoquinoline **3**.
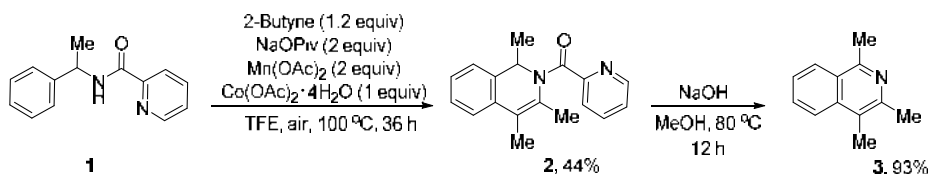

Scheme 1. The first example of cobalt-catalyzed picolinamide-directed C-H functionalization.

Cui and co-workers later, in 2017 expanded the utility of this method and published an extended study for the synthesis of isoquinoline derivatives **5** from benzylamines **4** and terminal or internal alkynes (Scheme 2).[9] In their report Co(OAc)$_2$·4H$_2$O catalyst in combination with KPF$_6$ additive in PEG$_{400}$ were found to be the best catalytic system for successful annulation reaction. Interestingly, the demonstrated methodology displayed picolinamide as a traceless directing group for the first time and gave the reaction products **5**, where the directing group was eliminated in situ. A diverse substitution pattern of benzene ring moiety was tolerated well under the reaction conditions, providing products in moderate to very good yields. In the case of *meta*-substituted benzylamine derivatives **4**, the reaction was generally unselective and yielded isoquinolines **5** as a regioisomer mixtures (ranging from 1:1 to 8:1). Alkyne scope study revealed good compatibility and regioselectivity with both diaryl- and dialkyl-acetylenes as well as terminal alkynes.
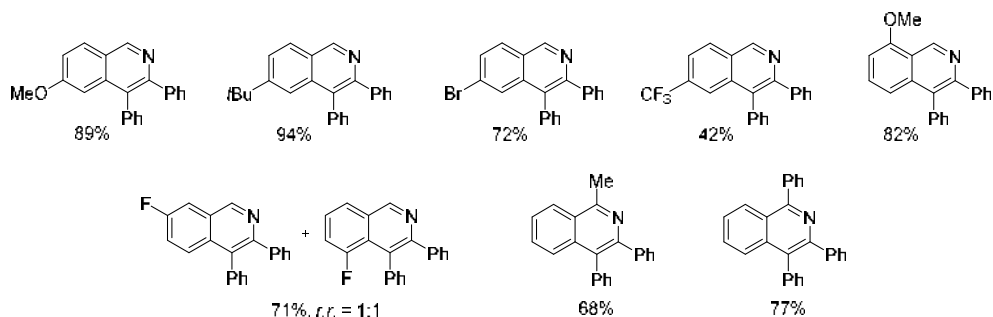
Scheme 2. Annulation reaction of benzylamine derivatives **4** with alkynes.

To gain insight into the reaction mechanism, mechanistic investigations were performed. The KIE (KH/KD) from two parallel reactions was found to be 1.1, indicating that C-H bond activation might not be involved as the rate-determining step. Subsequently, radical scavenger addition to the reaction mixture under standard reaction conditions did not inhibit the reaction, revealing that the radical processes are not involved

in the reaction mechanism. Considering the mechanistic investigations and literature precedents, authors proposed the plausible catalytic cycle (Scheme 3).[9] According the proposed mechanism, the reaction is initiated by the oxidation of Co(II) to Co(III), followed by coordination and ligand exchange with substrate **4** giving cobalt complex **6**. Then C-H bond activation *via* CMD mechanism takes place and intermediate **7** is formed. Subsequent coordination and migratory insertion of alkyne into Co-C bond furnishes complex **8**, which undergoes reductive elimination to give isoquinolinium salt **9**. Next, C-N bond cleavage gives isoquinoline product **5** and Co(I) species which is reoxidized by O_2 and returned into the catalytic cycle.
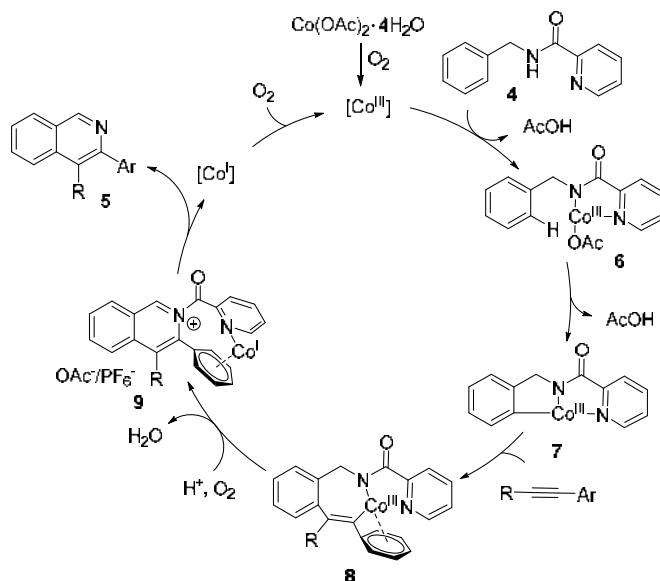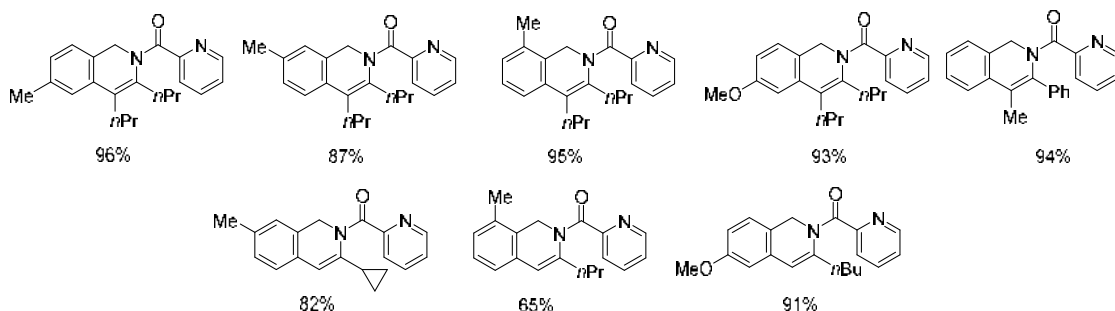

Scheme 3. Plausible reaction mechanism for the synthesis of isoquinolines **5**.

Shortly after, Carretero and co-workers published an approach towards the synthesis of 1,2-dihydroisoquinolines **11** (Scheme 4).[10]
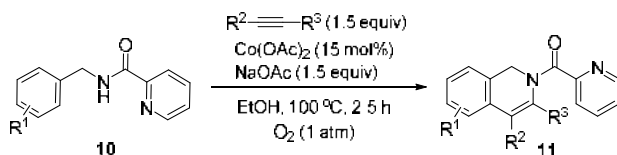

Scheme 4. Synthesis of 1,2-dihydroisoquinolines **11** *via* C-H bond functionalization with alkynes.

In contrast to the method reported by Cui and co-workers, this methodology allowed obtaining 1,2-dihydroisoquinolines **11** in non-traceless fashion, thus avoiding the dehydrogenation of benzylic position. During the optimization studies, authors determined that Co(OAc)$_2$ catalyst, NaOAc additive in ethanol was the best catalytic system where oxygen is used as the sole oxidant. The reaction conditions were mild, and tolerated a large scope of substituents at the benzene moiety. No significant sensitivity to *para*-substituent electronic effects were found, whereas electron-withdrawing substituents at *ortho*-position were less reactive. In the case of *meta*-substituted benzylamine derivatives **10**, activation and functionalization occurred at the more sterically accessible *ortho*-C-H bond, yielding products **11** with excellent regioselectivity. The alkyne scope study showed that reaction was not compatible with diarylacetylenes. Unsymmetrical dialkylacetylenes gave corresponding products **11** with poor regioselectivity. On the other hand, terminal alkyl- and aryl-alkynes displayed excellent regioselectivity and reactivity (Scheme 4).

Furthermore, authors demonstrated that the removal of picolinamide directing group was done efficiently without aromatization of heterocyclic ring under reductive acidic conditions (Scheme 5).[10] The resulting unprotected amine undergoes oxidation by atmospheric O$_2$ to furnish dihydroisoquinoline derivative **12** in excellent yield. The utility of the procedure was demonstrated by subjecting crude reaction product after C-H functionalization to Zn/HCl system to afford products in one pot manner in good and very good yields. On the other hand, commonly used base hydrolysis was also feasible and provided isoquinoline **13** in excellent yield.
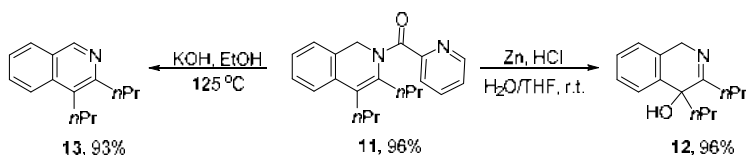
Scheme 5. The cleavage of picolinamide directing group.

Based on mechanistic experiments and literature precedents, authors proposed a simplified plausible catalytic cycle (Scheme 6).[10] Initially, Co(OAc)$_2$ coordination with substrate **10** and concomitant oxidation by O$_2$ forms cobalt complex **14**. Next, C-H bond cobaltation gives five membered cobaltacycle **15**, followed by alkyne coordination and migratory insertion in Co-C bond affording intermediates **17** or **18**. Finally, after reductive elimination 1,2-dihydroisoquinoline **11** is formed, and Co(I) is reoxidized and returned to the catalytic cycle.
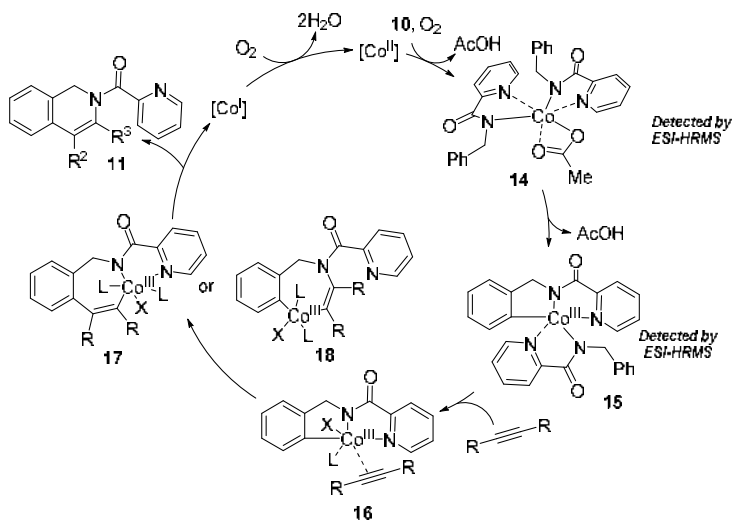
Scheme 6. The plausible reaction mechanism for the formation of isoquinolines **11**.

In 2019, Zhong and co-workers developed a novel *o*-arylaniline **19** C-H bond functionalization protocol to obtain dibenzoazepines **20** (Scheme 7).[11] The optimized reaction conditions included CoCl$_2$ as catalyst, NaOPiv additive, Mn(OAc)$_2$ co-oxidant and O$_2$ as the terminal oxidant. Authors devised a one-pot procedure and treated the crude reaction mixture from C-H bond functionalization step with NaOH in ethanol to cleave the picolinamide directing group. The reaction substrate scope studies revealed that benzene rings with electron rich substituents (Me, SMe, OMe) gave products **20** in better yields than electron poor ones (CF$_3$, F). Regarding the alkyne scope, electronic effect was reversed: electron poor alkynes gave products **20** in better yields than electron rich ones, although the majority of products were obtained in moderate yields. Interestingly, the unsymmetrical diaryl alkynes gave regioisomer mixtures in 1.2:1 ratio. An exception was the alkyne with strongly electron-biased substituents at *para*-position of the arenes (OMe and CF$_3$), providing the product in highly regioselective manner (>20:1). Unfortunately, dialkyl- or alkylaryl-alkynes were unreactive, whereas terminal alkynes turned out to be compatible coupling components and yielded products **20** predominately in moderate yields, albeit with excellent regioselectivity.
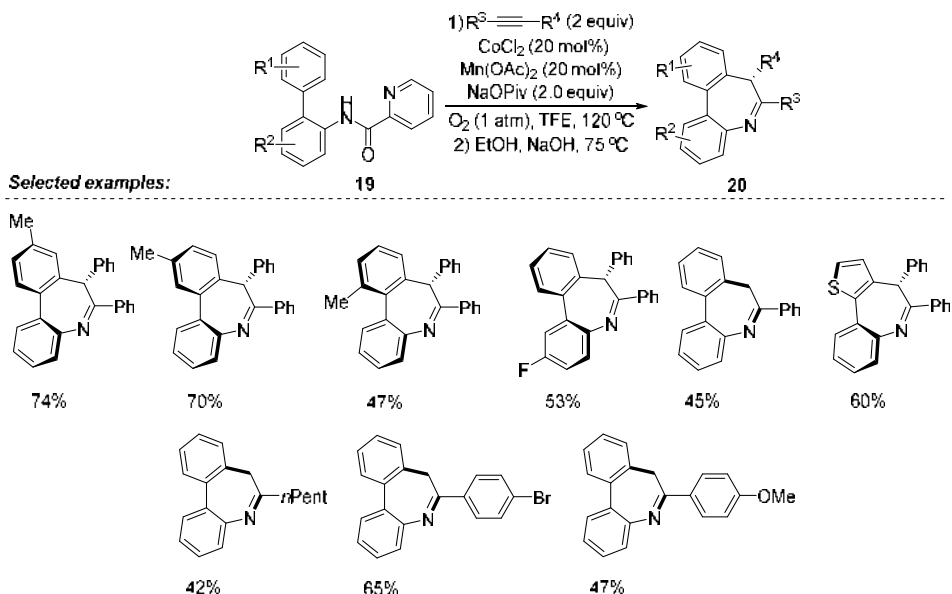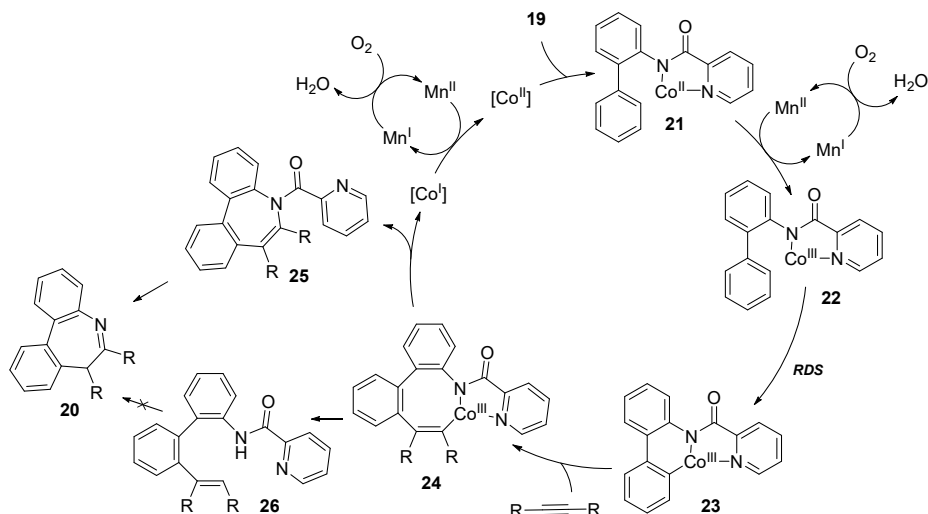

Scheme 7. Synthesis of dibenzoazepines **20** *via* C-H bond functionalization of *o*-arylanilines **19**.

The proposed catalytic cycle (Scheme 8)[11] is based on experimental data and the literature precedents. The reaction is initiated by the coordination of Co(II) to the substrate followed by oxidation with Mn(OAc)$_2$/O$_2$ oxidant system to generate Co(III) complex **22**. Next, cobalt complex **23** forms by C-H cobaltation of **22**, which as suggested by intermolecular KIE experiment is probably the rate-determining step. Besides, the increase of product **20** yield using electron rich substrates also implies that a base-assisted intramolecular electrophilic substitution-type mechanism could be operative within the C-H metalation. Subsequently, alkyne coordination and migratory insertion into Co-C bond gives intermediate **24**, which undergoes reductive elimination to give product **25**. Finally, hydrolysis and tautomerization of the double bond leads to more stable imine form **20**. Alternative pathway from complex **24** to open chain product **26** *via* protodemetalation mechanism followed by cyclization to form **20** was omitted, because the control experiment where **26** was subjected to standard reaction conditions gave no traces of product whatsoever.

Yang and co-workers in 2020 developed an efficient method for the synthesis of benzoquinolines **28** by cobalt catalyzed, picolinamide-directed naphthylamine **27** C-H bond functionalization with alkynes (Scheme 9).[12] The optimized reaction conditions required Co(OAc)$_2$ catalyst, NaOAc additive in xylene at 120 °C for successful transformation. Similarly, to other literature reports, in this transformation no additional external oxidant was necessary, as the atmospheric oxygen was capable to oxidize the cobalt

catalyst. The majority of the alkyne scope was demonstrated using terminal alkynes, only two examples with internal alkynes were shown. The authors found that electron-poor alkynes performed worse than electron-rich, and gave products in low and moderate yields. Influence of the naphthalene substituents showed that electron-donating group (Me) is compatible with the reaction conditions, on the other hand, naphthalene **27** substituted with electron-withdrawing group (NO$_2$) yielded product **28** in only 14% yield.

Scheme 8. Plausible reaction mechanism for the synthesis of dibenzoazepines **20**.
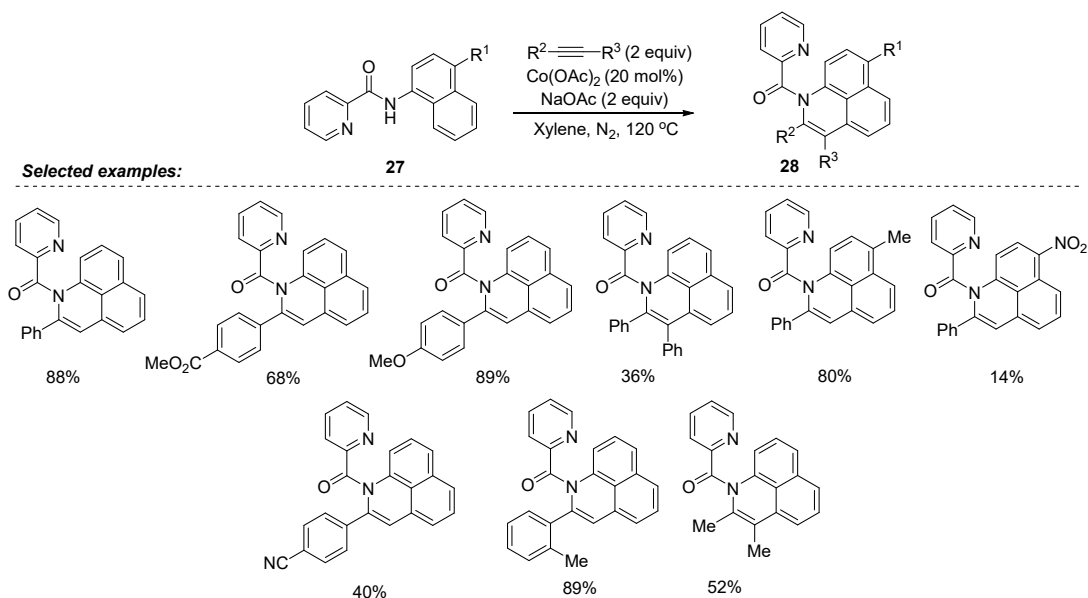
Scheme 9. Cobalt-catalyzed naphthylamine **27** annulation with alkynes.

In the same year, our group reported a cobalt-catalyzed, picolinamide-directed C-H functionalization of phenylglycinols **29** with alkynes to afford 1,2-dihydroisoquinolines **30** (Scheme 10).[13] We found that Co(dpm)$_2$ catalyst, NaOPiv base and Mn(OAc)$_3$·2H$_2$O/O$_2$ oxidant system in methanol at 80 °C is the most appropriate catalytic system for this transformation. Several different alcohol-protecting groups (MOM,

PMB and TBS) were viable and gave reaction products smoothly. In contrast, unprotected alcohol did not result in product formation, most likely due to possible cobalt coordination to oxygen atom thereby deactivating the cobalt catalyst. The reaction conditions are mild, tolerated wide variety of benzene substituents: electron-donor and electron-acceptor groups as well as halogen atoms, giving products mostly in very good yields and with complete regioselectivity towards less hindered *ortho*-C-H bond if *meta*-substituted substrates were used. Alkyne scope studies revealed that both terminal and symmetrical/unsymmetrical internal alkynes with diverse electronic properties were applicable and resulted in corresponding products with predominantly very good yields and excellent regioselectivity. An additional advantage of the developed methodology was the complete retention of original stereochemistry at α-position of substrate that allowed obtaining enantiopure products.
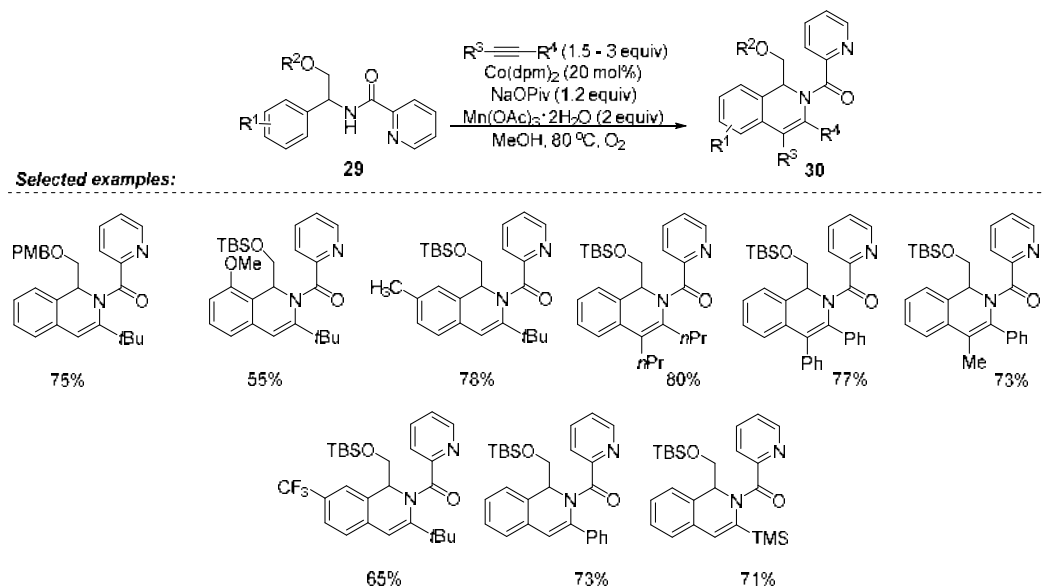
Scheme 10. Cobalt-catalyzed C-H annulation of phenylglycinols **29** with alkynes.

The synthetic utility of this transformation was demonstrated by accessing tetrahydroisoquinoline **33**. The reduction of 1,2-dihydroisoquinoline **31** in presence of Na/NH$_3$ led to the formation of **32** in highly diastereoselective manner. Subsequent directing group cleavage with LiAlH$_4$ gave tetrahydroisoquinoline **33** in very good yield and without enantiopurity loss (Scheme 11).[13]
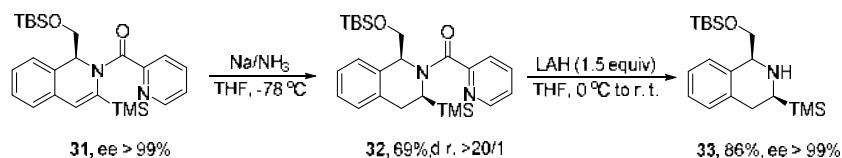
Scheme 11. 1,2-Dihydroquinoline **31** reduction and removal of the picolinamide directing group.

Based on experimental observations and literature precedents, we proposed a plausible catalytic cycle (Scheme 12).[14] Initially, oxidation of the Co(II) catalyst in the presence of phenylglycinol **29** generates Co(III) complex **34**. Subsequent C-H activation step forms cobaltacycle **35**. Next, alkyne coordination and insertion into Co-Ar bond gives intermediate **36**. Finally, reductive elimination step would give reaction product **30** and Co(I) species that after oxidation with Mn(III)/O$_2$ system returns to the catalytic cycle.

In 2020, Qi and co-workers reported the cobalt-catalyzed, picolinamide-directed hydroarylation of naphthylamines **37** with internal alkynes and diynes. Their catalytic system consisted of Co(OAc)$_2$·4H$_2$O

catalyst, KOAc base in TFE at 100 °C under air. This work was mainly focused on open-chain hydroarylation products, however a single example of C-H annulation product was also presented, albeit in a low yield (Scheme 13).[14]
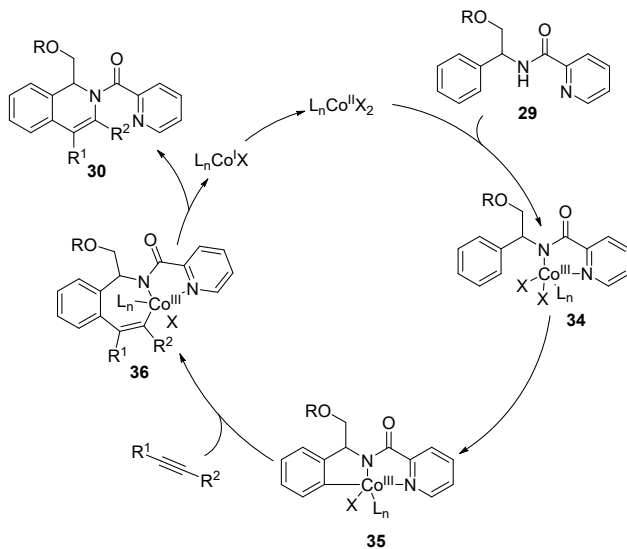
Scheme 12. Plausible mechanism for the annulation of phenylglycinols **29** with alkynes.
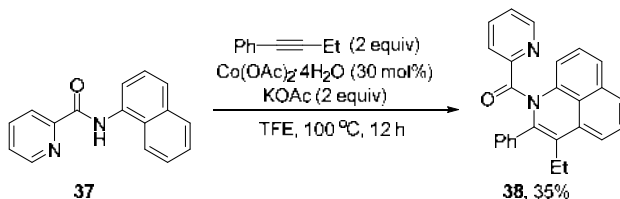
Scheme 13. Annulation of naphthylamine derivative **37**.

Our group continued investigations on cobalt-catalyzed, picolinamide-directed C-H bond functionalization methodology, and in 2021, we reported a study on phenylglycine **39** C-H bond functionalization.[15] Our previous results showed that phenylglycinols **29** were compatible substrates for the annulation reaction with alkynes. We set our goal to transfer the methodology to more challenging substrates: amino acids as a continuation of our research. The optimization studies showed that phenylglycine derivatives **39** are difficult substrates for C-H functionalization, mainly due to their instability under typical reaction conditions and tendency to form ketoesters **41** *via* oxidative cleavage (Scheme 14).[15] We managed to optimize phenylglycine **39** C-H bond annulation with *para*-methoxyphenylacetylene up to 36% yield.
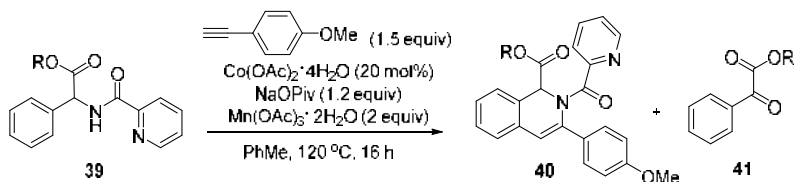
Scheme 14. Cobalt-catalyzed C-H bond annulation of glycine esters **39** with alkynes.

3. C-H functionalization with CO or CO surrogates

In 2017, Zhong and co-workers reported the first example of cobalt-catalyzed, picolinamide-directed carbonylation C(sp^2)-H bond (Scheme 15).[16] Under cobalt catalysis, using picolinamide directing group, benzylamines **42** were transformed into isoindolinone derivatives **43** in a traceless fashion. The developed catalytic system consisted of Co(OAc)$_2$·4H$_2$O catalyst, Ag$_2$CO$_3$ oxidant, PivOH additive and diethyl azodicarboxylate (DEAD) as the carbon monoxide surrogate. These mild reaction conditions provided good compatibility with alkyl, aryl, halogen and alkoxy substituents giving products in good to very good yields and excellent regioselectivity in the case of *meta*-substituted benzylamine derivatives **42**. Additionally, the authors found that developed carbonylation method was scalable up to 2 g. Besides, no loss of enantiopurity was observed when chiral starting materials were used.
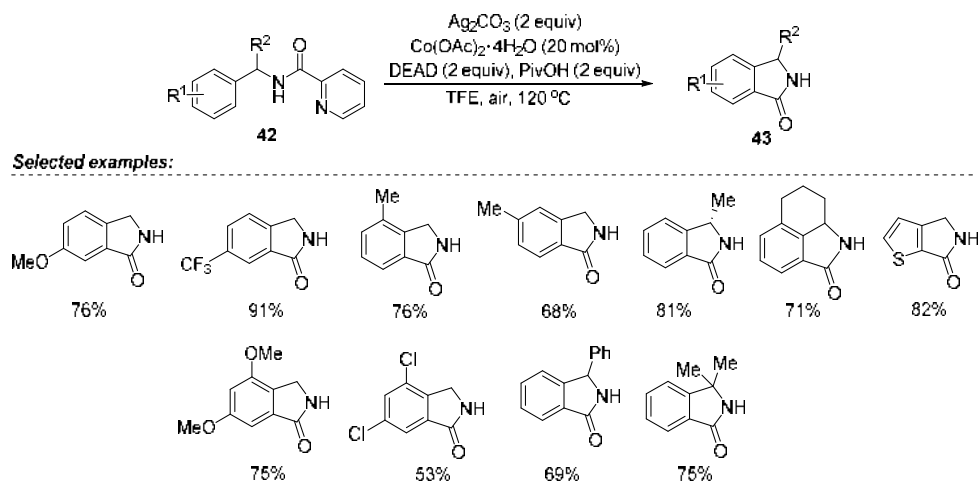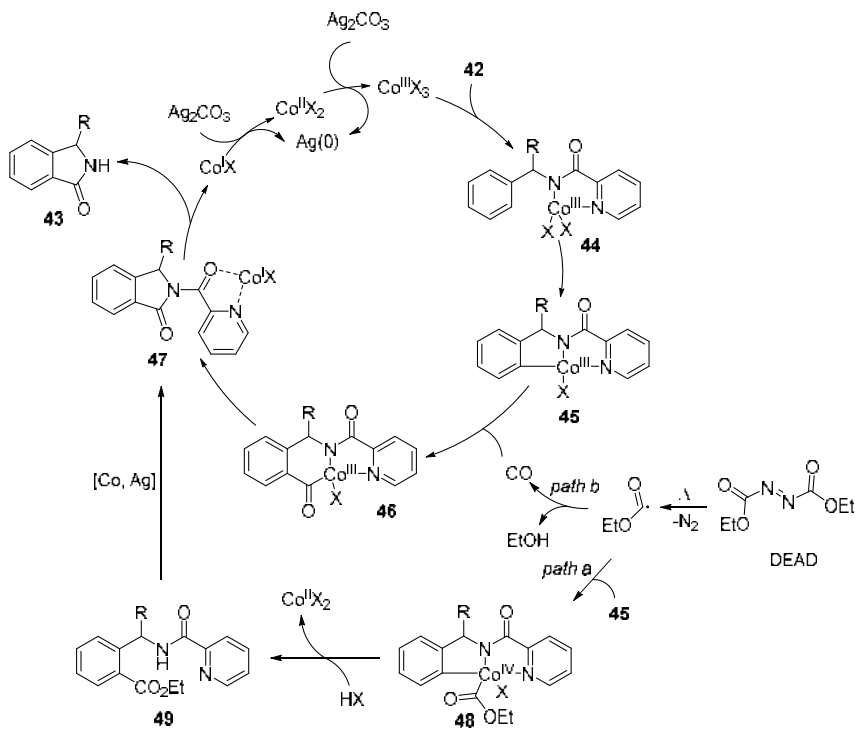

Scheme 15. Benzylamine **42** C(sp)^2-H bond carbonylation.

The plausible catalytic cycle for the carbonylation reaction is provided by the authors and is depicted in Scheme 16.[16] The reaction is initiated by the oxidation of Co(II) to Co(III) species and coordination to the substrate **42** to form complex **44**. Next, C-H cobaltation takes place and forms cobalt complex **45**. According to *path a*, the esteric radical, that is generated in situ from DEAD *via* thermolysis, attack to complex **45**, forming Co(IV) intermediate **48**. Subsequently, reductive elimination and intramolecular cyclization with successive directing group hydrolysis would give product **43** and Co(II) species. According to *path b*, esteric radical generates CO gas, which coordinates and migratory inserts into Co-C bond to give complex **46**. The reductive elimination and directing group cleavage steps would yield the product **43** and Co(I) species, that after oxidation with Ag$_2$CO$_3$ would be released back to the catalytic cycle. The mechanistic studies showed that only 10% of product was obtained if intermediate **49** was subjected to the reaction conditions, suggesting that *path a* is not the major reaction pathway.

Next year, Zhong and co-workers published a new methodology for the synthesis of *N*-unprotected phenanthridinones **51** from arylanilines **50** (Scheme 17).[17] In their study authors employed a traceless picolinamide directing group in combination with CoCl$_2$ catalyst, NaOPiv base and DIAD as a CO source. The use of external oxidants was unnecessary as the O$_2$ was sufficient to maintain the reaction. The developed reaction conditions were mild; therefore, authors offered a broad substrate scope and the majority of selected substrates tolerated reaction conditions extremely well, giving products predominantly in excellent yields and highly regioselective manner. Interestingly, besides benzene, thiophene was also compatible with the reaction conditions and gave product in very high yield.

Based on the control experiments and previous literature data, authors proposed the plausible reaction mechanism, which is depicted in Scheme 18.[17] First, the carbonylation reaction is initiated by the coordination of Co(II) salt with arylaniline **50** to form intermediate **52**. Next, oxidation of complex **52** to Co(III) complex **53** takes place, followed by the C-H activation step to generate cyclic intermediate **54**. The

coordination and migratory insertion of CO, which is released by thermal decomposition of DIAD, results in a cyclic Co(III) intermediate **55**. The reductive elimination results in complex **56**, which contains Co(I) species and is formed *via N,O*-coordination. Further hydrolysis of **56** gives phenanthridinone **51** and releases Co(I) which is oxidized to Co(II) and is returned to catalytic cycle.

Scheme 16. Proposed mechanism for the cobalt-catalyzed carbonylation of benzylamine **42** C-H bond.
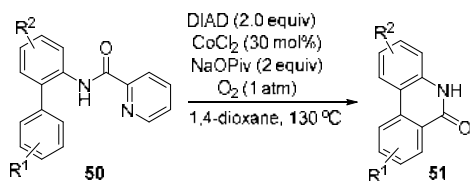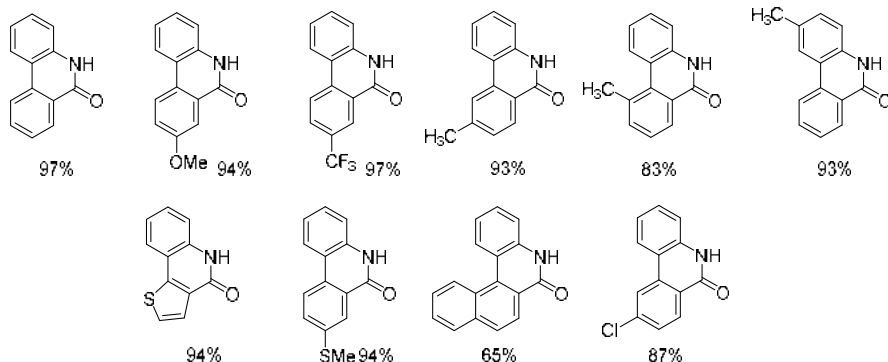
Scheme 17. Cobalt-catalyzed C-H carbonylation of phenanthridinones **50**.

The performed intermolecular competition experiment gave KIE value of $k_H/k_D=1.72$, while obtained KIE value from two parallel reaction was $k_H/k_D=2.24$. These KIE experiments indicated that C-H bond cleavage might occur in a rate-determining step. Besides, from experiments with a radical scavenger addition, authors found, that the esteric radical species, generated from DIAD, most likely are not the active carbonylation species, as addition of TEMPO showed only a slight influence on the reaction yield.
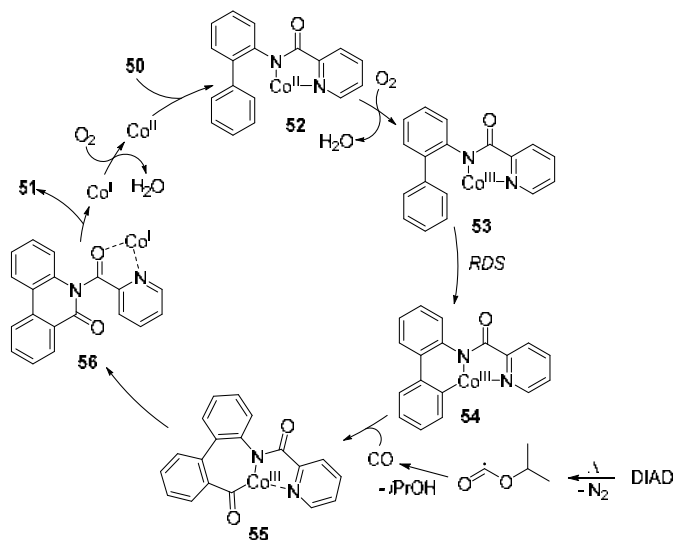
Scheme 18. Plausible reaction mechanism for the C-H bond carbonylation in arylanilines **50**.

In 2019, Wu and co-workers developed a methodology for the synthesis of benzoindolones **58** *via* C-H bond carbonylation of the naphthylamine derivatives **57** (Scheme 19).[18]
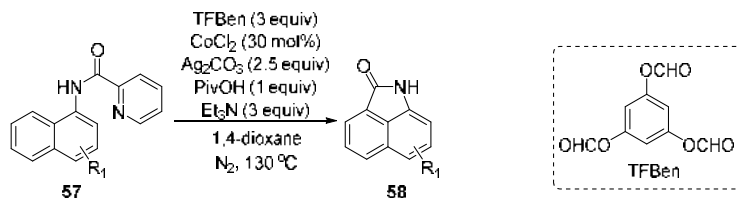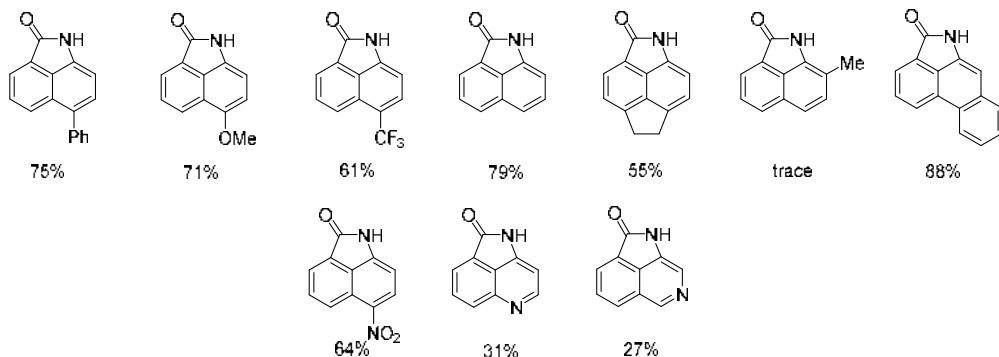
Scheme 19. Cobalt-catalyzed naphthylamine **57** C-H bond carbonylation.

Similarly to other C-H carbonylation reports, in this case picolinamide directing group was used in traceless fashion and was cleaved in situ under the reaction conditions. Benzene-1,3,5-triyl triformate (TFBen) was used as an efficient and solid CO gas surrogate. The authors demonstrated that the substitution pattern at C4 position is rather flexible. A large variety of functional groups: alkyl, aryl, heteroaryl, alkynyl, halogen, esters were well tolerated and gave products in yields ranging from low to very good. The only significant limitation was the lack of substitution at C2 position, in such case, only trace amount of product was detected. This result suggests that the steric effect play a very important role in a substrate design. This methodology is also scalable and can be realized up to 4 mmol of **57**, although 19% drop in yield was observed (Scheme 19).

The proposed plausible catalytic cycle was based on the experimental data and literature precedents (Scheme 20).[18] The catalytic cycle is initiated with the coordination of Co(II) to the substrate **57** followed by an o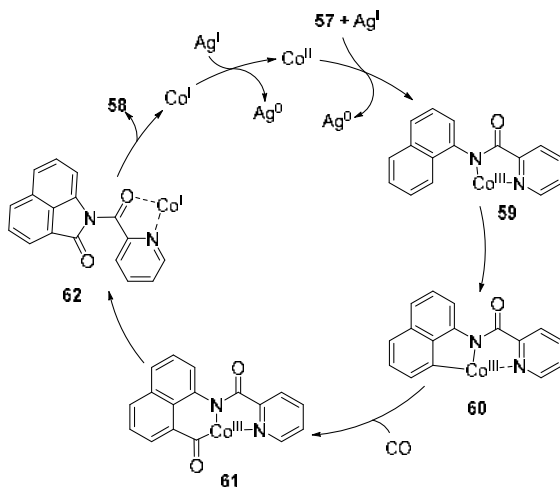xidation with Ag(I) to afford complex **59**. Subsequently, C-H activation step forms cobaltacycle **60**. The CO gas, which is generated in situ from TFBen coordinates and inserts into Co-C bond to give acyl cobalt species **61**. Next, the reductive elimination takes place, followed by the hydrolysis of the directing group in intermediate **62** yielding benzoindolone **58** and returning Co(I) to the catalytic cycle, where it is reoxidized to Co(II). The addition of TEMPO as the radical scavenger under the standard conditions did not affect the product yield, thereby excluding the radical process. Performed KIE experiments indicated that the C-H bond cleavage was not involved in the rate-determining step.

Scheme 20. Plausible catalytic cycle for the C-H bond carbonylation of naphthylamines **57**.

In 2020, we explored C-H bond carbonylation possibilities of amino alcohol derivatives **63**. This substrate design had proven to be effective for C-H bond annulation with alkynes, which we had reported earlier that year. In our work, we developed a catalytic system for the C-H bond carbonylation reaction using picolinamide as a traceless directing group to obtain isoindolinones **64** (Scheme 21).[19] From the perspective of alcohol protecting groups, we found similar reactivity pattern as previously.[13] Thus, TBS, PMB, MOM protecting groups could be used, although TBS group was superior over the others and gave product in higher yield. Unfortunately, unprotected amino alcohol derivatives did not gave corresponding carbonylation product **64**, that we attributed to excessive chelation and deactivation of the cobalt catalyst by an oxygen atom. Reactions using various *ortho-*, *meta-* and *para*-substituents were successful and in majority of cases products were obtained in good and very good yields with excellent regioselectivity in the case of *meta*-substituted amino alcohols **63**. We demonstrated that the reaction conditions are mild and no loss of enantiopurity of product **64** was detected under the reaction conditions. Furthermore, this methodology was transferred to more challenging quaternary and sterically hindered substrates, reactions yielded products in moderate yields, and higher catalyst loading and longer reaction times were required.
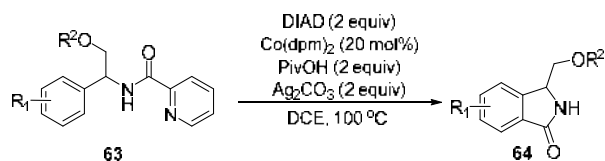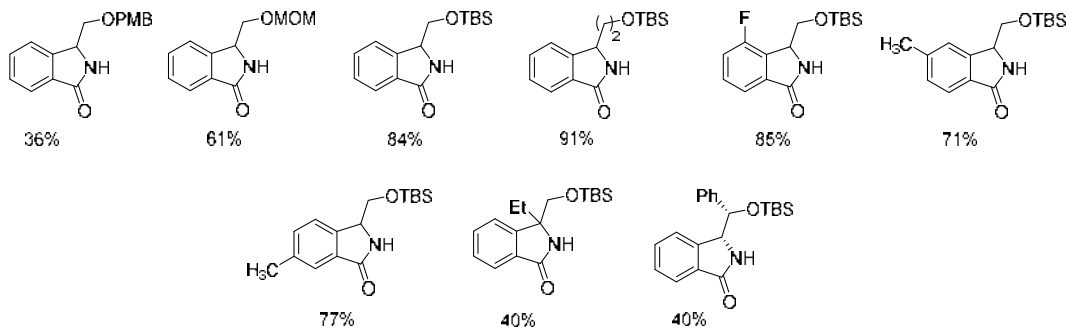
Scheme 21. Cobalt-catalyzed C-H bond carbonylation of amino alcohols **63**.

In 2021, Wu and co-workers reported an approach for the synthesis of free indoloquinoxalinones **66**. Their work involved the use of picolinamide as a traceless directing group for indolylaniline **65** C-H bond carbonylation employing TFBen as CO surrogate (Scheme 22).[20] The optimized reaction conditions tolerated several alkyl, alkoxy, halogen and ester functional groups, and gave corresponding products in moderate to good yields. Introduction of a substituent on the aniline moiety had negative impact on the reaction efficiency, as all of the products were obtained in lower yields and in some cases reaction required higher temperature or prolonged reaction time compared to substrates with non-substituted aniline.
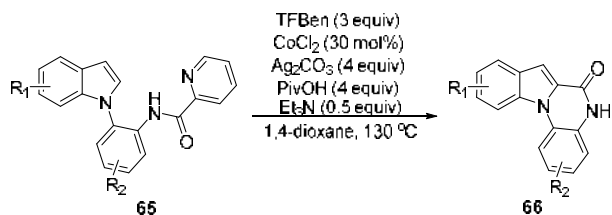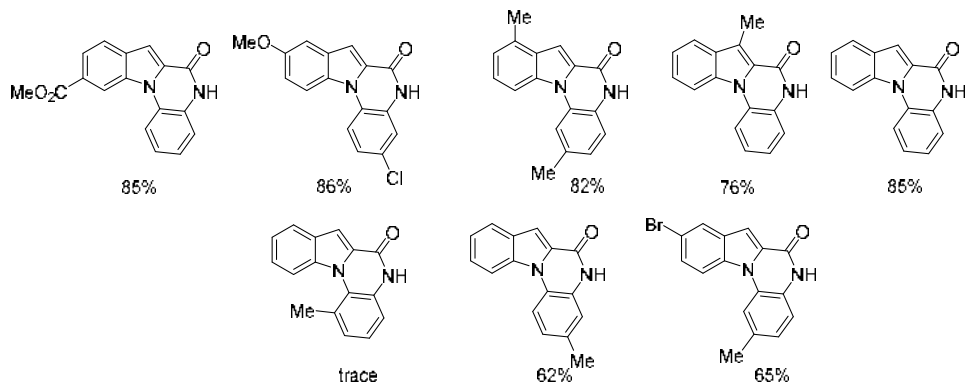
Scheme 22. Cobalt-catalyzed indolylaniline **65** C-H bond carbonylation.

If methyl substituent was introduced at the C6 position of the aniline, only product traces were obtained. The authors suggest that the steric effect of *ortho*-methyl group might interfere with the indole and aniline position in different plane that caused difficulty to form C-N bond. However, a series of indole-substituted substrates **65** were tested for C-H bond carbonylation, providing good reactivity (Scheme 22).

The proposed catalytic cycle for the cobalt-catalyzed synthesis of indoloquinoxalinones **66** is depicted in Scheme 23,[20] and is similar to C-H bond carbonylation of naphthylamines **57**. Initially, the Co(II) catalyst is coordinated to the substrate **65** and oxidized to Co(III) complex **67** by Ag(I) salt. Next, C-H bond activation takes place and forms complex **68**. Further, coordination and migratory insertion of CO, which is generated from TFBen, lead to acyl cobalt complex **69**. After the reductive elimination step, intermediate **70** is formed which then is hydrolysed to give product **66**. The released Co(I) species are reoxidized by Ag(I) and are returned to the catalytic cycle.

Scheme 23. Plausible mechanism for the C-H bond carbonylation of indolylanilines **65**.

Recently, our group demonstrated a novel method for the synthesis of 1,2-dihydroisoquinolinones **72** *via* C-H bond carbonylation of phenylalanine derivatives **71** (Scheme 24).[21] Developed catalytic system included Co(dpm)$_2$ catalyst, PivOH additive and Ag$_2$CO$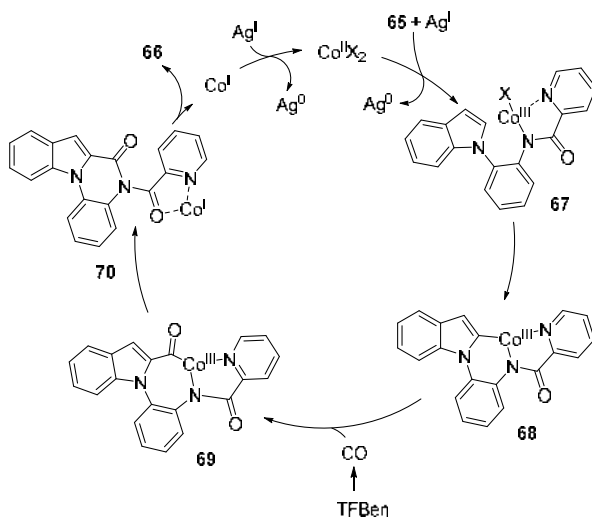_3$/Mn(OAc)$_3$·2H$_2$O oxidant system in chlorobenzene. Diverse functional groups were compatible with the reaction conditions and gave products mostly in good yields. The substrate scope studies showed that both electron-donating and electron-withdrawing substituents at *ortho*-, *meta*- and *para*-positions of the benzene were tolerated well. In the case of *meta*-substituted amino acid derivatives **71**, we obtained products arising from the functionalization of the less hindered C-H bond, even in the case of *meta*-fluoro substituent. Additionally, we demonstrated that our developed catalytic system were successful for the late stage functionalization of short dipeptides and tripeptides, and gave corresponding carbonylation products in acceptable to good yields. Unfortunately, under the reaction conditions partial racemization occurred.

To gain some insights into the reaction mechanism, we performed several control experiments, based on obtained results as well as literature precedents we proposed a plausible reaction mechanism (Scheme 25).[21] According to proposed catalytic cycle, initially phenylalanine **71** is converted to imine **73'** under oxidative conditions in the presence of Co(II) catalyst, which then tautomerizes to corresponding enamine **73**. The control experiments, where the addition of radical scavenger TEMPO significantly suppressed the carbonylation reaction of phenylalanine **71**, but only slightly affected the carbonylation if enamine **73** was used as the starting substrate, indicate that the radical pathway may be involved for the generation of enamine **73**. Next, enamine **73** coordinates to Co(II) and is oxidized to Co(III) complex **74**, followed by the C-H cobaltation to form complex **75**. Further, three possible pathways could be envisioned. According to

path a, Co(III) complex **75** is oxidized to Co(IV), followed by CO coordination and insertion, to give intermediate **76**, that after the reductive elimination step forms **77**.
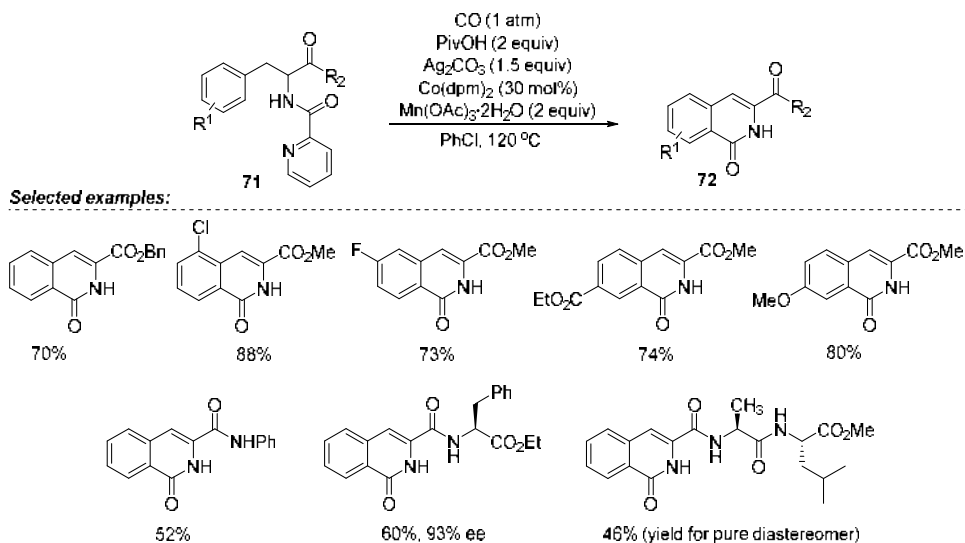
Scheme 24. Cobalt-catalyzed C-H bond carbonylation of phenylalanines **71**.
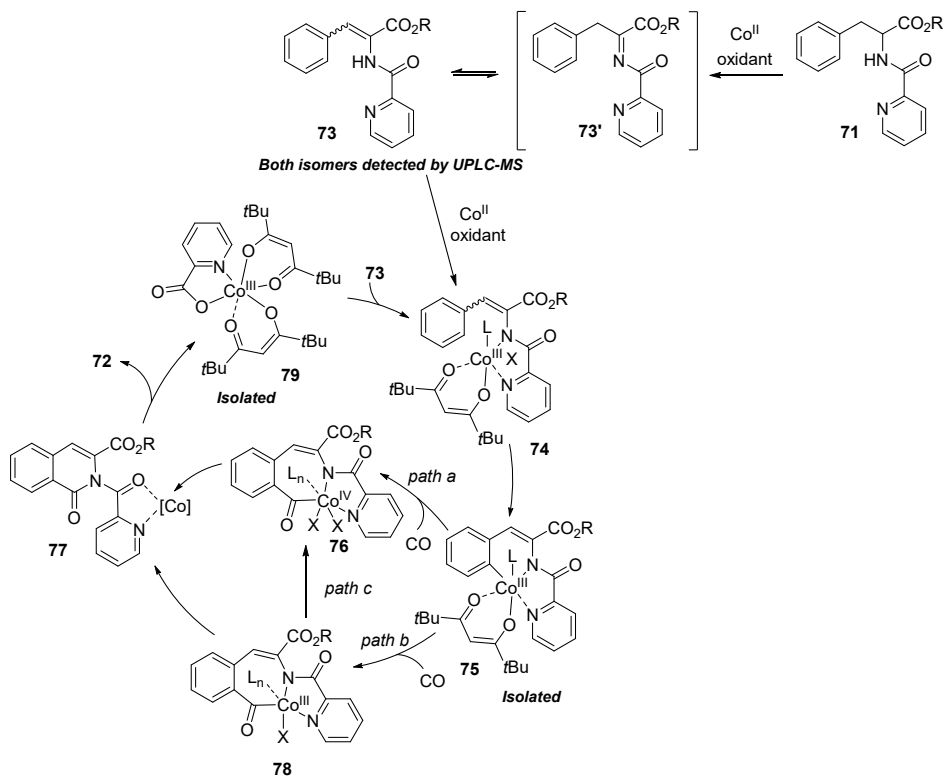
Scheme 25. Plausible mechanism for the C-H bond carbonylation of phenylalanines **71**.

Alternatively, formation of the cobalt intermediate **77** could occur *via* coordination and migratory insertion of CO in complex **75**, followed by the reductive elimination step (*path b*). Similarly, *path c* could also be possible according to which, CO coordination and migratory insertion in complex **75** takes place to furnish Co(III) intermediate **78**, followed by oxidation to Co(IV) complex **76**. Finally, after the hydrolysis of complex **77**, product **72** is formed and cobalt is reoxidized to Co(III) complex **79**, which *via* ligand exchange restarts the catalytic cycle. The performed control experiment, where C-H activation intermediate **75** was transformed into the carbonylation product in absence of external oxidant under CO atmosphere indicated that *path b* might be more favourable over the other pathways (Scheme 25).

4. C-H functionalization with heteroarenes

Wang and co-workers in 2020 reported the only example known so far of cobalt-catalyzed, picolinamide-directed arylaniline **80** C-H bond heteroarylation with heteroarenes **81** (Scheme 26).[22] The presented work provided an efficient access to 2-(2-arylphenyl)azole **82** motifs, which are known to possess antifungal and anti-inflammatory properties. The reported catalytic system consisted of Co(OAc)$_2$ catalyst, Ag$_2$CO$_3$ oxidant and sodium oleate base. The authors examined the generality of the method by testing several substitution patterns in both of arylaniline **80** aromatic moieties as well as substrate scope with the respect to azoles **81**. They found that R^1 substituent at aniline had only a slight effect on the product yield. Regardless of the substituent position or electronic pattern, the majority of products were obtained in moderate yields. However, R^2 substituent at the *ortho*-aryl ring had a greater influence on the substrate **80** reactivity. The use of substrates containing weak electron-withdrawing groups such as 4-F and 4-Cl slightly decreased the product **82** yield compared to unsubstituted substrates, whereas strong electron-withdrawing groups (-CF$_3$, -CO$_2$Me) displayed even poorer reactivity and gave corresponding products **82** in low yields. The less potent substrate reactivity was attributed to the decreased efficiency of the C-H bond activation step. The examination of the azole **81** substituent influence on the reaction yield showed that similarly to R^1 substituents, no significant change in reactivity was observed neither for the position nor for the electronic properties of the functional group. Additionally, the authors showed that benzothiazoles and oxazoles are also competent arylaniline **80** C-H bond functionalization counterparts.
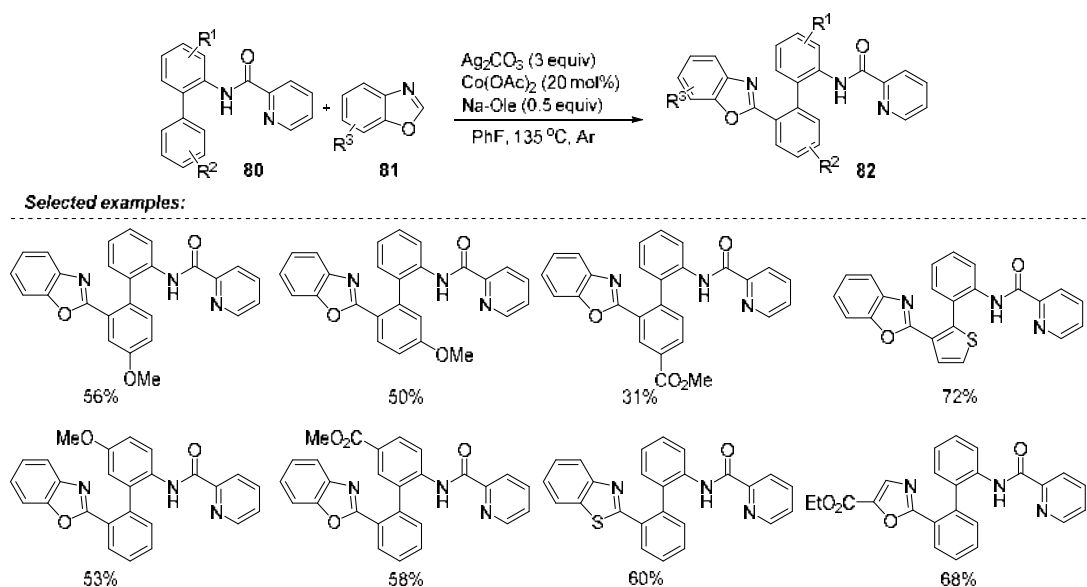
Scheme 26. Cobalt-catalyzed arylaniline **80** C-H bond functionalization with heteroarenes **81**.

On the basis of the conducted control experiments and literature data, authors proposed plausible mechanism for arylaniline **80** C-H bond functionalization with heteroarenes **81** (Scheme 27).[22] According to the proposal, first, Co(II) catalyst coordinates to the substrate, providing complex **83**, which is oxidized by

Ag$_2$CO$_3$ to Co(III) complex **84**. Next, irreversible C-H bond cobaltation takes place *via* base-assisted concerted metalation-deprotonation (CMD) mechanism to obtain cyclic C-H activation intermediate **85**. Subsequently azole **81** is coordinated to the cobalt centre to form intermediate **86**, followed by the reductive elimination to give the desired product **82** and Co(I) species, which are oxidized by Ag$_2$CO$_3$ to Co(II) and returned back to the catalytic cycle.
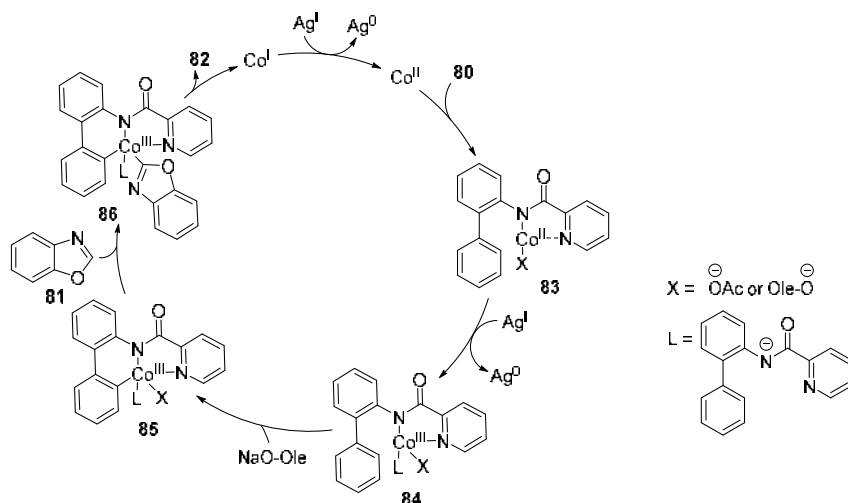
Scheme 27. Plausible mechanism for the arylaniline **80** C-H bond functionalization with heteroarenes **81**.

5. Conclusions

In this chapter, we have summarized the cobalt-catalyzed, picolinamide-directed C-H functionalization methodologies for the synthesis of various heterocyclic targets, which substructures are the key fragments in various natural products or pharmaceutically active compounds. We have compiled the published methods for C-H functionalization with alkynes yielding isoquinolines, 1,2-dihydroisoquinolines, dibenzoazepines and benzoquinolines, as well as C-H bond carbonylation methods to access isoindolinones, phenanthridinones, benzoindolones, indoloquinoxalinones and 1,2-dihydroisoquinolinones, and one C-H bond heteroarylation method, which allowed to obtain 2-(2-arylphenyl)azole derivatives. Results described in this review demonstrate that the bidentate directing group assisted cobalt-catalyzed C-H bond functionalization is a powerful tool for the construction of different types of heterocyclic compounds with the potential application in medicinal chemistry. One of the greatest advantage of the picolinamide directing group is the ability to act in a traceless fashion. Besides the developed methods described, this is still highly active field and many new discoveries might be expected in the nearest future.

Acknowledgements

References

1.	Selected reviews on transition metal-catalyzed C–H functionalization: (a) Lyons, T. W.; Sanford, M. S. *Chem. Rev.* **2010**, *110*, 1147-1169. (b) Ackermann, L. *Chem. Rev.* **2011**, *111*, 1315-1345. (c) Colby, D. A.; Tsai, A. S.; Bergman, R. G.; Ellman, J. A. *Acc. Chem. Res.* **2012**, *45*, 814-825. (d) He, J.; Wasa, M.; Chan, K. S. L.; Shao, Q.; Yu, J.-Q. *Chem. Rev.* **2017**, *117*, 8754-8786. (e) Gensch, T.; Hopkinson, M. N.; Glorius F.; Wencel-Delord, J. *Chem. Soc. Rev.* **2016**, *45*, 2900-2936. (f) Gao, K.; Yoshikai, N. *Acc. Chem. Res.* **2014**, *47*, 1208-1219. (g) Davies, H. M. L.; Morton, D. *J. Org. Chem.* **2016**, *81*, 343-350. (h)

Wu, Y.; Pi, C.; Wu, Y.; Cui, X. *Chem. Soc. Rev.* **2021**, *50*, 3677-3689. (i) Rej, S.; Das, A.; Chatani, N. *Coord. Chem. Rev.* **2021**, *431*, 213683-213719.

2. Rej, S.; Ano, Y.; Chatani, N. *Chem. Rev.* **2020**, *120*, 1788-1887.

3. Zaitsev, V. G.; Shabashov, D.; Daugulis, O. *J. Am. Chem. Soc.* **2005**, *127*, 13154-13155.

4. Grigorjeva, L.; Daugulis, O. *Angew. Chem., Int. Ed.* **2014**, *53*, 10209-10212.

5. Selected reviews on cobalt-catalyzed C–H functionalization: (a) Kommagalla, Y.; Chatani, N. *Coord. Chem. Rev.* **2017**, *350*, 117-135. (b) Gandeepan, P.; Müller, T.; Zell, D.; Cera, G.; Warratz, S.; Ackermann, L. *Chem. Rev.* **2019**, *119*, 2192-2452. (c) Lukasevics, L.; Grigorjeva, L. *Org. Biomol. Chem.* **2020**, *18*, 7460-7466. (d) Ujwaldev, S. M.; Harry, N. A.; Divakar, M. A.; Anilkumar, G. *Catal. Sci. Technol.* **2018**, *8*, 5983-6018. (e) Moselage, M.; Li, J.; Ackermann, L. *ACS Catal.* **2016**, *6*, 498-525. (f) Baccalini, A.; Vergura, S.; Dolui, P.; Zanoni, G.; Maiti, D. *Org. Biomol. Chem.* **2019**, *17*, 10119-10141. (g) Daugulis, O.; Roane, J.; Tran, L. D. *Acc. Chem. Res.* **2015**, *48*, 1053-1064. (h) Yoshikai, N. *Bull. Chem. Soc. Jpn.* **2014**, *87*, 843-857.

6. Selected examples: (a) Planas, O.; Whiteoak, C. J.; Company, A.; Ribas, X. *Adv. Synth. Catal.* **2015**, *357*, 4003-4012. (b) Kalsi, D.; Sundararaju, B. *Org. Lett.* **2015**, *17*, 6118-6121. (c) Cao, Y.; Yuan, Y.; Lin, Y.; Jiang, X.; Weng, Y.; Wang, T.; Bu, F.; Zeng, L.; Lei, A. *Green Chem.* **2020**, *22*, 1548-1552. (d) Nguyen, T. T.; Grigorjeva, L.; Daugulis, O. *Chem. Commun.* **2017**, *53*, 5136-5138. (e) Grigorjeva, L.; Daugulis, O. *Org. Lett.* **2014**, *16*, 4688-4690. (f) Qiu, S.; Zhai, S.; Wang, H.; Tao, C.; Zhao, H.; Zhai, H. *Adv. Synth. Catal.* **2018**, *360*, 3271-3276. (g) Zhou, S.; Wang, M.; Wang, L.; Chen, K.; Wang, J.; Song, C.; Zhu, J. *Org. Lett.* **2016**, *18*, 5632-5635. (h) Grigorjeva, L.; Daugulis, O. *Org. Lett.* **2014**, *16*, 4684-4687. (i) Hao, X. Q.; Du, C.; Zhu, X.; Li, P. X.; Zhang, J. H.; Niu J. L.; Song, M. P. *Org. Lett.* **2016**, *18*, 3610-3613. (j) Nguyen, T. T.; Grigorjeva, L.; Daugulis, O. *ACS Catal.* **2016**, *6*, 551-554. (k) Nallagonda, R.; Thrimurtulu, N.; Volla, C. M. R. *Adv. Synth. Catal.* **2018**, *360*, 255-260.

7. Selected examples for C-H functionalization using picolinamide DG: (a) Nadres, E. T.; Daugulis, O. *J. Am. Chem. Soc.* **2012**, *134*, 7-10. (b) Schreib, B. S.; Carreira, E. M. *J. Am. Chem. Soc.* **2019**, *141*, 8758-8763. (c) Rej, S.; Chatani, N. *ACS Catal.* **2018**, *8*, 6699-6706. (d) Martínez, Á. M.; Rodríguez, N.; Gómez-Arrayás, R. G.; Carretero, J. C. *Chem. Commun.* **2014**, *50*, 2801-2803.

8. (a) Biswas, S.; Bheemireddy, N. R.; Bal, M.; Van Steijvoort, B. F.; Maes, B. U. W. *J. Org. Chem.* **2019**, *84*, 13112-13123. (b) O'Donovan, D. H.; De Fusco, C.; Spring, D. R. *Tetrahedron Lett*. **2016**, *57*, 2962-2964.

9. Kuai, C.; Wang, L.; Li, B.; Yang, Z.; Cui, X. *Org. Lett.* **2017**, *19*, 2102-2105.

10. Martínez, Á. M.; Rodríguez, N.; Gómez-Arrayás, R.; Carretero, J. C. *Chem. Eur. J.* **2017**, *23*, 11669-11676.

11. Ling, F.; Xie, Z.; Chen, J.; Ai, C.; Shen, H.; Wang, Z.; Yi, X.; Zhong, W. *Adv. Synth. Catal.* **2019**, *361*, 3094-3101.

12. Yao, Y.; Lin, Q.; Yang, W.; Yang, W.; Gu, F.; Guo, W.; Yang, D. *Chem. Eur. J.* **2020**, *26*, 5607-5610.

13. Bolsakova, J.; Lukasevics, L.; Grigorjeva, L. *J. Org. Chem.* **2020**, *85*, 4482-4499.

14. Gao, Y.; Zhang, M.; Wang, C.; Yang, Z.; Huang, X.; Feng, R.; Qi, C. *Chem. Commun.* **2020**, *56*, 14231-14234.

15. Zagorska, P. A.; Grigorjeva, L.; Bolsakova, J. *Chem. Heterocycl. Compd.* **2021**, *57*, 159-165.

16. Ling, F.; Ai, C.; Lv, Y.; Zhong. W. *Adv. Synth. Catal.* **2017**, *359*, 3707-3712.

17. Ling, F.; Zhang, C.; Ai, C.; Lv, Y.; Zhong, W. *J. Org. Chem.* **2018**, *83*, 5698-5706.

18. Ying, J.; Fu, L.-Y.; Zhong, G.; Wu, X.-F. *Org. Lett.* **2019**, *21*, 5694-5698.

19. Lukasevics, L.; Cizikovs, A.; Grigorjeva, L. *Org. Lett.* **2020**, *22*, 2720-2723.

20. Gao, Q.; Lu, J.-M.; Yao, L.; Wang, S.; Ying, J.; Wu, X.-F. *Org. Lett.* **2021**, *23*, 178-182.

21. Lukasevics, L.; Cizikovs, A.; Grigorjeva, L. *Org. Lett.* **2021**, *23*, 2748-2753.

22. Wang, X.; Chen, Y.; Song, H.; Liu, Y.; Wang, Q. *Org. Lett.* **2020**, *22*, 9331-9336.

Lukasevics, L.; Grigorjeva, L. Mechanistic studies on cobalt-catalyzed, bidentate chelation-assisted C-H bond functionalization

Handbook of CH-Functionalization.

Mechanistic studies on cobalt-catalyzed, bidentate chelation-assisted C-H bond functionalization

Lukass Lukasevics[a] and Liene Grigorjeva[a]*
[a]Latvian Institute of Organic Synthesis, Aizkraukles 21, LV-1006, Riga, Latvia

Abstract

Over the last decade, cobalt-catalyzed C-H bond functionalization has proven to be a valuable tool for the synthesis of complex molecules. In particular, bidentate chelation-assisted C-H bond functionalization methodology has witnessed tremendous growth in a relatively short time, having numerous novel transformations developed for various substrate groups, utilizing a broad range of directing groups. Despite the progress made in this field, the understanding of mechanistic aspects for the transformations is not very well established as the majority of the proposed mechanisms rely on well-studied mechanistic aspects of precious transition metals. As a consequence, only a few studies actually explain the catalyst's mode of action in depth based on meaningful mechanistic experiments and theoretical calculations. In this chapter, we summarize the current understanding of the mechanisms for cobalt-catalyzed, bidentate chelation-assisted C-H bond functionalization with different coupling partners that are based either on experimental evidence or theoretical calculations.

Keywords
cobalt-catalysis, bidentate chelation, C-H functionalization, transition-metal catalysis, mechanistic study, C-H activation

[A]Introduction

Transition metal-catalyzed reactions in synthetic organic chemistry have seen tremendous growth over the last few decades. Precious transition metals (Pd, Rh, Ru, Ir) have been exploited as a versatile tool for a large variety of functionalization and coupling reactions demonstrating their important role in several applications in organic chemistry. C-H functionalization, in particular, has branched out as important tool for the synthesis of various relevant synthetic targets. Due to the step and atom economy that C-H bond functionalization provides, it can be considered as an attractive alternative to standard coupling reactions which often require pre-functionalization of starting materials (borylation, halogenation etc.). Third row transition metals (Fe, Co, Ni) have displayed a rapid increase in applicability in C-H bond functionalization reactions, having similar or even better reactivity than precious transition metal catalysts.[1] In particular, simple cobalt salts in combination with a directing group and oxidant, have shown a great potential in C-H bond functionalization methodologies, such as C-C, C-N, C-S or C-halogen bond forming reactions. Cobalt-catalyzed C-H functionalization dates back to 1955, when Murahashi reported the first example of cobalt-catalyzed C-H carbonylation of Shiff bases using Co_2CO_8 catalyst under CO atmosphere.[2] This work was followed by a long dormant period and only few examples were reported until 2010, when cobalt began to resurface as a potentially cost-effective catalyst and only during the past decade has truly become a hot topic and area of research among synthetic chemists.

Since the rediscovery of the usefulness of cobalt catalysis in C-H bond functionalization field, majority of the results were achieved using low-valent cobalt catalysts

by Yoshikai and co-workers where the active catalyst Co(0) or Co(I) species were generated *in situ* under reductive conditions.[3] In 2013 Matsunaga and Kanai reported a high-valent cobalt catalysis by developing Cp*Co(III) catalysts which, by an analogy to Rh or Ru catalysts, could perform in directed C-H bond functionalization reactions very well.[4] In 2014 Daugulis and co-worker published a novel approach towards generating high-valent Co(III) species *in situ* from simple Co(II) salts in combination with bidentate directing group assistance under oxidative conditions.[5]

1. General mechanisms for the C-H bond functionalization

Over time, the general idea of operative mechanisms in cobalt-catalyzed C-H bond functionalization has been gathered via direct or indirect evidence. Several reports for operating mechanisms of low-valent cobalt as well as Cp*Co(III) catalysts have been reported [6,7], so here we only cover the mechanistic aspects of high-valent cobalt catalysis where active Co(III) catalyst is generated *in situ* from Co(II) salts under oxidative conditions in the presence of a directing group. In the Figure 1.1, the general mechanism for C-H functionalization is depicted. It is believed to consist of 4 elementary steps:

1) Oxidation/coordination of cobalt catalyst to the directing group of substrate;
2) C-H bond activation;
3) C-H bond functionalization.
4) Re-oxidation and returning Co species to the catalytic cycle.
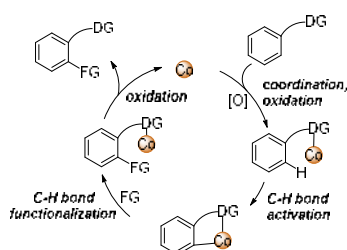
Figure 1.1 General mechanism for cobalt-catalyzed C-H functionalization

1.1. Coordination/oxidation

For the first step of catalytic cycle two pathways are plausible. On the one hand, the catalytic cycle could be initiated by the coordination of Co(II) pre-catalyst to the substrate molecule forming a Co(II) complex, followed by the oxidation of metal centre forming a Co(III) complex from which C-H activation could take place (Figure 1.2, path a). On the other hand, the Co(II) pre-catalyst could be oxidized directly to Co(III) before the coordination to substrate (Figure 1.2, path b). Both of these pathways could be competing and may happen either simultaneously or separately depending on the reaction conditions. Further in this chapter, we review examples of experimental evidence that support either of these pathways.
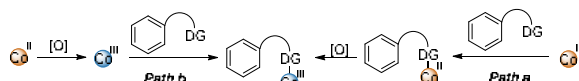
Figure 1.2 Plausible scenarios in coordination/oxidations step

In 2016, Maiti and co-workers reported a methodology for the C-H bond allylation of benzamides **1** with olefins **2** to obtain allyl benzamides **3** (Figure 1.3). In the reported work, the authors used Co(OAc)$_2$•4H$_2$O catalyst in the presence of Ag$_2$SO$_4$, Na$_2$CO$_3$ and 8-aminoquinoline directing group. As a part of their mechanistic investigation, authors determined the reaction order with the respect to the catalyst by monitoring the reaction profile with different catalyst loading using GC-MS analysis and an internal standard. The obtained data showed the reaction order of 0.5 for the Co(OAc)$_2$ catalyst. Such a result suggested that in the early stage of the reaction disproportionation of two Co(II) species is likely and would lead to the formation of Co(III) and Co(I). The presence of Ag(I) salt facilitates the oxidation of Co(I) to the active Co(III) catalyst. Subsequently, coordination to substrate **1** and C-H bond activation would take place.[7]
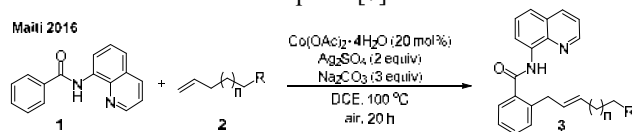
Figure 1.3 Allylation of benzamides **1**

In 2016, Ribas and co-workers described the preparation and characterization of Ar-Co(III) complexes, that could be used for the mechanism study of annulation of macrocyclic arenes with alkynes (Figure 1.4). In their study stochiometric amount of Co(II) salts reacted with macrocycle **4** in the presence of air. The authors found that ligand exchange could easily be achieved at room temperature in TFE to obtain Ar-Co(II) **5** complexes. By increasing the reaction temperature, the complexes **5** reacted further to form organometallic Ar-Co(III) complexes **7**. Performing the reaction under an inert atmosphere completely inhibited the reaction, when starting from Co(II) complexes **5**. However if the reaction was performed under an inert atmosphere in the presence of an external oxidant (i.e. Ag(I) salts), Ar-Co(III) complexes **7** formed, as evidenced by HRMS. When Co(acac)$_3$ was used instead of Co(OAc)$_2$, Ar-Co(III) organometallic complexes **7** formed as a major product. Further reaction of these complexes **7** with alkynes yielded annulation products **8** and **9**. These observations indicated that the Co(II) catalyst most likely first coordinated to form Co(II) complex **5**, then oxidized to a highly electrophilic 16e$^-$ Co(III) complex **6** which underwent rapid C-H bond activation.[8]
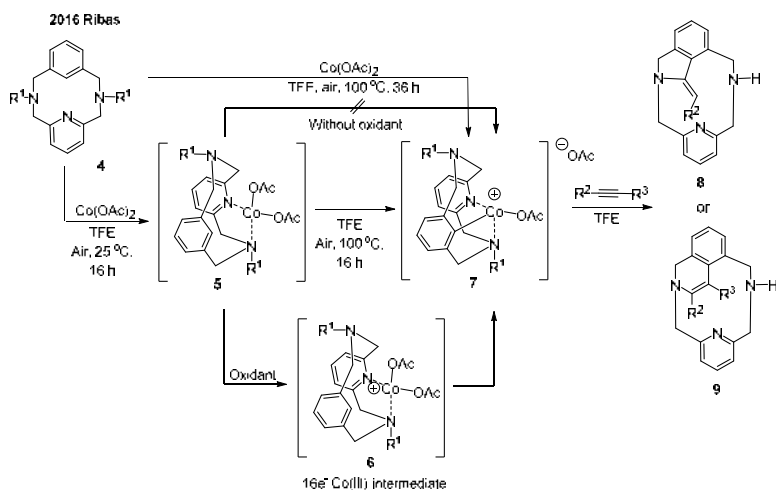
Figure 1.4 Synthesis of Ar-Co(III) complexes **7** via C-H activation of macrocycles **4**

In 2017 Sundaraju[9], Gaunt[10] and Lei[11] independently developed a methodology for C(sp^3)-H carbonylation of pivaloylamides **10** to obtain succinimides **11** using carbon monoxide as the carbonyl source (Figure 1.5). The developed catalytic systems were similar, and in all cases Co(acac)$_2$ was used as the catalyst and Ag$_2$CO$_3$ as the oxidant. As a part of the study, Sundararaju and co-workers performed several control experiments to gain insight into reaction mechanism. To probe the oxidation of cobalt species in the reaction media, the authors monitored the progress of the reaction with stochiometric loading of the catalyst using UV-Vis spectrometry. The analysis of the results showed that conversion of Co(II) to Co(III) could be achieved in 2 h. Thus, the authors concluded that the first step of the catalytic cycle is oxidation of Co(II) catalyst followed by coordination to the substrate **10**. Different results were obtained by Lei and co-workers. During their mechanistic investigations, the authors monitored the oxidation of and Co(acac)$_2$ by Ag$_2$CO$_3$ using XAS spectroscopy. The analysis of spectra revealed that the direct reaction between Co(II) and Ag(I) generated the mixture of Co(II) and Co(III) species, whereas oxidation of Co(II) by Ag(I) in presence of substrate **10** occurred more rapidly. Based on this result, the authors concluded that Co(III) catalyst is more likely to be generated via oxidation of coordinated Co(II) species rather than simple Co(acac)$_2$ complex.
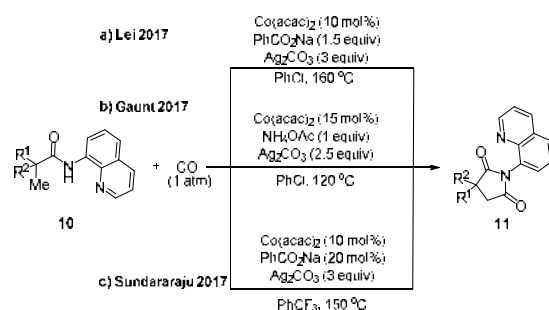
Figure 1.5 Carbonylation of pivaloylamides **10**

In 2018, Lei and co-workers reported the cobalt-catalyzed electrochemical C-H bond annulation of benzamides **1** with ethylene or ethyne (Figure 1.6) to obtain products **12**. To explore the reaction mechanism the authors performed cyclic voltammetry experiments. The results revealed that the substrate **1** and Co(acac)$_2$ alone have higher oxidation potentials than the mixture of substrate **1** and Co(acac)$_2$, suggesting that Co(III) species are generated predominantly via anodic oxidation of coordinated Co(II) complex.[12]
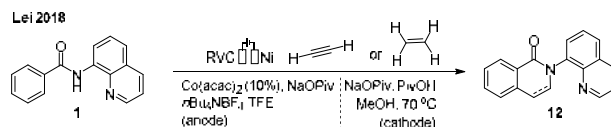
Figure 1.6 Electrochemical C-H annulation of benzamides **1** with ethylene or ethyne

Interestingly, one year later, the Ackermann group reported an electrochemical procedure for the C-H bond acyloxylation of benzamides **1a** with benzoic acid **13** and obtained different results (Figure 1.7). Cyclic voltammetry showed that the oxidation potential of the Co(II) catalyst is lower than that of substrate **1a** as well as the mixture of

substrate **1a** and Co(II), suggesting that Co(II) is oxidized to Co(III) before the coordination with substrate.[13]
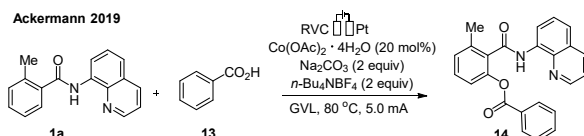
Figure 1.7 Electrochemical acyloxylation of benzamide **1a**

The same year, Ackerman and co-workers published a methodology for the cobalt-catalyzed C-H bond annulation of hydrazines **15** with allenes **16** to obtain products **17** (Figure 1.8). The mechanistic investigation study by a means of cyclic voltammetry revealed similar analytical results as Lei's report in 2018, oxidation potentials of substrate **15** and Co(OAc)$_2$ alone are considerably higher than the mixture of both, suggesting the oxidation of Co(II) to Co(III) occurs in coordinated complex.[14]
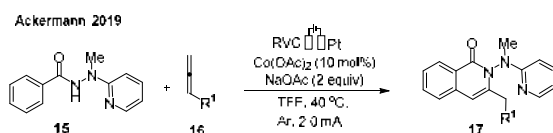
Figure 1.8 Electrochemical annulation of hydrazines **15** with allenes **16**

Thus far the evidence for the first step of the C-H bond functionalization mechanism supports both pathways, firstly coordination of Co(II) catalyst to the substrate followed by oxidation or vice versa. These processes are competitive and occur simultaneously. Based on the contradictory evidence in the variety of transformations, it seems that if one pathway is favoured over another, there is no clear indication why it happens, and most probably depends on variety of factors like catalyst, directing group, oxidant used, reaction temperature, etc.

[B]1.2. C-H bond Activation

Over the last decades many experimental efforts have been made to gain an understanding on the process of C-H bond activation.[6] Some of these mechanistic proposals are well established and some are introduced recently to the field. For high-valent cobalt catalysis several mechanisms are generally accepted (figure 1.9):

- ***Electrophilic aromatic substitution (S$_E$Ar)***. The Lewis acidic nature of cobalt enables it to coordinate to the electrons of π-system in arenes and subsequently make C-Co bond. This leads to the formation of positively charged Wheland intermediate and increases the acidity of C-H bond. These acidic intermediates could donate protons to the solvent or weak bases present in the reaction mixture to re-establish the aromaticity of the arene.[15]
- ***Base-assisted intramolecular electrophilic substitution (BIES)***. Generally, this reaction mechanism is very similar to S$_E$Ar, except the base location in the coordination sphere of the metal.[15]
- ***Concerted metalation deprotonation (CMD).*** This mechanism involves an approach of the cobalt catalyst to the close proximity of C-H bond usually with assistance of directing group. The metal coordination sphere contains Brønsted base which assists

with the deprotonation of the target C-H bond at the same time as C-Co bond is formed.[15]

- **_Single electron transfer (SET)_**. This mechanism does not involve direct formation of the Co-C bond and is devised into several processes: 1) Formation of cation radical from arene and Co(III); 2) Nucleophilic attack on cation radical by external nucleophile; 3) subsequent SET oxidation of arene; 4) re-aromatization.[15]
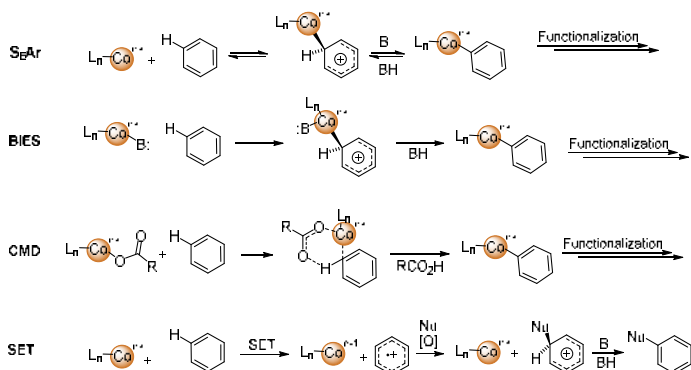
Figure 1.9 General mechanisms for the high-valent cobalt-catalyzed C-H bond activation

During mechanistic investigations, there are several control experiments one can perform to gain insight into the catalyst's mode of action in the terms of C-H activation, although often it is not an easy task. Typically key control experiments to distinguish between these reaction mechanisms are:

- _Kinetic isotope effect (KIE)_ provides the information about rate-determining step (RDS) of the catalytic cycle, based on the mass difference of hydrogen isotopes ^{1}H and ^{2}H. The mass difference makes the rate at which C-H bond is cleaved, vary if the C-H bond activation step is rate determining. The KIE can be determined both in parallel reactions and in competition experiments (Figure 1.10) and evaluated as a ratio of the kinetic constants of the deuterated and non-deuterated substrates (in parallel reactions KIE = K_H/K_D) or the relative quantities of the products formed (in competing reactions KIE = [P_H/P_D]).[16] Lack of KIE in C-H bond functionalization reactions (KIE = 1) indicates that the C-H bond activation step is not rate-determining and is usually associated with SET mechanism. On the other hand, large KIE value (KIE >> 1) suggests that the C-H bond activation step is potentially rate-determining and is associated with BIES or CMD mechanisms. Nevertheless, the interpretation of the results from KIE experiments is not simple and if not done carefully can lead to the incorrect conclusions. Even though the KIE determination in competition and parallel experiments fundamentally displays the same phenomenon – difference in reaction rate of deuterated and non-deuterated substrates, it does not necessarily provide indisputable evidence for the rate determining step of the reaction. Other factors and elementary steps of the mechanism (e.g. reversibility of C-H activation, ligand exchange or C-H functionalization and selectivity determining step etc.) could potentially affect the results obtained in one of the two experiments and not in the other.[17] Therefore, one should assess the KIE in both competition and parallel experiments, and draw the conclusions based on the results obtained from all of the experiments.
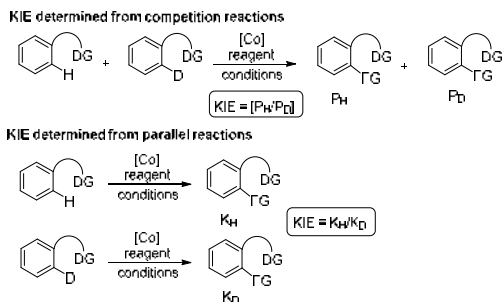
Figure 1.10 Determination of kinetic isotope effect

- *Competition experiments* are carried out with two substrates bearing electronically different substituents in the same reaction vessel. The ratio of the reaction products can indicate the preferred electronic effects which are favoured in particular C-H activation mechanism. Although, one cannot solely rely on competition experiments and usually are combined with other control experiments, especially if neither of the electronic effects are superior.[18,19] Typically, if the substrates bearing electron-withdrawing substituents are strongly favoured (product ratio >>1), CMD mechanism is likely operative and this can also be supported further by high KIE values (Figure 1.11, entries 1,7). The higher reactivity of electron-rich substrates along with low or non-existent KIE could suggest, that the S_EAr or BIES C-H activation mechanisms are operative (Figure 1.11, entries 4,8,9,11). Sometimes the competition experiments do not provide clear information about reaction mechanism, particularly if both of the electronic effects display similar reactivity and the ratio of the obtained products is 1 or close to 1 (Figure 1.11, entries 2,3,5,6). In such cases clear distinction between the operative mechanisms could be obtained with the help of other experiments like DFT calculations.
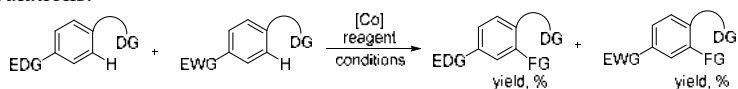
KIE	product ratio EWG:EDG	proposed C-H activation mechanism	ref
3.5	1:1.18	CMD	18a
1.23 (competitive) 1.26 (parallel)	1:1.06	Not S_EAr	18b
3.3 (competition)	1:1.2	Not S_EAr	18c
1.1 (parallel)	1:1.41	BIES	18d
-	1:1.2	Not S_EAr	18e
1.1 (competitive) 1.12 (parallel)	1.26:1	Not S_EAr	18f
1.4 (competitive) 1.6 (parallel)	1:0	CMD	19a
1.1 (competitive)	1:1.45	BIES	19b
0.53 (parallel)	-	S_EAr	19c
2.89 (competitive)	1:1.93	BIES	19d
1.0 (competitive) 0.97 (parallel)	1:3.7	S_EAr	19e

Similarly, Hammett analysis can also be used to gain useful information about the reaction mechanism. This was demonstrated in 2019 by Chatani and co-workers, where a Hammett plot for cobalt-catalyzed iodination of benzamides **18** showed nearly linear correlation with a negative slope (ρ = -3.22), indicating that the rate-determining transition state was stabilized by electron-donating substituent. Additionally, parallel KIE experiments revealed KIE to be 0.53. Such a result and Hammett analysis together gave a strong indication that the C-H bond activation step is not the RDS and the cleavage of C-H bond occurred via sp^2-sp^3 re-hybridization like in the electrophilic substitution mechanism (Figure 1.12).[19c]
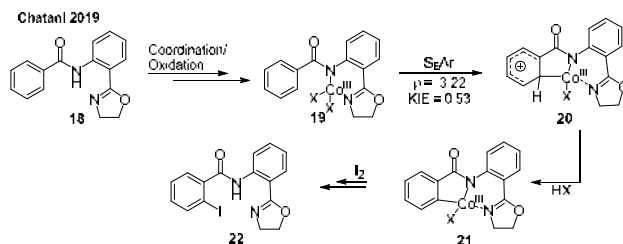
Figure 1.12 C-H bond activation of benzamides **18** via S_EAr mechanism

Addition of radical scavengers to the reaction mixture can sometimes give useful information about the reaction mechanism. Radical scavengers (TEMPO, BHT, AIBN, etc.) can partially or completely inhibit the reaction if SET processes are involved within the catalytic cycle.[20] Sometimes the SET step can be identified if the radical quenching products are isolated and characterized, giving convincing evidence of the involvement of the free radicals in the C-H bond activation or functionalization steps.

[C]1.2.1. Co-Ar(III) C-H Activation Complexes

The mechanistic understanding of cobalt-catalyzed C-H bond functionalization is unfortunately less developed compared to the noble metal catalysts. The instability of the key reaction intermediates often limits the methods that can be applied to elucidate the reaction mechanism. To the date, several research groups have been successful in the synthesis and isolation of the stable aryl-Co(III) complexes via direct C-H activation, although in general, this is rare. Isolation of such complexes is beneficial for the mechanistic studies and often serves as a direct evidence for the existence of the key reaction intermediates. The first isolated Ar-Co(III) complex was reported by the Daugulis group in 2014 (Figure 1.13a) and was characterized by 1D NMR spectroscopy.[21] In 2016, the Maiti group were successful in isolation of the similar complex and obtained XRD confirmation of the structure.[7] Since then several other structurally different complexes have been synthesized, isolated and used for the mechanistic investigations in the catalytic or stochiometric C-H functionalization reactions.[8,19c,22] Interestingly, in 2015, the Zhang group were able to detect the presence of C(sp^3)-Co(III) activated complex in the pivaloylamide alkynylation crude reaction mixture using MALDI-TOF analysis (Figure 1.13g).[23] Similarly, in 2018 the Ackermann group used ESI-MS to detect the presence of alkenyl-Co(III) intermediate in benzamide annulation reaction with alkyne (Figure 1.13i).[19b]
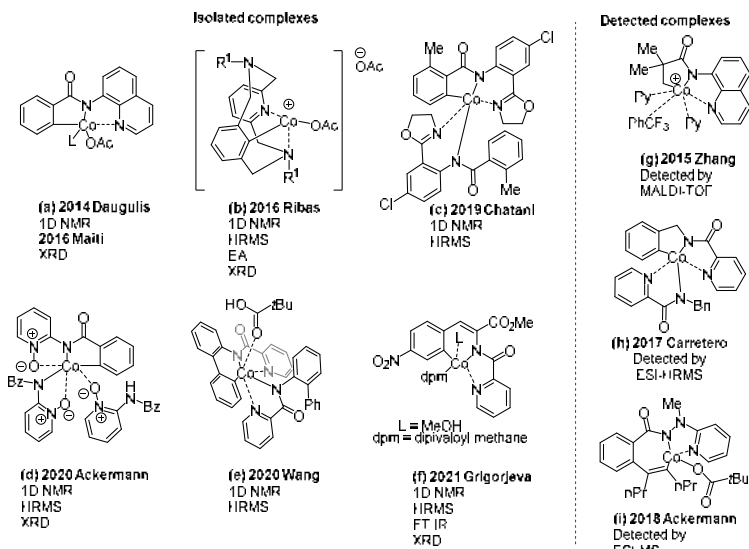
Figure 1.13 Isolated and detected Ar-Co(III) complexes in C-H bond functionalization reactions

[B]1.3. C-H Bond Functionalization

[C]1.3.1. C-H Bond Functionalization with Electrophiles
[D]1.3.1.1. Reaction with Alkynes

Since the first example in 2014[21], considerable attention has been directed towards the mechanistic understanding of cobalt-catalyzed C-H bond functionalization with terminal and internal alkynes. Depending on the reaction conditions and the reagent used, several types of products could be obtained. Terminal alkynes provide either alkynyl- or annulated products with variable cycle size whereas internal alkynes in almost every case form cyclic annulated products. The generally accepted reaction mechanism is depicted in the Figure 1.14. The reaction is initiated with the coordination/oxidation of Co(II) catalyst with the substrate **A** to form Co(III) complex **B**. Subsequent C-H bond activation gives intermediate **C**. The plausible intermediacy of Ar-Co(III) **C** has been evidenced by numerous groups by successfully exploiting such isolated or synthesized complexes as catalysts or substrates in stochiometric amounts to obtain alkynylation or annulation products. [8, 24] Depending on the alkyne used, two reaction pathways are possible. In 2016, Ribas and co-workers based on experimental observations and DFT calculations, proposed that terminal alkynes predominantly follow an acetylide mechanism, according to which alkyne first coordinates to the Ar-Co(III) intermediate **C** and with the base assistance forms complex **D**. Subsequently, reductive elimination furnishes Co(I) complex **E**, which undergoes protodemetalation to give alkynylation product **F** and Co(I) catalyst, which is reoxidized and returned to the cycle. Thereafter, cobalt-assisted intramolecular nucleophilic cyclization delivers **G** or **H**. In the reported study, the authors found that the site of nucleophilic attack is strongly dependent on the reaction temperature and solvent used as well as alkyne substitution pattern, giving either thermodynamic or kinetic product. Furthermore, such pathway has also been suggested by the Zhang group.[23] Alternatively, C-H bond functionalization with internal alkynes proceeds via the migratory insertion pathway, where coordination and migratory insertion of alkyne

forms complex **E'** which undergoes reductive elimination to give cyclic product **G'**. Protodemetalation and oxidative cyclization from complex **I** is unlikely, based on the experimental evidence obtained by the Daugulis and Song groups.[21,25]
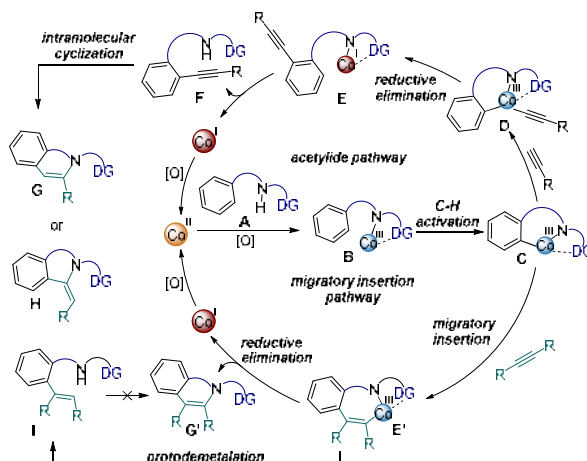
Figure 1.14 General mechanism for the C-H bond functionalization with internal and terminal alkynes

Alternative C-H bond functionalization mechanisms involving terminal alkynes have been proposed by several research groups. According to the mechanistic proposal, the reaction proceeds via Co(II/III/IV) catalytic cycle and involves the formation of an alkyne radical via SET or proton-coupled electron transfer (PCET) steps (Figure 1.15). Although this mechanism is not very popular, experimental evidence supported by DFT calculations has been obtained by Song[25b], Balaraman[26] and Wei[27], suggesting that this pathway is likely when silver oxidants are employed. Initially, coordination/oxidation of Co(II) catalyst with substrate **A** gives Co(III) complex **B** which undergoes C-H activation to give Ar-Co(III) intermediate **C**. An alkyne radical is generated *in situ* from halogen- or carboxylate-substituted alkynes in the presence of Ag(I) salts. DFT calculations suggested that the alkyne radical can also be obtained from terminal alkynes via a PCET mechanism.[27] Coordination of the alkyne radical to activated Ar-Co(III) intermediate **C** forms Co(IV) complex **D**, and upon reductive elimination and protodemetalation forms alkynylation product **F**. Intramolecular cyclization furnishes the cyclic product **G**.
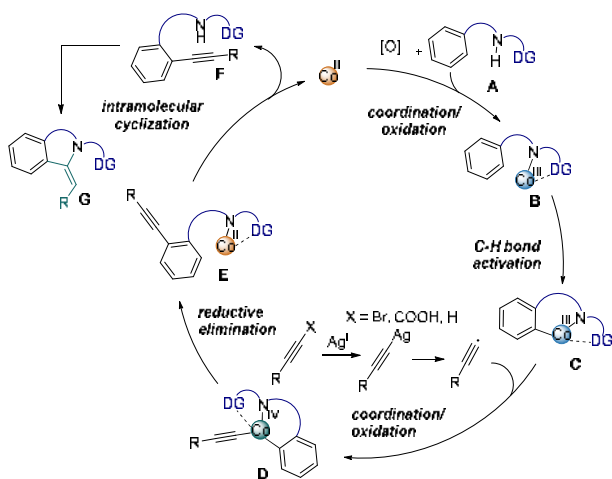
Figure 1.15 Alternative general mechanism for the C-H bond functionalization with terminal alkynes and their precursors

[D]1.3.1.2. Reactions with Alkenes and Allenes

Similarly to the C-H functionalization reactions with alkynes, alkenes and allenes are compatible coupling partners and provide a wide variety of products (Figure 1.16). Internal alkenes and allenes give cyclic annulation products, whereas terminal alkenes give either alkenylation and allylation or annulation products, depending whether β-hydrogens are present in the molecule.
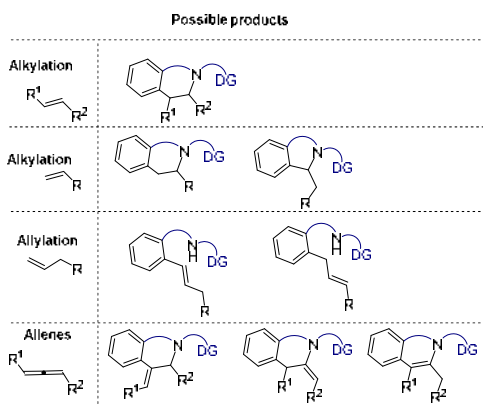
Figure 1.16 Possible products in the C-H bond functionalization with alkenes and allenes

Even though alkenes have been successfully employed in numerous C-H bond functionalization reactions as coupling partners, experimental evidence for the operative mechanisms of these transformations has not been reported as frequently as in the case of alkynes. Nevertheless, the general idea of operative mechanisms has been established based on the analogy to the precious transition metal catalysts. The cycle is initiated by the coordination/oxidation of Co(II) catalyst to substrate molecule **A**, forming Co(III) complex **B**. Subsequent C-H activation forms Ar-Co(III) intermediate **C** followed by coordination and migratory insertion of the alkene to give intermediate **D**. Finally, reductive elimination gives

annulation product **F**.[12,18f,24b,28] On the other hand, β-hydride elimination from intermediate **D** is possible, yielding either allylation **E** or alkenylation **E'** products, depending on which of the β-hydrogen is more accessible.[29] Finally, intramolecular Michael addition in **E'** yields cyclic product **G** (Figure 1.17).[19a]
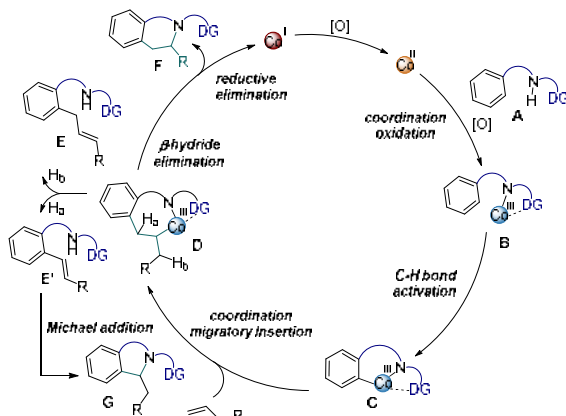
Figure 1.17 General C-H bond functionalization mechanism with alkenes

[D]1.3.1.3. Reactions with CO and Isocyanides

Cobalt-catalyzed C-H bond carbonylation methodologies have been extensively studied over the last decade and many novel transformation have been developed.[30] Although, similarly to alkenes, not much experimental evidence have been reported on this topic. Generally, the operative mechanism is assumed to be very similar to alkenes and alkynes (Figure 1.18). Initially, Co(III) complex **B** is formed via coordination/oxidation of the Co(II) catalyst to the substrate **A**. Further C-H bond activation yields Ar-Co(III) intermediate **C** which is coordinated by CO. Subsequent migratory insertion gives acyl-cobalt intermediate **E** followed by reductive elimination to furnish product **F** and Co(I) that is re-oxidized and returned to the catalytic cycle. Formation of Co(IV) intermediates thus far has not been proposed and are unlikely. This pathway was recently supported by control experiment where Ar-Co(III) intermediate **C** was able to form C-H carbonylation product **F** with gaseous CO in the absence of oxidant, indicating Co(I/III) catalytic cycle.[22c] It should be noted that C-H carbonylation, in which dialkyldicarboxylates (DIAD, DEAD, etc.) are used as CO surrogates, can proceed via Co(IV) intermediate as suggested by the Zhang's report.[31] Just like CO, isocyanides can also be employed for C-H functionalization and provide imine or carbonylation products **F** and **F'**. In this case, the reaction mechanism is believed to be the same.[32]
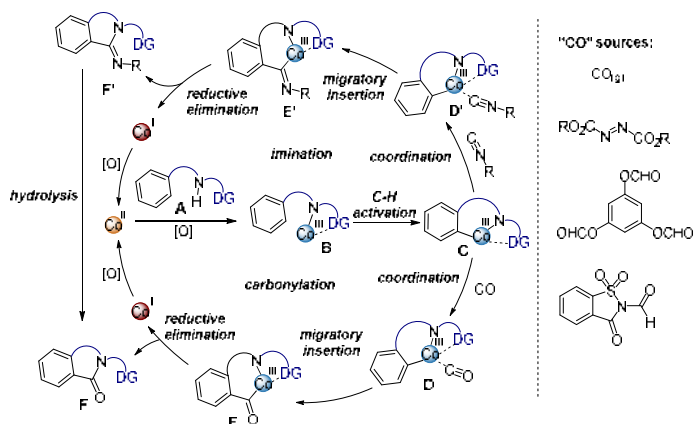
Figure 1.18 General mechanism for the C-H bond carbonylation or imination

[D]1.3.1.4. Reaction with Iodine

In 2019, Chatani and co-workers developed cobalt-catalyzed C-H iodination of the benzamide derivative **18** to obtain iodides **22**. The mechanistic experiments indicated that the C-H functionalization step involved redox neutral Co(III) pathway via electrophilic attack of I₂ in the transition state **23**. Subsequent protodemetalation and ligand exchange would regenerate Co(III) species (Figure 1.19).[19c]
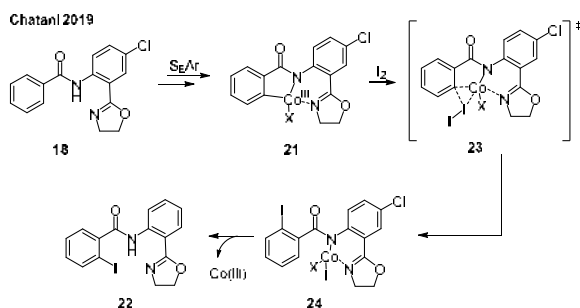
Figure 1.19 Cobalt-catalyzed C-H bond iodination

[C]1.3.2. Reaction with Nucleophiles

Operative mechanisms for the C-H bond functionalization with nucleophiles slightly differ from reactions with the electrophiles, where typically the C-H bond activation is followed by a migratory insertion. It is generally accepted that nucleophiles react with the Ar-Co(III) intermediate **C** via ligand exchange to form Ar-Co(III)-Nu complex **D,** followed by proximity-induced reductive elimination to form product **F** and Co(I), which is reoxidized to be reintroduced in the catalytic cycle (Figure 1.20). Interestingly, recently published mechanistic investigation report by the Ackermann group proposed different pathway for the electrochemical alkoxylation of benzamides.[22a] In the reported study the authors found that the reductive elimination did not occur at Ar-Co(III)-Nu complex **D** unless the external oxidant was introduced, thus indicating an additional oxidation-induced reductive elimination pathway, where Co(II/III/IV) cycle is operative via intermediate **E**. Either of these

mechanistic pathways could be applied for the C-H bond functionalization reactions with carbon[19e,22b], nitrogen[24a,33] or oxygen[22a,13,34] nucleophiles.
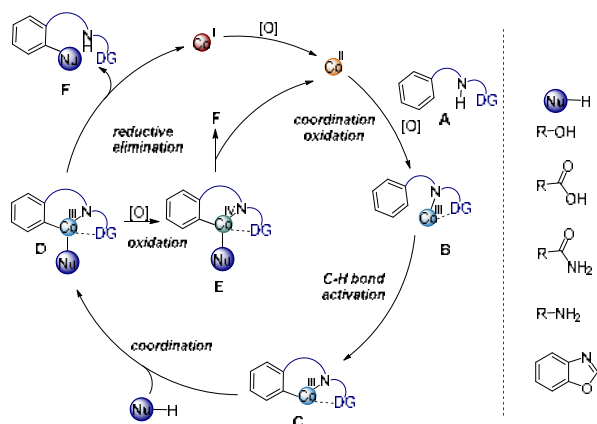
Figure 1.20 General mechanism for the cobalt-catalyzed C-H bond functionalization with nucleophiles

[C]1.3.3. SET Reaction

Interestingly, several research groups have obtained experimental evidence that support essentially different mechanism of action. Initially, the first example of the use of a cobalt catalyst for the C-H bond functionalization via SET mechanism was published by Kochi and co-workers in 1973.[35] In their work, the authors demonstrated the oxidizing properties of Co(III) salts by obtaining phenyltrifluoroacetates from benzene using stochiometric amounts of Co(OTf)$_3$ and TFA solvent. Since the report, this research direction has grown, more understanding about SET processes has been attained and new methodologies have been developed, employing various coupling partners. Typically, these transformations are inhibited by the addition of radical scavengers (TEMPO, BHT, etc.) and exhibit low or nonexistent primary KIE or show existence of single electron in EPR spectrum.[20b,c,f,g,36] According to this mechanism, the reaction is initiated by coordination/oxidation of Co(II) catalyst to the substrate **A**, forming Co(III) complex **B** (Figure 1.21). Next, a single electron is transferred from the aromatic system to the cobalt centre, forming radical cation **C** and reducing Co(III) to Co(II). Coordination of the nucleophile to Co(II) in the presence of the base yields Co(II)-Nu complex **D**. Subsequently, proximity-induced nucleophilic attack on the *ortho*-position of arene forms radical **E,** which is further oxidized to cation **F**. Rearomatization of the arene furnishes Co(II) complex **G**, from which product **H** and Co(II) catalyst are released upon protodemetalation to restart the catalytic cycle.[37]
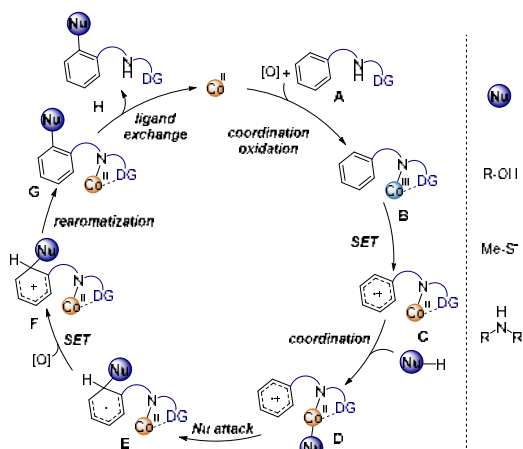
Figure 1.21 General SET mechanism for the cobalt-catalyzed C-H bond functionalization with nucleophiles

In 2015, Lu and co-workers reported Co(II) catalyzed C-H bond acylation of benzoxazoles **25** with oxocarboxylic acid **26**.[20e] The authors proposed a reaction mechanism depicted in the Figure 1.22. Initially, Co(II) is oxidized to Co(III) by Ag(I), which then reacts with substrate **25** via ligand exchange to generate Co(III) complex **28**. Oxocarboxylic acid **26** in the presence of Ag_2CO_3 forms acyl radical species **29**, that coordinates to the complex **28** and oxidizes Co(III) to Co(IV) intermediate **30**. Subsequent reductive elimination furnishes product **27** and returns Co(II) to the catalytic cycle. Interestingly, when 3 equivalents of radical scavenger TEMPO was added to the reaction mixture, product formation was completely inhibited and the authors observed formation of TEMPO-acyl adduct **31**, which supports their SET mechanism hypothesis.
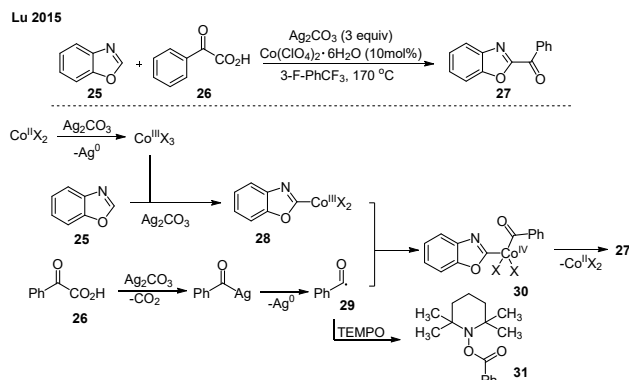
Figure 1.22 Cobalt-catalyzed C-H bond acylation of benzoxazoles via SET process

An interesting example of cobalt-catalyzed cross coupling was demonstrated by Song and co-workers using mixed directing-group strategy in oxidative C-H bond arylation under high-valent cobalt catalysis.[20d] In their work, the authors used benzamides **1** with the 8-aminoquinoline directing group in combination with 2-arylpyridines **32** to achieve tandem C-H bond activation and obtain heterocoupling products **36** (Figure 1.23). As a part of their

mechanistic investigation, the authors performed radical quenching experiments and observed complete suppression of the product **36** formation if TEMPO, BQ or BHT were added to the reaction mixture. Interestingly, the use of BHT led to the formation of **37**, which could be the result of a SET pathway initiated by Co(III) or Mn(II) species. Based on the mechanistic investigation, the authors proposed a possible reaction mechanism, where cobalt plays two-fold role in C-H bond activation. On the one hand, in the intermolecular SET reaction between benzamide **1** and Co(III), intermediate **34** is generated, while on the other hand direct C-H activation of arylpyridine **32** via CMD mechanism provides **33**. Subsequent coordination of **33** to Co(III) complex and loss of a proton leads to the formation of Co(IV) intermediate **35**, which undergoes reductive elimination to give product **36**.

Figure 1.23 Cobalt-catalyzed cross coupling using mixed directing group strategy

In 2017, Song and co-workers reported a method for C(sp^3)-H bond nitration of pyrimidine derivatives **38** using *tert*-butylnitrite as the nitrating agent (Figure 1.24). To elucidate the reaction mechanism, the authors performed control experiments with TEMPO as a radical scavenger and observed complete inhibition of the nitration reaction. Furthermore, TEMPO-NO$_2$ was detected by GC-MS in the crude reaction mixture, which confirmed involvement of SET mechanism. On basis of the literature precedents and above experiment, the authors proposed plausible catalytic cycle. First, a NO radical is generated via thermal decomposition of *tert*-butylnitrite, and then oxidized to a NO$_2$ radical under aerobic conditions. In the presence of oxygen, Co(II) could also be oxidized to Co(III), which then undergoes SET of pyrimidine **38** to generate the cation radical **40**. With the help of a *t*BuO radical, a H atom is abstracted from intermediate **40** to form intermediate **41**. Finally, product **39** is obtained via recombination of intermediate and NO$_2$ radicals.[38]

Figure 1.24 Nitration of pyrimidine **38** derivatives

In the same year, Das and co-workers published a methodology for the cobalt-catalyzed nitration of *N*-phenylpyridin-2-amines **42** using AgNO$_2$ as the nitro source (Figure 1.25).[20a] To gain insight into the reaction mechanism, the authors performed broad series of control experiments. First, addition of TEMPO to the reaction mixture completely inhibited the reaction. Second, no preference towards electron rich or electron poor substrates was observed in the competition experiments, suggesting that the SET mechanism is involved and direct C-H cobaltation is unlikely. Additionally, no KIE was observed in the competition experiments (KIE = 1), indicating that the C-H activation step is not the rate determining step. Lastly, DFT calculations were also employed to elucidate the reaction mechanism. Initially, Co(OAc)$_2$ is converted to Co(OAc)$_2$(NO$_3$) in the presence of silver nitrite, then coordinated to substrate **42** to form starting complex **44**. Following PCET (proton-coupled electron transfer), a hydrogen atom from the N-H bond is abstracted by acetate and an electron is delocalized to the cobalt which is reduced from Co(III) to Co(II), forming complex **45**. The hydrogen atom is then abstracted by AcO radical and Co(II) is oxidized back to Co(III). Simultaneously, single electron on nitrogen atom gets delocalized in the aniline ring and complex **46** is formed. Next, nitro group is transferred to the *ortho*-carbon of the aniline ring, which then adopts sp^3 hybridization and forms intermediate **47**. According to DFT calculations, this is the RDS of the reaction. The hydrogen in *ortho*- C-H bond is oriented towards acetate ligand, which facilitates the abstraction of proton and rehybridization of *ortho*-carbon generating intermediate **48**. Finally, intramolecular proton transfer and dissociation provides reaction product **43**.
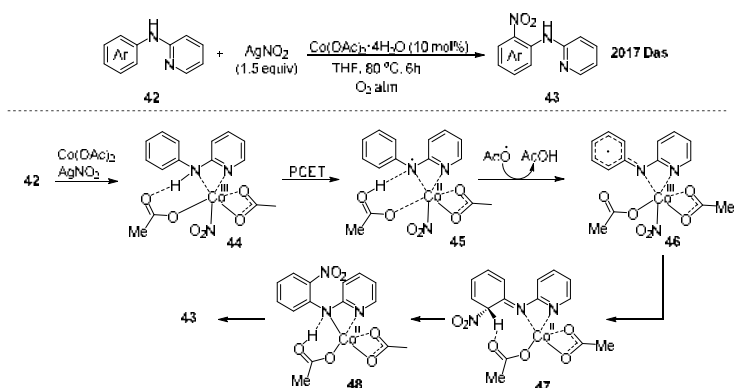

Figure 1.25 Nitration of *N*-phenylpyridin-2-amines **42**

In 2016, Whiteoak and Ribas reported the first example of a cobalt-catalyzed C-H bond nitration in 8-aminoquinolines **1** via SET pathway with *tert*-butyl nitrite (Figure 1.26).[39] Initially, the authors proposed a SET pathway, although after more thorough investigations using DFT calculations in 2020, a different mechanism was proposed, involving a high-spin remote induced radical coupling mechanism.[40] According to the obtained results, the reaction is initiated by H-atom abstraction from the amide by *t*BuO radical, which is generated *in situ* from the thermal decomposition of *t*BuONO. Further, coordination with the Co(II) catalyst results in the formation of a Co(II) species **A** with a partially delocalised radical in the C(5) and C(7) positions in the 8-aminoquinoline moiety, which then reacts with NO$_2$ radical to obtain intermediate **B**. Deprotonation of **B** followed by protodemetalation of chelated product **C** furnishes final nitration product **49**. Such a reaction pathway is consistent with the regioselectivity observed in sulfonation and perfluoroalkylation reactions reported earlier by Xia[41] and Song.[20g]
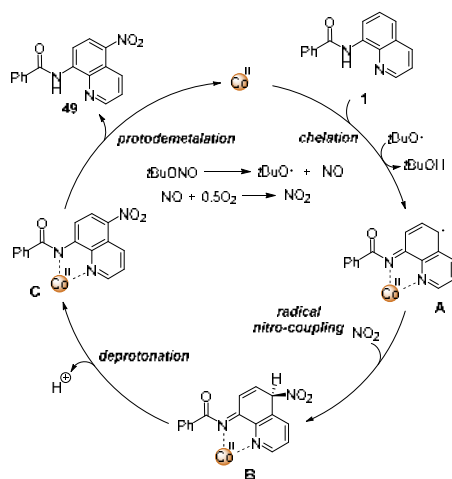
Figure 1.26 Co(II) catalyzed nitration via high-spin remote induced radical coupling

[A]2. Conclusions and Outlook

To conclude, we have summarized the generally accepted C-H activation and functionalization mechanisms under cobalt catalysis conditions. Despite the immense progress in the cobalt-catalyzed C-H functionalization field, not many studies have actually focused the efforts to understand the mode of action of the catalyst. Most of the mechanistic studies rely on the use of the isotope labelling and kinetic experiments as well as computational methods. Due to the instability of organometallic Co complexes and the reversibility of C-H activation step, isolation and characterisation of such complexes is a challenging task. Even though many research groups have successfully isolated and employed these complexes to prove the existence of key reaction intermediates, the reaction mechanism in lots of cases is still not fully confirmed, remains hypothetical and should be studied further.

Acknowledgements

References

1. Gandeepan P., Müller T., Zell D., et al. 3d Transition Metals for C-H Activation. Chem. Rev. 2019;119:2192–2452.
2. Murahashi S. Synthesis of Phthalimidines from Schiff Bases and Carbon Monoxide. J. Am. Chem. Soc. 1955;77:6403–6404.
3. Gao K., Lee P.S., Fujita T., et al. Cobalt-catalyzed hydroarylation of alkynes through chelation-assisted C-H bond activation. J. Am. Chem. Soc. 2010;132:12249–12251.
4. a) Yoshino T., Ikemoto H., Matsunaga S., et al. A Cationic High-Valent Cp*Co III Complex for the Catalytic Generation of Nucleophilic Organometallic Species: Directed C-H Bond Activation. Angew. Chem. Int. Ed. 2013;52:2207-2211. b) Lukaevics L., Cizikovs A., Grigorjeva, L. C–H bond functionalization by high-valent cobalt catalysis: current progress, challenges and future perspectives. Chem. Commun. 2021;57:10827-10841.

5. Grigorjeva L., Daugulis O. Cobalt-catalyzed, aminoquinoline-directed coupling of sp^2 C-H bonds with alkenes. Org. Lett. 2014;16:4684–4687.

6. Oliveria J.C.A., Dhawa U., Ackermann L. Insights into the Mechanism of Low-Valent Cobalt-Catalyzed C-H activation. ACS. Catal. 2021;11:1505–1515.

7. Planas O., Chirila P.G., Whiteoak C.J., et al. Current Mechanistic Understanding of Cobalt-Catalyzed C–H Functionalization. 1st ed. Vol. 69, Advances in Organometallic Chemistry. Elsevier Inc.; 2018. 209–282 p.

8. Planas O., Whiteoak C.J., Martin-Diaconescu V., et al. Isolation of Key Organometallic Aryl-Co(III) Intermediates in Cobalt- Catalyzed C(sp^2)−H Functionalizations and New Insights into Alkyne Annulation Reaction Mechanisms. J. Am. Chem. Soc. 2016;138:14388–13497.

9. Barsu N., Bolli S.K., Sundararaju B. Cobalt catalyzed carbonylation of unactivated C(sp^3)-H bonds. Chem. Sci. 2017;8:2431–2435.

10. Williamson P., Galván A., Gaunt M.J. Cobalt-catalysed C-H carbonylative cyclisation of aliphatic amides. Chem. Sci. 2017;8:2588–2591.

11. Zeng L., Tang S., Wang D., et al. Cobalt-Catalyzed Intramolecular Oxidative C(sp^3)-H/N-H Carbonylation of Aliphatic Amides. Org. Lett. 2017;19:2170–2173.

12. Tang S., Wang D., Liu Y., et al. Cobalt-catalyzed electrooxidative C-H/N-H [4+2] annulation with ethylene or ethyne. Nat. Commun. 2018;9:1–7.

13. Tian C., Dhawa U., Struwe J., et al. Cobaltaelectro-Catalyzed C—H Acyloxylation. Chinese J. Chem. 2019;37:552–556.

14. Mei R., Fang X., He L., et al. Cobaltaelectro-catalyzed oxidative allene annulation by electro-removable hydrazides. Chem. Commun. 2020;56:1393–1396.

15. a) Gellego D., Baquero A.E. Recent Advances on Mechanistic Studies on C–H Activation Catalyzed by Base Metals. Open Chem. 2018;16:1001–1058. b) Ackermann L. Carboxylate-assisted transition-metal-catalyzed C-H bond functionalizations: Mechanism and scope. Chem. Rev. 2011;111:1315–1345. c) Yang Y.F., She Y.. Computational exploration of Pd-catalyzed C–H bond activation reactions. Int J Quantum Chem. 2018;118:1–9.

16. Gallego D., Baquero A.E. Recent Advances on Mechanistic Studies on CH Activation Catalyzed by Base Metals. Open Chem. 2018;16:1001–1058.

17. Simmons E.M., Hartwig J.F. On the interpretation of deuterium kinetic isotope effects in C-H bond functionalizations by transition-metal complexes. Angew. Chem. Int. Ed. 2012;51:3066–3072.

18. Selected examples: a) Planas O., Whiteoak C.J., Company A., et al. Regioselective Access to Sultam Motifs through Cobalt-Catalyzed Annulation of Aryl Sulfonamides and Alkynes using an 8-Aminoquinoline Directing Group. Adv. Synth. Catal. 2015;357:4003–4012. b) Manoharan R., Jeganmohan. Cobalt-Catalyzed Oxidative Cyclization of Benzamides with Maleimides: Synthesis of Isoindolone Spirosuccinimides. Org. Lett. 2017;19:5883–5887. c) Kathiravan S., Nicholls I.A. Cobalt Catalyzed, Regioselective C(sp^2)-H Activation of Amides with 1,3-Diynes. Org. Lett. 2017;19:4758–4761. d) Tian C., Massignan L., Meyer T.H., et al. Electrochemical C−H/N−H Activation by Water-Tolerant Cobalt Catalysis at Room Temperature. Angew. Chem. Int. Ed. 2018;57:2383–2387. e) Thrimurtulu N., Nallagonda R., Volla C.M.R. Cobalt-catalyzed aryl C-H activation and highly regioselective intermolecular annulation of sulfonamides with allenes. Chem. Commun. 2017;53:1872–1875. f) Dey A., Thrimurtulu N., Volla C.M.R. Cobalt-Catalyzed Annulation Reactions of Alkylidenecyclopropanes: Access to Spirocyclopropanes at Room Temperature. Org. Lett. 2019;21:3871–3875.

19. Selected examples: a) Ma W., Ackermann L. Cobalt(II)-catalyzed oxidative C-H alkenylations: Regio- and site-selective access to isoindolin-1-one. ACS Catal. 2015;5:2822–2825. b) Mei R., Sauermann N., Oliveira J.C.A., et al. Electroremovable Traceless

Hydrazides for Cobalt-Catalyzed Electro-Oxidative C-H/N-H Activation with Internal Alkynes. J. Am. Chem. Soc. 2018;140:7913–7921. c) Kommagalla Y., Chatani N. Cobalt-Catalyzed C-H Iodination of Aromatic Amides with Molecular Iodine through the Use of a 2-Aminophenyloxazoline-Based Bidentate-Chelation System. Org. Lett. 2019;21:5971–5976. d) Ling F., Xie Z., Chen J., et al. Cobalt(II)-Catalyzed [5+2] C−H Annulation of o-Arylanilines with Alkynes: An Expedient Route to Dibenzo-[b,d]azepines. Adv. Synth. Catal. 2019;361:3094–3101. e) Yao Z., Cai Z., Zhen L., et al. Cobalt-Catalyzed Switchable Intramolecular Thioenolization/C-H Thiolation and C(sp^2)-H/C(sp^3)-H Dehydrogenative Coupling. Org. Lett. 2020;22:4505–4510.

20. a) Nageswar R.D., Rasheed S., Raina G., et al. Cobalt-Catalyzed Regioselective Ortho C(sp^2)-H Bond Nitration of Aromatics through Proton-Coupled Electron Transfer Assistance. J. Org. Chem. 2017;82:7234–7244. b) Zhang T., Zhu H., Yang F., et al. Cobalt(II)–catalyzed C8–H alkoxylation of 1-naphthylamine derivatives with alcohols. Tetrahedron. 2019;75:1541–1547. c) Hu L., Chen X., Yu L., et al. Highly mono-selective *ortho* - methylthiolation of benzamides *via* cobalt-catalyzed sp^2 C–H activation. Org. Chem. Front. 2018;5:216–221. d) Du C., Li P.X., Zhu X., et al. Mixed Directing-Group Strategy: Oxidative C−H/C−H Bond Arylation of Unactivated Arenes by Cobalt Catalysis. Angew. Chem. Int. Ed. 2016;55:13571–13575. e) Yang K., Chen X., Wang Y., et al. Cobalt-Catalyzed Decarboxylative 2-Benzoylation of Oxazoles and Thiazoles with α-Oxocarboxylic Acids. J. Org. Chem. 2015;80:11065–11072. f) Zhang L.B., Hao X.Q., Zhang S.K., et al. Cobalt-catalyzed C(sp2)-H alkoxylation of aromatic and olefinic carboxamides. Angew. Chem. Int. Ed. 2015;54:272–275. g) Suo J.F., Zhao X.M., Zhang K.X., et al. Cobalt-Catalyzed Perfluoroalkylation of Quinoline Amides at the C5 Position. Synthesis 2017;49:3916–3924.

21. Grigorjeva L., Daugulis O. Cobalt-catalyzed, aminoquinoline-directed C(sp^2)-H bond alkenylation by alkynes. Angew. Chem. Int. Ed. 2014;53:10209–10212.

22. a) Meyer T.H., Oliveira J.C.A, Ghorai D., et al. Insights into Cobalta(III/IV/II)-Electrocatalysis: Oxidation-Induced Reductive Elimination for Twofold C-H Activation. Angew. Chem. Int. Ed. 2020;59:10955–10960. b) Wang X., Chen Y., Song H., et al. Construction of 2-(2-Arylphenyl)azoles via Cobalt-Catalyzed C−H/ C−H Cross-Coupling Reactions and Evaluation of Their Antifungal Activity. Org Lett. 2020;22:9331–9336. c) Lukasevics L., Cizikovs A., Grigorjeva L. Cobalt-Catalyzed C(sp^2)−H Carbonylation of Amino Acids Using Picolinamide as a Traceless Directing Group. Org. Lett. 2021;23:2748–2753. d) Sanjosé-Orduna J., Sarria Toro J.M., Pérez-Temprano M.H. HFIP-assisted C–H functionalization by Cp*Co^{III}: Promoted Access to Key Reactive Cobaltacycles and Implication in Catalysis. Angew Chemie - Int Ed. 2018;57:11369–11373. e) Martínez de Salinas S., Sanjosé-Orduna J., Odena C., et al. Weakly Coordinated Cobaltacycles: Trapping Catalytically Competent Intermediates in Cp*Co^{III} Catalysis. Angew Chemie Int Ed. 2020;59:6239–6243.

23. Zhang J., Chen H., Lin C., et al. Cobalt-Catalyzed Cyclization of Aliphatic Amides and Terminal Alkynes with Silver-Cocatalyst. J. Am. Chem. Soc. 2015;137:12990–12996.

24. a) Du C., Li P.X., Zhu X., et al. Cobalt-Catalyzed Oxidative C-H/N-H Cross-Coupling: Selective and Facile Access to Triarylamines. ACS Catal. 2017;7:2810–2814. b) Kalsi D., Dutta S., Barsu N., et al. Room Temperature C-H bond Functionalization by Merging Cobalt- and Photoredox Catalysis. ACS Catal. 2018;8:8115–8120.

25. a) Nguyen T.T., Grigorjeva L., Daugulis O. Cobalt-Catalyzed Coupling of Benzoic Acid C-H Bonds with Alkynes, Styrenes, and 1,3-Dienes. Angew. Chem. Int. Ed. 2018;130:1–5. b) Zhang L.B., Hao X.Q., Liu Z.J., et al. Cobalt(II)-Catalyzed Csp^2-H Alkynylation/Annulation with Terminal Alkynes: Selective Access to 3-Methyleneisoindolin-1-one. Angew. Chem. Int. Ed. 2015;127.

26. Landge V.G., Jaiswal G., Balaraman E. Cobalt-Catalyzed Bis-alkynylation of Amides via Double C-H Bond Activation. Org. Lett. 2016;18:812–815.

27. Wang Y., Du C., Wang Y., et al. High-Valent Cobalt-Catalyzed C-H Activation/Annulation of 2- Benzamidopyridine 1-Oxide with Terminal Alkyne: A Combined Theoretical and Experimental Study. Adv. Synth. Catal. 2018;360:2668–2677.

28. Kathiravan S., Nicholls I.A. Cobalt-Catalyzed Oxidative Annulation of Benzothiophene-[b]-1,1-dioxide through Diastereoselective Double C-H Activation. Org. Lett. 2019;21:9806–9811.

29. Yamaguchi T., Kommagalla Y., Aihara Y., et al. Cobalt-catalyzed chelation assisted C–H allylation of aromatic amides with unactivated olefins. Chem. Commun. 2016;52:10129–10132.

30. Lukasevics L., Grigorjeva L. Cobalt-catalyzed carbonylation of the C-H bond. Org. Biomol. Chem. 2020;18:7460–7466.

31. Ni J., Li J., Fan Z., et al. Cobalt-Catalyzed Carbonylation of C(sp^2)–H Bonds with Azodicarboxylate as the Carbonyl Source . Org. Lett. 2016;18:5960–5963.

32. Zhao H., Shao X., Qing Z., et al. Cobalt-Catalyzed 2-(1-Methylhydrazinyl)pyridine-Assisted Direct C−H/N−H Functionalization of Benzoyl Hydrazide with Isocyanide: Efficient Synthesis of Iminoisoindolinone Derivatives. Adv. Synth. Catal. 2019;361:1678–1682.

33. a) Wu X., Yang K., Zhao Y., et al. Cobalt-catalysed site-selective intra-and intermolecular dehydrogenative amination of unactivated sp3carbons. Nat. Commun. 2015;6:6462-6472. b) Sauermann N., Mei R., Ackermann L. Electrochemical C−H Amination by Cobalt Catalysis in a Renewable Solvent. Angew. Chem. Int. Ed. 2018;57:5090–5094. c) Gao X., Wang P., Zeng L., et al. Cobalt(II)-Catalyzed Electrooxidative C-H Amination of Arenes with Alkylamines. J. Am. Chem. Soc. 2018;140:4195–4199.

34. a) Sauermann N., Meyer T.H., Tian C., et al. Electrochemical Cobalt-Catalyzed C-H Oxygenation at Room Temperature. J. Am. Chem. Soc. 2017;139:18452–18455. b) Lin C., Chen Z., Liu Z., et al. Direct ortho-Acyloxylation of Arenes and Alkenes by Cobalt Catalysis. Adv. Synth. Catal. 2018;360:519–532. c) Ueno R., Natsui S., Chatani N. Cobalt(II)-Catalyzed Acyloxylation of C-H Bonds in Aromatic Amides with Carboxylic Acids. Org. Lett. 2018;20:1062–1065.

35. Kochi J.K., Tang R.T., Bernath T. Mechanisms of Aromatic Substitution. Role of Cation-Radicals. J. Am. Chem. Soc. 1972;19:7114–7123.

36. Zhang L.B., Zhang S.K., Wei D., et al. Cobalt(II)-Catalyzed C-H Amination of Arenes with Simple Alkylamines. Org. Lett. 2016;18:1318–1321.

37. Guo X.K., Zhang L.B., Wei D., et al. Mechanistic insights into cobalt(II/III)-catalyzed C–H oxidation: a combined theoretical and experimental study. Chem. Sci. 2015;6:7059–7071.

38. Zhou Y., Tang Z., Song Q. Co-catalyzed highly selective C(sp^3)-H nitration. Chem. Commun. 2017;53:8972–8975.

39. Whiteoak C.J., Planas O., Company A., et al. A First Example of Cobalt-Catalyzed Remote C-H Functionalization of 8-Aminoquinolines Operating through a Single Electron Transfer Mechanism. Adv. Synth. Catal. 2016;358:1679–1688.

40. Chu M., Planas O., Company A., et al. Unravelling the mechanism of cobalt-catalysed remote C-H nitration of 8-aminoquinolinamides and expansion of substrate scope towards 1-naphthylpicolinamide. Chem. Sci. 2020;11:534–542.

41. Wang K., Wang G., Duan G., et al. Cobalt(II)-catalyzed remote C5-selective C-H sulfonylation of quinolines: Via insertion of sulfur dioxide. RSC. Adv. 2017;7:51313–51317.